Mississippi State University
Scholars Junction

Theses and Dissertations | Theses and Dissertations

1-1-2013

Evaluation of Catalytic and Non-Catalytic Production of Biodiesel from Wet Microbial Media and Reaction Schemes

Adebola Titilope Coker

Follow this and additional works at: https://scholarsjunction.msstate.edu/td

Recommended Citation
Coker, Adebola Titilope, "Evaluation of Catalytic and Non-Catalytic Production of Biodiesel from Wet Microbial Media and Reaction Schemes" (2013). *Theses and Dissertations*. 2004.
https://scholarsjunction.msstate.edu/td/2004

This Dissertation - Open Access is brought to you for free and open access by the Theses and Dissertations at Scholars Junction. It has been accepted for inclusion in Theses and Dissertations by an authorized administrator of Scholars Junction. For more information, please contact scholcomm@msstate.libanswers.com.

www.manaraa.com

Evaluation of catalytic and non-catalytic production of biodiesel from wet microbial media and reaction schemes

By

Adebola Titilope Coker

A Dissertation
Submitted to the Faculty of
Mississippi State University
in Partial Fulfillment of the Requirements
for the Degree of Doctor of Philosophy
in Chemical Engineering
in the Dave C. Swalm School of Chemical Engineering

Mississippi State, Mississippi

December 2013

www.manaraa.com

Copyright by

Adebola Titilope Coker

2013

www.manaraa.com

Evaluation of catalytic and non-catalytic production of biodiesel from wet microbial media and reaction schemes

By

Adebola Titilope Coker

Approved:

_____

Rafael A. Hernandez
(Major Professor)

_____

W. Todd French
(Committee Member)

_____

Priscilla J. Hill
(Committee Member)

_____

L. Antonio Estevez
(Committee Member)

_____

Keisha B. Walters
(Graduate Coordinator)

_____

Jerome A. Gilbert
Interim Dean
Bagley College of Engineering

www.manaraa.com

Name: Adebola Titilope Coker

Date of Degree: December 14, 2013

Institution: Mississippi State University

Major Field: Chemical Engineering

Major Professor: Rafael Hernandez

Title of Study: Evaluation of catalytic and non-catalytic production of biodiesel from wet microbial media and reaction schemes

Pages in Study: 275

Candidate for Degree of Doctor of Philosophy

Biodiesel is a renewable fuel that can supplement petroleum fuel supply. A major deterrent to commercial biodiesel production from traditional feedstock like soybean, canola or rapeseed oils is the high cost of feedstock: 70 - 95% of total biodiesel production cost. Therefore, a relatively cheaper feedstock is needed to make the price of biodiesel cost-competitive with petroleum diesel. Activated sludge from wastewater treatment plants is a relatively cheaper feedstock and relatively easy to obtain. However, drying of this sludge prior to oil extraction is a major operating cost of this process, as high as 50% of biodiesel production cost.

The goal of this research is to address this challenge by investigating the feasibility of using activated sludge from municipal wastewater for cost-efficient biodiesel production with little or no drying of the feedstock. First, the use of water-tolerant catalysts for biodiesel production was investigated to determine the level of water tolerance of these catalysts for the case where the sludge could be dried to an extent. The study investigated porous metal oxide and zeolite catalysts with tunable basicities, acidities and hydrophobicities and proposed a reaction mechanism for the most active

www.manaraa.com

catalyst. Next, the alternative where the catalysts were not very tolerant of moisture was considered, and the feasibility of a non-catalytic means of producing biodiesel from wet microbial media using supercritical methanol was also investigated. A model system of oleaginous yeast, *Rhodotorula glutinis*, was used to evaluate the production of biodiesel in a system similar to sludge.

Since the non-catalytic method showed the highest tolerance for water at 90% moisture content, the optimum reaction conditions for highest FAME yields were determined. Two methods of the non-catalytic process, 1-step and 2-step processes, that could produce high FAME yields were studied and compared in terms of FAME yields and kinetic rate constants. With these results, an economic analysis was performed to investigate the cost efficiency of both methods of the non-catalytic process and recommend one with great potential for producing biodiesel from activated sludge at a cost-competitive price.

www.manaraa.com

DEDICATION

All the praise and glory goes to God. I would like to dedicate this dissertation to my family, especially my parents, Mrs. Adesola O. Coker and the later Mr. Emmanuel O. Coker, who sacrificed a lot to send me to study in the United States. Their unending love, support and sacrifice helped make this happen. I would also like to dedicate this to my wonderful fiancé, Ayobami M. Oyedeji, who has provided such great moral support encouragement and constructive criticism when needed. Thank you for your love and support during these past few years and for continually speaking words of wisdom and positivity for every time I got frustrated, I am incredibly blessed to have you in my life and so very grateful. I love you!

www.manaraa.com

ACKNOWLEDGEMENTS

A deep, profound thank you goes to my advisor, Dr. Rafael Hernandez, who is a great inspiration to me and has been very encouraging and quite patient with me. His exemplary leadership is a high one to live up to and I am very grateful for the opportunity to have him as a mentor. I would like to thank Dr. Alexei Iretskii for his invaluable mentoring and guidance especially in my first year here. Special thanks go to Dr. Mark White for being such a wonderful teacher and consultant, listening to your explanations always made everything so much easier and more understandable. My deep gratitude goes to Mr. William Holmes whose assistance and technical expertise was extremely crucial to completing this project. I would like to thank Dr. Todd French for being a great advisor also, for his sense of humor and his encouragement. My appreciation goes to my other committee members, namely Dr. Antonio Estevez and Dr. Priscilla Hill, for your valuable input in making me the best researcher I can be. I would like to thank the undergraduate students that provided invaluable help with experiments on this project: Vicdaly Williams, Ranjita Bandi, Jerry Layne Smith, Phillip Jamison, Robert Callahan, Allison Forks, and especially Janice Cunningham whose invaluable time, dedication and attention to details helped me complete the numerous experiments that were needed.

A big thank-you goes to the Renewable Fuel and Chemicals group, members of which made work a better experience and made the environment like family. They include Dr. Emmanuel Revellame, Dr. Jaclyn Hall, Dr. Andro Mondala, Dr. Patrisha

www.manaraa.com

Pham, Dr. Mary Hetrick, Dr. Guochang Zhang, and Scott Crymble. The assistance from Dr. Darrell Sparks, Dr. Patrisha Pham, Mr. Jimmy Cain, Ms. Linda McFarland contributed very much to this work as well. I would like to thank my fellow graduate students Erick Vasquez-Guardado, Marta Amirsadeghi, Hien Nguyen, Ersan Eyiler, Dhan Fortella, Maryam Dadgarmoghaddam, Amy Parker and Dr. Sheena Reeves for their helpful assistance at different times and for adding memorable experiences to make this journey worth it. Thank you to Dr. Xiangu Yan and Dr. Fei Yu for use of their catalyst pelletizer.

I would also like to thank the Chemical Engineering office staff: Ms. Sherre Denson, Ms. Sandra Shumaker, and Ms. Ellen Weeks for all their valuable assistance with administrative needs. Thank you to the Sustainable Energy Research Center (SERC) and General Atomics (GA) for financial support.

www.manaraa.com

TABLE OF CONTENTS

www.manaraa.com

www.manaraa.com

www.manaraa.com

www.manaraa.com

www.manaraa.com

www.manaraa.com

www.manaraa.com

LIST OF TABLES

www.manaraa.com

www.manaraa.com

LIST OF FIGURES

www.manaraa.com

www.manaraa.com

www.manaraa.com

www.manaraa.com

www.manaraa.com

www.manaraa.com

CHAPTER I

INTRODUCTION

1.1 World Energy Needs

Energy is among the most important needs for daily survival in many parts of the world. It is one of the largest industries on the planet with total global annual energy consumption in 2011 being 12,275 billion tonnes of oil equivalent (BP 2012). Of this global energy consumption, oil was the leading fuel accounting for 33.1% (4059.1 million tonnes), followed by coal at 30.3% as seen in Figure 1.1 below (BP 2012).

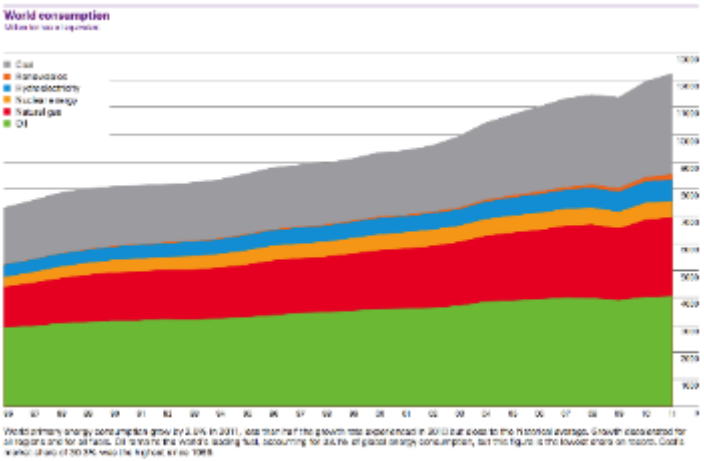

Figure 1.1 World energy consumption Source

(EIA 2012)
*1 tonne of crude oil = 42 Giga Joules = 7.3 barrels of oil

www.manaraa.com

The U.S. Department of Energy's Energy Information Administration (EIA) projects that world energy consumption will increase by 47% from 2010 through 2035, based on the assumption that current laws and regulations remain unchanged throughout the projections shown in Figure 1.2 (EIA 2012). Most of this increase is attributed to robust economic growth which is usually accompanied by increased demand for energy. For example, countries like China and India are reported to account for half the growth in world energy use (EIA 2012). Thus, there is a great need to meet this growing demand with diverse supply options for reasons that include: availability and economic impact, environmental impact, and government regulations.

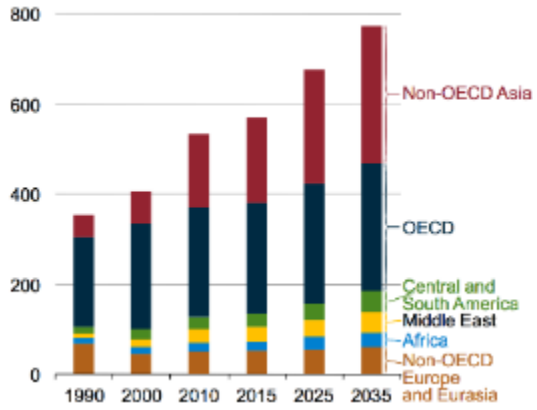

Figure 1.2 Projected increase in energy consumption (quadrillion Btu) by region till 2035 Source

(EIA 2012)

1.1.1 Availability and economic impact

Currently the world largely depends on fossil fuels like crude oil, as the predominant energy source for liquid transportation fuel. Of the total petroleum and other liquids consumption, the transportation sector accounted for 57 % in 2009 (OPEC 2012).

www.manaraa.com

This number is expected to grow as the global population growth increases from 6.9 billion in 2010 to 8.6 billion in 2035 (OPEC 2011). Corresponding with that population growth, the International Energy Agency (IEA) expects the world's energy demand to increase by more than one-third over the period to 2035, with 60% by 2030 driven largely by growth of energy use and population in India, China and the Middle East (IEA 2012).

In addition to this projected increase, the volatility in oil prices (Figure 1.3), often due to risks in the international financial system, natural disasters, and social unrest in different oil-producing parts of the world, indicates the need for countries to independently produce more of their own fuel supply locally for energy and economic security. While some countries like the U.S. have experienced a significant increase in onshore crude oil production (especially from shale and other tight formations) that puts them closer to energy independence, more important factors need to be addressed: sustainability and environmental impact. Furthermore, not every country is on the path to energy independence, and in most cases their economic growth will be accompanied by a parallel increase in transport and energy demand. Therefore, it is important to invest in diverse, sustainable energy sources in a timely manner to meet future energy demands for the economic and energy security of the country.

www.manaraa.com

Figure 1.3 Oil prices over the last 5 years

(Source:(Oil-Price.net))

1.1.2 Environmental impact

Unfortunately, utilization of fossil fuels is one of the main causes of environmental pollution. The combustion of these non-renewable fossil fuels emits excessive toxic greenhouse gases such as carbon monoxide (CO), carbon dioxide (CO_2), sulfur dioxide (SO_2), nitrogen oxide (NO) and nitrogen dioxide (NO_2). These greenhouse gases cause the green house effect phenomenon as they trap heat in the atmosphere and subsequently cause global warming and acid rain (Tan and Lee 2011). Continued and increasing use of petroleum fuels will increase local air pollution and intensify the global warming problems caused by CO_2 (Ma and Hanna 1999). Thus, another important reason for investing in more renewable fuels: the positive environmental impact of the fuels. Renewable fuels like biodiesel are reported to be cleaner than the corresponding petroleum fuel, having less sulfur and generating less particulate matter. The environmental impacts span more than just the exhaust emissions of cars and can have far-reaching impacts on the health and economy of a nation. The need for a more environmental friendly fuel is clear.

www.manaraa.com

1.1.3 Government regulations

Renewable fuels are an alternative to supplement conventional energy supply since individual countries can produce what they need and would not have to depend on unstable regions of the world for supply. Places like the U.S. and Europe recognize this need and have instituted mandates to boost renewable fuel supply. For example, the U.S. government instituted a mandate to boost the use of renewable fuels in 2005: the Renewable Fuel Standard. This standard requires the volume of renewable fuel blended into transportation fuels to be 36 billion gallons by 2022 (EPA 2013).

The high volumes required by mandates, fluctuating rise in crude oil prices, environmental and future supply concerns with petroleum-based fuels, and sustainability are some of the many reasons why additional renewable fuels are needed to supplement the supply of transportation fuels from fossil sources.

1.2 Renewable Energy Alternatives

Renewable energy is derived by utilizing infinite natural resources such as sunlight, tidal, wind and geothermal heat energy. Thus, when compared to non-renewable fossil fuels, the net impacts of renewable fuels introduce less harmful particulates and gases to the environment, and they have the potential to mitigate climate change and environmental pollution (Tan and Lee 2011). Of the total global energy consumption in 2011, renewable fuels comprised only 1.6% - an increase of 18% from 2010 (BP 2012). The growth of renewable fuels worldwide still has a long way to go and has numerous benefits to give such as jobs, economic improvements, cleaner environment, etc.

There are several kinds of renewable energy sources currently being developed including: wind, hydrothermal, solar, and biofuels. Solar, wind and hydrothermal are

www.manaraa.com

stationary sources and not practical for transportation applications that need liquid fuels. Biofuels are most likely to have the biggest impact and can be produced from local feedstocks in many parts of the world.

1.3 Biofuels

Biofuels refer to liquid or gaseous fuels for the transport sector that are predominantly produced from biomass (Demirbas 2007b), e.g. ethanol, hydrogen, biodiesel, methane, etc. Biomass as a feedstock is a renewable resource that could be sustainably developed. It has positive environmental qualities as it causes no net releases of carbon dioxide and has very low sulfur content (Demirbas 2007b). Some potential advantages of biofuels on the environment include: 1) better waste utilization, 2) reduction of local pollution, 3) reduction of net GHG emissions, and 4) more efficient use of landfill sites (Nigam and Singh 2011).

Biofuels can be produced from biomass via thermochemical and biological routes. They are broadly classified as primary and secondary biofuels. Primary biofuels are used in their natural, unprocessed form typically for heating, cooking or for electricity production e.g. wood pellets, fuel wood, crop residues, etc. (Nigam and Singh 2011, Singh et al. 2011). Secondary biofuels are modified primary biofuels that are produced by processing the biomass. They can be solids (e.g. charcoal), liquids (e.g. biodiesel and ethanol), or gases (e.g. biogas and hydrogen) that can be used in vehicles and industrial processes (Nigam and Singh 2011). These secondary liquid biofuels are further classified as first, second and third generation liquid biofuels based on the raw materials and technology used in their production (Singh et al. 2011).

www.manaraa.com

First generation liquid biofuels are generally produced from food and oil crops (e.g. sugars, grains or seeds) as well as animal fats using relatively simple and conventional production technologies (Nigam and Singh 2011, Singh et al. 2011). The most popular first generation liquid biofuel is ethanol, which is typically made by fermenting sugars extracted from corn or other starchy crops. Biodiesel produced from straight vegetable oils of oleaginous plants and bioethanol produced from organic-based matter with high sugar content fermented by enzymes produced by yeast are other examples (Nigam and Singh 2011). The challenge with first generation biofuels is the competition with food, which consequently raises the cost of the edible crops, and thus, the biofuel. Additionally, using edible crops require a lot of arable land, water and fertilizer requirements. High demand and sustainability highlight the need to find non-edible alternatives for producing biofuels (Singh et al. 2011).

Second-generation liquid biofuels are generally produced by biological and thermochemical processing of lignocellulosic biomass, which include non-edible residues of food crops, or non-edible whole plant biomasses, e.g. grasses (Nigam and Singh 2011). Examples are lignocellulosic ethanol and Fischer-Tropsch liquids. The advantage with second-generation biofuels is avoidance of the food vs. fuel issue. However, there is still concern over competing land use since large portions of land are needed for growth of the non-edible biomass.

Third generation liquid biofuels are obtained using microbial-based feedstock. Microbes such as yeast, fungi and algae can be used as a source of feedstock for the production of biofuels since they biosynthesize and store large amounts of fatty acids in their biomass (Nigam and Singh 2011). Third generation biofuels address the drawbacks

www.manaraa.com

of the first- and second- generation fuels by not competing with food, and in some cases, not requiring significant land change and contributing to waste reduction. Key benefits of third generation biofuels are the utilization of CO_2 (e.g. algae) and/or organic waste (e.g., oleaginous microorganisms), which contributes to positive and sustainable environmental impacts.

Some of the more common liquid biofuels include: ethanol and biodiesel. Ethanol has the largest market share of all the renewable fuels and is most commonly produced by fermentation of simple sugars. The heating value of ethanol as a fuel is typically reported as 101, 000 Btu/gal (Hodge 2010), and it can be blended with gasoline in different ratios. Current issues with ethanol include disagreement on its feedstock (corn) competing with food supply and the need for a lot of fresh water. Biodiesel comes behind ethanol and is a direct alternative for petroleum diesel. Biodiesel is discussed in greater detail in the next section.

1.4 Biodiesel

Biodiesel is a renewable fuel that can meet energy demands in conjunction with other fuel sources. It has similar properties to petroleum diesel that allow it to be blended in all ratios, and it can be used in existing infrastructure.

1.4.1 History and Significance

Biodiesel is a form of renewable energy that is mostly produced from oil crops, which absorb carbon from the atmosphere during growth. This carbon will eventually be released to the atmosphere during combustion; therefore, biodiesel is regarded as a carbon neutral source of energy as no additional emission is discharged to the

www.manaraa.com

environment from the carbon cycle (Tan and Lee 2011). It consists mainly of fatty acid alkyl esters typically obtained by the transesterification reaction of triglycerides with alcohols utilizing a catalyst. These triglycerides come from vegetable oils or animal fats. In the US, the main feedstock for biodiesel production is soy bean oil (Schuchardt et al. 1998, Balat 2008).

Vegetable oils had previously been tested as a fuel in engines more than 100 years ago (Demirbaş 2003). They have heat contents about 90% that of diesel fuel but have problems such as high viscosity, nearly 10 times that of diesel fuel (Schwab et al. 1987) and were more expensive than petroleum fuels (Demirbaş 2003). Other problems with using neat vegetable oil as a fuel include: injector coking, ring sticking, more engine deposits, thickening of the engine lubricant, lower volatility and the reactivity of the unsaturated hydrocarbon chains (Demirbaş 2003). There are 5 methods that can be used to address the viscosity problem: 1) dilution, 2) microemulsification, 3) pyrolysis, 4) transesterification (Schwab et al. 1987), and 5) catalytic cracking (Rathore and Madras 2007). Of these alternatives, the transesterification method seems to be the best choice for relatively small scale and distributed applications as the physical and chemical characteristics of the esters formed are very close to diesel fuel (Schuchardt et al. 1998), and the simple process of transesterification serves the purpose of reducing the viscosity of the oil (Demirbaş 2003).

Capacity for biodiesel production has been growing for the last 15 years. The National biodiesel board reports that the U.S. biodiesel industry reached a key milestone of producing more than 1 billion gallons of biodiesel fuel in 2011, shown in Figure 1.4 below.

www.manaraa.com

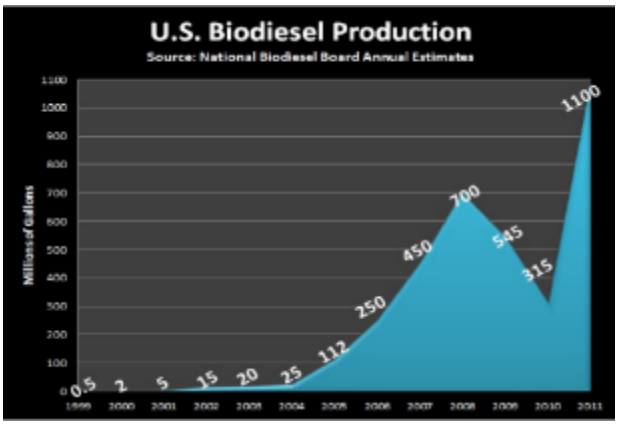

Figure 1.4 Graph of biodiesel production in U.S. from National Biodiesel Board annual estimates

(Board 2013)

The Board found that biodiesel production of 1 billion gallons supports 39,027 jobs around the country and more than $2.1 billion in household income (Board 2013). This growth will need to increase to satisfy the volume requirement of the Renewable Fuel Standard by 2022. In order to increase biodiesel supply, challenges related with feedstock cost and availability, as well as feedstock quality and consistency will need to be overcome.

1.4.2 Advantages

Some of the advantages of biodiesel that encourage its use include the following:

- Properties and Performance as renewable fuel

  Biodiesel has the advantages of biodegradability, great lubricity, and miscibility with petrodiesel (Knothe et al. 2005, Al-Zuhair 2007, Knothe 2008). Other advantages include: a higher flash point and no modification needed in the diesel engine as biodiesel is compatible with existing engine models. It can be

www.manaraa.com

commercially blended with diesel as a transportation fuel (Tan and Lee 2011) or serve as a substitute.

- Environmental Impact and Safety

  Biodiesel has a cleaner impact on the environment due to almost zero sulfur emissions and almost no particulate matter (Marchetti et al. 2007). It has a lower CO_2 footprint, is non-toxic, and causes less exhaust emissions (Demirbaş 2003). Additionally, biodiesel compares better than diesel fuel on environmental impact in terms of its sulfur content, ash point, and biodegradability (Demirbas 2007b).

- Economic and Energy Security

  Biodiesel also has the potential of offering sustainable development since more than 40% of the world's total energy consumption is in liquid form, whereas other sources like solar, hydrothermal and wind are only able to generate thermal energy or electricity (Tan and Lee 2011). In addition, the fact that it is domestically produced reduces dependence on imported petroleum fuels (Demirbaş 2003) and improves energy security.

Notwithstanding these many advantages, biodiesel production still faces some challenges that are discussed in the next section.

1.4.3 Production of Biodiesel

Biodiesel consists mainly of fatty acid alkyl esters (FAAEs) and can be produced by two methods: 1) transesterification of fats and oils, or 2) esterification of fatty acids discussed below:

www.manaraa.com

1.4.3.1 Transesterification

Biodiesel can be obtained from the transesterification reaction of a vegetable oil or animal fat with an alcohol. This reaction, also known as alcoholysis, produces fatty acid alkyl esters (FAAEs), which are the biodiesel product. For the transesterification reaction, two types of alcohols can be used to produce biodiesel: methanol and ethanol. Methanol is the most commonly used alcohol for biodiesel production because it is generally the cheapest alcohol (Schuchardt et al. 1998). Thus, methyl esters are the most common form of biodiesel in the US.

In the transesterification reaction, the oil or fats (consisting mainly of triglycerides) are reacted with an alcohol (usually methanol) in the presence of an acid or base catalyst to generate fatty acid methyl esters (FAMEs) and glycerol as a by-product (Knothe et al. 2005). The reaction consists of a 3-step reversible mechanism (see Chapter 3). The objective of the transesterification reaction is to reduce the viscosity of vegetable oils to a value similar to conventional diesel since neat vegetable oils cannot be used directly in a diesel engine due to its high viscosity and low volatility, both of which could contribute to coking (Tan and Lee 2011). The overall reaction schematic is shown in Figure 1.5.

www.manaraa.com

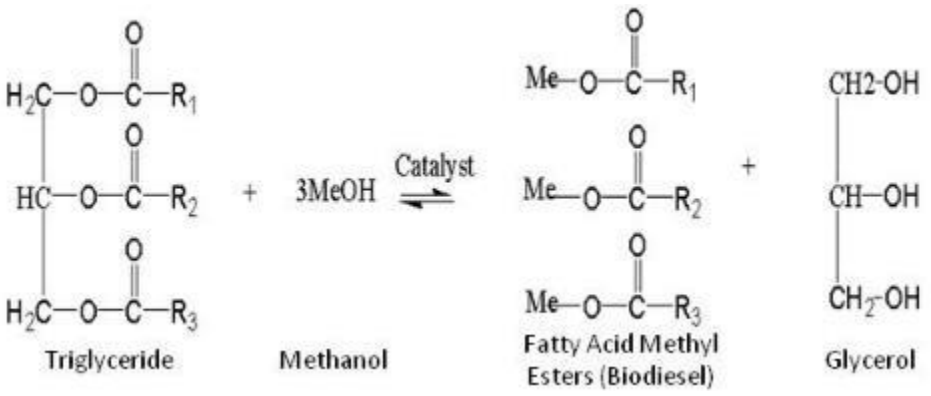

Figure 1.5 The transesterification reaction

* R_1, R_2 and R_3 are alkyl groups representing long fatty acid chains

The most important factors affecting the transesterification reaction are the molar ratio of oil to alcohol, catalyst amount and type, reaction time, reaction temperature, and the content of free fatty acids and water in the oil feedstock (Demirbaş 2003). The optimization of each of these factors is crucial to improving biodiesel yield and making it cost-effective.

1.4.3.2 Esterification

Esterification occurs when fatty acids react with methanol in the presence of a catalyst to form fatty acid methyl esters (FAMEs) and water (Kamarudin et al. 1998). This reaction is shown in Figure 1.6. The main difference between esterification and transesterification lies in the reactants and products: in esterification, fatty acids are used instead of triglycerides and water is produced instead of glycerol.

www.manaraa.com

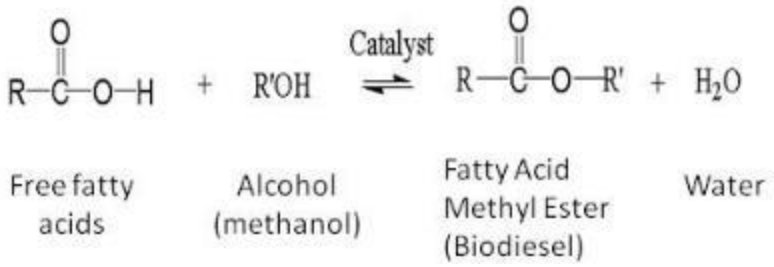

Figure 1.6 The esterification reaction

* R and R' are alkyl groups

Esterification is a one-step reaction; thus, the process requires milder reaction conditions than the transesterification reaction. Similarly, factors affecting the yield also include the molar ratio of fatty acids to alcohol, catalyst type and amount, reaction time, reaction temperature, and the content of water in the feedstock.

The fatty acids used in the esterification may be present in the feedstock supplied e.g. waste frying oils (Chung et al. 2008) or may be produced by hydrolysis of the triglycerides present in an oil/fats feedstock. Hydrolysis is a 3-step reaction where water molecules split a triglyceride molecule to form fatty acids and glycerol as seen in Figure 1.7 below:

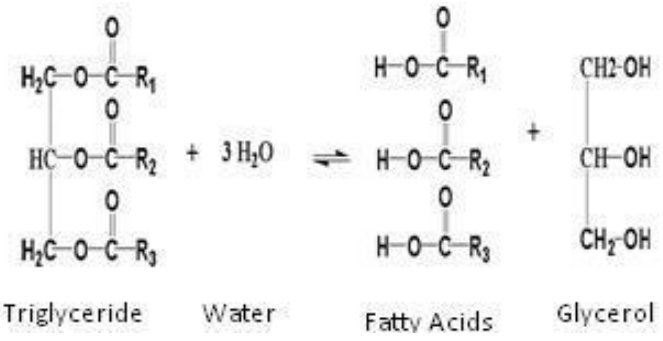

Figure 1.7 The Hydrolysis reaction

www.manaraa.com

1.5 Issues with Feedstock

Unfortunately, while biodiesel is an excellent alternative and supplement to petroleum-based fuels, it has a relatively high production cost predominantly due to the feedstock. It is estimated that, depending on the feedstock, biodiesel costs about one and a half times the cost of petroleum diesel (Zhang et al. 2003b). Zhang et al. state that 70 - 95% of biodiesel production cost is attributed to the feedstock cost (Zhang et al. 2003b).

Feedstock typically used for biodiesel production include vegetable oils such as soybean, rapeseed, coconut, palm, canola, jatropha oils, etc, animal fats such as tallow, and microalgae (Knothe et al. 2005, Chisti 2007). However, use of edible oils such as soybean and canola oils limits how much can be supplied for the biodiesel industry when there is a strong competition on its availability for the food industry. This would inevitably raise the price of food crops, which consequently raises the price of biodiesel. Some feedstock prices are shown in Table 1.1.

Table 1.1 Typical biodiesel feedstock and their prices

Feedstocks	Sep. 2011 Prices ($/lb.)
Soybean oil	0.55
Rapeseed oil	0.59
Coconut Oil	0.59
Oil palm	0.45
Sunflower oil	0.76

Source: (IndexMundi 2011)

Since the fatty acid reactants for the esterification method can also be obtained from the oil by hydrolysis, this high cost affects the esterification process as well. Therefore, there is a need to find relatively inexpensive feedstocks to make biodiesel production more cost effective.

www.manaraa.com

Researchers have investigated the use of different kinds of feedstocks to deal with these challenges. Non-edible feedstocks evaluated include: waste cooking oil (Zhang et al. 2003a), *Jatropha curcas* (Shuit et al. 2010), and microalgae (Chisti 2008). The use of microbial oils is gaining attention. Many researchers are working to develop an economic process to make biodiesel produced from these oils cost-competitive with petroleum diesel (Huang et al. 2010, Levine et al. 2010).

From the literature review, the qualities of a great feedstock for biodiesel production include factors like: 1) non-edible 2) not requiring large portions of land, 3) relatively inexpensive 4) not requiring expensive pre-processing, 5) available year-round and in any region, and 6) integration to waste management.

One alternative, high - potential feedstock is activated sewage sludge obtained from wastewater treatment plants, which is relatively inexpensive, since it is considered a waste, and it is readily available in any region. Some cities in the US have more than one wastewater treatment facility.

1.6 Activated Sewage Sludge as a feedstock

Activated sludge is the solid or semisolid that is produced by the biological treatment of wastewaters. It contains many living microorganisms that use oxygen to feed on wastewater and reduce the organic content (Dufreche et al. 2007). Sludge is a complex heterogeneous mixture of organic and inorganic materials (Fonts et al. 2009) and is the major waste produced in the urban wastewater treatment process (Fonts et al. 2012). The lipids/oily content of the activated sludge (also referred to as sewage sludge) contains significant concentrations of lipids derived from the direct adsorption of lipids into the sludge (Kargbo 2010) that can be used to produce biodiesel.

www.manaraa.com

1.6.1 Benefits to using activated sludge

There are many advantages to using sludge which include the following:

- Valuable inherent properties

  Sludge contains the lipids that are needed for biodiesel production. Dufreche et al. report that it contains approximately 20% ether-soluble fats that can be converted to FAMEs (Dufreche et al. 2007) and Kargbo states that the significant concentration of lipids present in sludge can make biodiesel production from sludge profitable (Kargbo 2010). The wastewater from which it is obtained has properties conducive to microbial growth, and sludge microbes can be enhanced to increase lipid yield by growing under specific conditions (Mondala et al. 2012). In addition, sludge does not compete with food supply or require additional acreage like edible crops. It also has the benefit of current infrastructures already in place for its production and supply.

- Positive environmental impact

  The positive environmental impact of using sludge as biodiesel feedstock includes reduction of the volume of waste sludge that is produced at the municipal wastewater treatment plants (MWWTPs). Sludge is currently an unwanted waste product of the MWWTPs and its disposal poses a high cost for treatment facilities. Dufreche et al. report that activities associated with sludge treatment represent about 30 to 80% of the electrical power consumed at a wastewater treatment facility (Dufreche et al. 2007). Furthermore, the U.S. EPA states that 3-4% of the national electricity consumption (about $4 billion) is used in providing drinking water and wastewater services each year. With water and wastewater

www.manaraa.com

utilities typically being the largest consumers of energy in municipalities, that represents about 30-40% of the total energy consumed (EPA 2012). Thus, using the waste to produce a renewable fuel instead of paying additional expenses to dispose of it would be more cost efficient.

- Ease of availability to potential biodiesel producers

  Sludge is plentiful and is available in municipal wastewater treatment plants across the world, which makes it a potentially valuable feedstock that can be harnessed in many regions of the world to produce fuels locally for economic development. In the USA, wastewater facilities generate approximately 6.2×10^6 t (dry basis) of sludge annually (Dufreche et al. 2007), and this will continue to increase as global population also increases. There are more than 16,000 sewage treatment plants in the U.S. that treat more than 32 billion gallons per day of wastewater (United States Environmental Protection Agency: Office of Wastewater Management June 2011). Most of these treatment plants use the activated sludge process, which reduces sludge treatment time (Spellman 2009, Michael et al. 2013). Since activated sludge is a waste product from wastewater treatment operations, processes developed to extract the oil could start with a positive income stream due to tipping fees.

- Economic development

  Kargbo reports that studies have shown that integrating lipid extraction in 50% of all existing U.S. municipal wastewater treatment plants and transesterification of those extracted lipids could produce 1.8 billion gallons of biodiesel, which is approximately twice the total biodiesel produced in the US in 2011 (Kargbo

www.manaraa.com

2010). This not only increases biodiesel supply but provides jobs and allows economic development for municipalities.

For these many reasons, identifying an alternative method to turn this waste into a valuable product rather than disposing of it is very important. Currently, the commonly used sludge disposal methods are landfills, land application in farms, or incineration. These existing disposal methods are not beneficial to the environment. For example, landfills are not environmentally friendly and cause accumulation of more waste into valuable land. Incineration has the benefit of reducing waste volume by 70% while destroying pathogens and toxic organic compounds, but is a high cost alternative (Fonts et al. 2012). The land application on farms method is feasible since sludge contains organic matter, nitrogen and phosphorus, making it suitable as fertilizer. However, sludge also concentrates heavy metals, pathogens, and some organic compounds, which could negatively affect the environment (Fonts et al. 2012). Fonts et al. state that even use as fertilizers cannot be done all year round because fertilizers are only applied once or twice a year, while sludge is generated year round; therefore, the sludge would need to be stored for long periods (Fonts et al. 2012).

With the decreasing availability and increasing price of land for landfilling, thermal utilization of sewage sludge is growing as a means of managing sewage sludge, especially since the heating value of dried sludge is similar to that of coal (Tian et al. 2002). There are several processes proposed for the thermal utilization of sewage sludge which include co-briquetting with coal, co-combustion with coal, using sewage sludge pyrolysis volatiles as a reburn fuel, and in the air-staged combustion of coal as well as incineration/combustion of sewage sludge alone (Tian et al. 2002). However, one

www.manaraa.com

challenge with these thermal utilization processes is that the NO_x emissions must meet the increasingly stringent environmental standards, which is difficult especially since sewage sludge has a nitrogen content of 9 wt % which is 6.5 wt % higher than that of coal (Tian et al. 2002).

The high output of sewage sludge that is constantly increasing over the years as well as the high cost and limitations of sludge disposal points to the need to find an alternative method of utilizing this waste and adding value to it. This study investigates a path to potentially recovering some of the energy and the capital that goes into sludge treatment and disposal by converting inexpensive raw materials/waste to environment-friendly fuels, thus solving two problems – waste disposal and low renewable fuel supply.

The origin of activated sludge from wastewater treatment plants is described in the following sections.

1.6.2 Wastewater Treatment

Municipal wastewater treatment plants are facilities that treat both domestic and industrial wastewater with the objective of producing a cleaner, environmentally safe liquid stream and solids that are suitable for disposal or re-use. Domestic inputs into wastewater are constituted mainly of detergents, kitchen wastewater and fecal organic matter, while industrial inputs consist of a wide range of wastes from petroleum to food-processing by-products and depend on the economic activity of the wastewater catchment area (Jardé et al. 2005). Most conventional wastewater treatment plants generally have a preliminary, primary, secondary, and sometimes a tertiary stage that have different

www.manaraa.com

biological and physicochemical processes at each stage (Spellman 2009, Michael et al. 2013). A schematic of a typical MWWTP is shown in Figure 1.8 increase font of labels:

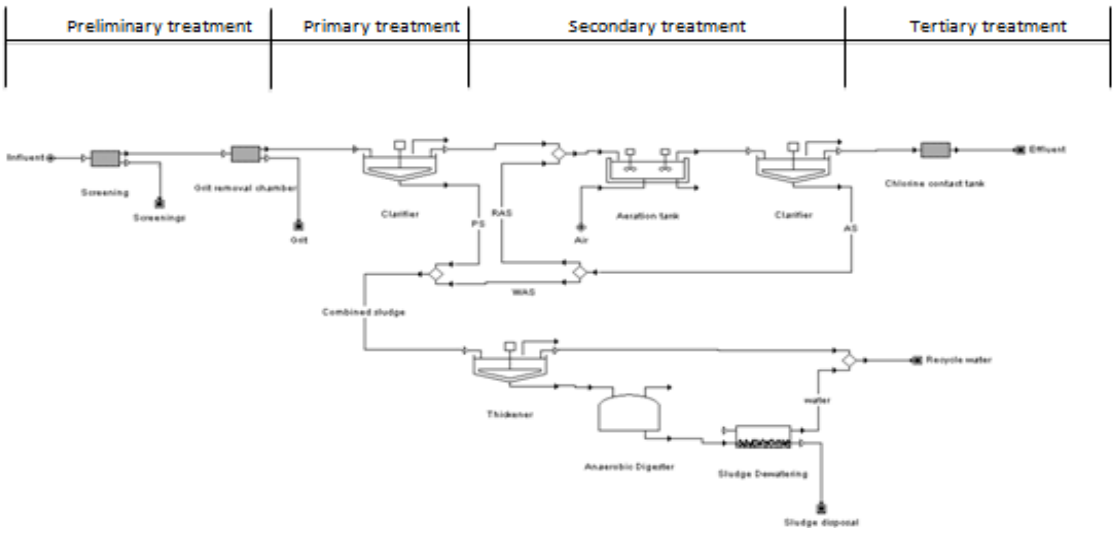

Figure 1.8 Schematic of MWWTP with activated sludge system

(Redrawn and modified from (Spellman 2009)) *
*PS – Primary sludge; AS – Activated sludge; RAS – Return activated sludge; WAS – Waste activated sludge

In most MWWTPs, the collected wastewater goes into a preliminary treatment stage where large solid particles are removed by shredding, screening and grit removal before proceeding to the primary treatment stage where settleable organics and floatable solids are removed by sedimentation in a clarifier. The primary treatment can remove as much as 90 - 95% settleable solids and 40 – 60% total suspended solids (Spellman 2009). The effluent from primary treatment then proceeds to the secondary treatment stage where biological processes are used to remove organic matter with aerobic or anaerobic systems (Michael et al. 2013). The aim of the secondary treatment is to convert the dissolved and suspended organic wastes to more stable solids that can be removed by

www.manaraa.com

settling or that can be discharged safely to the environment (Spellman 2009). There are multiple types of biological treatments used in MWWTPs which include trickling filters, rotating biological contactors (Spellman 2009), fixed bed bioreactors, membrane bioreactors, and moving bed biofilm reactors, but the most widely used technology is the conventional activated sludge system (Michael et al. 2013).

Activated sludge processes use dissolved oxygen to foster the growth of a biological floc, which extensively removes the organic material and nitrogen at given conditions (Michael et al. 2013). Both primary and secondary treatment processes generate waste solids, known as sewage sludge or biosolids. For the final stage, tertiary wastewater treatment processes could be applied to remove phosphorus by precipitation and in some cases, the effluent is disinfected before being released into the environment (Michael et al. 2013).

1.6.3 How Activated Sludge works

The activated sludge process was discovered in 1914 by Arden and Lockett in England when they recognized that the aeration of sewage formed flocculent suspended particles. This was important because the flocculent form could reduce the treatment time to remove organic contaminants from days to hours (Rittmann and McCarty 2001). A schematic is shown in Figure 1.9 below.

www.manaraa.com

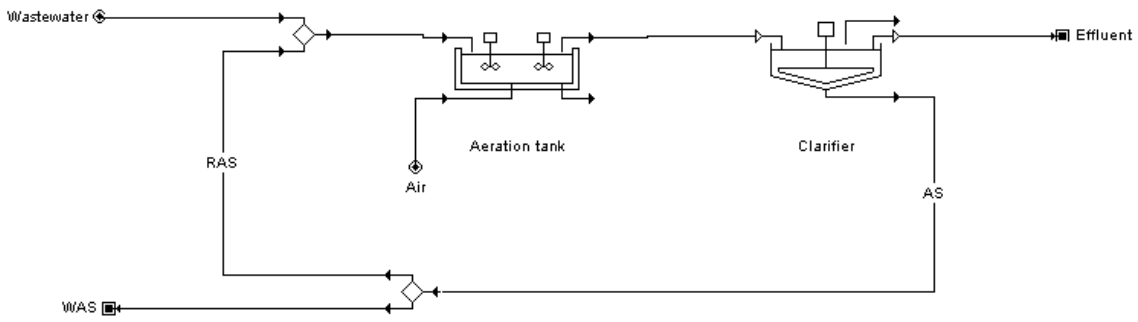

Figure 1.9 Schematic of the activated sludge system

*PS – Primary sludge; AS – Activated sludge; RAS – Return activated sludge; WAS – Waste activated sludge)

The main components of the activated sludge process are: the aeration tank, a settling tank/clarifier, a solids recycle from the settling tank to the aeration tank, and a sludge wasting line. The aeration tank serves as a suspended-growth reactor where the microorganisms metabolize and biologically flocculate the organic wastes (Spellman 2009). The microbial aggregates (flocs) of microorganisms is the activated sludge (Rittmann and McCarty 2001). This activated sludge is maintained in the reactor via aerated mixing until it flows to the settling tank/clarifier where the flocs are removed by settling. The treated wastewater is removed as an effluent, and the settled flocs are recycled to the aeration tank or wasted to control the solids retention time. The recycling of the collected flocs (RAS) to the aeration tank is crucial to the activated sludge process because that leads to a much higher concentration of microorganisms in the reactor than could have been achieved without the settler and recycle, hence called “activated”. This high biomass concentration is what allows the liquid detention time to be shorter, making the process more cost effective (Rittmann and McCarty 2001). The sludge-wasting line (WAS) helps control the solid retention time of the solids.

www.manaraa.com

1.6.4 Microbial community and lipids in activated sludge

Activated sludge contains a wide variety of microorganisms that include prokaryotes (bacteria), eukaryotes (protozoa, nematodes and rotifers), bacteriophage (bacterial viruses), and fungi. The dominant members of this community (by mass) are the heterotrophic bacteria, and they are the primary consumers of organic wastes (Rittmann and McCarty 2001).

For producing biodiesel via transesterification, lipidic compounds are needed. Kargbo states that the cell membranes of the activated sludge microorganisms are a major component of the sewage sludge and are composed mainly of phospholipids, which are approximately 25% of the dry mass of the cell (Kargbo 2010). He reports that other energy-containing lipids present in sewage sludge consist of lipids like triglycerides, diglycerides, monoglycerides, phospholipids and free fatty acids contained in the oils and fats (Kargbo 2010). These lipids also characterized as oils, greases and fats are approximately 30 – 40% of the total chemical oxygen demand in municipal wastewater (Chipasa and Mędrzycka 2006). Since treatments in wastewater treatment plants are not consistent, the composition and characteristics of sewage sludge will vary depending on factors like wastewater origin, wastewater treatment, stabilization treatment of the sludge, time and storage conditions of the sewage sludge, and coagulants used (Fonts et al. 2009).

Jarde et al. report that the lipidic fraction of sewage sludge is a composite organic fraction including natural hydrocarbons, surfactants, fatty acids, sterols and micropollutants (Jardé et al. 2005). They state that fatty acids are the predominant family of compounds in the polar fraction of all sludges regardless of origin, usually in the range

www.manaraa.com

of C10-C18. This can be expected because kitchen wastes produced from vegetable oils and animal fats show distributions of fatty acids dominated by C16:0 (palmitic acid), C18:0 (stearic acid), C18:1 ω 9 (oleic acid) and C18:2 ω 6 (linoleic acid) (Jardé et al. 2005). This composition is also beneficial because fatty acids in that range form good quality biodiesel.

1.6.5 Issues with activated sludge

The use of activated sludge as a feedstock still has some challenges to be overcome for biodiesel production to be cost effective. Some of these challenges include: 1) identifying how to collect the sludge fractions and treat them for maximum lipid extraction, 2) production challenges with efficient optimal reaction conditions and selecting a suitable catalyst, 3) bioreactor design to select and increase growth of microorganisms that have oil-producing capabilities, 4) bringing down production costs when processing costs are two-thirds of the biodiesel price (Kargbo 2010).

1.6.5.1 Current Status of Lipids/Biodiesel from Sewage Sludge/Work done on Activated sludge

Dufreche et al. (2007) used 3 solvent extraction methods (organic solvent mix, supercritical CO_2 and in situ transesterification) and extracted as high as 20% lipids (Dufreche et al. 2007). Mondala et al. (2009) conducted in situ transesterification of primary and secondary sludge and obtained maximum FAME yields of 14.5% and 2.5% respectively at 75 °C, 5% (v/v) H_2SO_4 and 12:1 methanol:solid mass ratio (Mondala et al. 2009). Revellame et al. (2010) optimized in situ transesterification of dry activated sludge and got an optimum biodiesel yield of 4.9% at 55 °C, 25ml/g MeOH:solid ratio and 4%

www.manaraa.com

sulfuric acid (Revellame et al. 2010). To investigate FAME yields in the presence of moisture, Revellame et al. (2011) also conducted an optimization study for the in situ transesterification of wet activated sludge and got a yield of 3.78% at 75 °C, 30ml/g methanol:solid ratio, and 10% vol sulfuric acid concentration (Revellame et al. 2011). In addition, Mondala et al. (2011) demonstrated that lipid content of sludge can be enhanced for biodiesel production by cultivating at high C:N ratios, producing lipid yield of ~ 18% and FAME yield of ~10% instead of 11 % lipid yield and 3 % FAME yield on raw activated sludge (Mondala et al. 2012).

A limiting factor with sludge use, however, is the high cost of dewatering which consists of methods like filtration, centrifugation, and freeze-drying (Hellstrom and Kvarnstrom 1997). An earlier cost analysis conducted by Dufreche et al. (2007) shows that the highest cost in the production estimate for sludge biodiesel is the drying operation and maintenance cost, which accounts for approximately 41% of the total cost (Figure 1.10).

	Cost per gallon ($)
Centrifuge O&M	0.43
Drying O&M	1.29
Extraction O&M	0.34
Biodiesel processing O&M	0.60
Labor	0.10
Insurance	0.03
Tax	0.02
Depreciation	0.12
Capital P&I service	0.18
Total cost	3.11

Assuming 7.0% overall transesterification yield
O&M operation and maintenance, *P&I* protection and indemnity

Figure 1.10 Production Cost Estimate for Sludge Biodiesel (Dufreche et al. 2007)

www.manaraa.com

Mondala et al. also performed a cost analysis on the production of biodiesel from sludge and found that more than 50% of the production cost accounts for drying the sludge using these de-watering methods. The drying cost to obtain $3.23 break-even biodiesel price was 53% of the total production cost (Mondala et al. 2009). Since drying is so expensive, an option of proceeding with wet transesterification reaction could make sludge biodiesel more cost effective and competitive with petroleum diesel.

1.7 Extractions of lipids

There are two main alternatives to extracting lipids from cells for biodiesel production: 1) extraction of the lipids prior to reaction, and 2) combined extraction and reaction of the lipids. These alternatives can be pursued using the following methods to extract lipids from sludge; solvent extraction and reactive extraction.

Solvent extraction can include the use of single solvents like *n*-hexane, methanol, acetone, supercritical CO_2 (Dufreche et al. 2007), toluene and chloroform (Boocock et al. 1992) to extract the lipids from the microbial mixture. Solvent extraction could also include methods like the Folch and Bligh & Dyer extraction methods (Ramalhosa et al. 2012). The Folch extraction method involves homogenizing the lipid-bearing cells with a 2:1 chloroform-methanol mixture and washing the extract with an additional 0.2 of its volume in water to form a biphasic system. The upper phase contains non-lipidic substances and negligible amounts of the lipid, while the lower phase contains the lipids (Folch et al. 1957). The Bligh and Dyer method uses a mixture of chloroform, methanol and water to extract the lipids into a single-phase system initially. This is followed by addition of more solvents to separate the system into two phases with the aqueous phase in the top layer and the lipids in the bottom, chloroform layer (Bligh and Dyer 1959). The

www.manaraa.com

bottom phase of both methods can then be evaporated to obtain the dry lipid yield. Some concerns with solvent extraction methods are that: 1) lipids might still have some water concentration, 2) the extraction method could be costly to use at large scale, depending on the volumes used, 3) re-extraction steps to ensure complete lipid isolation are still required and have long preparation times (Ramalhosa et al. 2012), and 4) depending on which solvent is used, solvents may be selective to certain lipids.

In the case where these extractions are costly or take too long, researchers have also evaluated the use of supercritical fluids for reaction and extraction due to the low viscosities and high diffusivities (Patil et al. 2011). The combined extraction and reaction method, also known as reactive extraction, involves the reaction with alcohol to produce biodiesel from the cells directly without separating the lipids from the cells prior to reaction as in the case of in situ transesterification reactions at sub-critical and supercritical methanol reaction conditions (Mondala et al. 2009, Levine et al. 2010, Revellame et al. 2010).

1.8 Catalytic and non-catalytic processes

The biodiesel production reactions, both transesterification and esterification, at sub-critical conditions are very slow without the addition of a catalyst and would not be economical without using a catalyst to increase the yields and speed up the reaction time. For example, Diasakou et al. reported that without a catalyst, methyl esterification of soybean oil required 10 hours to obtain 85% yield at a relatively high temperature of 235°C (Diasakou et al. 1998) while Di Serio et al. show that with a heterogeneous catalyst such as magnesium oxide, transesterification of soybean oil can achieve FAME

www.manaraa.com

yield of 90% in 1 hour of reaction time at 180 °C (Di Serio et al. 2007). This shows the need for a catalyst if aiming for an efficient process.

1.8.1 Catalyst selection for biodiesel production

Some important considerations to make when selecting a catalyst are to consider: activity and selectivity, stability, heterogeneous nature and cost (Lee and Saka 2010). The purity of the feedstock also plays an important role. The presence of free fatty acids and water in the feedstock causes soap formation, consumes the catalyst and reduces catalyst effectiveness, all negative effects that lead to low conversion (Demirbas 2007a). Even refined oils and fats contain some amounts of water and free fatty acids and either need to be pretreated or used with a tolerant catalyst.

Some catalysis issues include leaching, which is the loss of active compounds in the catalyst to the reaction media. Leaching is known to be accelerated in metal oxide catalysts, such as ZnO and CaO, when there are free fatty acids or water present (Lee and Saka 2010). Leaching is affected by the active compound type, the porous support, and the polarity of the reaction media (Lee and Saka 2010). Another catalyst issue is one where organic deposits foul the pores of the catalyst, thus deactivating the catalyst. In a study of transesterification of palm kernel oil using CaO-ZnO catalyst, the deactivation was caused by more than 12 wt % of organic deposits on the catalyst (Ngamcharussrivichai et al. 2008); this is another factor to consider during catalytic reactions.

www.manaraa.com

1.8.2 Homogeneous versus Heterogeneous biodiesel catalysts

Homogeneous catalysts are advantageous because they form a uniform mixture with the reactant, eliminating mass transfer limitations, and affording high reaction rates (Lestari et al. 2009). However, the homogeneous (liquid catalyst in liquid reactants) system used has disadvantages that include difficulty in products separation, impossibility of catalyst recovery from reactant-product mix, limitation in establishing a continuous process, and reactor corrosion from dissolved acid/base species. Also, the biggest problem with using homogeneous catalysts like sodium hydroxide (NaOH) is soap formation which adds complexity to product separation. This occurs when water reacts with esters formed to produce carboxylic acids, which rapidly react with alkaline metals to form soaps such as $RCOO^{-}Na^{+}$ (Lee et al. 2009, Zabeti et al. 2009). This study will be using heterogeneous catalysts (solid catalyst in liquid reactants) for the proposed project since they address many of the drawbacks of a homogeneous system, and the reactions being studied have high water content. The most common problem of the heterogeneously catalyzed processes is its slow reaction rate compared to the homogeneous process. This can be compensated for by increasing reaction temperature (100 – 250 °C), catalyst amount (3- 10 wt %), and methanol/oil molar ratio (10:1 – 25:1) (Lee et al. 2009).

1.8.3 Acidic versus Basic catalysts

The most commonly used alkali catalysts are sodium hydroxide, sodium methoxide and potassium hydroxide. Sulfuric acid, hydrochloric acid and sulfonic acid are usually used as acid catalysts (Demirbas 2007b). Although acid-catalyzed transesterification promotes high FAME yields, it suffers from a slow reaction rate: 1 –

www.manaraa.com

45 hours, compared with base-catalyzed transesterification: 1- 8 hours (Demirbas 2007b). Thus, the acid-catalyzed reaction needs relatively higher temperatures and catalyst loadings to complete conversion (Lee et al. 2009).

Another disadvantage of acid-catalyzed transesterification is the sensitivity of the reaction to water content in the system due to a competitive parallel reaction occurring that converts a carbocation intermediate in the reaction mechanism to carboxylic acids instead of FAMEs (Schuchardt et al. 1998, Lee et al. 2009). Schuchardt et al. reported that this suppressed the biodiesel yield; therefore, acid-catalyzed transesterification should only be conducted in the absence of water (Schuchardt et al. 1998).

1.8.4 Issues with current catalysts/processes

There are two main issues that limit the use of heterogeneous catalysts in biodiesel production processes, especially with wet feedstock: catalyst cost and its response to the presence of impurities like water in the feedstock.

1.8.4.1 Cost

Some catalysts may be suitable for transesterification reactions, producing high yields, but the catalyst may so expensive that the production of biodiesel on a large scale is not feasible or may not be readily available on a large scale e.g. Amberlyst BD20 catalyst (Park et al. 2010b).

1.8.4.2 Effect of Water

Park et al. conducted a study on the effects of water on the esterification of free fatty acids (FFA) using heterogeneous acid catalysts: Amberlyst 15 and Amberlyst BD20. They illustrated that Amberlyst 15 demonstrated good efficiency on oils with a low FFA

www.manaraa.com

content of 2.5 wt% but was hindered by water. The Amberlyst BD20 catalyst showed significant catalytic activity for high FFA oils, higher tolerance for water, and its activity did not decrease with re-use. The difference was explained by showing that the presence of pores on the Amberlyst 15 catalyst allowed water to adsorb on the inner surface of the catalyst which prevented oil with a hydrophobic property from being converted. Amberlyst BD20, which had no pores, maintained its activity despite the presence of water. While the Amberlyst BD20 catalyst is very attractive, it is an expensive catalyst and is not readily available (Park et al. 2010b). Other studies conducted on the effects of water include work done by Liu et al. (2006) which studies the effect of water on sulfuric acid-catalyzed esterification. In this homogeneous reaction, they reported that there is a decrease in initial reaction kinetics as water concentration increases and indicated that catalysis is impaired as esterification proceeds (Liu et al. 2006b). This work gives an initial hypothesis on how water could affect the reactions in the proposed project.

Based on current literature, this study identified three reaction processes that look promising for these reactions in the presence of water: transesterification with porous metal oxides (PMOs), esterification with zeolites for and a noncatalytic process with supercritical methanol.

1.8.5 Basic – Porous Metal Oxides (PMOs)

PMOs are hydrotalcite-based catalysts with basicities and surface areas that can be tuned by modifying the hydrotalcite chemical composition and preparation procedures (Lee et al. 2009). A hydrotalcite is a layered Mg^{2+}/Al^{3+} double hydroxide of the formula, $[Mg_6Al_2(OH)_{16}CO_3]\bullet 4H_2O$ (Antunes et al. 2008, Lee et al. 2009). Its structure comprises brucite-like layers where the substitution of Al^{3+} for Mg^{2+} cations generates an excess of

www.manaraa.com

positive charges that are compensated for by the carbonate anions located with water molecules in the interlayer space (Kustrowski et al. 2004, Antunes et al. 2008). The Mg/Al ratio can range from 2 to 4, with 3 being the best in terms of basic activity as noted by other researchers (Di Cosimo et al. 1998, Lee et al. 2009). Substituted hydrotalcite-like materials are formed by substituting a certain molar percentage of the Mg^{2+} ions with a divalent ion such as copper, and/or substituting a molar percentage of the Al^{3+} ions by a trivalent ion such as iron or gallium. The substituted hydrotalcites that are used in this work have the formula:

$$[(Me_z^{2+}Mg_{1-x})_{1-x}\ Al_x(OH)_2](CO_3)_{x/2}\bullet nH_2O \qquad (1.1)$$

where Me^{2+} = Cu, z = 0.1- 0.2; x = 0.25 and

$$[Mg_{1-x}(Me_y^{3+}Al_{1-y})_x(OH)_2](CO_3)_{x/2}\bullet nH_2O \qquad (1.2)$$

where Me^{3+} = Ga, Fe or La, y = 0.05 – 0.2; x = 0.25.

PMOs are formed when hydrotalcites are calcined to release CO_2 and water. These catalysts are known to have large surface areas, which is advantageous because it allows more exposure of the active sites to the reactants. Macala et al. show that the Brunauer-Emmett-Teller (BET) surface areas for uncalcined Fe-10 and unsubstitued hydrotalcites are 68.6 m^2/g and 87.1 m^2/g respectively (Macala et al. 2008). For calcined species (PMOs), they report that unsubstituted hydrotalcite, Fe-10, and Fe-20 PMOs have BET surface areas of 111.8 m^2/g, 123.6 m^2/g, and 161.1 m^2/g respectively when calcined at 460 °C. They are reported to be tunable and tolerant of water (Di Serio et al. 2007), hence the investigation.

www.manaraa.com

1.8.6 Acidic - Zeolites

Zeolites are microporous crystalline solids with well-defined structures usually containing silicon, aluminum, and oxygen in their framework (Chung et al. 2008). A common characteristic used to distinguish zeolites is their silica-to-alumina (SiO_2:Al_2O_3) ratio, which determines the acidity (number of total acid sites) and hydrophobicity of the catalyst. The acidity decreases with decreasing Al content, so a catalyst with larger silica: alumina ratio has lower acidity (Chung et al. 2008, Shirazi et al. 2008). The hydrophobicity increases with increasing silica-to-alumina ratio (Navalon et al. 2009). These catalysts also offer tenability in determining if a particular zeolite with a specific silica-to-alumina is more tolerant to water during the biodiesel reaction.

1.8.7 Non-catalytic alternative - Supercritical Methanol

A supercritical fluid is a fluid existing at conditions above its critical temperature and pressure and having the viscosity of a gas and density of a liquid. Under these conditions, the supercritical fluid has outstanding transport properties coupled with highly tunable solvent properties (de Boer and Bahri 2011).

Supercritical methanol addresses several of the limitations occurring with conventional heterogeneous catalytic processes. These limitations include complicated separation and purification of biodiesel, long reaction times, sensitivity to high water and fatty acid content, and exorbitant cost of catalysts which make some of those processes uneconomical (Tan and Lee 2011). All these limitations point to the use of catalysts in the transesterification reaction. Hence in recent years, many more researchers have worked on developing technologies using supercritical fluids that can overcome limitations of heterogeneous catalysis.

www.manaraa.com

For example, unlike conventional transesterification processes that need pretreatment, supercritical methanol allows the use of the original feedstock instead of extracted and purified oil as the source of triglycerides for transesterification. Additional fatty acids present in the feedstock will undergo esterification simultaneously with the transesterification reaction, and water present typically has minimal effect on the conversion (Kusdiana and Saka 2004a). Also, water present in the feedstock can cause hydrolysis of the triglycerides to fatty acids which are simultaneously converted to esters through the faster esterification reaction. Thus, the supercritical methanol process can work with any lipid-containing feedstock and allows for cost savings on the solvent extraction process**.** The supercritical conditions allow the usually immiscible nonpolar oil and polar methanol to form a one-phase solution, and hence the supercritical condition increases the reaction rate due to the enhanced contact area between the two reactants. By reducing the multiple process steps to extract oil before producing alkyl esters, the use of additional reagents, solvents and unit operations is reduced, bringing down the cost of the final product. In addition, downstream separation of the products can be relatively easier with the supercritical methanol process.

Challenges with the supercritical methanol process include: energy consumption, cost and safety issues (Tan and Lee 2011). The high temperature and pressures used in the process cause a concern. These intense reaction conditions require high pressure equipment such as reactors, furnaces and pumps that are part of the capital costs in addition to costs of solvent needed to produce biodiesel. However, there is room to counter these costs by the amounts that would be saved by: 1) not using any catalyst, 2)

www.manaraa.com

not having feedstock pretreatment steps that include drying and extraction, 3) no additional post-processing steps for separating catalysts, etc.

1.9 Remarks

It has been demonstrated that activated sludge is a promising feedstock for biodiesel production with the main challenge being reducing or avoiding the cost of dewatering the sludge before conversion to biodiesel. This has been investigated in this study in two ways: 1) by seeking to identify water-tolerant catalysts and the maximum water content the catalyst would tolerate efficiently, and 2) evaluating a process that skips the drying step altogether. To avoid this de-watering cost, the purpose of this project was to examine the feasibility of using sludge with high water content to produce biodiesel commercially by investigating the effects of water on biodiesel yield from the two reaction methods and the catalysts used. The effect of water on transesterification and esterification reactions, the reaction mechanism behind it, and the deactivating effect of water on the catalysts are areas that have been given minimal attention in the literature. It is possible that these reactions will proceed in the presence of high water content; however, the effects of water may be detrimental on the transesterification and esterification reactions. In addition, an understanding of the transesterification and esterification kinetics is required to increase the efficiency of the reaction.

While these catalytic and non-catalytic processes have been used on other feedstock for biodiesel, they have not been used with microbial cells evaluating them at water content as high as 90%. One of the goals of this project is to have a better understanding of reaction mechanisms in these 3 processes with high water content and determine an economically feasible process that can be used for wet sludge as a

www.manaraa.com

feedstock. Since water could have a negative effect on the mechanism, identifying how it works could help improve the reaction process for better yields. This work reports the effect of water on each process and catalyst.

www.manaraa.com

1.10 References

Al-Zuhair, S. (2007). "Production of biodiesel: possibilities and challenges." Biofuels Bioproducts & Biorefining-Biofpr **1**(1): 57-66.

Antunes, W. M., C. D. Veloso and C. A. Henriques (2008). "Transesterification of soybean oil with methanol catalyzed by basic solids." Catalysis Today **133**: 548-554.

Balat, M. (2008). "Biodiesel fuel production from vegetable oils via supercritical ethanol transesterification." Energy Sources, Part A: Recovery, Utilization and Environmental Effects **30**(5): 429-440.

Bligh, E. and W. Dyer (1959). "A Rapid method of total lipid extraction and purificatin " Canadian Journal of Biochemistry and Physiology **37**(8): 911-917.

Board, N. B. (2013). "Production Statistics." Retrieved 01/30/2013, 2013, from http://www.biodiesel.org/production/production-statistics.

Boocock, D. G. B., S. K. Konar, A. Leung and L. D. Ly (1992). "Fuels and chemicals from sewage sludge. 1. The solvent extraction and composition of a lipid from a raw sewage sludge." Fuel **71**(11): 1283-1289.

BP (2012). BP Statistical Review of World Energy June 2012, British Petroleum (BP): 45.

Chipasa, K. B. and K. Mędrzycka (2006). "Behavior of lipids in biological wastewater treatment processes." Journal of Industrial Microbiology and Biotechnology **33**(8): 635-645.

Chisti, Y. (2007). "Biodiesel from microalgae." Biotechnology Advances **25**(3): 294-306.

Chisti, Y. (2008). "Biodiesel from microalgae beats bioethanol." Trends in Biotechnology **26**(3): 126-131.

Chung, K. H., D. R. Chang and B. G. Park (2008). "Removal of free fatty acid in waste frying oil by esterification with methanol on zeolite catalysts." Bioresource Technology **99**(16): 7438-7443.

de Boer, K. and P. A. Bahri (2011). "Supercritical methanol for fatty acid methyl ester production: A review." Biomass and Bioenergy **35**(3): 983-991.

Demirbas, A. (2007a). "Biodiesel from sunflower oil in supercritical methanol with calcium oxide." Energy Conversion and Management **48**(3): 937-941.

Demirbas, A. (2007b). "Recent Developments in Biodiesel Fuels." International Journal of Green Energy 4(1): 15-26.

www.manaraa.com

Demirbaş, A. (2003). "Biodiesel fuels from vegetable oils via catalytic and non-catalytic supercritical alcohol transesterifications and other methods: a survey." Energy Conversion and Management **44**(13): 2093-2109.

Di Cosimo, J., V. K. Diez, M. Xu, E. Iglesia and C. Apesteguia (1998). "Structure and Surface and Catalytic Properties of Mg-Al Basic Oxides." Journal of Catalysis **178**.

Di Serio, M., R. Tesser, L. Pengmei and E. Santacesaria (2007). "Heterogeneous Catalysts for Biodiesel Production." Energy & Fuels **22**(1): 207-217.

Diasakou, M., A. Louloudi and N. Papayannakos (1998). "Kinetics of the non-catalytic transesterification of soybean oil." Fuel **77**(12): 1297-1302.

Dufreche, S., R. Hernandez, T. French, D. Sparks, M. Zappi and E. Alley (2007). "Extraction of lipids from municipal wastewater plant microorganisms for production of biodiesel." Journal of the American Oil Chemists Society **84**(2): 181-187.

EIA, U. S. (2012). Annual Energy Outlook 2012, U.S. Energy Information Administration**:** 239.

EPA, U. S. (2012, 09/14/12). "Water & Energy Efficiency." Retrieved 02/04/13, from http://water.epa.gov/infrastructure/sustain/waterefficiency.cfm.

EPA, U. S. E. P. A. (2013, 01/31/13). "Renewable Fuel Standard (RFS)." Retrieved 02/04/13, 2013, from http://www.epa.gov/otaq/fuels/renewablefuels/index.htm.

Folch, J., M. Lees and G. H. S. Stanley (1957). "A simple method for the isolation and purification of total lipides from animal tissues." Journal of Biological Chemistry 226(1): 497-509.

Fonts, I., M. Azuara, G. Gea and M. B. Murillo (2009). "Study of the pyrolysis liquids obtained from different sewage sludge." Journal of Analytical and Applied Pyrolysis **85**(1–2): 184-191.

Fonts, I., G. Gea, M. Azuara, J. Ábrego and J. Arauzo (2012). "Sewage sludge pyrolysis for liquid production: A review." Renewable and Sustainable Energy Reviews **16**(5): 2781-2805.

Hellstrom, D. and E. Kvarnstrom (1997). "Natural sludge dewatering. I: Combination of freezing, thawing, and drying as dewatering methods." Journal of Cold Regions Engineering **11**(1): 1-14.

Hodge, B. K. (2010). Alternative Energy Sources, John Wiley & Sons, Inc.

Huang, G. H., F. Chen, D. Wei, X. W. Zhang and G. Chen (2010). "Biodiesel production by microalgal biotechnology." Applied Energy **87**(1): 38-46.

www.manaraa.com

IEA (2012). World Energy Outlook 2012 Executive Summary, International Energy Agency**:** 9.

IndexMundi. (2011). "Commodity price indices." Retrieved 10/11/11, from http://www.indexmundi.com/commodities/?commodity=soybean-oil

Jardé, E., L. Mansuy and P. Faure (2005). "Organic markers in the lipidic fraction of sewage sludges." Water Research **39**(7): 1215-1232.

Kamarudin, R., N. Nordin, N. Buang and S. Ahmad (1998). "A Kinetic Study on the Esterification of Palmitic Acid in Methanol." Pertanika Journal of Science & Technology **6**(1): 71-79.

Kargbo, D. M. (2010). "Biodiesel Production from Municipal Sewage Sludges." Energy & Fuels **24**(5): 2791-2794.

Knothe, G. (2008). ""Designer" biodiesel: Optimizing fatty ester (composition to improve fuel properties." Energy & Fuels **22**(2): 1358-1364.

Knothe, G., J. Van Gerpen and J. Krahl (2005). The Biodiesel Handbook, AOCS Press.

Kusdiana, D. and S. Saka (2004a). "Effects of water on biodiesel fuel production by supercritical methanol treatment." Bioresource Technology **91**(3): 289-295.

Kustrowski, P., L. Chmielarz, E. Bozek, M. Sawalha and F. Roessner (2004). "Acidity and basicity of hydrotalcite derived mixed Mg-Al oxides studied by test reaction of MBOH conversion and temperature programmed desorption of NH3 and CO2." Materials Research Bulletin **39**(2): 263-281.

Lee, D. W., Y. M. Park and K. Y. Lee (2009). "Heterogeneous Base Catalysts for Transesterification in Biodiesel Synthesis." Catalysis Surveys from Asia **13**(2): 63-77.

Lee, J.-S. and S. Saka (2010). "Biodiesel production by heterogeneous catalysts and supercritical technologies." Bioresource Technology **101**(19): 7191-7200.

Lestari, S., P. Mäki-Arvela, J. Beltramini, G. M. Lu and D. Y. Murzin (2009). "Transforming triglycerides and fatty acids into biofuels." ChemSusChem **2**(12): 1109-1119.

Levine, R. B., T. Pinnarat and P. E. Savage (2010). "Biodiesel Production from Wet Algal Biomass through in Situ Lipid Hydrolysis and Supercritical Transesterification." Energy & Fuels **24**(9): 5235-5243.

Liu, Y., E. Lotero and J. G. Goodwin (2006b). "Effect of water on sulfuric acid catalyzed esterification." Journal of Molecular Catalysis A: Chemistry **245**(1/2): 9p.

www.manaraa.com

Ma, F. and M. A. Hanna (1999). "Biodiesel production: a review." Bioresource Technology **70**: 1-15.

Macala, G. S., A. W. Robertson, C. L. Johnson, Z. B. Day, R. S. Lewis, M. G. White, A. V. Iretskii and P. C. Ford (2008). "Transesterification Catalysts from Iron Doped Hydrotalcite-like Precursors: Solid Bases for Biodiesel Production." Catalysis Letters **122**(3/4): 5p.

Marchetti, J. M., V. U. Miguel and A. F. Errazu (2007). "Heterogeneous esterification of oil with high amount of free fatty acids." Fuel **86**(5-6): 906-910.

Michael, I., L. Rizzo, C. S. McArdell, C. M. Manaia, C. Merlin, T. Schwartz, C. Dagot and D. Fatta-Kassinos (2013). "Urban wastewater treatment plants as hotspots for the release of antibiotics in the environment: A review." Water Research **47**(3): 957-995.

Mondala, A., K. W. Liang, H. Toghiani, R. Hernandez and T. French (2009). "Biodiesel production by *in situ* transesterification of municipal primary and secondary sludges." Bioresource Technology **100**(3): 1203-1210.

Mondala, A. H., R. Hernandez, T. French, L. McFarland, J. W. Santo Domingo, M. Meckes, H. Ryu and B. Iker (2012). "Enhanced lipid and biodiesel production from glucose-fed activated sludge: Kinetics and microbial community analysis." AIChE Journal **58**(4): 1279-1290.

Navalon, S., M. Alvaro and H. Garcia (2009). "Highly dealuminated Y zeolite as efficient adsorbent for the hydrophobic fraction from wastewater treatment plants effluents." Journal of Hazardous Materials **166**(1): 553-560.

Ngamcharussrivichai, C., P. Totarat and K. Bunyakiat (2008). "Ca and Zn mixed oxide as a heterogeneous base catalyst for transesterification of palm kernel oil." Applied Catalysis A: General **341**(1–2): 77-85.

Nigam, P. S. and A. Singh (2011). "Production of liquid biofuels from renewable resources." Progress in Energy and Combustion Science **37**(1): 52-68.

Oil-Price.net. "Crude Oil and Commodity Prices." Retrieved 02/04/13, from http://www.oil-price.net/.

OPEC (2011). World Oil Outlook 2011, Organization of the Petroleum Exporting Countries (OPEC)**:** 304.

OPEC (2012). World Oil Outlook 2012, Organization of the Petroleum Exporting Countries (OPEC)**:** 284.

Park, J. Y., D. K. Kim and J. S. Lee (2010b). "Esterification of free fatty acids using water-tolerable Amberlyst as a heterogeneous catalyst." Bioresource Technology **101**: S62-S65.

www.manaraa.com

Patil, P. D., V. G. Gude, A. Mannarswamy, S. Deng, P. Cooke, S. Munson-McGee, I. Rhodes, P. Lammers and N. Nirmalakhandan (2011). "Optimization of direct conversion of wet algae to biodiesel under supercritical methanol conditions." Bioresour Technol **102**(1): 118-122.

Ramalhosa, M. J., P. Paíga, S. Morais, M. Rui Alves, C. Delerue-Matos and M. B. P. P. Oliveira (2012). "Lipid content of frozen fish: Comparison of different extraction methods and variability during freezing storage." Food Chemistry **131**(1): 328-336.

Rathore, V. and G. Madras (2007). "Synthesis of biodiesel from edible and non-edible oils in supercritical alcohols and enzymatic synthesis in supercritical carbon dioxide." Fuel **86**(17–18): 2650-2659.

Revellame, E., R. Hernandez, W. French, W. Holmes and E. Alley (2010). "Biodiesel from activated sludge through *in situ* transesterification." Journal of Chemical Technology and Biotechnology **85**(5): 614-620.

Revellame, E., R. Hernandez, W. French, W. Holmes, E. Alley and R. Callahan Ii (2011). "Production of biodiesel from wet activated sludge." Journal of Chemical Technology & Biotechnology **86**(1): 61-68.

Rittmann, B. E. and P. L. McCarty (2001). Environmental Biotechnology: Principles and Applications. New York, NY, McGraw-Hill.

Schuchardt, U., R. Sercheli and R. Vargas (1998). "Transesterification of Vegetable Oils: a Review." Journal of the Brazilian Chemical Society **9**(1): 199-210.

Schwab, A. W., M. O. Bagby and B. Freedman (1987). "Preparation and properties of diesel fuels from vegetable oils." Fuel **66**(10): 1372-1378.

Shirazi, L., E. Jamshidi and M. R. Ghasemi (2008). "The effect of Si/Al ratio of ZSM-5 zeolite on its morphology, acidity and crystal size." Crystal Research and Technology **43**(12): 1300-1306.

Shuit, S. H., K. T. Lee, A. H. Kamaruddin and S. Yusup (2010). "Reactive extraction and in situ esterification of Jatropha curcas L. seeds for the production of biodiesel." Fuel **89**(2): 527-530.

Singh, A., S. I. Olsen and P. S. Nigam (2011). "A viable technology to generate third-generation biofuel." Journal of Chemical Technology & Biotechnology **86**(11): 1349-1353.

Spellman, F. R. (2009). Handbook of water and wastewater treatment plant operations. Boca Raton, Taylor & Francis.

www.manaraa.com

Tan, K. T. and K. T. Lee (2011). "A review on supercritical fluids (SCF) technology in sustainable biodiesel production: Potential and challenges." Renewable and Sustainable Energy Reviews **15**(5): 2452-2456.

Tian, F.-J., B.-Q. Li, Y. Chen and C.-Z. Li (2002). "Formation of NOx precursors during the pyrolysis of coal and biomass. Part V. Pyrolysis of a sewage sludge." Fuel **81**(17): 2203-2208.

United States Environmental Protection Agency: Office of Wastewater Management. (June 2011). "Introduction to the National Pretreatment Program." Retrieved January 31, 2013, from http://www.epa.gov/npdes/pubs/pretreatment_program_intro_2011.pdf.

Zabeti, M., W. M. A. W. Daud and M. K. Aroua (2009). "Activity of solid catalysts for biodiesel production: A review." Fuel Processing Technology **90**(6): 770-777.

Zhang, Y., M. A. Dube, D. D. McLean and M. Kates (2003a). "Biodiesel production from waste cooking oil: 1. Process design and technological assessment." Bioresource Technology **89**(1): 1-16.

Zhang, Y., M. A. Dube, D. D. McLean and M. Kates (2003b). "Biodiesel production from waste cooking oil: 2. Economic assessment and sensitivity analysis." Bioresource Technology **90**(3): 229-240.

www.manaraa.com

CHAPTER II

RESEARCH HYPOTHESIS AND STUDY OBJECTIVES

2.1 Statement of the Problem

Researchers have shown that biodiesel can be obtained from activated sludge. However, due to the high cost of drying - 50% of biodiesel production cost, there is opportunity for the economics of the biodiesel production process to be improved if the drying costs are reduced or removed.

The main motivation for this work was to improve the cost-competitiveness of biodiesel production from activated sludge and to reduce the sludge waste. A chemical approach was taken to solve this problem by selecting the most efficient process after evaluating the use of three different reaction processes and evaluating their biodiesel yields, kinetics, mechanisms and economics.

2.2 Research Hypothesis

The guiding hypothesis for this work was that biodiesel can be produced from wet activated sludge at a relatively high yield and for a competitive price if: 1) a strong, water-tolerant catalyst was used, particularly one with tunable catalytic properties. This assumed that by tuning specific catalytic properties, an optimal catalyst for high water content reactions can be obtained; or 2) a non-catalytic process was used to avoid adding

www.manaraa.com

a catalyst that could be deactivated by the water content. These two approaches could either reduce the cost of drying or remove it altogether if they perform excellently.

However, while the literature shows that it is possible that the transesterification and esterification reactions will proceed with water present in the system initially, it points out that high water content might pose a problem for catalytic reactions by poisoning the acidic/basic sites on the solid catalyst or causing reverse hydrolysis, thus reducing the biodiesel yield.

Therefore, in selecting the best catalyst, the acidity, basicity and hydrophobicity of the catalysts play a significant role in the biodiesel yield obtained from reactions with high water content. If catalysts are used, they need to be highly water-tolerant.

2.3 Goal and Objectives

The overall goal of this work was to develop an economically-efficient biodiesel production process using activated sludge with high water content as a feedstock and to determine the feasibility of building a large-scale biodiesel production plant using the optimal reaction process developed in this study that can produce relatively high biodiesel yields and sell biodiesel at a cost-effective price. This goal has been split into 3 specific objectives:

2.3.1 Primary Objective 1: Evaluation of the effect of water on base-catalyzed transesterification of soybean oil with methanol over porous metal oxides (PMOs)

Chosen for their versatile basicity tuning properties as well as indication of their water tolerance in the literature, these catalysts show promise for use with wet activated

www.manaraa.com

sludge. This study evaluates if tuning these basic catalysts could make the catalyst more tolerant of high water content.

The study evaluates: 1) the effects of varying water content on transesterification of soybean oil (surrogate of triglycerides in sludge oil/fats) using PMOs, searching for an optimum water concentration that promotes the highest yield of biodiesel in the reaction; and 2) kinetic experiments on the transesterification reaction with and without water to determine reaction parameters and understand the effect of water on the reactions and catalysts for potential full-scale reactor design.

2.3.2 Primary Objective 2: Evaluation of the effect of water on the esterification of palmitic acid with methanol using acidic zeolite catalysts

Chosen for their versatile acidity and hydrophobicity properties, these catalysts also show promise for use with wet activated sludge. Tuning the silica:alumina ratios of the acidic catalysts (zeolites) might identify a catalyst that is reasonably tolerant of high water content due to an optimal combination of hydrophobicity and acidity. Palmitic acid was chosen as a surrogate of the fatty acids as it is one of the predominant lipids extracted from sludge.

This study evaluates: 1) the effects of varying initial water content on esterification of palmitic acid to identify an optimum water concentration that promotes the highest yield of biodiesel; and 2) kinetic experiments on the esterification reaction to determine reaction parameters and propose a mechanism to understand the effect of water on the reactions and zeolites for potential full-scale reactor design.

www.manaraa.com

2.3.3 Primary Objective 3: Evaluation of the feasibility of using a non-catalytic process (supercritical methanol) for biodiesel production from wet microorganisms and activated sludge

Using supercritical methanol to serve as both a reactant and catalyst would accelerate the reaction and could allow the sludge drying step to be skipped, thus saving money by: no catalyst use, no drying and no pretreatment step to remove water and/or fatty acids as in conventional methods.

A model oleaginous (oil-retaining) microorganism, *Rhodotorula glutinis*, was used for most of the reaction condition optimization studies to reduce the variations between sludge batches. This study evaluates: 1) the optimum reaction conditions for this non-catalytic process, 2) the effect of water on FAME yields, 3) kinetic experiments on the reactions with and without water to determine rate constants and rate expressions, and 4) an economic analysis to determine if biodiesel production from sludge with high water content is cost-effective.

This work is important because little work has been conducted on biodiesel production from sludge with high water content in the literature. Researchers who have conducted transesterification research work with sludge have typically dried or concentrated the sludge first before reaction. This research shows water tolerance of the catalysts at various compositions and generates various kinetic data on each process.

The identification of a process and catalyst to produce biodiesel with high water tolerance will be of intellectual interest to the academic, governmental and industrial communities. Knowledge of the reaction mechanisms proposed, the optimum reaction conditions, and the deactivating effects of water on the catalyst can be used in the design of efficient large-scale reactors which can optimize conversion of sludge oil to biodiesel.

www.manaraa.com

This research could enable commercial production of biodiesel at a relatively low cost from a readily available, non-food feedstock and also presents a means of utilizing wastewater and increasing global supply of fuels.

www.manaraa.com

CHAPTER III

EFFECT OF WATER ON BASE-CATALYZED TRANSESTERIFICATION OF SOYBEAN OIL WITH METHANOL OVER PROMOTED HYDROTALCITE-DERIVED CATALYSTS

3.1 Introduction

One of the most widely used methods of biodiesel production is the transesterification reaction of oil and alcohol. Although very common, it faces some challenges that have limited its ability to be cost-competitive with petroleum diesel. The main issue, as discussed in Chapter 1, is the feedstock cost. Researchers in the literature have addressed this problem by evaluating the use of various feedstock that are inexpensive and do not compete with food, such as waste oils and microalgae. In particular, a number of researchers have shown the potential of activated sewage sludge as a relatively less expensive and readily available feedstock (Dufreche et al. 2007, Mondala et al. 2009, Kargbo 2010) .

Activated sludge, as described in Section 1.6 of Chapter 1, is the solid or semisolid that is produced by the biological treatment of wastewaters containing many living microorganisms that use oxygen to feed on wastewater and reduce the organic content (Dufreche et al. 2007). It can also be a high-potential feedstock for the transesterification reaction since sewage sludge contains significant concentrations of

www.manaraa.com

lipids derived from the direct adsorption of lipids into the sludge (Kargbo 2010) that can be used to produce biodiesel.

The limiting factor with sludge use however is the high cost of dewatering to separate the sludge fats/oil. This high cost can be reduced by drying sludge partially and identifying a water-tolerant catalyst that can produce high FAME yields in the transesterification reactions with sludge lipids of high moisture content. Since it is likely that the catalyst will be affected by the presence of water, the aim of this study was to determine the extent of water tolerance. Different water compositions were studied to simulate the drying extent and the maximum tolerable level of water content for the catalyst.

3.1.1 Transesterification reaction

The transesterification reaction is a catalyzed chemical reaction that uses alcohols (e.g. methanol) to convert triacylglycerols (triglycerides) to fatty acid alkyl esters (e.g. fatty acid methyl esters or FAMEs) and a glycerol by-product. Triacylglyerols or triglycerides, the main component of vegetable oil, are made up of 3 long chain fatty acids connected to a glycerol backbone. The reaction is shown below in Figure 3.1.

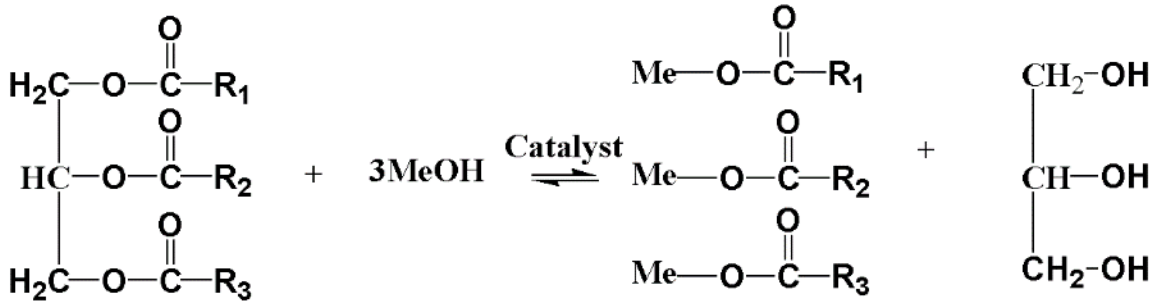

Figure 3.1 Transesterification reaction using methanol

www.manaraa.com

When the triglycerides react with the alcohol, the fatty acid chains are released from the glycerol skeleton to form the fatty acid methyl esters and glycerol as a by-product (Zhang et al. 2003a). This takes place in a 3-step reversible reaction (Figure 3.2) that converts triglycerides to diglycerides, the diglycerides to monoglycerides, and finally monoglycerides to fatty acid methyl esters. Thus, 3 moles of fatty acid methyl esters are formed when 1 mole of triglycerides combines with 3 moles of alcohol.

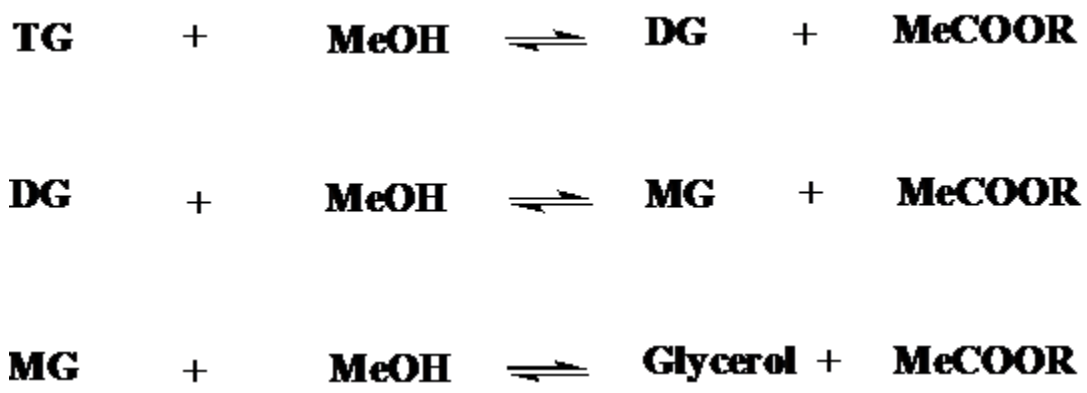

Figure 3.2 The 3 reversible steps in the transesterification reaction

For transesterification, vegetable oils from various feedstocks such as corn, soybean, rapeseed, coconut, oil palm, and canola oils are often used (Ma and Hanna 1999, Knothe et al. 2005, Chisti 2007). However, as discussed in Chapter 1, the need to find a less expensive, non-edible alternative to make biodiesel an economically competitive alternative fuel has led to research on the use of activated sludge as a feedstock. In this study, soybean oil will be used as a model compound for sludge oil to evaluate the effect of water on the reaction and catalyst since it contains triglycerides that would also be present in the extracted/reacted sludge oil.

www.manaraa.com

Transesterification reactions can be catalyzed by a base, acid, or enzyme (Lee et al. 2009). In the acid-catalyzed homogeneous process, the hydrogen from the acid protonates the carbonyl group of the ester and forms a carbocation which, after a nucleophilic attack of the alcohol, produces a tetrahedral intermediate. This intermediate eliminates glycerol to form the new ester and regenerate the H^+ (Schuchardt et al. 1998, Lee et al. 2009). The mechanism is shown in Figure 3.3.

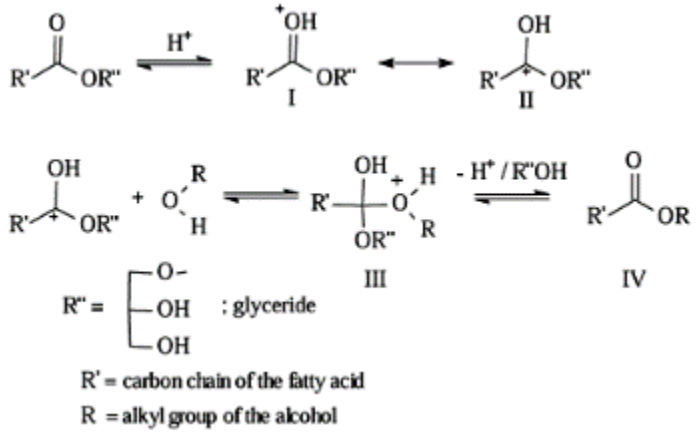

Figure 3.3 Mechanism of the acid-catalyzed transesterification of vegetable oils (Schuchardt et al. 1998).

The main drawbacks for an acid-catalyzed transesterification is a low rate of reaction compared with base-catalyzed transesterification, and the need for higher temperatures sometimes to reach complete conversion (Lee et al. 2009). Furthermore, Revellame et al. (Revellame et al. 2010) showed that acid-catalyzed *in situ* transesterification of sludge is complicated by an acid-catalyzed polymerization of unsaturated fatty acids at temperatures above 60°C, which significantly decreases biodiesel yield. In their study, activated sludge obtained from a municipal wastewater

www.manaraa.com

treatment plant was concentrated, freeze-dried, and transesterified with methanol for 24 hours using sulfuric acid as the catalyst. It was shown that acid-catalyzed production of estolides (oligomeric fatty acid esters) proceeds at a slow reaction rate at 50°C and significantly faster at 75°C, despite a lower concentration of acid catalyst. Another disadvantage of the acid-catalyzed transesterification is its sensitivity to water content in the reaction system. As seen in the mechanism, carboxylic acids can be formed by the reaction of the carbocation with water present in the reaction instead of alkyl esters thus reducing the biodiesel yield (Schuchardt et al. 1998, Lee et al. 2009).

In the homogeneous base-catalyzed mechanism (Figure 3.4), the base abstracts a hydrogen ion from the alcohol, and an alkoxide is produced. A nucleophilic attack of the alkoxide at the carbonyl group of the triglyceride results in a tetrahedral intermediate that rearranges to form the alkyl ester and the corresponding anion of the diglyceride, which deprotonates the catalyst. Thus, the active species are regenerated and can react with another molecule of alcohol and start another catalytic cycle. Diglycerides and monoglycerides are converted to alkyl esters and glycerol by this continuous mechanism (Schuchardt et al. 1998, Lee et al. 2009).

www.manaraa.com

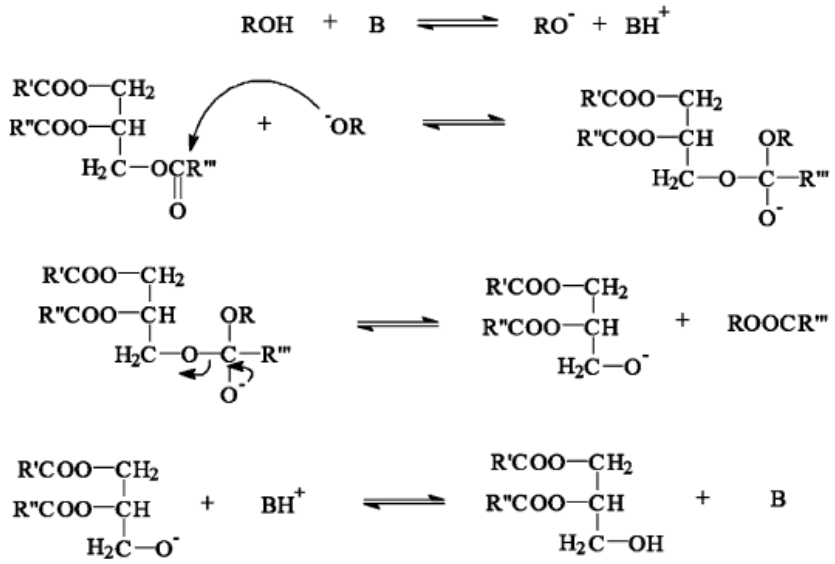

Figure 3.4 Mechanism of the base-catalyzed transesterification of vegetable oils (Schuchardt et al. 1998)

While the homogeneous system allows great mixing as well as faster reaction, the drawbacks include soap formation (if fatty acids are present), difficulty in separation of products, impracticality of catalyst recovery from reactant-product mix, limitation in establishing a continuous process, and reactor corrosion from dissolved acid/base species (Lee et al. 2009). Also, the alkaline and acidic wastewater generated from the separations require additional cost for disposal (Tan and Lee 2011).

The heterogeneously-catalyzed transesterification processes address most of the drawbacks of the homogeneous system, however, its major problem is its slow reaction rate compared with the homogeneous process as reported by Lee (Lee et al. 2009). This can be compensated for by increasing reaction temperature, catalyst amount, and methanol/oil molar ratio (Lee et al. 2009). Thus, it was decided to focus on basic heterogeneous catalysts for transesterification in this part of the study. Basic catalysts were chosen for the transesterification reaction in this study due to the numerous

www.manaraa.com

disadvantages of acid-catalyzed transesterification outlined in the literature, as discussed in section 1.8, Chapter 1.

The most important factors affecting the transesterification reaction are the molar ratio of oil to alcohol, catalyst amount and type, reaction time, reaction temperature, and the content of free fatty acids and water in the oil feedstock (Demirbaş 2003). These variables need to be selected wisely as they all contribute not only to the biodiesel yield but to the cost of production as well. Typical reaction conditions for base heterogeneous catalytic reactions are temperature of 100 – 250 °C, catalyst amount of 3- 10 wt %, and methanol/oil molar ratio of 10:1 – 25:1 (Lee et al. 2009).

The presence of heterogeneous catalysts in the reaction mixture causes a three-phase system of oil-methanol-catalyst to be formed, which inherently inhibits the reaction because of diffusion limitations (Xie et al. 2006) and points to the fact that the reaction mixing is very important as well.

Increasing reaction temperature helps improve phase miscibility and allows better reaction kinetics especially in this potentially diffusion-limited process. Stoichiometrically, three moles of methanol are needed for the transesterification of 1 mole of triglyceride to occur. It is expected that using excess methanol will help drive the reaction to form the desired FAMEs product since it is a reversible reaction. Liu et al. observed that for a set reaction time of 2 hours, poultry fat conversion steadily increased from 23% to 75% when methanol:oil ratio was increased from 6 to 60 (Liu et al. 2007). At the 60 ratio, it took 3 hours to reach 91% TG conversion, but it took 15-fold this reaction time to do the same when using a ratio of 6. Xie et al., however, found that the benefit of molar ratio increase approached saturation at a molar ratio of 15:1 (Xie et al.

www.manaraa.com

2006) and do not recommend higher ratios. Liu et al. believe this is because they used a fixed mass ratio of catalyst:triglyceride (Liu et al. 2007).

In the proposed study, the type of catalyst is important due to the uniquely high moisture content of the proposed feedstock, activated sludge. Since the organic, nonpolar oil and the inorganic, polar alcohol are not very miscible to form one phase of solution, there will be poor contact between the reactants which causes the reaction to proceed relatively slowly. Increasing temperature and mixing rates could help; however, one other useful change is adding a catalyst at an elevated temperature to increase the reaction rate.

3.1.2 Catalysts typically used

Previous studies have used various catalysts such as metal oxides: MgO, CaO (Di Serio et al. 2007), BaO (Hattori 1995); and supported catalysts like Na/NaOH/γ-Al_2O_3 (Kim et al. 2004). The Na/NaOH/γ-Al_2O_3 tested by Kim et al. worked as a superbase giving yields similar to a homogeneous base catalyst. Liu et al. found that catalytic activities for biodiesel synthesis using alkali earth oxides like MgO and CaO had poor performance due to low surface area and limited concentrations of edge and corner defect sites (Liu et al. 2007).

3.1.3 Choice of catalysts

Based on the catalyst selection criteria described in section 1.5, we selected hydrotalcite-derived catalysts called porous metal oxides (PMOs) to take advantage of the following properties: 1) the basicity and surface area of the PMOs can be tuned by modifying the chemical composition and preparation procedures (Lee et al. 2009), 2) large surface areas (Macala et al. 2008), 3) tolerant to water (Di Serio et al. 2007).

www.manaraa.com

The basicity directly impacts the reaction conversion. Additionally, a large catalytic surface area is essential for heterogeneous catalysts, because more access of the substrates to the active sites will improve conversion rates. For example, Liu et al. states that the solid catalysis of reactions with large molecules can be restricted by limited surface site concentration and steric hindrance of the reactants. Limited surface concentration may also be made up for by increasing catalyst loading (Liu et al. 2007). Finally, the catalysts selected needed to be tolerant to water due to the inherent high moisture content of the feedstock – activated sludge.

3.1.4 Hydrotalcites

Hydrotalcites are precursors for a wide range of metal oxides (Li et al. 2011). They are also called layered double hydroxides (LDHs) and have the general formula of $[M_{1-x}^{2+} M_x^{3+}(OH)_2][A^{n-}]_{x/n} \cdot yH_2O$, where M^{2+} and M^{3+} are divalent and trivalent cations in the octahedral sites within the hydroxyl layers, and A^{n-} is an exchangeable interlayer anion. x is equal to the ratio of $M^{3+}/(M^{2+}+ M^{3+})$ and typically has a value in the range of 0.17 – 0.50. M^{2+} and M^{3+} should typically have their ionic radii close to 0.65Å, which is characteristic of Mg^{2+}, to form a stable hydrotalcite structure (Kustrowski et al. 2004).

Divalent cations such as Mg, Mn, Fe, Co, Ni, Cu, Zn and Ga; and trivalent metal cation such as Al, Cr, Mn, Fe, Co, Ni, and La are often used. Some interlayer anions could be CO_3^{2-}, OH^-, NO_3^-, SO_4^{2-} or ClO_4^- (Li et al. 2011). In naturally-occuring hydrotalcite (e.g. $Mg_6Al_2(OH)_{16}CO_3 \cdot 4H_2O$), the interlayer anion is carbonate, although various inorganic, complex and organic anions can be used. Thus, hydrotalcites give the opportunity to prepare tailor-made materials for particular applications by varying the cations and anions used (Kustrowski et al. 2004).

www.manaraa.com

The hydrotalcite structure comprises brucite-like layers where the substitution of Al^{3+} for Mg^{2+} cations generates an excess of positive charges that are compensated for by the anions located with water molecules in the interlayer space (Kustrowski et al. 2004, Antunes et al. 2008). Figure 3.5 below shows 3 common distances that are typically measured to characterize or identify a hydrotalcite compound: the basal spacing, the layer thickness, and the interlayer spacing. The Mg/Al ratio (which is the inverse of x) can range from 1 to 5, with 3 being the best in terms of basic activity as noted by other researchers (Di Cosimo et al. 1998, Lee et al. 2009).

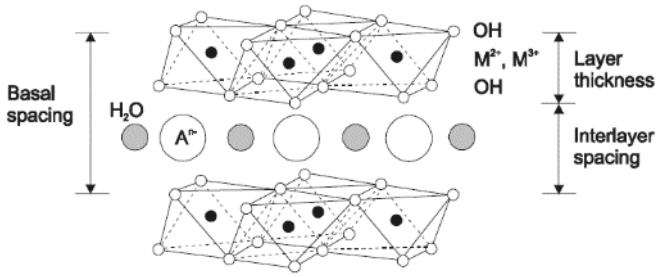

Figure 3.5 Hydrotalcite-like structure

(Hutson and Attwood 2008)
*M^{2+} and M^{3+} are divalent and trivalent cations, A^{n-} is an exchangeable interlayer anion

Hydrotalcites have a broad spectrum of applications in anion exchangers, adsorbents, ionic conductors, as well as catalyst supports and precursors (Pérez-Ramírez et al. 2007). They as well as their derived metal oxides are used in chemical processes such as aldol and Knoevangel condensations, alkylation, Michael addition, and transesterification (Kustrowski et al. 2004).

To take advantage of making specific hydrotalcites for particular applications, substituted hydrotalcite-like materials are formed by substituting a certain molar

www.manaraa.com

percentage of the Mg^{2+} ions by a divalent ion such as copper, and/or substituting a molar percentage of the Al^{3+} ions by a trivalent ion such as iron or gallium. The substituted hydrotalcites that were used in this work have the formula:

$$[(Me_z^{2+}Mg_{1-z})_{1-x}\ Al_x(OH)_2](CO_3)_{x/2}\bullet nH_2O \qquad (3.1)$$

where Me^{2+} = Cu, z = 0.1- 0.2; x = 0.25 and

$$[Mg_{1-x}(Me_y^{3+}Al_{1-y})_x(OH)_2](CO_3)_{x/2}\bullet nH_2O \qquad (3.2)$$

where Me^{3+} = Ga, Fe or La, y = 0.05 – 0.2; x = 0.25.

With the substituted hydrotalcites, the recommended 3:1 Mg/Al ratio (also expressed as Al/(Al+Mg) = 0.25) will be maintained. For example, the molar ratio for an iron-doped hydrotalcite will be Mg/(Al+Fe) = 3:1. The optimum Mg/Al ratio is dependent on the target reaction. For soybean oil methanolysis, Mg/Al = 3 gave the maximum activity (Debecker et al. 2009). There are various methods of preparing hydrotalcites that include: 1) Co-precipitation method, 2) anion exchange, 3) reconstruction, 4) hydrothermal, and 5) urea methods (Li et al. 2011).

The co-precipitation method is the most widely used and is based on the reaction of a solution containing the M^{2+} and M^{3+} cations in adequate proportions with an alkaline solution (Cheng et al. 2012). Lee et al. report that mixed oxides prepared by co-precipitation have the advantage of less of a leaching problem than the parent compounds, stating that proper formulation of the catalyst can overcome the leaching obstacle (Lee and Saka 2010).

www.manaraa.com

3.1.5 X-ray diffraction

X-ray diffraction (XRD) is an experimental technique that uses the scattering of rays on a material to identify information about its crystal structure and its lattice parameters. It can give information on the spacing between lattice planes or layers of atoms, using hkl Miller indices. The size and shape of a unit cell of the material can be calculated from the positions of the XRD peaks and the positions of the atoms in the unit cell can be determined from the intensities of the diffraction peaks.

For hydrotalcites, the X-ray diffraction also gives a breadth of information on the crystalline sample analyzed such as the *d*, *a*, and *c* parameters to calculate the atom positions/separation inside the molecule.

Indexing of the hydrotalcite XRD pattern is typically done using a hexagonal cell with the space group of trigonal symmetry (Brito et al. 2009). The parameter *a* corresponds to the cation-cation distance in the hydroxide (brucite-like) layers, while the parameter *c* refers to the layer thickness (Cheng et al. 2012). It corresponds to three times the distance between adjacent brucite-like layers (Brito et al. 2009). Di Cosimo et al. indicated that the brucite-like sheets in hydrotalcites can accommodate Al^{3+} cations within a wide compositional range since the *a* lattice parameter of hydrotalcite samples decreased monotonically as the Al content increased (Di Cosimo et al. 1998). The *d* parameter is the interplanar spacing or distance between parallel planes of atoms and ions.

The peaks assigned to the 003 and 110 reflections were used to calculate hexagonal parameters *a* and *c*. The presence of d_{003} in the particular position of the XRD plot shows the layered structure of the samples. The position of the diffraction plane

www.manaraa.com

(003) is used to calculate the *c* lattice parameter as $c = 3d_{003}$, whereas the *a* parameter representing the average metal-metal distance in the frame work is calculated from the diffraction plane (110) as $a = 2d_{110}$ (Parida et al. 2012). Comparing the *a* and *c* parameters, you can tell if synthesis methods were consistent (Cheng et al. 2012).

3.1.6 Porous Metal Oxides

Solid base porous metal oxides (PMOs) are hydrotalcite-based catalysts with basicities and surface areas that can be tuned by modifying the hydrotalcite chemical composition and preparation procedures (Lee et al. 2009, Lestari et al. 2009). They are formed by the decomposition of the LDHs at moderate temperatures, producing high specific surface areas and reactivity that are useful in catalytic applications. The decomposition of the hydrotalcite has two steps: 1) the loss of the interlayer water, forming an intermediate structure, and 2) the collapse of the layered structure and decomposition of the interlayer anions (Li et al. 2011). The structure and surface properties of hydrotalcites and their corresponding mixed oxides depend strongly on chemical composition and production methods (Di Cosimo et al. 1998). At the calcination temperature, the interlayer water loss and decarbonization occurs with the release of CO_2 and H_2O to form a porous, amorphous structure with larger surface area (Figure 3.6) (Antunes et al. 2008, Lee et al. 2009).

www.manaraa.com

Figure 3.6 Conversion of hydrotalcite to PMO and regeneration (Pérez-Ramírez et al. 2007).

This calcination process is reversible, and it is important to protect these catalysts from water and CO_2 after being calcined to prevent them from reverting back to the inactive hydrotalcite state. This phenomenon is called the 'memory effect', where porous metal oxides formed from calcining the hydrotalcite can be restored to the original hydrotalcite structure upon contact with water or aqueous solutions containing certain anions (Pérez-Ramírez et al. 2007). Reconstruction of the oxide with water vapor or by immersion in decarbonated water leads to the formation of meixnerite (Figure 3.6), which is similar to a hydrotalcite but has OH- anions in the interlayer instead of the original carbonates. This new structure is reported to possess bronsted basic character and can catalyze a number of organic reactions such as the aldol and Knoevenagel condensations, and Michael additions (Pérez-Ramírez et al. 2007).

The calcination temperature is reported to be an important parameter affecting the surface basicity of the porous metal oxide, i.e., the site strength, site concentration and accessibility (Di Cosimo et al. 1998, Xie et al. 2006, Liu et al. 2007). When testing PMOs that were calcined at different temperatures in the range of 400 - 800 °C, Liu et al. found that poultry fat conversion in the transesterification reaction increased to a maximum of 75% with PMO that was calcined at 550 °C and then decreased on catalysts with higher calcination temperatures. Thus, they determined 550 °C as their optimum calcination

www.manaraa.com

temperature (Liu et al. 2007). Xie et al., on the other hand, found the optimum to be 500 °C. This variation could be due to their different preparation methods. The hydrotalcite used by Liu et al. was purchased from Sigma Aldrich and had a Mg/Al ratio of 2.3. Xie et al. prepared their hydrotalcite to a composition of Mg/Al = 3. However, Liu et al. stated that calcining at 500 °C generates high activity for the transesterification reaction. Di Cosimo also reported that hydrotalcites calcined at 500 °C displayed strong basicity and were more active than pure MgO (Di Cosimo et al. 1998). Macala et al. (2008) with Mg/Al ratio of 3:1 suggest calcining in air at 460 °C (Macala et al. 2008) for soybean oil methanolysis application and this temperature was used for this study.

3.1.7 Past Studies with Hydrotalcite and PMOs

Liu et al. used calcined Mg-Al hydrotalcites (PMO) to catalyze the transesterification of poultry fat with methanol and found that these PMOs showed high activity for triglyceride transesterification with methanol (methanolysis) without signs of catalyst leaching. They conducted reaction in a Parr 4590 at 120°C and 100 psi after charging the reactants and purging oxygen with N_2. Methanol:oil molar ratio was 30:1 and stirring was 1417 rpm. Catalyst concentration was 10 - 20 wt%. They also reported catalytic activity on hydrotalcite samples that were not calcined (Liu et al. 2007). At 120°C, it took 2 hr to reach 60% conversion, and after 8 hr reaction time, it achieved 93% conversion. Brito et al. also reported that the PMO from Mg/Al LDH was highly effective in catalyzing the transesterification reaction of waste oil with methanol. They showed that these catalysts achieved more than 90% conversion at 120 °C after 6 hr. Gao et al. prepared KF/Ca-Mg-Al hydrotalcites and report that the hydrotalcite-derived PMOs had low activities at low temperatures, but could achieve as high as 90% conversion of

www.manaraa.com

soybean oil or acid cottonseed oil when at high temperatures (Gao et al. 2009). Xie et al. also found PMO active for methanolysis of soybean oil and achieved a conversion of 67% after 9hr when reacted at methanol reflux, methanol:oil ratio of 15:1, and catalyst amount of 7.5% (Xie et al. 2006). Corma et al. studied the glycerolysis (a different kind of transesterification) of triglycerides in triolein and rapeseed oil using Mg/Al hydrotalcites at 240 °C for 5 hr and achieved a conversion of 92%. The Al/(Al+Mg) ratio of the hydrotalcite used was 0.2 and calcination temperature was 450 °C.

Studies done by Di Serio et al. (Di Serio et al. 2006) on transesterification of soybean oil to biodiesel using heterogeneous basic catalysts show a correlation between the yield and the catalyst basicity and structural texture. They show that stronger basic sites promote the transesterification reaction at a very low temperature (100°C), while medium strength basic sites need higher temperatures to promote that same reaction (Di Serio et al. 2007). In addition, they show that their tested magnesium oxide and calcined hydrotalcite catalysts were resistant to moisture presence in the reaction environment. In their work, the Al-Mg hydrotalcite used had a ratio of ~ 0.2. This catalyst was tested in an autoclave of 1 L, using 250 g soybean oil, 114 g of methanol, and 2.5 g of calcined hydrotalcite catalyst (CHT). The esteric phase from the reaction products had results of 94% w/w methyl esters (Di Serio et al. 2006). They also carried out some runs at 180°C to test the effect of water in the transesterification of soybean oil with methanol at a water concentration of 10000 ppm. Their best magnesium oxide catalyst produced a biodiesel yield of 78% in the absence of water and 77% at 10000 ppm. While the calcined hydrotalcite produced a biodiesel yield of 92% both in the absence of water and with 10000 ppm moisture content, showing the catalysts' tolerance of water at a low level. The

www.manaraa.com

Mg/Al ratio used was 5 (Di Serio et al. 2006). Although it looked promising, the effect of water on the catalyst was not tested at higher water compositions and will be evaluated in this study.

These data indicated promising results for the use of PMOs in the proposed study. The PMOs used for this project had Mg-Al ratios of 3 since it is reported to have a higher basic activity (Lee et al. 2009).

3.1.8 Selection of Metal Dopants for Catalysts

All hydrotalcites used were synthesized and characterized for this project since only the unsubstituted hydrotalcites are available for purchase commercially. The eight PMO catalysts used for this study are outlined in Table 1 below:

Table 3.1 PMO catalysts for transesterification reactions

10% Copper-substituted (Cu-10)	5% Gallium-substituted (Ga-5)
20% Copper-substituted (Cu-20)	10% Gallium-substituted (Ga-10)
10% Iron-substituted (Fe-10)	5% Lanthanum-substituted (La-5)
20% Iron-substituted (Fe-20)	Unsubstituted (HTC)

The hypothesis for adding dopants to these catalysts was that adding transition metals could generate PMOs with higher basicities and catalyst activity for transesterification reactions especially with some initial moisture content.

Copper was tested as a dopant because copper- based catalysts are often used in methanol synthesis and steam reforming of methanol due to their high selectivity and activity (Cunha et al. 2012) . Cunha also states that copper dispersion is favored with

www.manaraa.com

lower copper loadings. Gallium was tested because Yavuz et al. demonstrated that gallium substitution reinforced the layered structure and increased CO_2 adsorptivity and stability, compared to unsubstituted hydrotalcites (Yavuz et al. 2009). Iron-doped hydrotalcites were tested because Macala et al. found them to be much stronger bases than the Gallium-doped hydrotalcites, and were effective catalysts for the methanol transesterification of triacetin and soybean oil (Macala et al. 2008). Lanthanum was tested because, as a rare earth metal, it has been known to improve stability in zeolites used as FCC catalysts in the refining industry (Moreira et al. 2010). Lanthanum (III) was added in this study to stabilize the Al in the framework of the hydrotalcite and keep it from coming out. The reason for evaluating stabilization is because NMR has shown the movement of Al in zeolites especially with high temperature steam cite, which could be present in our reaction mix if wet sludge is used.

These catalysts are also known to have large surface areas, which is advantageous because it allows more exposure of the active sites. Di cosimo reports hydrotalcite surface areas to fall in the range of 65 – 85 m^2/g (Di Cosimo et al. 1998). Macala et al. show that the Brunauer-Emmett-Teller (BET) surface areas for uncalcined Fe-10 and unsubstitued hydrotalcites are 68.6 m^2/g and 87.1 m^2/g respectively (Macala et al. 2008). For calcined species, they report that unsubstituted hydrotalcite, Fe-10, and Fe-20 PMOs have BET surface areas of 111.8 m^2/g, 123.6 m^2/g, and 161.1 m^2/g respectively when calcined at 460 °C. The effects of the varying dopants (substituted metals) on the conversion will be examined in this project.

The aim of this study is to find the maximum concentration of water that the transesterification of soybean oil can tolerate with the solid PMO catalysts used. The

www.manaraa.com

specific goals are to: 1) prepare strong, solid base catalysts with tunable basic properties and reactivities by homogeneous introduction of various dopants into the unsubstituted hydrotalcite (HTC) lattice, 2) screen these catalysts for highest conversion, 3) determine the effect of water at different compositions on these catalysts and 4) determine kinetic parameters on the reactions run at 0% water and at the optimal water composition.

3.2 Materials and Methods

3.2.1 Chemicals and Gases

The following chemicals were obtained from Fisher Scientific (Pittsburgh, PA, USA): high performance liquid chromatography (HPLC)-grade methanol (Acros Organic, 99.9%), soybean oil (Best Yet Vegetable Oil), magnesium chloride hexahydrate, $MgCl_2.6H_2O$ (99%), aluminum chloride hexahydrate, $AlCl_3.6H_2O$ (99%), sodium carbonate, Na_2CO_3 (100.3%), copper (II) chloride dihydrate, $CuCl_2.6H_2O$ (99%), iron (III) chloride hexahydrate, $FeCl_3.6H_2O$ (99%), lanthanum (III) chloride hexahydrate, $LaCl_3.6H_2O$ (99%), and sodium hydroxide, NaOH (99.4%). Triolein, 1,3-diolein, monoolein, tricaprin, and MSTFA were purchased from Sigma Aldrich and used to prepare calibration standards. Soybean oil was obtained from a local grocery store in Starkville, MS. All the gases used (He, H_2, and air) for gas chromatography were of high purity grade and distributed by NexAir (Columbus, MS, U.S.A.). All chemicals, standards, and gases were used as received without further purification.

3.2.2 Apparatus

Figure 3.7 - Figure 3.10 show some of the apparatus used in this study:

1. 450ml batch Parr® reactor

www.manaraa.com

Figure 3.7 Parr 5522 - 450ml reactor

(Parr Instrument Company, Moline, IL, U.S.A)

2. Rotary evaporator

Figure 3.8 Büchi R-205 rotary evaporator

(Brinkmann Instruments, Inc., Westbury, NY, U.S.A.)

www.manaraa.com

3. Vacuum filtration set-up

Figure 3.9 Gast Oil-less Vacuum pump set-up for catalyst filtration (Fisher Scientific, Pittsburgh, PA, USA)

4. Chemglass 1000ml reactor set

Figure 3.10 1000ml 3-necked reactor equipped with stirrer and temperature controller (Chemglass Inc., Vineland, NJ, USA)

3.2.3 Catalyst Preparation

The PMO catalysts used for the transesterification were synthesized in a Chemglass 1000 ml Process Reactor System (Figure 3.10) using the co-precipitation method (Macala et al. 2008). Each catalyst was characterized using X-ray diffractography

www.manaraa.com

to ensure that hydrotalcite compound and no other phases were formed. The catalysts were ground to powder form and stored in air-tight vials to avoid water and CO_2 poisoning. Catalysts were freshly calcined for an hour at 460°C before use, to remove moisture and provide the best activity.

3.2.3.1 Protocol for the Mg/Al hydrotalcite (HTC) preparation

The hydrotalcite was prepared using a method similar to that used by Macala et al. (Macala et al. 2008). Hydrotalcite solids were prepared to have a molar ratio of Mg/(Al+dopant) = 3. A solution of 30.5 g (0.15 mol) of $MgCl_2.6H_2O$ in 125 ml of distilled water was combined with a solution of 12.1 g (0.05 mol) of $AlCl_3.6H_2O$ in 125 ml of distilled water and added drop wise to 375 ml of a Na_2CO_3 (5.3 g, 0.05 mol solution) at pH = 10 and 60°C under vigorous stirring. The pH was kept constant by adding appropriate volume of 1M NaOH during precipitation. The addition of the combined solution took almost 3 hours. The suspension obtained was kept at 80°C for 24 h, and then filtered and washed thoroughly with abundant amount of distilled water until the pH was 7. This was checked using a Whatman indicator paper strip. This hydrotalcite precipate was exchanged with carbonate at 80°C by re-suspending it in 0.02 M Na_2CO_3 solution to remove any remaining chloride ions from the interlayer, and left to age for 48 h. The resulting precipitate was dried at 120°C for 24 h, and then calcined overnight at 460°C to form the porous metal oxides. The dried catalyst was crushed in a mortar and pestle and stored in a glass vial till use.

If a divalent cation, Me^{2+} was substituted, then the number of moles of (Mg^2 + Me^{2+}) would sum up to a total of 0.15 moles. Likewise, when a trivalent cation, Me^{3+}, was substituting Al^{3+}, the number of moles of (Al^{3+} + Me^{3+}) would sum to a total of 0.05

www.manaraa.com

moles to keep the recommended 3:1 divalent:trivalent cation ratio. Pictures of a sample hydrotalcite and PMO are shown in Figure 3.11 and Figure 3.12.

Note: For copper, additional precautions were taken to ensure that temperature did not exceed 70°C during aging. Also, lanthanum was left to age for 7 days so its larger ion radii could be properly inserted into the lattice.

Figure 3.11 Filtered and dried Fe -10 hydrotalcite

Figure 3.12 Ground, calcined Fe-10 hydrotalcite

www.manaraa.com

3.2.4 Catalyst Characterization

3.2.4.1 Crystallinity

The uncalcined hydrotalcite was characterized for crystallinity by powder X-ray diffraction (XRD) performed on a Rigaku Ultima III diffraction system using Cu Kα radiation (k=1.54059 Å), 40 kV and 44 mA to identify the crystalline phases. Analysis was conducted with a step size of 0.02 degrees over a 2θ range of 3 - 70° with a scanning speed of 5°/min. The resulting patterns were compared to reference patterns for hydrotalcite mineral. This characterization is to check that the hydrotalcite phase was formed properly and only that phase was present.

3.2.4.2 Surface area

The PMO surface area characterization was performed using the Brunauer, Emmett, Teller method (BET) method by nitrogen adsorption which measures the specific surface area of a material by adsorption/desorption of nitrogen on a solid surface at 77 K (Brunauer et al. 1938). The instrument used was the Tristar II 3020 system at the Micromeritics Analytical Services lab in Norcross, GA. This characterization was done on the best catalyst before and after reaction to ensure that any attrition in the reactor was not causing increase in the surface area.

3.2.5 Experimental Design

The investigative procedure for the feasibility of using wet sludge to produce biodiesel will be evaluated using the flowchart shown in Figure 3.13 below:

www.manaraa.com

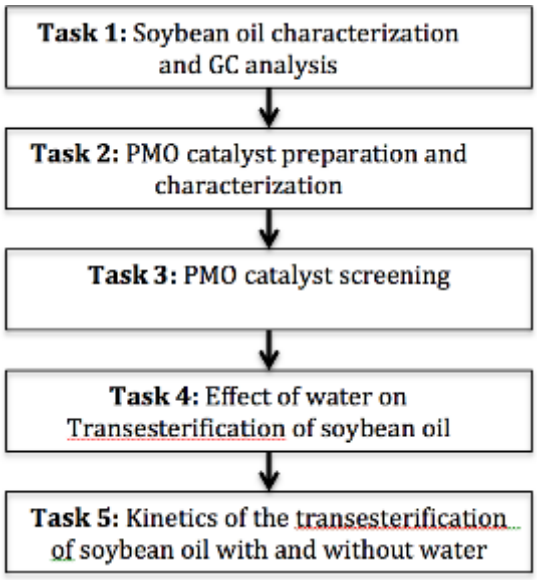

Figure 3.13 Flowchart illustrating tasks for the project

3.2.5.1 Catalyst screening

Catalyst screening tests based on highest conversions to pick the best catalysts were conducted at the same reaction conditions for 8 catalysts. The eight hydrotalcite-based catalysts as listed in Table 1 were synthesized and tested with the transesterification procedure described above in section 3.2.6.2. On the basic Parr® set up, both oil and methanol were charged at the same time before heating, and the start of the reaction was not tracked due to the 20 min heat up time. The tests were conducted at 150 °C at 240 rpm stirring for 1 hour. These tests were performed in duplicates. After the reaction, the transesterification products were treated and analyzed for the conversion of soybean oil.

www.manaraa.com

3.2.5.2 Effect of Temperature

The influence of temperature was studied on the dry transesterification of soybean oil with methanol using 2 wt% of the best catalyst (Fe-20 PMO), 10g oil and 100ml methanol and stirring speed of 240 rpm. Four temperatures were studied to test the effect of temperature on oil conversion: 120 °C, 150 °C, 180 °C and 210 °C.

3.2.5.3 Effect of Water on Transesterification of Soybean Oil

For studying the effect of water, the transesterification reaction was modified by adding the corresponding mass percentage of water (based on oil mass) to the 10g of soybean oil. The water compositions were 1, 5, 10, and 20% (w/w). The effect of water on the transesterification reaction with respect to substrate conversion and FAME yield was determined.

3.2.5.4 Kinetics on the Transesterification of Soybean Oil with and without water

The kinetic transesterification reaction of soybean oil was studied at 0% and 10% water content at 150°C starting out with 10g oil and 100ml methanol using the best catalyst, Fe-20 PMO.

3.2.6 Experimental Procedure

All reactions were done in duplicates

3.2.6.1 Soybean oil characterization and GC analysis

Soybean oil was obtained from the local grocery store and used without further purification. It was characterized for initial triglyceride and ester content by gas chromatography using a Varian 3600 GC with Rtx®-Biodiesel TG column (Restek Corporation) equipped with a flame ionization detector (FID). The specific method used

www.manaraa.com

to analyze all samples for glyceride content is discussed in the Analytical Method section of this chapter.

3.2.6.2 Non-kinetic transesterification reaction procedure

Prior to each run, the PMO catalyst was freshly calcined at 460°C for an hour and cooled in a dessicator containing NaOH to protect from carbon dioxide and moisture adsorption. Ten grams of soybean oil and 100 ml of methanol were charged into the 450 ml Parr® batch reactor (Figure 3.7), and 0.2 g (2 wt% based on oil) of freshly calcined catalyst was added. Reaction temperature was set for 150°C and stirring for 240 rpm. The vessel took about 23 minutes to heat up to 150°C and was left to run for 1 hour after it reached the set point of 150°C.

After an hour, the reaction was quenched by cooling the reactor with an ice bath. The reactor contents were transferred to a 250 ml beaker and the reactor was rinsed with heptane and pooled with the contents in the beaker. The reaction products were transferred to a 250 ml round bottom flask and methanol was removed from the products at 45°C under a vacuum pressure of 300 mbar using the Büchi rotary evaporator (Figure 3.8). The catalyst was removed by vacuum filtration of the product using a 30 ml Buchner funnel and washed with heptane on the filter (Figure 3.9).

3.2.6.3 Reactor modifications for kinetics of transesterification

Kinetic experiments for the transesterification reaction were performed on soybean oil with the best catalyst determined from the screening tests, using a modified set-up.

www.manaraa.com

When the first, basic set-up described in section 1.2.6.2, would not work due to long heat-up time, a first modification was made to allow accurate calculation of kinetics, but did not work for reasons described below. After a series of further modifications to the reactor, a final set-up was obtained.

3.2.6.3.1 First modification to 450ml batch Parr® reactor for kinetic reactions

The simple set-up of the 450 ml Parr® reactor (Figure 3.14) was used for the catalyst screening since all catalysts were being screened at the same conditions and not being studied for kinetics. However, the inability to control the start time of the reaction with the heater's inconsistent heating times indicated that the simple set-up of the Parr® batch reactor would prevent the accurate determination of reaction kinetics as it could take as high as 23 minutes to reach a set point of 150 °C.

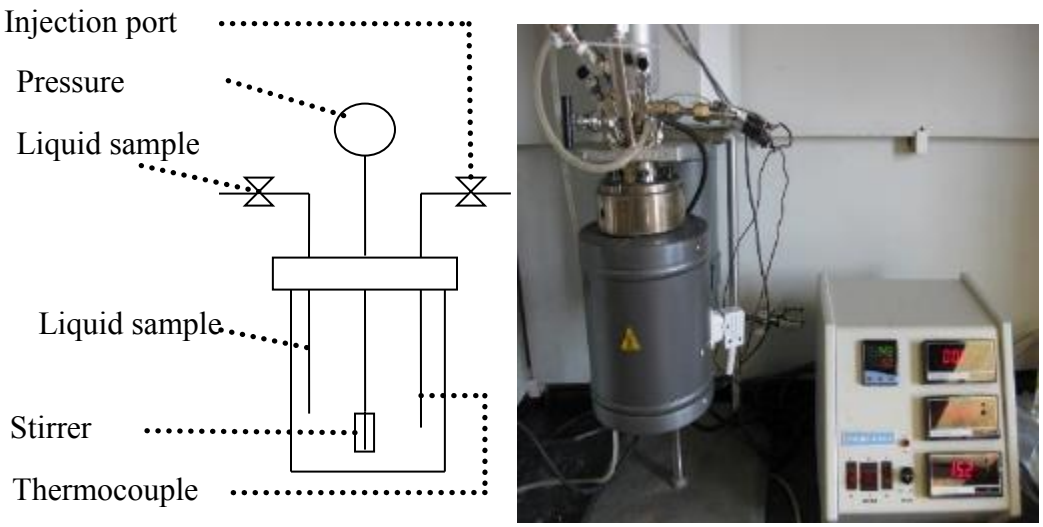

Figure 3.14 Schematic and picture of unmodified 450 ml Parr® batch reactor with temperature and pressure control interface used for catalyst screening in transesterification of soybean oil

www.manaraa.com

We proposed to modify this set-up by charging the reactor with methanol and catalyst first, heating to the desired temperature, and then using a pressure-equalizing loop added to two ports on the reactor to use the methanol pressure entering the loop on one end of the loop to push down oil in a reservoir on the other end of the loop into the reactor while the stirrer mixed the contents. After the addition, the timer was started to track the reaction time. The parts needed to change the reactor set-up were assembled as shown in Figure 3.15 and the description is as follows:

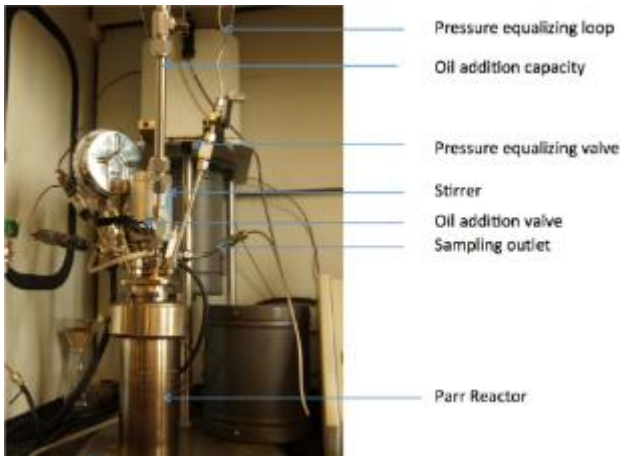

Figure 3.15 First modification to reactor

On two vacant ports (at the reactor head) that were previously plugged, a loop of stainless steel tubing was used to connect the reactor opening at one port to the oil reservoir (made of 3/8-inch tubing), which was connected to the reactor opening at the second port. Valves were added just before the entrance to both ports. The assumption was that opening the valve on the first port would release the pressurized methanol vapor (formed when the reactor had come to the temperature set point with methanol in it) to

www.manaraa.com

flow toward the oil reservoir and push oil into the reactor when the valves before and after the oil reservoir were opened consecutively.

This set-up eventually did not work because there was concerns about not getting all the oil into the reactor, losing some of the reactant mixture to the pressure-equalizing loop, improper introduction of oil into the methanol body because the methanol vapor would disperse it everywhere (this dispersion was neither uniform nor could it be controlled between replicates), and not being able to conduct the reaction completely in the liquid phase. Hence, there was a need to find another method to add the 2nd reactant in so all the expected amount introduced would react.

3.2.6.3.2 Final modification to 450ml batch Parr® reactor for kinetic reactions

Figure 3.16 Final modification to 450-ml Parr® reactor used for final kinetic study in transesterification of soybean oil

a) front view b) side view c) sample vials

To get accurate kinetic information, a final modification was made to the batch reactor such that soybean oil and catalyst in the reactor were heated up to the set point before addition of methanol. This required the addition of a methanol reservoir, and a

www.manaraa.com

tubing connection for additional pressure supplied by a nitrogen tank. Similar to the previous modification, a methanol reservoir was made from 14 inches of 1-inch 316 stainless steel tubing and was added to one of the reactor's ports with a valve between. The other port was connected to the reactor while the tubing loop had a tee in it that had a tubing connection to the nitrogen tank.

3.2.6.4 Kinetic transesterification procedure with and without water

The kinetic transesterification reaction of soybean oil was studied at 0% and 10% water content at 150°C starting out with 10g oil and 100ml methanol using 0.2g of the best catalyst, Fe-20 PMO. The reactor was charged with soybean oil and the catalyst. To avoid oxidation of the reactants, nitrogen was used to purge the reactor (after sealing) with a pressure of 700 psi and then the reactor was heated to 150 °C. Stirrer was turned on at 500 rpm. Once at 150 °C, the valve for the line from the nitrogen tank (via tee) was first opened at 800 psi pressure to push all the methanol down into the reactor after which the valve between the methanol reservoir and the reactor was opened next. The reaction time was started. A sample was taken for the 0 min sample and 6 more samples were taken at 10-minute intervals. A 60ml vial containing 30ml of methanol placed in a beaker of ice was used to collect the sample to prevent methanol vapor loss when the sample came out of the reactor from high pressure to atmospheric pressure. To do this, the metal 1/8-inch tubing was inserted through the silicone/Teflon septum of the 60ml vial until it was below the level of the cold liquid so the vapor would cool and condense. The nitrogen supply was left on during reaction to maintain constant pressure in the reactor and keep reactants in the liquid phase. Figure 3.16 shows the modified reactor and the sample vials used.

www.manaraa.com

After the reaction, the volume of each sample was measured, and then methanol was evaporated using a Turbovap since the glyceride concentrations would be measured on an oil basis. The dried residual lipids were weighed and 2 portions were taken out: one was dissolved in a toluene diluent containing 100ppm BHT and 200ppm DCB, which was the internal standard used for FAME analysis on the Agilent 6890 GC (Figure 3.17). The second portion was derivatized and analyzed using high temperature gas chromatography (GC) with the Varian 3600 GC (Figure 3.18) for quantification of FAMEs and glycerides.

Figure 3.17 Agilent 6890 series GC system with DA Stabilwax column for quantifying FAMEs and FFA Initial and final temperatures of 50 °C and 250 °C

Figure 3.18 High temperature GC, Varian 3600

www.manaraa.com

3.2.7 Analytical Method

3.2.7.1 Derivatization Method

Derivatization is the chemical change of a compound to a new compound that has more suitable properties for an analytical method. In this case, glyceride samples had to be derivatized before analysis on the GC to be accurately quantified because they have a low volatility which will affect the reproducibility of the peak areas and shapes. Thus, derivatization improves the resolution and analyte response during chromatography. A silylation process was used to derivatize the glyceride by adding N-methyl-N-(trimethylsilyl)-trifluoroacetamide (MSTFA) to the sample. The MSTFA then replaces the active hydrogen on the glycerides with silyl groups, making it more volatile and improving the resolution.

The proposed method that was selected for analyzing the glyceride content of the sample is the "ASTM D6584 Test Method for Determination of Free and Total Glycerin in B-100 Biodiesel Methyl Esters By Gas Chromatography" (ASTM). This test is typically used to quantify glycerol and glycerides in biodiesel samples.

3.2.7.1.1 Calibration Preparation for derivatization standards

FAMEs mix C8-C24 of saturated, mono-unsaturated and poly-unsaturated fatty acid methyl esters (Supelco, Bellefonte, PA) were used to calibrate for FAME compounds with internal standard of dichlorobenzene (DCB). Triolein, 1,3-diolein, monoolein purchased from Sigma Aldrich were used as glyceride reference compounds for the high temperature GC calibration. A 5-level calibration standard containing these glycerides and tricaprin as an internal standard was made and derivatized. The reaction products were also converted to volatile trimethylsilylether derivatives with N-methyl-N-

www.manaraa.com

(trimethylsilyl)-trifluoroacetamide (MSTFA), using a modified form of the method described in the ASTM D6584 method for Determination of Free and Total Glycerin in B-100 Biodiesel Methyl Esters (ASTM). After 20 min at room temperature, the products were dissolved in chloroform and were analyzed by high temperature gas chromatography (GC).

3.2.7.1.1.1 Procedure for Standard Preparation and Derivatization

Triolein, diolein, monoolein were obtained from Sigma Aldrich and derivatized with tricaprin as an internal standard before making calibration samples at 5 levels from 500 µg/ml to 31.25 µg/ml. For the 500 µg/ml calibration standard, one hundred and twenty five microliters (125 µL) of 8mg/ml tricaprin in pyridine was added to 400 µL each of triolein, diolein, and monoolein dissolved in pyridine at concentrations of 5000 µg/ml. One hundred microliters (100 µL) of MSTFA was added, and the mixture was allowed to sit for at least 20 minutes, after which 575 µL of pyridine and 2000 µL of chloroform were added to achieve a total volume of 4000 µL (4ml). This gave a tricaprin internal standard concentration of 250 µg/ml. For the remaining 4 levels, the volumes of triolein, diolein, and monoolein were appropriately reduced and the chloroform level was increased appropriately while keeping the total volume at 4ml and the tricaprin internal standard concentration constant at 250 µg/ml.

3.2.7.1.1.2 Procedure for Sample Derivatization

All glyceride samples were derivatized using this modified ASTM D6584 method before analysis. One hundred and twenty five microliters (125 µL) of 8mg/ml tricaprin in pyridine and 100 µL MSTFA were added to the mass being analyzed (~ <10mg), allowed

www.manaraa.com

to sit at least 20 min, and diluted with 3,775 µL of plain chloroform before being filtered and injected on the high-temperature GC. Accuracy of the method was confirmed by using the calibration obtained on the GC with the standards prepared to calculate a known concentration of soybean oil derivatized using the method above and it matched. All kinetic samples were derivatized and the GC analysis provided a quantitative analysis of the triglyceride (TG), diglyceride (DG), monoglyceride (MG) and FAMEs needed for the kinetic study.

3.2.8 Gas Chromatograph and method

3.2.8.1 Gas Chromatograph for FAME analysis

The concentrations and amounts of FAMEs in the chloroform phase were analyzed and quantitated using the Agilent GC 6890N gas chromatograph equipped with a flame ionization detector (GC-FID) (Agilent, Santa Clara, CA, USA. Approximately 4 mg of crude extract was dissolved in 1ml standard solution (toluene diluent containing 100 µg/ml BHT and 200 µg/ml DCB, which was the internal standard for GC analysis). One µL of this solution was injected in splitless mode on an Agilent 6890 Gas Chromatograph (Agilent Technologies, Santa Clara, CA) at a constant injector temperature of 260 °C. The GC was equipped with a 30 m × 0.25 mm ID Restek 11023 Stabilwax DA Capillary Column (Restek, Bellefonte, PA) having a 0.25-µm film thickness. The GC oven was programmed at an initial temperature of 50 °C, held for 2 min, ramped up to 250 °C at 10 °C min^{-1}, and held for 18 min, giving a total of 40 min analysis time. A flame ionization detector (FID) operating at 260°C and using helium carrier gas (14 psi, 53.5 mL/min flow rate) was used to detect the FAMES. The instrument was calibrated using a standard FAME mixture containing 14 FAMEs from

www.manaraa.com

C8 – C24 (Sigma-Aldrich, St. Louis, MO). The total FAME concentration obtained was used to estimate the total biodiesel yield from each reactor set.

3.2.8.2 High Temperature Varian Gas Chromatograph for glyceride analysis

The high temperature GC was used to characterize the soybean oil and to analyze the glyceride content in the reaction products for quantification. The equipment used was the Varian 3600 GC (Figure 3.18) equipped with a flame ionization detector (FID). The column used was the ZB-5HT Inferno™ (Phenomenex, Torrance, CA, USA) having dimensions of 15m, internal diameter of 0.32mm and film thickness of 0.10μm, and 400 °C maximum temperature. The initial and final injector temperatures will be 50°C and 380°C respectively and the FID temperature of 380°C in accordance with the ASTM Method D 6584 (ASTM). The GC oven was programmed at an initial temperature of 50°C for 1 minute, then ramped to 180°C at 15°C/minute, to 230°C at 7°C/minute, and then to 370°C/minute at 10°C/minute was held constant at 380°C for 5 minutes.

3.2.9 Conversion Calculations

3.2.9.1 Conversion calculation for Catalyst Screening

The molecular weight of soybean oil is assumed to be 879.38 g/mol, assuming each of the alkyl group is linoleic acid (the largest fatty acid in the soybean oil composition) and that soybean oil is trilinolein.

The stoichiometry of the transesterification reaction below was used to relate the number of moles of FAMEs to the conversion of substrate given the relative GC response factor and the ratio of the peak areas.

www.manaraa.com

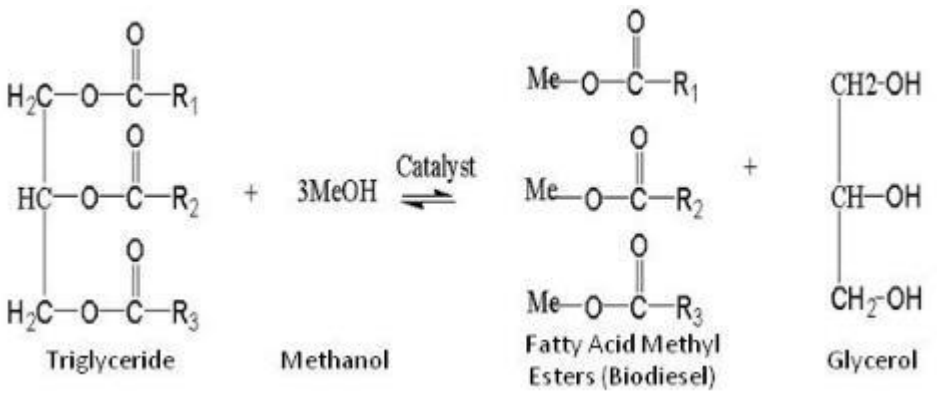

Figure 3.19 The transesterification reaction with methanol

Creating a parameter, α, on the assumption that:

$$\alpha = \frac{moles\ FAME\ (n_{FAME})}{moles\ Triglyceride\ (n_T)} = \frac{Area\ of\ FAME}{Area\ of\ Triglyceride} * Relative\ GC\ Response\ factor \tag{3.3}$$

Having calculated the relative GC response factor = 0.4, we calculated the conversion (f) using the following equations:

$$n_T = {n_T}^0 * (1 - f) \tag{3.4}$$

$$n_{FAME} = 3{n_T}^0 f \tag{3.5}$$

where ${n_T}^0$ is the initial number of moles of triglyceride, n_T is the number of moles of triglyceride, f is the conversion, α is ratio of moles of fame to triglyceride.

Thus,

$$\alpha = 0.4 * \frac{Area\ of\ FAME}{Area\ of\ Triglyceride} = \frac{(n_{FAME})}{(n_T)} = \frac{(3{n_T}^0 f)}{{n_T}^0 * (1-f)} = \frac{3f}{(1-f)} \tag{3.6}$$

Conversion, f, is given by:

$$f = \frac{\alpha}{3+\alpha} \tag{3.7}$$

www.manaraa.com

Thus, the fractional conversion of substrate was calculated from the peak area.

3.2.9.2 Conversion calculation for Kinetics

Samples were weighed, the internal standard was added to a portion which was derivatized and then analyzed on the GC. The GC analysis provided a quantification of the triglyceride (TG), diglyceride (DG), monoglyceride (MG), and FAMEs concentrations needed for the kinetic study.

3.3 Results

3.3.1 Soybean oil Characterization

The results obtained from the GC run were compared with a reference chromatogram (Figure 3.20) from the ASTM Method D 6584, Determination of Free and Total Glycerine in B-100 Biodiesel Methyl Esters, to identify retention time of esters and triglycerides. Figure 3.21 shows the GC trace of soybean oil before transesterification, which has strong peaks in the triglyceride region (22.5 – 25 minutes) and little or no peaks in the methyl ester region (8 – 11 minutes). In Figure 3.22, the GC trace of the transesterification product (FAMEs) after methanol had been evaporated shows strong peaks in the methyl ester region and a significant decrease in the peak size of the triglycerides, which indicates significant substrate conversion. To make a quantitative analysis of conversion, the ratio of the integrated areas under the methyl ester to triglyceride peaks was used.

www.manaraa.com

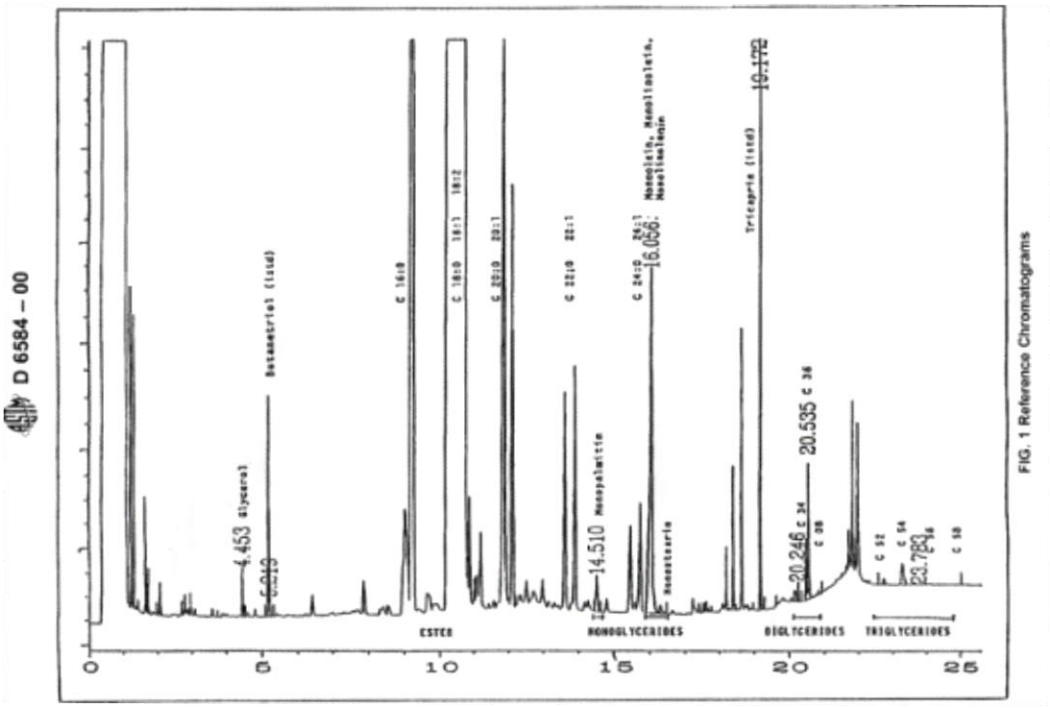

Figure 3.20 Reference chromatogram from ASTM method D6584.

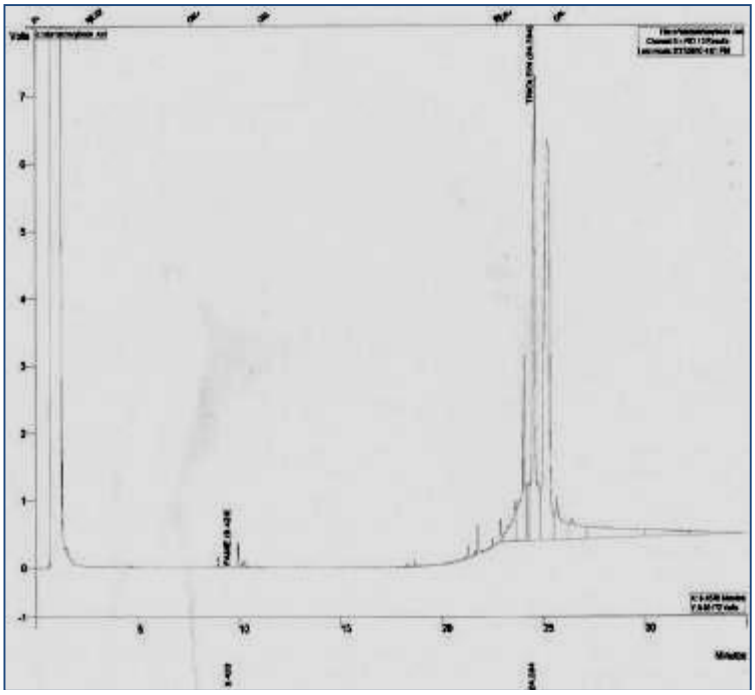

Figure 3.21 Gas chromatograph trace of soybean oil prior to transesterification.

www.manaraa.com

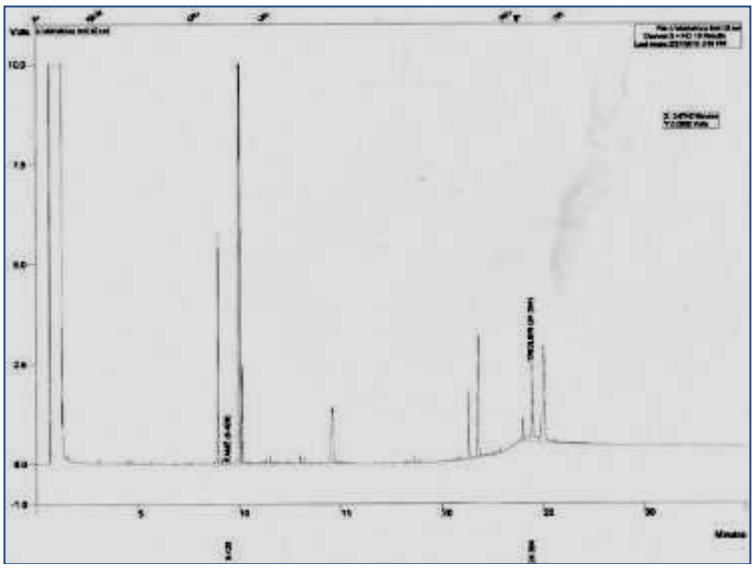

Figure 3.22 Gas chromatograph trace of soybean oil after transesterification

3.3.2 Catalyst Characterization

3.3.2.1 XRD

Our goal was the preparation of stable, strong solid base catalysts with tunable basic properties and reactivities by homogeneous introduction of various dopants into the HTC lattice. All samples exhibited the characteristic reflections of the hydrotalcite-like structure, which included sharp, symmetric reflections for the (003), (006), (110) and (113) planes, and also broad and asymmetric reflections for the (102), (105), and (108) planes as usually observed (Cheng et al. 2012, Pavel et al. 2012). Only the hydrotalcite phase was formed, no other phases present. A sample XRD is shown in Figure 3.23. For the substituted hydrotalcites, that indicated that the metal ions had been incorporated into the layers. The *a* and *d* parameters of the compounds were calculated and presented in the Table 3.2.

www.manaraa.com

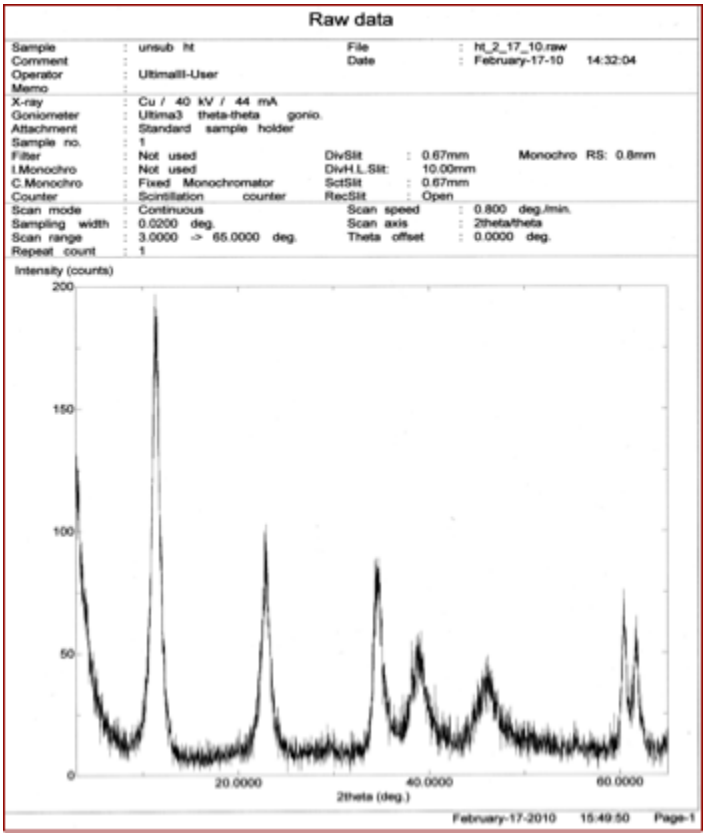

Figure 3.23 A sample XRD of the unsubstitued hydrotalcite sample

Table 3.2 d-spacing and *a* parameter of the catalysts used for the transesterification of soybean oil

Catalyst	Date Xrd Analyzed	d_{003} (Å)	d_{110} (Å)	a	c
cu 10	1/22/2010	7.7553	1.5335	3.067	23.2659
cu20	3/10/2010	7.6913	1.5305	3.061	23.0739
cu20	2/17/2010	7.6888	1.5286	3.0572	23.0664
ga5	4/15/2010	7.7697	1.5336	3.0672	23.3091
ga10	4/13/2010	7.7424	1.5314	3.0628	23.2272
fe10	4/15/2010	7.7704	1.535	3.07	23.3112
fe20	4/12/2010	7.7416	1.535	3.07	23.2248
la5	4/12/2010	7.8103	1.5359	3.0718	23.4309
ht	2/17/2010	7.7015	1.5313	3.0626	23.1045
Fe 20 A	10/19/2012	7.728	1.5345	3.069	23.184

www.manaraa.com

These values are similar to those for hydrotalcite materials found in literature (Pavel et al. 2012). From these results, it was observed that the *a* parameter of the metal-doped hydrotalcites remained very similar to the unsubstituted hydrotalcite (HTC), indicating that the metal cations were properly inserted. Pavel et al. also observed that the *a* cell parameter for their substituted samples was close to that of the unsubstituted HT (a=3.05 ± 0.01Å), showing no variation in the mean intermetallic distances in the brucite-like layers and corroborates these results. This was considering the low transition metal cation content that was in the samples (Pavel et al. 2012). Pavel et al. also noted that the specific surface area of the unsubstituted mixed oxide decreased from 224 m^2/g to a range of 161 – 213 m^2/g upon introducing the transition metal cations in the structure, e.g. CuMgAlO had slightly lower surface area than FeMgAlO. However, Macala et al. observed that the doped PMOs had larger surface areas than the undoped PMOs (Macala et al. 2008).

Hydroxides of ions of same valency as Mg or Al and having radii differing by about 15% (Hume-Rothery rules) are expected to form a solid solution with HTC. While the substitution of Cu for Mg (R_{Mg2+} = 0.72 Å, R_{Cu2+} = 0.73 Å, relative size difference = 1.4%) and Fe or Ga for Al (R_{Fe3+} = 0.55Å, R_{Ga3+} = 0.62 Å, R_{Al3+} = 0.54 Å, relative size differences for Fe and Ga with respect to Al are 1.9 and 14.8% correspondingly) is expected to be isomorphous, the doping of HTC with Lanthanum (La) is more complicated due to a large difference in the size of the cations (R_{La3+} = 1.03Å, R_{Al3+} = 0.54 Å). The value of the ratio R_{La3+}/R_{OH^-} = 0.752 (compared to R_{Al3+}/R_{OH^-} = 0.394 or R_{Mg2+}/R_{OH^-} = 0.526) suggests that La^{3+} ion is significantly larger than an interstitial octahedral site formed by 6 OH^- groups of the lattice and probably is not incorporated

www.manaraa.com

into it but just finely dispersed throughout. However, elevated temperatures where the expansion of structure provides greater tolerance for size variation favor substitution of smaller ions by larger ones. Thus, an attempt was made to substitute only 5 mol% of La for Al and increase the duration of the aging process at 80°C to 7 days instead of 2 days. However, La ions were not successfully incorporated into the lattice as evidenced by the size of the lattice parameter (*a*) of La5-HTC being almost the same size as the HTC instead of larger (Table 8.2). A separation of La_2CO_5 and $La_2(CO_3)_2(OH)_2$ phases, similar to what was found by Bîrjega et al. (Birjega et al. 2005) was possibly what occurred. (All values of ionic radii for octahedral environment were taken from Handbook of Chemistry and Physics (Lide 2010 CD-ROM Version)).

3.3.2.2 Surface Area

The surface area obtained on Fe 20 catalyst was 178 m^2/g which compares well with the 161 m^2/g obtained by Macala et al. on their Fe-20 catalyst (Macala et al. 2008) shows that the Brunauer-Emmett-Teller (BET) surface areas for uncalcined Fe-10 and unsubstitued hydrotalcites are 68.6 m^2/g and 87.1 m^2/g respectively. For calcined species, they show that unsubstituted, Fe-10, and Fe-20 have BET surface areas of 111.8 m^2/g, 123.6 m^2/g, and 161.1 m^2/g respectively when calcined at 460°C.

Based on consistent preparation methodology and similarity in d-spacings and *a* parameters, the surface areas of all 8 catalysts were not expected to have significant variation, especially between substituted catalysts, since the aim of the screening was to identify the most active catalyst.

www.manaraa.com

3.3.3 Catalyst Screening

The best catalysts were selected based on highest conversion of soybean oil. The results of the conversion-based screening tests on the 8 porous metal oxides are shown in Figure 3.24 below with the Fe-20, unsubstituted hydrotalcite, and Cu-10 catalysts having conversions of 44%, 41%, and 40% respectively. The order of catalyst conversion from highest to lowest was: Fe 20 >Unsustituted > Cu10 > Fe 10 > Ga 10 > Cu 20 > Ga 5 > La 5.

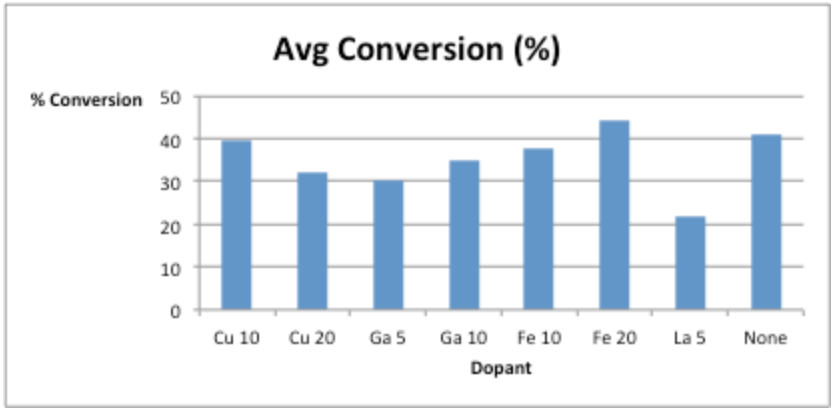

Figure 3.24 Percent conversion of soybean oil transesterification with 8 porous metal oxides.

Finding Fe-20 substituted porous metal oxides as the most active is similar to results found by Macala et al. (Macala et al. 2008) from testing six porous metal oxides on the transesterification of triacetin. The porous metal oxides used were Fe-substituted, Ga-substituted, and unsubstituted. For this transesterification, 4.4 ml triacetin was combined with 5.6 ml anhydrous methanol (6:1 methanol to triglyceride molar ratio), and 0.2 wt% catalyst at 60°C. The results showed that the undoped PMO had the least activity

www.manaraa.com

after 60 minutes (~18% conversion), while the Ga 5 and Ga 10% gave approximately 40% conversion and 80% conversion respectively. However, the Fe doped porous metal oxides were much more active than either the undoped or the Ga doped PMOs. The 5%, 10% and 20% Fe doped PMOs gave approximately 99% conversion at the same conditions.

For triacetin, Fe 10% was most active. It is important to note that triacetin is completely miscible with methanol even at room temperature (Liu et al. 2007), unlike soybean oil, and that property would contribute to the higher conversions observed as compared to the reactions with soybean oil in this case.

3.3.4 Effect of Temperature

As mentioned in the introduction, increasing temperature is usually beneficial on the reaction rate and substrate conversion, which is seen in the results as temperature was increased from 120 °C to 180°C (Figure 3.25):

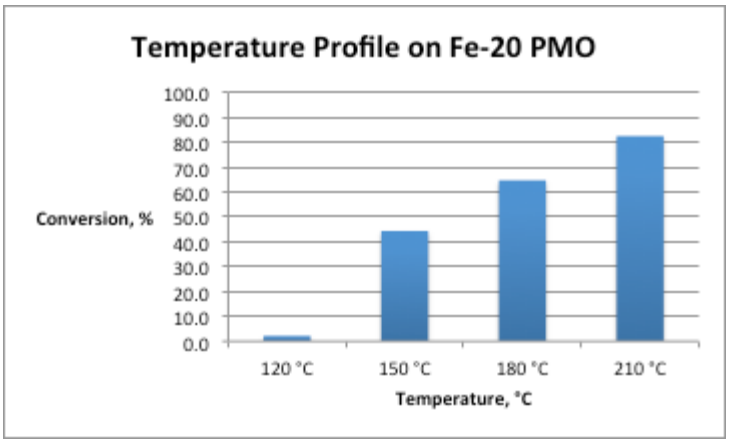

Figure 3.25 Effect of temperature on the transesterification conversion of soybean oil on Fe 20 catalyst at anhydrous condition.

www.manaraa.com

At 120 °C, there was ~2% conversion in 1hr, whereas at 210 °C it was 83% conversion in 1 hour. Experiments at 180°C on the Fe-20 catalyst produced approximately 65% conversion, and 83% conversion was obtained at 210 °C. The temperature profile in Figure 3.25 shows that these catalysts can tolerate high temperatures and maximum conversion can be achieved at a greater temperature, as also seen in literature (Macala et al. 2008). However, it is important to keep in mind that the higher temperatures will have higher costs associated with biodiesel production due to a more expensive reactor with insulation and also because the reactor would need to be rated for higher pressures to keep the methanol in the liquid phase; Liu et al. states than an increase in temperature from 120 to 170 °C can double the estimated costs while an increase from 60 to 120 °C would cause an increase of approximately 30% (Liu et al. 2007) and operating temperature should be selected based on economic and sensitivity analyses.

3.3.5 Transesterification of Soybean Oil with and without water

The results of water tests done on the most active catalyst, Fe-20, and three other porous metal oxides, Fe-10, Cu-20, and unsubstituted hydrotalcites are shown in Figure 3.26 - Figure 3.29.

www.manaraa.com

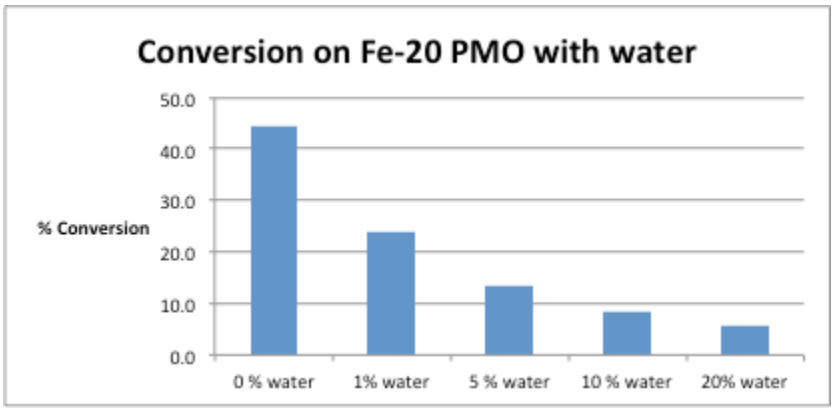

Figure 3.26 Effect of water content on the transesterification conversion of soybean oil on Fe 20 catalyst at 150°C.

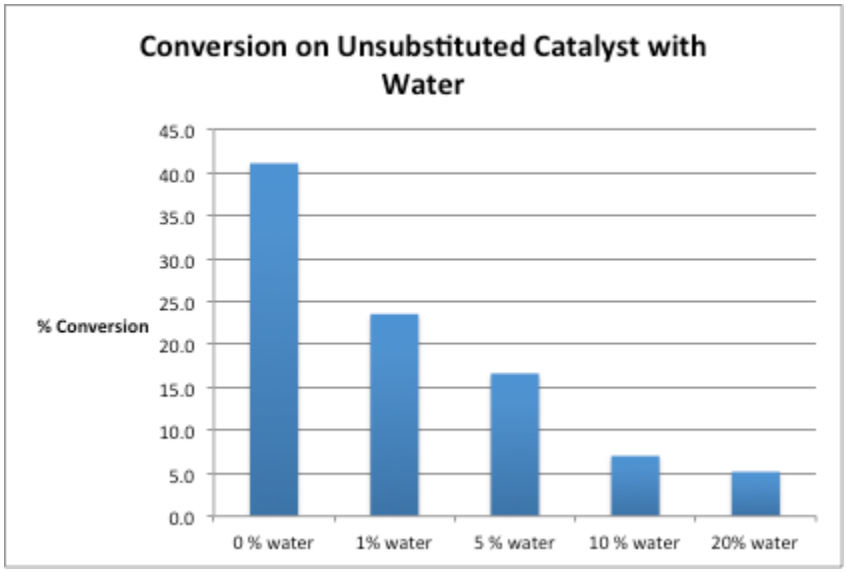

Figure 3.27 Effect of water content on the transesterification conversion of soybean oil on unsubstituted catalyst at 150°C.

www.manaraa.com

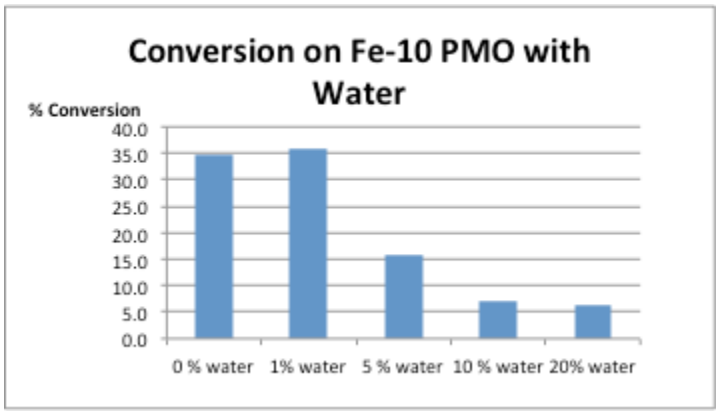

Figure 3.28 Effect of water content on the transesterification conversion of soybean oil on Fe 10 catalyst at 150°C.

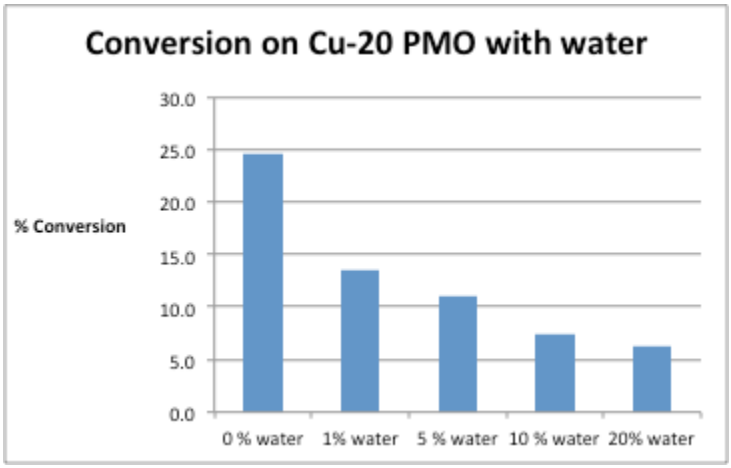

Figure 3.29 Effect of water content on the transesterification conversion of soybean oil on Cu 20 catalyst at 150°C.

In Figure 3.26, the most active, catalyst, Fe-20, appears to have the largest vulnerability to water. There is a 45% decrease in conversion from 44% conversion with no water present to 24% conversion with moisture content of 1%. It gives 6% conversion with water content of 20%, which is an 86% decrease in conversion from the original anhydrous condition. The decrease in conversion with the undoped catalyst as water

www.manaraa.com

content is increased is less steep than the Fe-20 but at 20% water content, its overall decrease in conversion is the same as Fe-20, at 88%.

The Fe-10 catalyst appeared to have a slight increase at 1% water content but had an 83% decrease in conversion from its original 35% conversion in the absence of water, to 6% conversion at 20% water content. The Cu-20 catalyst appears to have the highest tolerance of water at 20% water content. Similar to the Fe -20 catalyst, the conversion declined 45% when 1% water was introduced but declined 76% from 0% to 20% water content.

We presume that the effect of water acts in 3 ways: 1) deactivating the active site of the catalyst when present, 2) blocking access of the oil and methanol to the active sites, and 3) substituting the anions from the water molecules into the interlayer space, thus converting the porous metal oxide back to its precursor (hydrotalcite) which has less surface area and is not as active. This is the memory effect mentioned in the introduction (section 1.1.4). Liu et al. report that "water can also be formed by the reaction of brønsted sites with the alcohol molecules to produce the active methoxide species. Free fatty acids can then react with basic sites on the catalyst neutralizing them for further reaction. In addition, water itself may cluster around strong base sites and/or activated methanol thus limiting their contact with TGs through hydrophobic repulsion" (Liu et al. 2007) and this could be an occurrence to explain the deactivation.

Overall, all catalysts had similar patterns of conversion at the varying water compositions. However, the conversions obtained in the presence of water between 0 and 20% were poor as these water concentrations are nowhere close to the water concentration in sludge.

www.manaraa.com

Compared to work done by Di Serio et al. at 180°C showing no change in conversion at 10000 ppm (1%) water, our results obtained at 150°C indicate that there is a 41% decrease in conversion at the 1% water level of the unsubstituted hydrotalcite (Di Serio et al. 2007).

3.3.6 Kinetics on the Transesterification of Soybean Oil with and without water

There was some difficulty in completing the mass balance on the triglyceride component most likely due to strong adsorption on the catalysts. Thus, a mole balance on the remaining components: diglycerides, monoglycerides and FAMEs were used to calculate the mole balance for the triglycerides. Literature suggests pseudo first-order kinetics at large molar excess of alcohol (Noureddini and Zhu 1997, Kamarudin et al. 1998) and second-order kinetics at lower alcohol excess level based on work with kinetics of acid- and alkaline-catalyzed.

First-order kinetics was assumed for this study. The kinetic data obtained was fitted to a first order model based on the rate of decrease of triglyceride (TG). The rate constant was determined based on decreased amount of the triglycerides starting with the expression:

$$Rate = -d\frac{[TG]}{dt} \tag{3.8}$$

which can be written as

$$-d\frac{[TG]}{dt} = k[TG] \tag{3.9}$$

where [TG] is the concentration of triglycerides at a given time, t. Integrating,

$$ln[TG,0] - ln[TG,t] = kt \tag{3.10}$$

www.manaraa.com

Rearranging,

$$-\ln(\frac{[TG,t]}{[TG,0]}) = kt \qquad (3.11)$$

where *TG,0* is the initial species concentration at time zero, and *TG,t* is the concentration of the species at time, *t*. The apparent rate constant, *k*, was obtained by the linear fit of Equation 3.6 and the plots are shown in Figure 3.30.

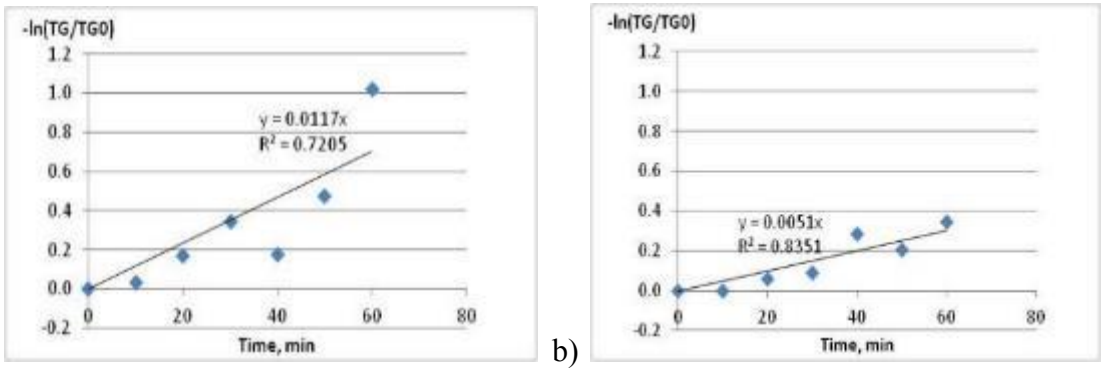

Figure 3.30 Kinetics for transesterification of soybean oil with: a) 0% water, b) 10% water

The rate constant, k, is equivalent to the slope. Converting to units of s^{-1}, rate constants of 1.95×10^{-4} s^{-1} ($\pm 2.4 \times 10^{-5}$) and 8.5×10^{-5} s^{-1} ($\pm 3.6 \times 10^{-5}$) were obtained for the reactions with 0% and 10% water respectively. This shows the significant effect of water on the rate constant as it decreased by more than 50% when water was added to only 10% composition.

Literature shows that a rate constant of 3×10^{-4} s^{-1} was obtained at 230 °C for the noncatalytic transesterification of soybean oil (Dasari et al. 2003). Under different reaction conditions, Chantrasa et al. report a power law rate expression of $-r = 3.43 \times 10^{-}$

www.manaraa.com

$^{5}C_{TCP}^{0.54}C_{MeOH}^{1.10}$ for the transesterification of tricaprylin (TCP) and methanol at 120 °C (Chantrasa et al. 2011).

Liu et al. reported that methanol had to be contacted with the catalyst before reaction because the reverse of contacting the oil with the catalyst first would impair the catalyst activity due to strong adsorption of triglycerides on the active sites. This was observed when they recognized differences in catalytic activity after comparing a methanol-catalyst pre-contacting case with a triglyceride-catalyst pre-contacting case at 120 °C. The methanol-catalyst pre-contacting case did not appear to have mass diffusion limitations, but the triglyceride-catalyst pre-contacting case did and was temperature dependent.

This was indicated in the conversion results by a test of the catalyst surface area before and after reaction. They ascribe these results to the fact that the triglyceride compounds in lipid feedstocks are large bulky molecules with linear saturated and unsaturated chains and also point out that adsorption is an exothermic reaction and is less favored thermodynamically at higher temperatures. (Liu et al. 2007). This phenomenon may have also affected the results.

3.4 Conclusions

In the methanol transesterification of soybean oil, porous metal oxides prepared from substituted and nonsubstituted hydrotalcites have high activity at 150°C. Using 8 different porous metal oxides, the highest conversions were produced by Fe-20, unsubstituted, and Cu-10 PMOs. Unsubstituted PMOs can be used since it gives a conversion that is only 4% less than the highest, Fe-20 PMO catalyst, and its precursor is available commercially. The effect of various concentrations of water on the

www.manaraa.com

transesterification of soybean oil using these catalysts was evaluated to determine their activity and usability in the presence of water. The unsubstituted hydrotalcite has the best tolerance for water at 1% water content with a 26% decrease in conversion, while the Cu-20 catalyst has the best tolerance for water at 20% water content.

In terms of kinetics, the rate of the reaction of 1.95×10^{-4} s^{-1} was decreased by more than 50% when 10% water was added

Generally, the results indicate that the porous metal oxides obtained from hydrotalcites can work well at high temperatures, but are significantly affected by water even at concentrations as low as 1% water during reaction. The most reactive catalyst (43% conversion) was Fe-20 PMO. Therefore, for best FAME yields, it is recommended to completely avoid the presence of water in the reaction as the rapid deactivation of these catalysts does not pose a benefit for the economics of the biodiesel production process from wet sludge which has significantly higher water content.

www.manaraa.com

3.5 References

Antunes, W. M., C. D. Veloso and C. A. Henriques (2008). "Transesterification of soybean oil with methanol catalyzed by basic solids." Catalysis Today **133**: 548-554.

ASTM "ASTM D6584 - 00 Test Method for Determination of Free and Total Glycerin in B-100 Biodiesel Methyl Esters By Gas Chromatography." ASTM International.

Birjega, R., O. D. Pavel, G. Costentin, A. Che and E. Angelescu (2005). "Rare-earth elements modified hydrotalcites and corresponding mesoporous mixed oxides as basic solid catalysts." Applied Catalysis a-General **288**(1-2): 185-193.

Brito, A., M. E. Borges, M. Garín and A. Hernández (2009). "Biodiesel Production from Waste Oil Using Mg−Al Layered Double Hydroxide Catalysts." Energy & Fuels **23**(6): 2952-2958.

Brunauer, S., P. H. Emmett and E. Teller (1938). "Adsorption of Gases in Multimolecular Layers." Journal of the American Chemical Society **60**(2): 309-319.

Chantrasa, A., N. Phlernjai and J. G. Goodwin Jr (2011). "Kinetics of hydrotalcite catalyzed transesterification of tricaprylin and methanol for biodiesel synthesis." Chemical Engineering Journal **168**(1): 333-340.

Cheng, W. P., J. Z. Zhao and J. G. Yang (2012). "MgAlFeCu mixed oxides for SO 2 removal capacity: Influence of the copper and aluminum incorporation method." Catalysis Communications **23**: 1-4.

Chisti, Y. (2007). "Biodiesel from microalgae." Biotechnology Advances **25**(3): 294-306.

Cunha, A. F., Y. J. Wu, J. C. Santos and A. E. Rodrigues (2012). "Steam reforming of ethanol on copper catalysts derived from hydrotalcite-like materials." Industrial and Engineering Chemistry Research **51**(40): 13132-13143.

Dasari, M. A., M. J. Goff and G. J. Suppes (2003). "Noncatalytic alcoholysis kinetics of soybean oil." JAOCS, Journal of the American Oil Chemists' Society **80**(2): 189-192.

Debecker, D. P., E. M. Gaigneaux and G. Busca (2009). "Exploring, Tuning, and Exploiting the Basicity of Hydrotalcites for Applications in Heterogeneous Catalysis." Chemistry-a European Journal **15**(16): 3920-3935.

Demirbaş, A. (2003). "Biodiesel fuels from vegetable oils via catalytic and non-catalytic supercritical alcohol transesterifications and other methods: a survey." Energy Conversion and Management **44**(13): 2093-2109.

Di Cosimo, J., V. K. Diez, M. Xu, E. Iglesia and C. Apesteguia (1998). "Structure and Surface and Catalytic Properties of Mg-Al Basic Oxides." Journal of Catalysis **178**.

www.manaraa.com

Di Serio, M., M. Ledda, M. Cozzolino, G. Minutillo, R. Tesser and E. Santacesaria (2006). "Transesterification of Soybean Oil to Biodiesel by Using Heterogeneous Basic Catalysts." Industrial & Engineering Chemistry Research **45**(9): 3009-3014.

Di Serio, M., R. Tesser, L. Pengmei and E. Santacesaria (2007). "Heterogeneous Catalysts for Biodiesel Production." Energy & Fuels **22**(1): 207-217.

Dufreche, S., R. Hernandez, T. French, D. Sparks, M. Zappi and E. Alley (2007). "Extraction of lipids from municipal wastewater plant microorganisms for production of biodiesel." Journal of the American Oil Chemists Society **84**(2): 181-187.

Gao, L., G. Teng, J. Lv and G. Xiao (2009). "Biodiesel Synthesis Catalyzed by the KF/Ca−Mg−Al Hydrotalcite Base Catalyst." Energy & Fuels **24**(1): 646-651.

Hattori, H. (1995). "Heterogeneous basic catalysis." Chemical Reviews **95**(3): 537-558.

Hutson, N. D. and B. C. Attwood (2008). "High temperature adsorption of CO2 on various hydrotalcite-like compounds." Adsorption-Journal of the International Adsorption Society **14**(6): 781-789.

Kamarudin, R., N. Nordin, N. Buang and S. Ahmad (1998). "A Kinetic Study on the Esterification of Palmitic Acid in Methanol." Pertanika Journal of Science & Technology **6**(1): 71-79.

Kargbo, D. M. (2010). "Biodiesel Production from Municipal Sewage Sludges." Energy & Fuels **24**(5): 2791-2794.

Kim, H.-J., B.-S. Kang, M.-J. Kim, Y. M. Park, D.-K. Kim, J.-S. Lee and K.-Y. Lee (2004). "Transesterification of vegetable oil to biodiesel using heterogeneous base catalyst." Catalysis Today **93–95**(0): 315-320.

Knothe, G., J. Van Gerpen and J. Krahl (2005). The Biodiesel Handbook, AOCS Press.

Kustrowski, P., L. Chmielarz, E. Bozek, M. Sawalha and F. Roessner (2004). "Acidity and basicity of hydrotalcite derived mixed Mg-Al oxides studied by test reaction of MBOH conversion and temperature programmed desorption of NH3 and CO2." Materials Research Bulletin **39**(2): 263-281.

Lee, D. W., Y. M. Park and K. Y. Lee (2009). "Heterogeneous Base Catalysts for Transesterification in Biodiesel Synthesis." Catalysis Surveys from Asia **13**(2): 63-77.

Lee, J.-S. and S. Saka (2010). "Biodiesel production by heterogeneous catalysts and supercritical technologies." Bioresource Technology **101**(19): 7191-7200.

Lestari, S., P. Mäki-Arvela, J. Beltramini, G. M. Lu and D. Y. Murzin (2009). "Transforming triglycerides and fatty acids into biofuels." ChemSusChem **2**(12): 1109-1119.

www.manaraa.com

Li, Z., Y. Song, J. Wang, Q. Liu, P. Yang and M. Zhang (2011). "Study of structural transformations and phases formation upon calcination of Zn–Ni–Al hydrotalcite nanosheets." Bulletin of Materials Science **34**(2): 183-189.

Lide, D. R. (2010 CD-ROM Version). CRC Handbook of Chemistry and Physics, CRC Press/Taylor and Francis, Boca Raton, FL.

Liu, Y., E. Lotero, J. G. Goodwin Jr and X. Mo (2007). "Transesterification of poultry fat with methanol using Mg-Al hydrotalcite derived catalysts." Applied Catalysis A: General **331**(1): 138-148.

Ma, F. and M. A. Hanna (1999). "Biodiesel production: a review." Bioresource Technology **70**: 1-15.

Macala, G. S., A. W. Robertson, C. L. Johnson, Z. B. Day, R. S. Lewis, M. G. White, A. V. Iretskii and P. C. Ford (2008). "Transesterification Catalysts from Iron Doped Hydrotalcite-like Precursors: Solid Bases for Biodiesel Production." Catalysis Letters **122**(3/4): 5p.

Mondala, A., K. W. Liang, H. Toghiani, R. Hernandez and T. French (2009). "Biodiesel production by *in situ* transesterification of municipal primary and secondary sludges." Bioresource Technology **100**(3): 1203-1210.

Moreira, C. R., N. Homs, J. L. G. Fierro, M. M. Pereira and P. Ramírez de la Piscina (2010). "HUSY zeolite modified by lanthanum: Effect of lanthanum introduction as a vanadium trap." Microporous and Mesoporous Materials **133**(1–3): 75-81.

Noureddini, H. and D. Zhu (1997). "Kinetics of transesterification of soybean oil." Journal of the American Oil Chemists' Society **74**(11): 1457-1463.

Parida, K., M. Satpathy and L. Mohapatra (2012). "Incorporation of Fe 3+ into Mg/Al layered double hydroxide framework: Effects on textural properties and photocatalytic activity for H 2 generation." Journal of Materials Chemistry **22**(15): 7350-7357.

Pavel, O. D., D. Tichit and I. C. Marcu (2012). "Acido-basic and catalytic properties of transition-metal containing Mg-Al hydrotalcites and their corresponding mixed oxides." Applied Clay Science **61**: 52-58.

Pérez-Ramírez, J., S. Abelló and Niek M. van der Pers (2007). "Memory Effect of Activated Mg-Al Hydrotalcite: *In Situ* XRD Studies during Decomposition and Gas-Phase Reconstruction." Chemistry - A European Journal **13**(3): 870-878.

Revellame, E., R. Hernandez, W. French, W. Holmes and E. Alley (2010). "Biodiesel from activated sludge through *in situ* transesterification." Journal of Chemical Technology and Biotechnology **85**(5): 614-620.

www.manaraa.com

Schuchardt, U., R. Sercheli and R. Vargas (1998). "Transesterification of Vegetable Oils: a Review." Journal of the Brazilian Chemical Society **9**(1): 199-210.

Tan, K. T. and K. T. Lee (2011). "A review on supercritical fluids (SCF) technology in sustainable biodiesel production: Potential and challenges." Renewable and Sustainable Energy Reviews **15**(5): 2452-2456.

Xie, W., H. Peng and L. Chen (2006). "Calcined Mg-Al hydrotalcites as solid base catalysts for methanolysis of soybean oil." Journal of Molecular Catalysis A: Chemistry **246**(1/2): 9p.

Yavuz, C. T., B. D. Shinall, A. V. Iretskii, M. G. White, T. Golden, M. Atilhan, P. C. Ford and G. D. Stucky (2009). "Markedly improved CO2 capture efficiency and stability of gallium substituted hydrotalcites at elevated temperatures." Chemistry of Materials **21**(15): 3473-3475.

Zhang, Y., M. A. Dube, D. D. McLean and M. Kates (2003a). "Biodiesel production from waste cooking oil: 1. Process design and technological assessment." Bioresource Technology **89**(1): 1-16.

www.manaraa.com

CHAPTER IV

EFFECT OF WATER ON THE ESTERIFICATION OF PALMITIC ACID USING METHANOL OVER ZEOLITE CATALYSTS

4.1 Introduction

Biodiesel is usually obtained by transesterification of oils to get the fatty acid methyl esters (FAMEs). In the case of a feedstock with high fatty acid and/or water content, however, a second method of generating biodiesel from oil without transesterification is to convert the lipids to free fatty acids by hydrolysis followed by esterification to obtain the fatty acid methyl esters (biodiesel).

Chapter 3 investigated the use of basic porous metal oxides to produce FAMEs from a wet feedstock. However, the PMOs were adversely affected by the presence of water that caused significant decrease in FAME yields. This chapter investigates the use of acidic zeolites to determine if these catalysts are more tolerant of high water content in the feedstock.

While transesterification is a 3 – step reaction of triglyceride with methanol to produce FAMEs and glycerol, esterification is a 1-step reaction of fatty acids with methanol to produce FAMEs and water as a by-product. Hydrolysis of oils and fats is a reversible reaction where water molecules split a triglyceride molecule to form fatty acids and glycerol. It is a 3-step mechanism where one molecule of triglyceride is hydrolyzed to 1 molecule of diglyceride and 1 mole of fatty acid (FA), in a continuous process until

www.manaraa.com

one molecule of monoglyceride is hydrolyzed to 1 molecule of glycerol and FA giving a total of 3 fatty acids. The transesterification, hydrolysis and esterification reactions are shown in Figures 4.1 - 4.3.

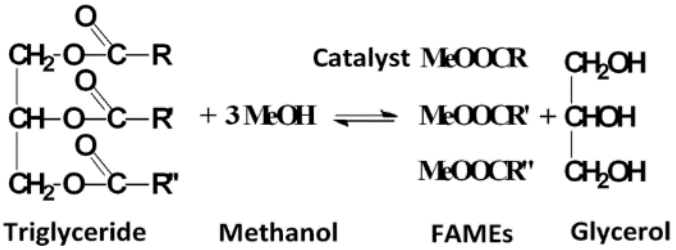

Figure 4.1 Transesterification reaction.

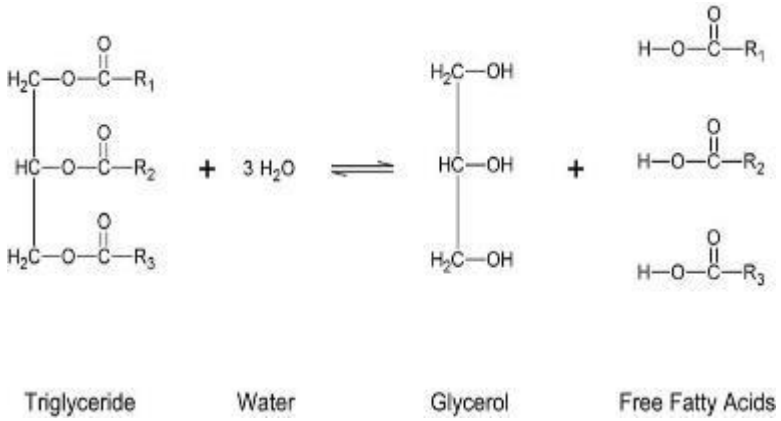

Figure 4.2 Hydrolysis of triglyceride.

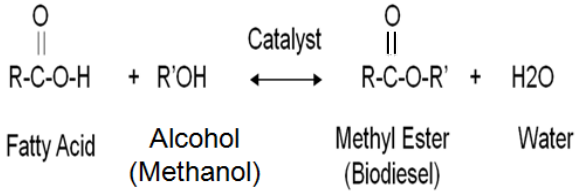

Figure 4.3 Esterification reaction.

www.manaraa.com

The benefits of using hydrolysis before esterification may be useful especially where there is a high water content initially in the feedstock. This water can be used for the hydrolysis.

4.1.1 Esterification Reaction

Direct esterification can be catalyzed or proceed in a spontaneous fashion depending on the miscibility of the reactants, the temperature and acidity of the carboxylic acid (Hoydonckx et al. 2004). The reactivity of alcohols and carboxylic acids toward esterification strongly depends on the steric hindrance of both the alcohol and carboxylic acid (Hoydonckx et al. 2004). As expected the larger the molecules are (e.g. tertiary alcohol and acid), the slower the reaction rates. While Lee and Saka point out that bronsted acid sites are more effective for FFA conversion (Lee&Saka 2010), Hoydonckx et al. report that the acid strength of the carboxylic acid has a minor effect on esterification reaction rate (Hoydonckx et al. 2004). In the esterification reaction, there is a lower mass transfer limitation since free fatty acids (FFA) are polar components and are miscible with methanol (Lee&Saka 2010). This makes the esterification of fatty acids faster than transesterification of triglycerides in addition to the fact that it is a one step reaction, while transesterification consists of three stepwise reactions (Aranda et al. 2008).

For the esterification reaction, an acidic catalyst is needed to reduce the reaction time, and this could be homogeneous or heterogeneous. Some of the most commonly used catalysts in industry for esterification include: sulfuric acid and phosphoric acid (Hoydonckx et al. 2004, Aranda et al. 2008). Aranda et al. were able to achieve over 90%

www.manaraa.com

conversion in 1 hour of reaction when 0.1% (w/w) sulfuric acid was used to catalyze the esterification of a fatty acid mix with anhydrous methanol at 130 °C (Aranda et al. 2008).

The use of heterogeneous catalysts has advantages over homogeneous catalysts that include: 1) ease of separation from products, 2) removes the corrosive environment, and 3) increases the purity of the products since side reactions are either eliminated or less significant (Xin et al. 2008). Di Serio et al. state that the reaction mechanism in esterification reactions promoted by solid acid Bronsted catalysts is similar to the homogeneous one (Di Serio et al. 2007)

With esterification particularly, the choice of catalysts is important because a basic catalyst might give challenges with soap formation upon reacting with the acid. Thus, an acid catalyst is needed.

One phenomenon to pay attention to in esterification is the reverse reaction (also called hydrolysis of esters) because excess water could push the reaction equilibrium backwards and reduce yield of FAMEs. Typically an excess of one of the reagents is used to shift the equilibrium, or water is continuously removed during the reaction by using codistillation or adsorption on drying agents (United States Environmental Protection Agency: Office of Wastewater Management June 2011).

4.1.2 Zeolites

In the search for a suitable catalyst for this process, it was determined that a heterogeneous, acidic catalyst that was tolerant to water was needed. Zeolites were chosen for this study because of the tunability of their acidicity and hydrophobicity.

Zeolites are microporous crystalline solids with well-defined, shape-selective structures usually containing silicon, aluminum, and oxygen in their framework (Chung

www.manaraa.com

et al. 2008). They are also known as molecular sieves and commonly used in applications such as ion-exchange, separations and catalysis (Larsen 2007). Zeolites are widely used in the petrochemical industry, especially in fluid catalytic cracking and hydrocracking, because of their numerous pores, active sites, thermal stability and shape selectivity (Askari et al. 2013).

A common characteristic used to distinguish zeolites is their silica-to-alumina (SiO_2/Al_2O_3) ratio, which gives an indication of the acidity (number of total acid sites) and hydrophobicity of the catalyst. The acidity (concentration of Bronsted acid sites) decreases with decreasing Al content so a catalyst with larger silica:alumina ratio has lower acidity (Chung et al. 2008, Shirazi et al. 2008, Lestari et al. 2009). Bronsted acid sites are more effective for the conversion of FFA and so the number of Bronsted acid sites is an important criterion for selecting a catalyst for esterification (Lee and Saka 2010).

As the acidity decreases with increasing Si/Al ratio, the hydrophobicity increases (Shirazi et al. 2008). Lower aluminum in the zeolite framework leads to a more hydrophobic catalyst because it decreases the hydrophilicity of the internal voids, thus increasing their adsorption capacity towards hydrophobic compounds (Navalon et al. 2009). Since the Si^{4+} and Al^{3+} ions in the zeolite framework are of similar ionic radius, the Al^{3+} ion can replace silicon in the zeolite lattice. When that happens, a negative charge is induced in the framework that requires a charge-balancing cation in the micropores. Consequently, the presence of the framework aluminum produces an increased affinity of the zeolite pores for water (Navalon et al. 2009). Thus, the catalyst with the higher silica/alumina ratio is more hydrophobic.

www.manaraa.com

There are various kinds of zeolites which include: ZSM-5 and Y zeolites, also known as Faujasite. Y zeolites are the most widely used in refineries especially in the area of fluid catalytic cracking because of its large pore openings and high surface area (Lestari et al. 2009). Pore size is reported to be 5.6 Å for ZSM-5 and 7.4 Å for zeolite Y (Jungsuttiwong et al. 2005). Structures are shown in Figure 4.4 below.

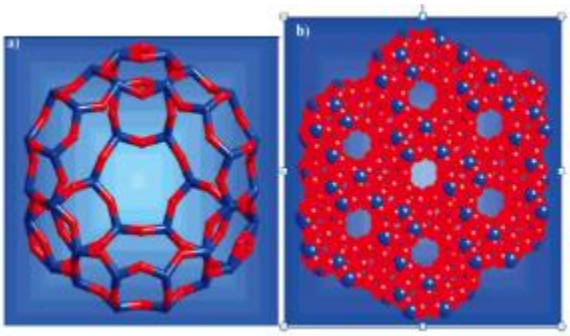

Figure 4.4 Structures of a) H-Y zeolite, and b) ZSM-5 zeolite (Larsen 2007)

An interesting phenomenon with ZSM-5 zeolites that will be examined is the knowledge that water molecules in ZSM-5 are driven out of the crystallites by polar organic molecules which substantiates the hydrophobicity of these catalysts (Ison and Gorte 1984, Kasai and Jones 1984). This phenomenon is significant and allows us to pose a hypothesis that the esterification reactions with water could proceed normally unless the temporary presence of water has hindered the activity of the catalyst. This could make the ZSM-5 catalyzed reactions have higher activity/conversion of fatty acids if methanol displaces any adsorbed water during reaction.

www.manaraa.com

The 5 zeolites used in this project are available commercially and were supplied by Zeolyst International. Their properties are given in Table 7.1. They are of the 2 basic types: H-Y and ZSM-5 zeolites.

Table 4.1 Properties of the 5 Zeolites proposed for use in this study

Property	**ZSM-5 (30) (CBV 3024E)**	**ZSM-5 (50) (CBV 5524G)**	**ZSM-5 (80) (CBV 8014)**	**H-Y (30) (CBV 720)**	**H-Y (80) (CBV 780)**
SiO_2/Al_2O_3 Mole Ratio	30	50	80	30	80
Nominal Cation Form	Ammonium	Ammonium	Ammonium	Hydrogen	Hydrogen
Surface Area	400 m^2/g	425 m^2/g	400 m^2/g	780 m^2/g	780 m^2/g

Source: (Zeolyst International)

The nominal cation form refers to the chemical state of the catalyst when supplied. A zeolite in ammonium form is inactive and needs to be calcined at 550°C (Jun et al. 2003) to convert it to the active hydrogen form (i.e. H-ZSM-5) before use. Conversely, the zeolite with hydrogen cation is already active and does not require calcination. The acidic sites responsible for the reaction are mainly inside the pores of the zeolites. This site (of the H^+) is characterized as a Brønsted acid site, and is responsible for the major catalytic activity of ZSM-5. Brønsted acids are proton donors, while Lewis acids are electron acceptors. Once the zeolite has been calcined, the name H-ZSM-5 is used hereafter to denote that it is in the acidic form. The value of x in H-Y (x) or H-ZSM-5 (x) henceforth denotes the SiO_2/Al_2O_3 ratio. The H-ZSM-5 Catalysts studied were: H-ZSM-5 (30, 50, 80) while H-Y catalysts studied were: H-Y (30, 80).

www.manaraa.com

4.1.3 Literature review on esterification catalysis

Catalysts such as Amberlyst-15 and sulfuric acid were investigated in the esterification of oleic acid with methanol for the effect of water. Park et al. varied the water content using 0, 1, 2, 5, 10 and 20% of oil at temperature conditions of 60 °C and 80 °C with oil to methanol ratios of 1:3 and 1:6 (Park et al. 2010a). They found that FAME content gradually decreased as initial water content increased (even as low as 1%) and the catalysts were not very tolerant of water, especially the Amberlyst 15 due to water poisoning the acidic sites and the reverse of the esterification reaction occuring (Park et al. 2010a).

Zeolites have also been used in esterification reactions (Kirumakki et al. 2004, Kirumakki et al. 2006). In terms of kinetic mechanisms, the Langmuir-Hinshelwood (LH) and the Eley-Rideal (ER) models are often used to correlate kinetic data for solid-catalyzed esterification reactions (Kirumakki et al. 2004) (Kirumakki et al. 2006, Bedard et al. 2012). These two models are derived based on the assumption that the rate-determining step is the surface reaction on the catalyst between two adsorbed molecules (LH) or between a molecule in the bulk solution and an adsorbed molecule (ER).

There are mixed reviews in the literature on whether the mechanism for the esterification of acids follows the Eley-Rideal or the Langmuir-Hinshelwood mechanism. Altiokka and Citak studied the esterification of acetic acid and isobutanol catalyzed by cation-exchange resin (Amberlte IR-120) between 318 K and 368 K and proposed that the mechanism occurred via a single-site Eley-Rideal (ER) pathway in which an adsorbed alcohol molecule reacts with an acid molecule in the bulk phase (Altiokka and Çitak 2003). Chu et al. researched the gas-phase esterification of acetic acid with ethanol and

www.manaraa.com

butanol over carbon-supported heteropolyacids and reported a Langmuir-Hinshelwood mechanism for the esterification with ethanol, but an Eley-Rideal mechanism for esterification with butanol (Chu et al. 1996). They ascribed the change in mechanisms to the different alcohols, stating that the steric hindrance of butanol could be the cause.

Both mechanisms have also been proposed for esterification on zeolites specifically as well. Kirumakki et al. investigated esterification of acetic acid with C_3 and C_4 alcohols on Hβ, HY, and HZSM-5 zeolites in the temperature range of 383 – 403 K and observed a decrease in initial rate with an increase in alcohol concentration which suggested that the alcohol blocks the adsorption of the acetic acid was needed for esterification to proceed (Kirumakki et al. 2006). These observations led to the conclusion that the esters are formed via an ER mechanism where an adsorbed acid molecule reacts with alcohol in the bulk phase.

The mechanism of the process is strongly dependent on the catalysts and reactants, and may vary depending on gas- or liquid-phase operations (Kirumakki et al. 2006). This study will evaluate the mechanism occurring during the esterification reaction on ZSM-5 zeolites and the effect of water.

The purpose of this project is to examine the feasibility of using sludge with high water content to produce biodiesel by investigating the effects of water on biodiesel yield and on the catalysts used in the esterification reaction. This is because the resistance of the solid acid catalysts to water poisoning is an important characteristic in determining their use for commercial esterification processes (Liu et al. 2006a). The effect of different water concentrations on esterification reactions and the mechanism behind it is an area that has been given minimal attention in the literature. The effect of water on

www.manaraa.com

esterification with respect to parameters like the reaction rate, reaction order, rate constants, activation energy, substrate conversion, and FAME yield were determined. Obtaining kinetic data and determining the reaction rate is essential for reactor design and scale-up feasibility studies.

4.2 Experimental Materials and Methods

4.2.1 Chemicals and Gases

All chemicals (palmitic acid (98%), methyl palmitate (95%), methanol (99.9%), sodium sulfate (99%), sodium chloride (99.9%), chloroform (99.8%), 1,3-dichlorobenzene (1,3-DCB) >99%, and butylated hydroxytoluene (BHT)) were purchased from Fischer Scientific (Pittsburgh, USA). Octadecane (C18) at 99% purity was obtained from Fisher Scientific (Pittsburgh, PA, USA) and used as an internal standard when FAMEs and fatty acids were and analyzed. The gases used (He, H_2, and N_2) were of high purity grade and were obtained from NexAir (Columbus, MS, USA). All chemicals, standards, and gases were used as received without further purification.

4.2.2 Apparatus

The experimental runs were performed in 60 mL borosilicate vials (I-Chem) placed in a heated aluminum block that was part of an Instatherm® block system (Ace Glass Inc., Vineland, NJ, USA) complete with a temperature controller that controls within ± 2°C. A stirring plate was used in conjunction with magnetic stir bars in the vial to provide agitation during the reaction.

www.manaraa.com

4.2.3 Procedures

4.2.3.1 Catalyst Preparation

The ZSM-5 catalysts were converted from the initial ammonium (NH_4^+) form to the active hydrogen (H-ZSM-5) form, releasing ammnonia (NH_3) by calcination at 550°C for 2.5 hours before use (Zeolyst). This site (of the H^+) is characterized as a Brønsted acid site, and is responsible for the major catalytic activity of ZSM-5. The H-Y zeolites were provided in the hydrogen form and did not need calcination but were heated at 250°C for 1 hour to drive off any moisture present before use. Both catalysts were stored in a desiccator until use.

4.2.3.2 Sample Preparation and Reaction Procedure for Esterification of Palmitic Acid

The kinetics of palmitic acid esterification was studied using 60 mL vials heated by the Instatherm® block system. The temperature controller was calibrated to produce a system temperature of 65 °C ± 1.5 °C in the vials. Batch runs were conducted at the same temperature for different sampling times. Eight 60ml vials were used for each reaction set with each vial used to represent the samples taken at each time interval for one reaction. One vial was used for monitoring internal temperature, where a thermometer was inserted through the vial's silicone/Teflon septum into the liquid in the vial to validate internal temperature. The remaining seven vials were labeled as: '0 min' (removed right before catalyst addition), '15 min', '30 min', '1 hr', '2 hr', '3 hr' (included catalyst and removed at the respective time points) and 'Control' (without catalyst and removed at 3 hour time point) samples.

www.manaraa.com

With this method for kinetics, there was a concern for methanol loss while opening the vial to add catalyst. This concern was addressed by weighing a known amount of methanol in the vial before heating to temperature (since methanol boils at 65 °C), and re-weighing it after opening the vial for 1 minute (assumed maximum time to add catalyst). It was determined that the difference in mass or methanol loss is insignificant.

At the start of the reaction, 0.5 g of palmitic acid was added to the 60 mL glass vials with 10 mL of solvent (either methanol only or a mixture of methanol and water) and a magnetic stirring bar (15 mm width × 10 mm length). Stirring rate was set to the respective speed. The vials were sealed and then placed in the already-heated Instatherm block and allowed to equilibrate to temperature set-point for an hour before adding the catalyst and starting the timer (Figure 4.5). When the vial contents have stabilized at the desired set point (by internal thermometer), (after about an hour), the 0 min sample was taken out and dropped into an ice bath to stop the reaction. (Initial GC analyses of the 0 min sample were conducted to confirm that there wasn't significant conversion in the first 1 hour of preheating. Literature also shows that the extent of reaction without catalyst is negligible compared to when it reacts with catalyst (Liu et al. 2006b).). Then 0.05 g of the appropriate calcined catalyst was quickly added to the respective labeled vials and sealed. The reaction timing was started using a countdown timer once the catalyst was placed in the vial. Samples were taken out at the designated time intervals of 0, 15, 30, 60, 120, and 180 minutes and placed in an ice bath to quench the reaction.

www.manaraa.com

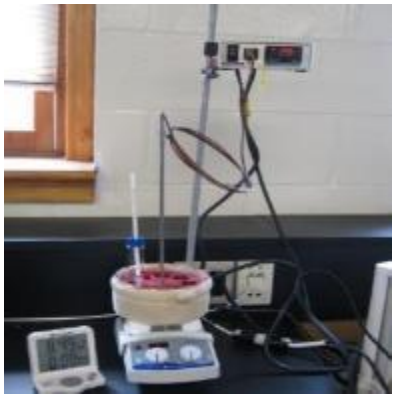

Figure 4.5 Reaction set-up for the esterification of palmitic acid with zeolite as catalyst

4.2.3.3 Extraction procedure - modified Bligh & Dyer method

The yield of FAME and conversion of fatty acid was determined after performing a chloroform extraction process using a modified form of the Bligh and Dyer method (Bligh and Dyer 1959) on each vial, and analyzing the resulting solutions by gas chromatography. This method uses a pre-determined mixture proportion of chloroform, water, and methanol to extract lipids into one phase (the chloroform phase) for easier identification.

The reaction products from each sample were extracted by first making up the vial contents to a mixture of 20 ml chloroform, 10 ml methanol, and 50 ml water (mass percentage ratio of chloroform:methanol:water being 34% : 9% : 57%), and combining in a 125ml separating funnel (Figure 4.6). After shaking vigorously and leaving to settle, the mixture separated into 2 phases with chloroform on the bottom and an aqueous layer containing methanol and water on top. The chloroform layer was withdrawn in a beaker containing a magnetic stirrer and sodium sulphate to dry any possible water molecules. The extraction was done twice (after confirming that a 3rd extraction was not needed) and

www.manaraa.com

the chloroform layers pooled, followed by vacuum filtration to remove the sodium sulphate. The extracted chloroform layer was diluted down to a maximum concentration of 400 μg/ml and subsequently analyzed by gas chromatography.

This ratio was selected when it yielded the best phase separation after testing a number of different ratios from the biphasic region of the chloroform-methanol-water phase diagram.

Prior to this, the method of using a rotary evaporator to remove the methanol content from the reaction products followed by dissolution in chloroform was tested. However there were challenges with getting the water content out especially at higher initial water concentrations, and concerns that the heating during evaporation could drive the reaction forward if there was any catalyst in mixture and thus invalidating the accuracy of the results.

Figure 4.6 Sample extraction in a separating funnel

www.manaraa.com

4.2.4 Analytical Method

4.2.4.1 Gas chromatography (GC) analysis

The fatty acid and FAME in the chloroform phase were analyzed using the Agilent GC 6890N gas chromatograph equipped with a flame ionization detector (GC-FID) (Agilent, Santa Clara, CA, USA). Octadecane, C18, was added to the chloroform diluent as an internal standard. The column used was a Restek Stabilwax-DA capillary column (Restek, Bellefonte,PA, USA) having dimensions of 30m x 0.25mm ID and 0.25 µm film thickness. Analyses were conducted using helium as a carrier gas with a constant injector temperature of 260 °C in splitless mode. Sample injection volume was 1 µL. The FID temperature was held at 260 °C for the duration of the analysis. The GC oven (Figure 4.7) was programmed at an initial temperature of 50 °C, held for 2 min, ramped up to 250 °C at 10 °C min^{-1}, and held for 18 min, giving a total of 40 min analysis time. The yield of methyl palmitate and conversion of palmitic acid were calculated using these results.

Figure 4.7 HP 6980 series GC system with DA Stabilwax column for quantifying FAMEs and FFA Initial and final temperatures of 50 °C and 250 °C

www.manaraa.com

4.2.4.2 Standard preparation and dilution

Palmitic acid and methyl palmitate purchased from Fisher Scientific (Pittsburgh, PA, USA) were used to prepare 5-level calibration standards in Chloroform with C18 as internal standard. All calibrations were corrected for purity. Calibrations based on maximum and zero conversion will be completed for palmitic and oleic acids and their esters at concentrations of 500, 250, 125, 62.5, 31.25, 15.625µg/ml.

Conversion of palmitic acid was calculated using the Equation 4.1 below:

$$Conversion\ of\ PA = \left(\frac{C_{PA0} - C_{PA}}{C_{PA0}}\right) \times 100 \quad (4.1)$$

FAME yield was calculated using the Equation 4.2:

$$FAME\ yield\ (\%) = \left(\frac{Mass\ of\ FAME\ produced}{Initial\ mass\ of\ PA\ reacted}\right) \times 100 \quad (4.2)$$

4.2.5 Experimental Design

Experiments were designed by varying temperature, mixing speed, zeolite catalyst type, initial water content and reaction duration to obtain various kinetic parameters. Three total temperatures of 55, 65 and 85°C were studied; additional water concentrations of 10, 20, 50, 70, and 90% were also investigated. The investigative procedure in this study include: 1) screen 5 purchased zeolite catalysts for most active, 2) check for mass transfer limitations, 3) evaluate effect of water on the best catalyst using 4 water compositions: 0%, 10%, 20%, 50%, 70%, and 90% and determine maximum concentration of water that catalyst will tolerate while producing relatively high FAME yield, and the influence of the silica:alumina (SiO_2/Al_2O_3) ratio, 4) determine activation energy and other kinetic parameters like rate constants, 5) determine heterogeneous

www.manaraa.com

catalytic rate laws and constants, and 6) propose reaction mechanisms with and without addition of water.

Triplicate runs were conducted for each reaction condition except where noted.

4.2.5.1 Catalyst Screening

For catalyst screening, the five zeolite catalysts discussed in the introduction were studied at the same reaction condition of 0% water, 0.5 g palmitic acid (PA), 10 mL methanol and 0.05 g catalyst at 65°C and 700 rpm to determine the zeolite catalyst(s) with highest activity. Palmitic acid was used as a surrogate because it is one of the predominant fatty acids in sludge. Composition is 56% in sewage lipids(Angerbauer et al. 2008). Catalysts were screened and the catalyst with the highest conversion was selected after normalizing with differing surface area values.

4.2.5.2 Investigation of External Diffusion significance

Although esterification has a lower mass transfer limitation than transesterification due to the fact that fatty acids are polar and more miscible with methanol, the reaction still needs to be investigated for the presence of any of those effects. External diffusion limitation has been shown to be directly related to stirring speed (Müller 2001). To ensure that the reactions were kinetically-limited and not mass transfer limited, the esterification reaction was conducted on the 80:1 ZSM-5 catalyst at 3 different stirring speeds: 600, 700, and 900 rpm, and the same reaction conditions of 65°C.

www.manaraa.com

4.2.5.3 Effect of water on yields and kinetics

The esterification reaction of palmitic acid with methanol was studied at different levels of initial water content varying from 0%, 10%, 20%, 50%, 70% and 90% water at the same reaction conditions of 65°C and 700 rpm for 3 hours. Additional reactions were also conducted at 55 °C and 85 °C using 0% and 50% water added initially.

For reactions investigating the effect of water, the appropriate combination of water and methanol was used according to Table 4.2 below to keep the total volume constant at 10 ml. All vials in a reaction set heated at the same time had the same starting water concentration. The reaction mixture was continuously stirred during the reaction using magnetic stirrers.

Table 4.2 Composition and volumes of water and methanol for the esterification of palmitic acid over zeolite

Water composition, % volume	Water volume (ml)	Methanol volume (ml)	Total volume (ml)
0	0	10	10
10	1	9	10
20	2	8	10
50	5	5	10
70	7	3	10
90	9	1	10

Based on the yield and conversion results, a reaction mechanism was proposed. The phenomenon of methanol driving water out of the catalyst pores will be examined at this point and it will be determined if water affects ester production negatively at all

www.manaraa.com

concentrations or if it improves ester yield at some concentrations, the maximum concentration would be beneficial in the production of biodiesel from sludge.

4.2.5.4 Influence of reaction time

The esterification reaction was conducted in the temperature range of 55 – 85°C while keeping the PA, methanol and catalyst concentrations constant. Timed samples taken at 0 min, 15 min, 30 min, 1 hr, 2 hr, and 3 hr were evaluated based on FAME yields. Also, added 5 hr and 7 hr reaction times to two reaction conditions to evaluate the effect.

4.2.5.5 Influence of reaction temperature

The esterification reaction was studied kinetically using the best catalyst, H-ZSM-5 (80), in the temperature range of 55 – 85°C while keeping the PA, methanol and catalyst amounts constant at 0.5g PA, 10ml methanol, and 0.05g catalyst for the 0% water composition and 0.5g PA, 5 ml methanol, 5 ml water, and 0.05g catalyst for the 50% water composition. The temperature dependency of the rate constants obtained from the data at 55 °C, 65°C, and 85 °C was used to determine the activation energy for this reaction using the Arrhenius equation at both conditions.

4.2.5.6 Effect of initial amount of fatty acids

Since all reactions had been conducted using 0.5g of palmitic acid, a set of duplicate reactions using 0.25g palmitic acid, 10 ml methanol, 0.05g catalyst, 700 RPM at 65°C and 0% water was conducted to determine the effect of changing concentrations on yields.

www.manaraa.com

4.2.6 Kinetics and mechanism determination

The Langmuir-Hinshelwood (LH) and Eley-Rideal (ER) mechanisms as well as some modified forms were considered as heterogeneous models that could predict the rate law of the reactions. The kinetic rate law with the best fit was chosen and optimum kinetic parameters can be used for process design.

Fatty acid concentrations were determined from samples taken at different reaction times via GC analysis and used to calculate the reaction rate. Experimental data was tested using the method of iterative non-linear regression in Microsoft® Excel to fit the experimental data to the proposed model function. The aim of this data fitting procedure was to minimize the mean square differences between the experimental values of the rate (r_{exp}) and the calculated values of the rate (r_{calc}), as seen in Equation 4.3. The Microsoft® Excel 'Solver' tool was used.

$$\text{Minimize } y = \sum(r_{calc} - r_{exp})^2 \tag{4.3}$$

The experimental rate was obtained using Equation 4.4:

$$r_{exp} = \frac{dC_a}{dt} \tag{4.4}$$

where C_a = concentration of acid at a given time, t. A plot of C_a vs. t was created for each data set and a second-order trend line was fitted to the data. The derivative of the quadratic equation of the trend line was used to determine the experimental rate ($\frac{dC_a}{dt}$).

www.manaraa.com

4.3 Results and Discussion

4.3.1 Catalyst Screening

Screening tests based on the highest FAME yields were conducted using the 5 catalysts in Table 1 to pick the best catalyst. The results are presented in Figure 4.8.

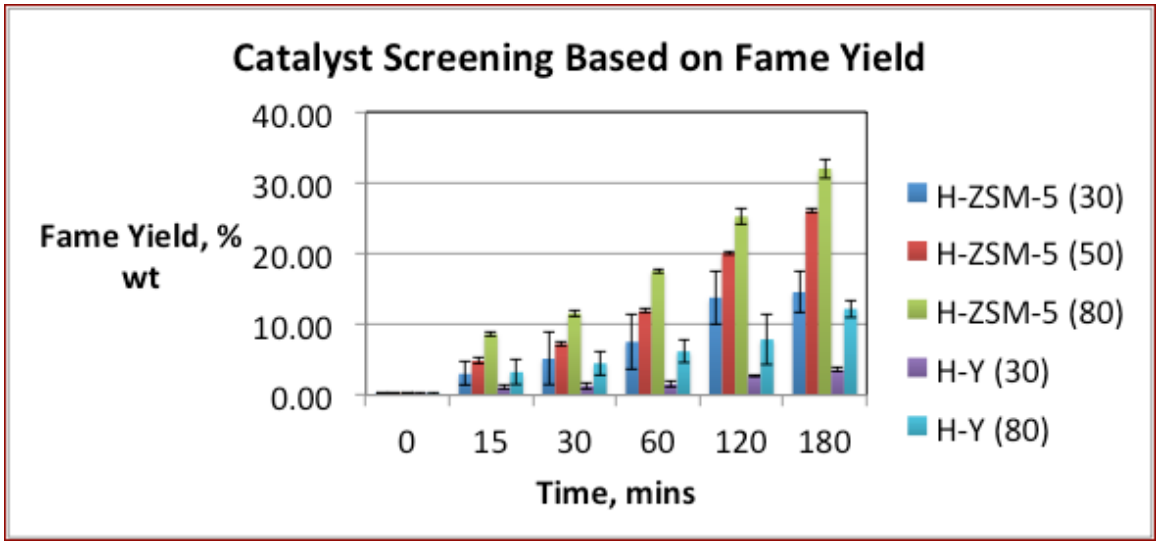

Figure 4.8 Catalyst screening results on esterification of palmitic acid with methanol effect of catalyst type – Methanol:Palmitic Acid = 127:1 (molar ratio), 0.05 g catalyst (H-ZSM-5 (80)), reaction temperature 65°C, 0% water, reaction time 0 - 3 h.

The results show that the best catalyst for the esterification reaction from the screening is the H-ZSM-5 (80) and it was significantly different in FAME yields from the other catalysts tested. The yields were normalized for the different catalyst surface areas. The yield of FAMEs decreased in the order:

H-ZSM-5 (80) > H-ZSM-5 (50) > H-ZSM-5 (30) > H-Y (80) > H-Y (30)

Since the activity of zeolites is directly related to the concentration of the acid sites (Zheng 2002), the initial hypothesis was that the H-ZSM-5 catalyst with the lowest silica/alumina ratio, H-ZSM-5 (30), could produce the highest conversion since it has the

www.manaraa.com

highest acidity. Nonetheless, there is the factor of the degree of hydrophobicity of the catalyst to consider. Literature shows that lower aluminum in the zeolite framework leads to a more hydrophobic catalyst. From these results it appears that the effect of higher acidity, based on lower SiO_2:Al_2O_3 ratio, was not significant in producing higher FAMEs yields. Rather, the results imply that the differences in conversion can be attributed more significantly to the hydrophobicity of the catalysts. From studying the H-ZSM-5 catalysts, it is seen that the FAMEs yields increased significantly as the SiO_2/Al_2O_3 increased from 30 to 80, which is the same trend of increasing hydrophobicity. The need for the hydrophobicity comes into play as water is produced from the forward reaction and could compete with the palmitic acid and methanol for the active catalyst sites. Although the catalysts with lower silica:alumina ratios are higher in acidity (number of acid sites), the effect of hydrophobicity seems to dominate as the catalysts with 80:1 silica:alumina ratios produced more FAMEs. This is presumed to be due to their higher water resistance (or preference for organic compounds) due to strong hydrophobic properties resulting from the high SiO_2/Al_2O_3 ratio. This is also corroborated by work done by Jun et al. who conducted a study in search of a zeolite with high water tolerance that could be used in the production of dimethyl ether by a methanol dehydration process which inherently produces a lot of water (Jun et al. 2003). They found that of all the zeolites tested, H-ZSM-5 zeolites had high water-resistance in methanol. The catalysts they tested included H-Y (12, 60) and H-ZSM-5 (30, 50, 80).

Between the 2 types of zeolites, H-ZSM-5 and H-Y, the H-Y zeolites have significantly lower FAMEs yields at both the 30:1 and 80:1 ratios. This is important because the H-Y zeolites are reported to have almost twice the surface area of the H-

www.manaraa.com

ZSM-5 catalysts and the pore size of the H-Y zeolite is larger than the H-ZSM-5 zeolite. Referring to the work of Ison & Gorte, it is possible that the displacement of water molecules from the acid sites by methanol on the H-ZSM-5 catalysts is what makes the H-ZSM-5 zeolites more active than their H-Y counterparts in the esterification reactions (Ison and Gorte 1984).

A control test was run to evaluate the yield in the absence of catalyst and it was found to produce only 1% FAMEs after reacting for the same time of 3 hours at 65°C.

To ensure that the palmitic acid molecules could get access to the catalytic active sites, calculations were made on Spartan® (a molecular modeling software) to determine palmitic acid dimensions. Palmitic acid width was estimated at 3.05 Å and its length at 21.68 Å, which indicates that the palmitic acid molecule can enter both catalyst pores if going in end-first. Pore size is reported to be 5.6 Å for ZSM-5 and 7.4 Å for zeolite Y (Jungsuttiwong et al. 2005).

4.3.2 Investigation of External Diffusion significance

The reactions at the different speeds produced FAMEs yields and rate constants that were not significantly different, thus indicating that the reaction was kinetically-limited. The first order rate constants were calculated and compared. Figure 4.9 shows the rate constants were not significantly different and Figure 4.10 below shows the yield of FAMEs over time for each speed at the same reaction conditions mostly overlapping. At these three different mixing rates, there appears to be no mass transfer limitations since there are only slight variations between the rate constants. Thus, limitation due to external diffusion or mass transfer can be neglected.

www.manaraa.com

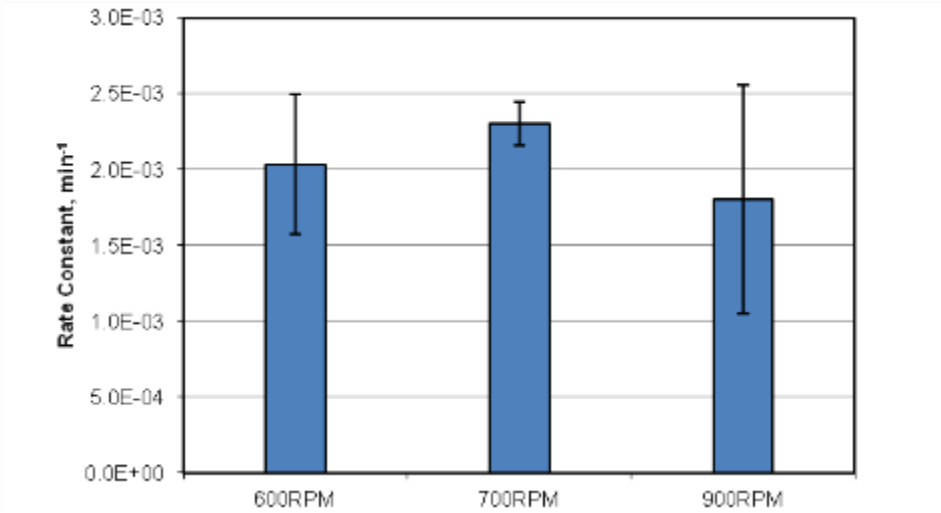

Figure 4.9 Rate constants as a function of mixing speed for the esterification of palmitic acid using H-ZSM-5 (80)

65°C, Methanol:Palmitic acid =127:1 (molar ratio), 0% water.

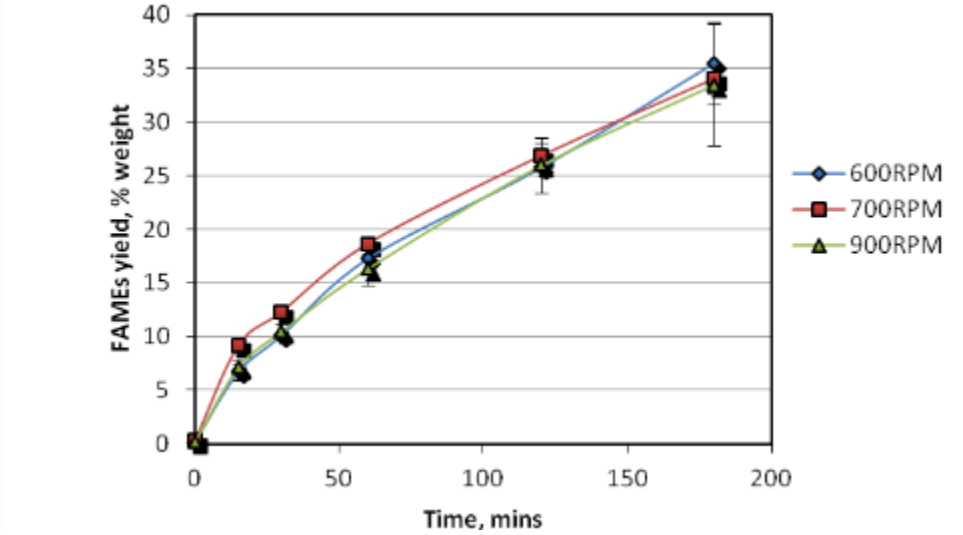

Figure 4.10 FAMEs yield at different mixing speeds for the esterification of palmitic acid using H-ZSM-5 (80)

65°C, Methanol:Palmitic acid =127:1 (molar ratio), 0% water.
* Lines are not from a model and were only added to show the trend

www.manaraa.com

4.3.3 Effect of water on yields and conversions

The esterification reaction was studied at different levels of initial water content varying from 0 – 90% water at the same reaction conditions of 65°C, 700 rpm for 3 hours. Figure 4.11 below shows the comparison of FAME yields at each water level and varying times.

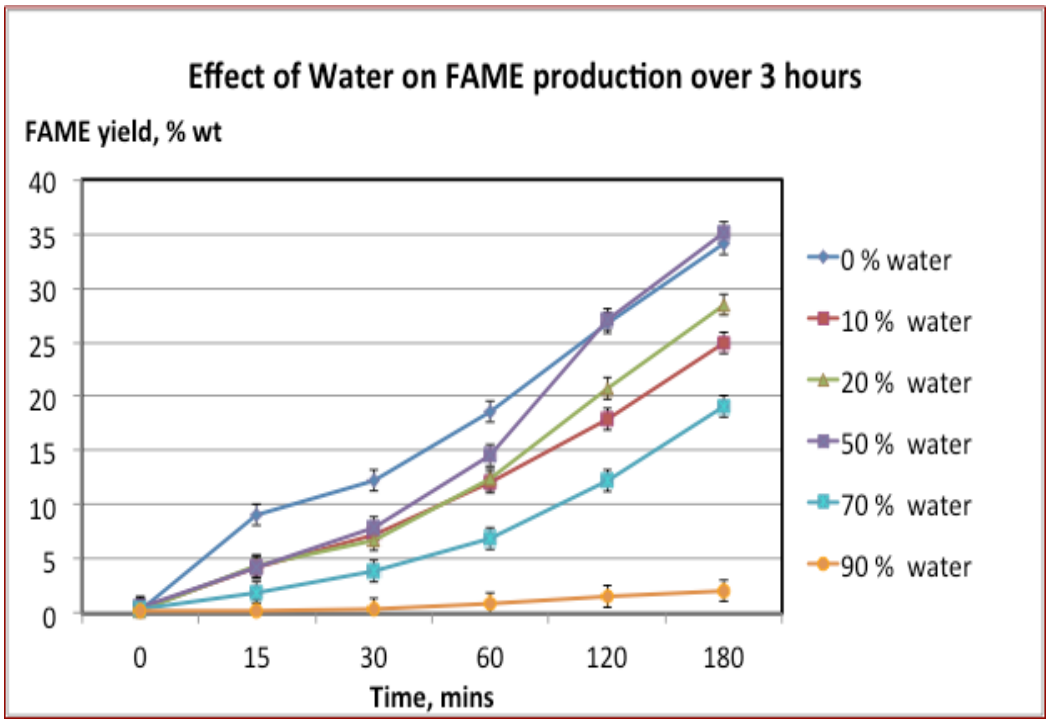

Figure 4.11 Effect of water on esterification of Palmitic acid over H-ZSM-5 (80) for 3-hour reaction time at 65°C and 700 rpm.

* Lines are not from a model and were only added to show the trend

In Figure 4.11, we see that addition of water affected the reaction negatively (compared to 0% water added) at all water levels except the 50% water content reaction. While the 0% water reaction showed the highest initial activity in the first hour of reaction, the presence of water in all other reactions reduced the FAME yields

www.manaraa.com

significantly from the beginning of the reaction. The effect of 10%, 20% and 50% water were not significantly different in FAME yields during the first 30 minutes. However, with longer reaction time, the 50% water reaction increases in activity and achieves the same FAMEs yield as the 0% water reaction after 2 hours. Testing other water levels higher than 50% had a drastically negative impact on FAMEs yield, indicating that 50% water is the optimum water content for these reactions. Overall, the FAME yield decreases with increasing water concentration.

Since this was an unexpected occurrence, further experiments were conducted for the 0% and 50% water content reactions for reaction times of 5 and 7 hr to examine if the trend would continue after a longer duration. The result is shown in Figure 4.12, where it is seen that the yield from the 50% water reaction does overtake that in the absence of water as reaction times increased. This is explained with the mechanism in Section 4.3.8.

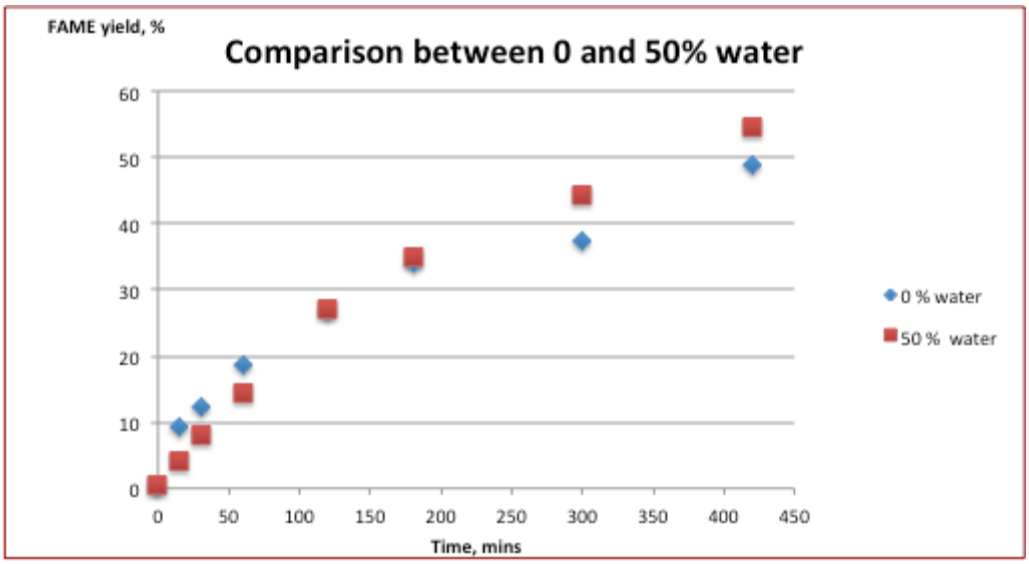

Figure 4.12 Effect of water on esterification of Palmitic acid over H-ZSM-5 (80) for 5- and 7-hour reaction times at 65°C and 700 rpm.

* Lines are not from a model and were only added to show the trend

www.manaraa.com

Interestingly, in a sensitivity analysis conducted by Revellame et al. (Revellame et al. 2011) to determine how the break-even biodiesel price changes with moisture content of the feedstock for producing biodiesel from wet activated sludge, they found that 50% moisture content was the optimum for producing the lowest break-even biodiesel price.

Possible reasons why water helps at 50%:

1. Regenerates the catalyst: It could be that there is an intermediate formed that blocks the catalyst's active site and thus inhibits formation of the ester. Then possibly the presence of water at 50% helps remove that intermediate and frees up the acid site for methanol to react with palmitic acid (since methanol also displaces the water according to Ison and Gorte (Ison and Gorte 1984)). This may not have happened for water levels less than 50% because the water content helped form the intermediate but was not enough to remove the intermediate from the acid sites. And at water concentrations higher than 50%, the water was present in such a high amount that the methanol could not displace all of it from blocking the catalytic active sites and the reverse reaction had to take place. In the study by Jun et al. to identify a zeolite with high water-tolerance for use in the methanol dehydration process, they found that coke formation (from polymerization of olefins on strong acid sites) blocked the supercage of the large-pore H-Y zeolite catalysts, unlike the medium-pore ZSM-5 catalysts which formed coke deposits much slower under comparable conditions and has no supercage (Jun et al. 2003). In studying the effect of

www.manaraa.com

water when added during the reaction, they found that all H-ZSM-5 catalysts tested were regenerated by adding water. This was attributed to the fact that water can remove the carbon deposited on the pore of the H-ZSM-5 catalysts but not in the H-Y catalyst because they have a supercage that gets blocked by the carbon deposit and thus prevents water from entering to remove deposits. They also had activation energy increase with the addition of water, possibly due to the blocking of the active sites by water (Jun et al. 2003), and thus, a similar occurrence could be taking place here.

2. At 50% water content, the effect of the reverse of esterification reaction is not as pronounced because there is roughly equal amount of reactant (methanol) and product (water) on both sides of the reaction, so the reaction proceeds as in the absence of water after about 2 hours have elapsed.

The initial hypothesis that the reaction could proceed normally because water was displaced by methanol was false. It is possible that the temporary presence of water has hindered the activity of the catalyst at certain water concentrations.

Hoydonckx et al. report that zeolites are active catalysts for esterification but they catalyze the reaction slowly due to steric hindrance of the bulk fatty acids, or due to poor adsorption inside the zeolite pores (Hoydonckx et al. 2004).

4.3.4 Influence of reaction time

The esterification reaction was carried out in the temperature range of 55 – 85°C while keeping the PA, methanol and catalyst concentrations constant. Equilibrium was

www.manaraa.com

not reached at the maximum reaction time studied (3 hours) because conversion was still increasing and had not leveled off. Additional reactions to obtain samples at 5 and 7 hours reaction times at 0 and 50% water content reactions were conducted to determine if the trend of the FAME yield in the 50% water reaction increased past that of the 0% water reaction continued on the 8014 catalyst. For reactions without water added initially, it was observed that the conversion of palmitic acid increased from about 12% in the first 30 minutes to around 35 % in 3 hours. When the reaction time was extended to 7 hours, the FAME yield got as high as 49 %, but still was not near completion, which indicates how slow this acid-catalyzed reaction is. For the 50% water reaction, the palmitic acid conversion was only about 8% at the 30 min point, increased to 35 % also by the 3 hr time point and ended up with a slightly higher conversion of 55 % after 7 hours of reaction time. The data indicate that the reaction with 50% water content continues to produce higher conversion than the 0% water reaction after 3 hours almost like the water at that content starts to serve as an acidic catalyst.

We also observed that for longer reaction times, the presence of additional water favored the production of FAMEs. For example, the 10% and 20% water reactions started off with the same FAMEs yield in the first 1hr and after that, the 20% water reaction had higher yield of FAMEs than the 10% water reaction. This was contrary to our initial hypothesis that adding water as a reactant would promote the backward reaction of ester hydrolysis (instead of the forward reaction of esterification) and thus reduces the ester yield. However, that observation was not noticed until after using greater than 50% water content initially. As seen in Figure 4.11, the 70% and 90% water content reactions dropped off in FAMEs yield significantly.

www.manaraa.com

4.3.5 Influence of reaction temperature

Activation energy was calculated on the reaction with best catalyst at 0% water and best water composition of 50% water.

The esterification reaction was studied using the best catalyst, H-ZSM-5 (80), in the temperature range of 55 – 85°C while keeping the PA, methanol and catalyst concentrations constant. It was observed that the production of methyl ester and the first order rate constants increased with increase in reaction temperature as expected. The increase in methyl ester production in the absence of additional water as a reactant was 67% when temperature was increased from 55°C to 65°C and increased by 104% when temperature was increased from 65°C to 85°C; for an overall rate constant increase of 240% from 0.0017 min^{-1} at 55°C to 0.0058 min^{-1} at 85°C.

The activation energy for the esterification reaction on H-ZSM-5 (80) at 0% water was calculated and found to be 39.3 kJ/mol from the plots in Figure 4.13and Figure 4.14 below.

www.manaraa.com

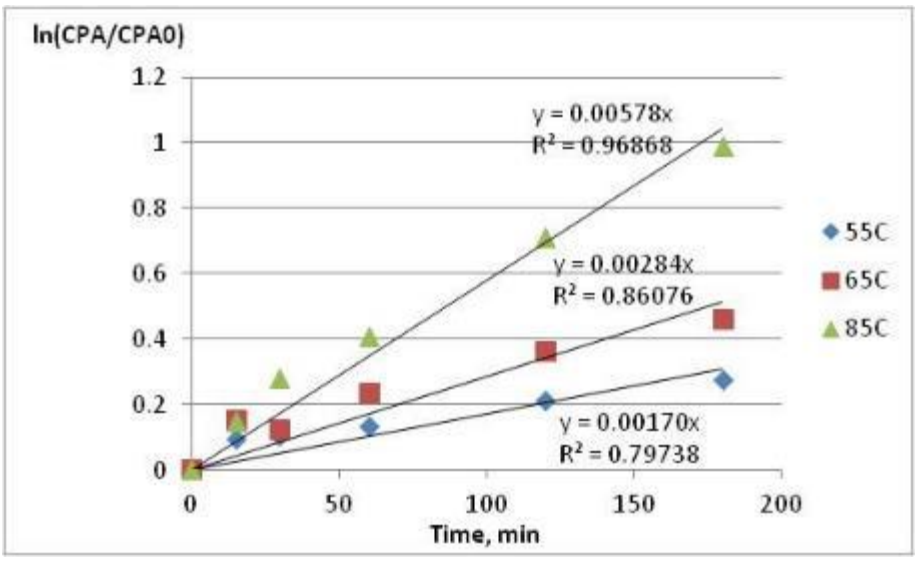

Figure 4.13 Linearized plots for the determination of the first order rate constants for the esterification of Palmitic acid using H-ZSM-5 (80)

0% water, 700 rpm.

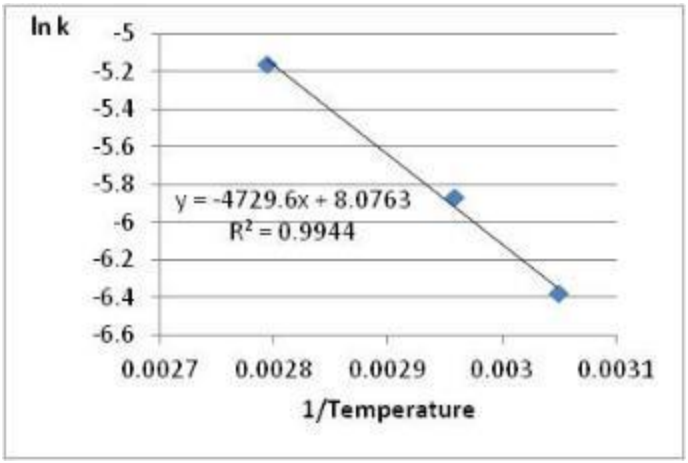

Figure 4.14 Arrhenius plot for activation energy determination on the esterification of Palmitic acid using H-ZSM-5 (80)

0% water, 700 rpm.

Since the optimum water for this reaction is 50%, the activation energy was calculated for this condition and found to be higher at 64.8 kJ/mol (Figure 4.15 and

www.manaraa.com

Figure 4.16). This correlates with the findings of Jun et al. (Jun et al. 2003) of a higher activation energy when water was added.

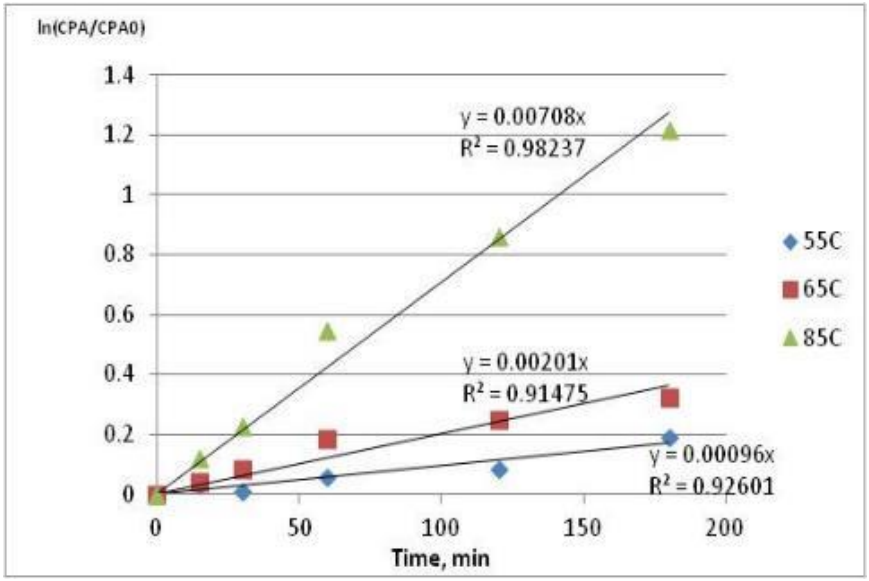

Figure 4.15 Linearized plots for the determination of the first order rate constants for the esterification of Palmitic acid using H-ZSM-5 (80)

50% water, 700 rpm.

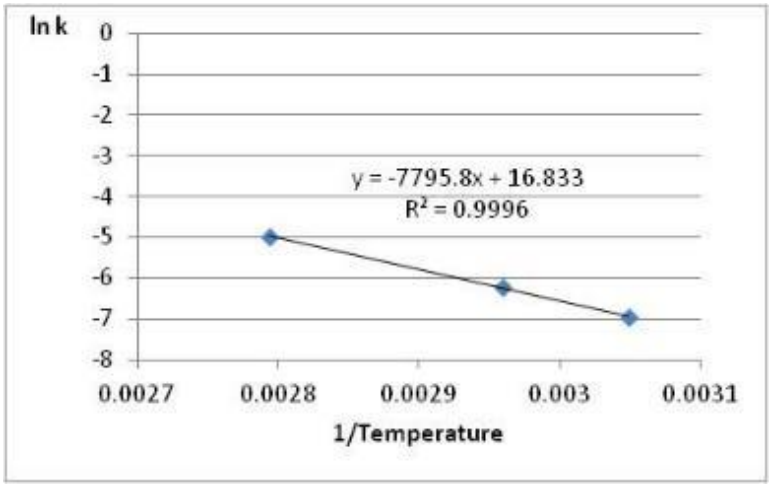

Figure 4.16 Arrhenius plot for activation energy determination on the esterification of Palmitic acid using H-ZSM-5 (80)

0% water, 700 rpm.

www.manaraa.com

The activation energy of 39.3 kJ/mol compares very well with the 35.2 kJ/mol obtained by Kamarudin et al. (1998) using homogeneous acidic thionyl chloride ($SOCl_2$) as catalyst for palmitic acid esterification (Kamarudin et al. 1998), and 40.8kJ/mol using HZSM5 zeolites by Kirumakki et al. (2004) (Kirumakki, 2004). The increase in activation energy from the 0% water reaction to the 50% water reaction indicates more competition for the reactant molecules to access the active sites on the catalyst with the increase in volume of water initially. The activation energy also indicates that there are no issues with internal diffusion limitations.

4.3.6 Effect of initial amount of fatty acids

Upon testing a lower starting amount of palmitic acid (0.25g), it was observed that the reaction rate and FAME yields increased (Figure 4.17). The increase in rate when a lower amount of fatty acid was used could indicate that the adsorption of methanol is an important step of the mechanism as it also indicates the presence of more competition between palmitic acid and methanol for catalytic sites at the higher concentration of palmitic acid. Otherwise, more fatty acid should have produced more yields. Or another possible and more likely reason for this result is that a higher starting concentration of palmitic acid could have lower yields because more water is produced in that reaction that could adsorb on the zeolite site and compete with palmitic acid adsorption and reaction on the catalytic site, thus affecting the yields. This explanation is substantiated by the proposed model that is identified in the next 2 sections.

www.manaraa.com

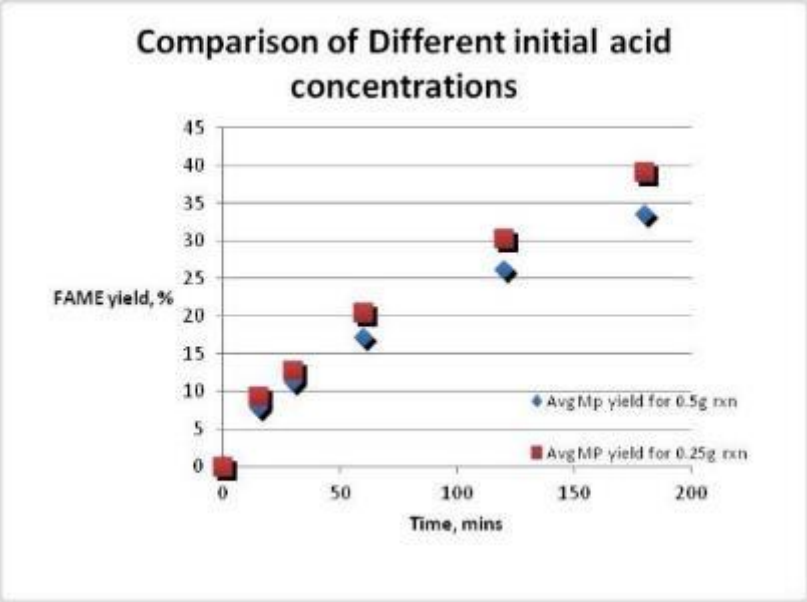

Figure 4.17 Comparison of different initial palmitic acid concentrations

4.3.7 Reaction kinetics with and without water, rate expressions for heterogeneous catalysts

Having tested several models that varied different factors such as: a) reversibility, b) different permutations of the 1, 2, 3 or 4 of the reaction components being adsorbed onto the catalytic site, and c) one or two different sites being utilized; the top 3 models out of ~ 30 models tested were further investigated for best fit. The top 3 were selected based on excellent fits with the experimental data at all 9 different reaction conditions tested. Thus, the best model (ERF2) was selected from these as it explained the changes in water concentrations and temperature realistically and fit the experimental data excellently well. Figure 4.18 shows the top 13 models tested that fit at least 7 of the 9 different reaction conditions.

www.manaraa.com

	65 C									
Water concentration and Temperature	0%	10%	20%	50%	70%	0%,55C	50%,55C	0%, 85C	50%, 85C	No of cond
ra = kKaCaCb/(1+KaCa+KcCc+KdCd)^2	0.845	0.931	0.890	0.868	0.912	0.797	0.976	0.883	0.895	9
ra = kCaCb/(1+KaCa+KcCc)^2	0.840	0.930	0.930	0.890	0.922	0.797	0.981	0.883	0.911	9
ra = k(CaCb-CcCd/Ke)/(1+KaCa+KdCd)^2	0.840	0.990	0.999	0.998	0.999	0.797	0.985	0.999	0.999	9
ra = k(CaCb-CcCd/Ke)/(1+KACa+KMCc+KdCd)	0.810		0.973	0.978	0.999	0.720	0.982	0.871	0.620	8
ra = k(CaCb-CcCd/Ke)/(1+KACa+KdCd)	0.810		0.973	0.978	0.999	0.760	0.982	0.873	0.600	8
ra = kKbCb/(1+KbCb+KcCc)^2	0.790	0.910	0.894	0.863	0.910	0.758	0.985		0.800	8
ra = kCaCb/(1+KaCa+KcCc)	0.750	0.870	0.860	0.700	0.840	0.760		0.870	0.810	8
ra = kCa/(1+KaCa+KcCc)^2	0.840	0.930	0.930	0.890	0.920	0.800	0.980		0.910	8
ra = k(CaCb-CcCd/Ke)/(Cd+KACaCd+KAKsCaCb)	0.999	0.993	0.999	0.998	0.999	0.003	0.998	0.999	0.988	8
ra = k(CaCb-CcCd/Ke)/(1+KBCb+KdCd)	0.991	0.976		0.978	0.999	0.780	0.982	0.921	0.940	8
ra = k(CaCb-CcCd/Ke)/(1+KACb+KMCc)	0.990	0.977	0.973	0.978	0.999	0.350	0.974	0.921		7
ra = kKaCa/(1+KaCa+KcCc)^2		0.930	0.935	0.892	0.922	0.800	0.984		0.910	7
ra = k(CaCb-CcCd/Ke)/(1+KBCb+KMCc+KdCd)		0.976	0.973	0.978	0.999		0.982	0.927	0.937	7

Figure 4.18 Top 13 models tested and their R^2 fits, the best model is highlighted in green

Temperature (°C)	Water Content (%)	R-square value
55	0	0.797
55	50	0.985
65	0	0.840
65	10	0.990
65	20	0.999
65	50	0.998
65	70	0.999
85	0	0.999
85	50	0.999

Figure 4.19 R^2 fits for the best model at all 9 different conditions

The best model for all 9 conditions analyzed was a modified Langmuir-Hinshelwood model with palmitic acid and water adsorbed on two different sites and was represented by:

$$r = k\frac{(C_aC_b - \frac{C_cC_d}{K_e})}{(1+K_aC_a+K_dC_d)^2} \quad (4.5)$$

where r is the reaction rate, k is the apparent rate constant, C_a, C_b, C_c, and C_d represent the concentrations of palmitic acid, methanol, methyl palmitate, and water respectively.

www.manaraa.com

K_a represents the equilibrium constant/affinity for the adsorption of palmitic acid onto the catalyst site and K_d represents the equilibrium constant/affinity for the adsorption of water onto the catalyst site. K_e is the overall reaction equilibrium constant. Figure 4.20 graphically illustrates the fit of the model for one of the 9 conditions.

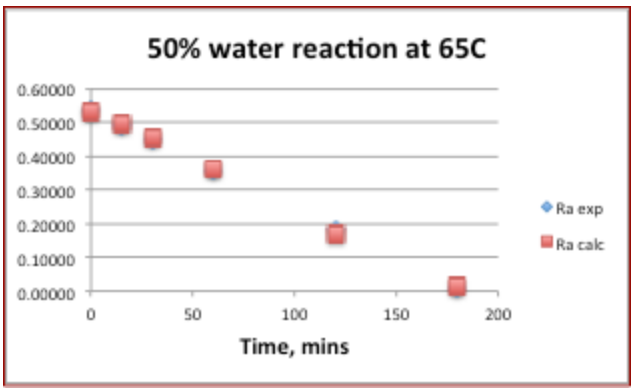

Figure 4.20 Fit of experimental data to the model for the 50% water reaction at 65 °C on H-ZSM-5 (80)

The values for the model parameters obtained are shown in Table 4.3. Here, k has units of mol/m^{3}min (same as the overall rate, r), K_a and K_d have units of m^3/mol, and K_e is dimensionless.

Table 4.3 Parameters for the best model at 9 different reaction conditions

Best model	**65 °C**					**55 °C**		**85 °C**	
Water content	**0 %**	**10%**	**20%**	**50%**	**70%**	**0 %**	**50%**	**0 %**	**50%**
k	0.027	0.111	0.223	0.332	0.425	0.012	0.089	0.066	3.001
K_a	2.242	4.489	4.155	4.220	2.625	1.973	3.312	3.032	5.844
K_d	2.411	0.065	0.052	0.015	0.027	6.191	0.016	1.784	0.043
K_e	0.001	0.142	0.287	1.142	1.250	0.987	1.196	0.012	6.058

www.manaraa.com

As seen in Table 4.3, the adsorption of palmitic acid (K_a) increases as water concentration increases (up to 70% water) which is reasonable because fatty acids are more hydrophobic than water and are more likely to adsorb to the hydrophobic catalyst surface than water is. Similarly, the adsorption of water (K_d) decreases as water content increases and is explained by water molecules joining the rest of their polar, hydrophillic bulk rather than the hydrophobic catalyst. The rate constants, k, increase as water content increases because the decreasing affinity of water for the catalytic sites as water content increases makes more sites available for the preferentially-adsorbed palmitic acid to react and move the reaction forward faster. This is supported by the corresponding increase in K_a, the affinity for fatty acid adsorption.

Upon using this best model to test a 10th reaction condition, with the initial palmitic acid mass changed from 0.5g to 0.25g, the model had a similar trend and fit experimental data excellently as shown in Figure 4.21 with R^2 fit of 0.992 further validating the model. The K_a and K_d for this reaction condition shows that there was increased adsorption of palmitic acid and decreased adsorption of water when compared to the 0.5g reaction at 65C and 0% water. This illustrates that at 0 % water, the smaller water product that was formed due to lower initial PA concentration, allowed a higher rate to be observed because there was less competition for acidic sites by the water molecules.

www.manaraa.com

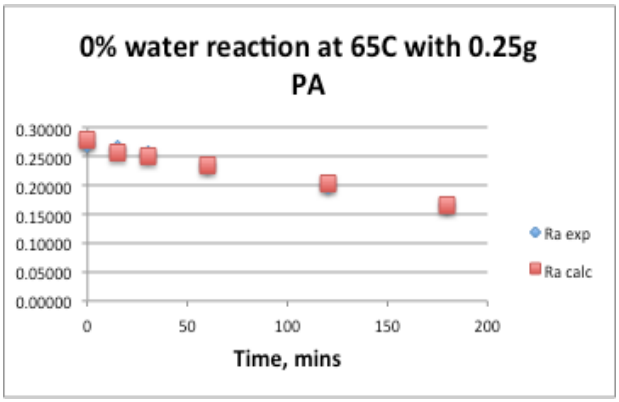

	0 %, 65 °C, 0.25g
k	0.047
K_a	4.749
K_d	0.006
K_e	1.115

Figure 4.21 a) Fit of experimental data to the model for the 0% water reaction at 65 °C on H-ZSM-5 (80) with initial PA mass of 0.25g, b) model parameters

Other models tested in literature had methanol and acid adsorbed and no reversibility: $r = \frac{kK_aC_aC_b}{1+K_aC_a+K_bC_b}$ (Kirumakki et al. 2006). However, these did not work for our system.

4.3.8 Proposed reaction mechanism

Having determined the best model to be:

$$r = k\frac{(C_aC_b - \frac{C_cC_d}{K_e})}{(1+K_aC_a+K_dC_d)^2} \quad (4.6)$$

We see from the numerator that reversibility of the reaction is significant, and we also see from the squared denominator that there are two different sites present in the reaction mechanism. This model was developed based on the assumption that surface reaction (rather than adsorption or desorption) was the rate-determining step.

The proposed mechanism assumes that palmitic acid (PA) is adsorbed onto a catalytic site (S_1) and then the adsorbed intermediate (PA·S_1) reacts with methanol (M) in the bulk solution with an available site (S_2) nearby. Methyl palmitate (MP) and water (W) are

www.manaraa.com

formed but water adsorbs onto the nearby available site (S_2) to form an intermediate ($W \cdot S_2$). Then the intermediate, $W \cdot S_2$, desorbs the water molecule formed into the bulk solution as shown in the steps below:

$$PA + S1 \Leftrightarrow PA \cdot S1 \tag{4.7}$$

$$PA \cdot S_1 + S_2 + M \Leftrightarrow MP + W \cdot S_2 + S_1 \tag{4.8}$$

$$W \cdot S_2 \Leftrightarrow W + S_2 \tag{4.9}$$

This mechanism would be very straightforward if reversibility did not play an important role, but it does, as each of the above steps are reversible. This is what plays into the unique water effect phenomenon discussed in Section 4.3.3.

It is possible that the reaction needs a neighboring empty site so the produced water can adsorb on it and the reaction rate may be hindered if there are not enough S_2 sites, due to the reverse reaction of equation 7 or water initially present occupying the catalytic sites. The proposed mechanism is illustrated in Figure 4.22.

www.manaraa.com

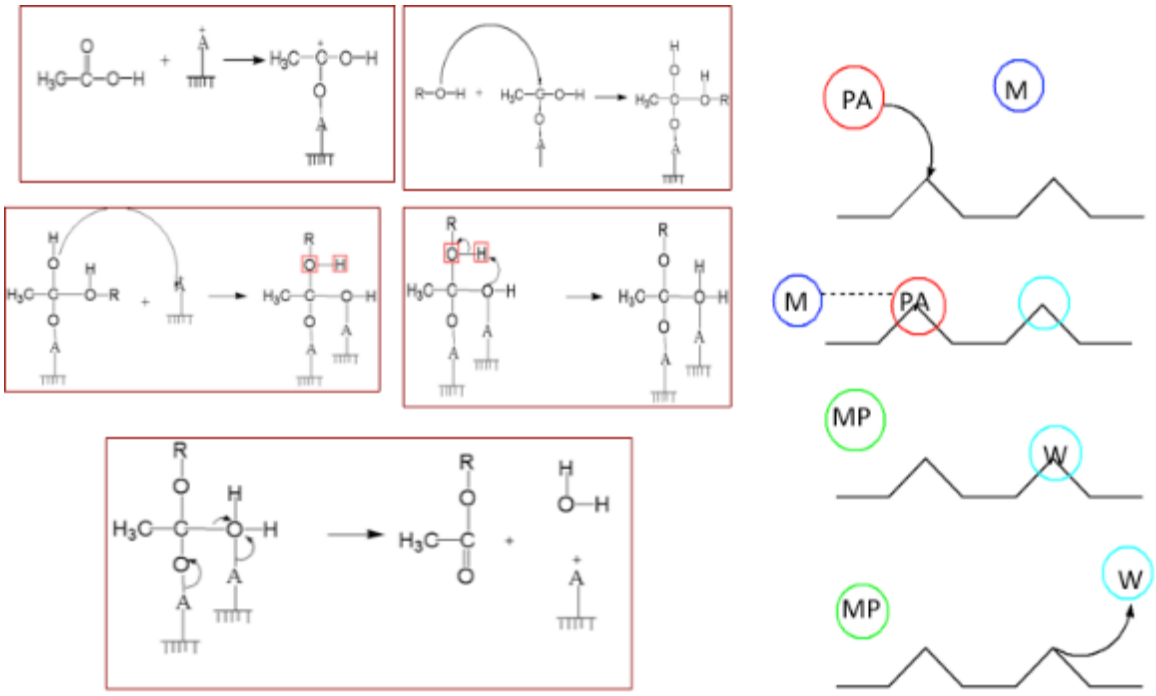

Figure 4.22 The proposed mechanism

This proposed model also shows that reversibility in the numerator is significant, which would be expected as the water content increased. It was also observed that none of the top 3 models had methanol adsorption.

The reason for the 50 % behavior can be explained by the rate of transfer of water in and out of the catalyst in Equation 4.7 being equal, causing a net higher FAME yield than at other concentrations where the rate of transfer of water into the catalyst might dominate the rate of transfer out, causing more catalytic sites to be used up and unavailable for palmitic acid adsorption. The reason for the 70 % low yield despite high rate constants is that the water concentration is so high that the water concentration driving force dominates FAME production.

www.manaraa.com

In the case of the 90% water reaction, the R^2 obtained on over 20 models tested never exceed 0.22. This could be due to the fact that there was so much water in the reaction mixture that there could have been inefficient mixing between organic palmitic acid and inorganic water that there wasn't a proper esterification. Also, the reaction dynamic is expected that there would be different reaction vapor pressures as water content increased and could contribute to 90% water reaction behaving differently.

4.4 Conclusions

In the study of the effect of water on esterification of palmitic acid to determine the optimum water content for FAME production, the 80:1 ZSM-5 catalyst was the most active catalyst of the 5 zeolites tested. It was determined that the optimum water content was 50%. Adding water affected the FAME yield negatively for all water levels except 50% and the rate constants for all reactions with water added were significantly lower than that for the reaction in the absence of water. Assuming this behavior is the same with the fatty acids in the sludge, sludge would need to be dried down to 50% moisture before reaction for highest FAME yield. This 50% water content can be used to hydrolyze and proceed with esterification without removing the water since esterification usually requires milder reaction conditions than transesterification and it is also a 1-step reaction instead of a 3-step reaction as with transesterification. The heterogeneous catalytic rate law that worked best was a modified Langmuir-Hinshelwood model indicating a reversible reaction with palmitic acid and water adsorbed on two different sites and was depicted by:

$$r = k\frac{(C_a C_b - \frac{C_c C_d}{K_e})}{(1+K_a C_a + K_d C_d)^2} \quad (4.10)$$

www.manaraa.com

If water is still an issue, the use of a water adsorption apparatus in tandem with the esterification reactor can be considered where biodiesel production has been shown to increase from 61 to 91% (Lucena et al. 2008), or consider using codistillation or adsorption on drying agents for water removal.

www.manaraa.com

4.5 References

Altiokka, M. R. and A. Çitak (2003). "Kinetics study of esterification of acetic acid with isobutanol in the presence of amberlite catalyst." Applied Catalysis A: General **239**(1-2): 141-148.

Angerbauer, C., M. Siebenhofer, M. Mittelbach and G. M. Guebitz (2008). "Conversion of sewage sludge into lipids by Lipomyces starkeyi for biodiesel production." Bioresource Technology **99**(8): 3051-3056.

Aranda, D. G., R. P. Santos, N. O. Tapanes, A. Ramos and O. Antunes (2008). "Acid-Catalyzed Homogeneous Esterification Reaction for Biodiesel Production from Palm Fatty Acids." Catalysis Letters **122**(1-2): 20-25.

Askari, S., S. Miar Alipour, R. Halladj and M. Davood Abadi Farahani (2013). "Effects of ultrasound on the synthesis of zeolites: a review." Journal of Porous Materials **20**(1): 285-302.

Bedard, J., H. Chiang and A. Bhan (2012). "Kinetics and mechanism of acetic acid esterification with ethanol on zeolites." Journal of Catalysis **290**: 210-219.

Bligh, E. and W. Dyer (1959). "A Rapid method of total lipid extraction and purificatin " Canadian Journal of Biochemistry and Physiology **37**(8): 911-917.

Chu, W., X. Yang, X. Ye and Y. Wu (1996). "Vapor phase esterification catalyzed by immobilized dodecatungstosilicic acid (SiW12) on activated carbon." Applied Catalysis A: General **145**(1–2): 125-140.

Chung, K. H., D. R. Chang and B. G. Park (2008). "Removal of free fatty acid in waste frying oil by esterification with methanol on zeolite catalysts." Bioresource Technology **99**(16): 7438-7443.

Di Serio, M., R. Tesser, L. Pengmei and E. Santacesaria (2007). "Heterogeneous Catalysts for Biodiesel Production." Energy & Fuels **22**(1): 207-217.

Hoydonckx, H., D. De Vos, S. Chavan and P. Jacobs (2004). "Esterification and Transesterification of Renewable Chemicals." Topics in Catalysis **27**(1-4): 83-96.

Ison, A. and R. J. Gorte (1984). "The Adsorption of Methanol and Water on H-ZSM-5." Journal of Catalysis **89**(1): 150-158.

Jun, K. W., H. S. Lee, H. S. Roh and S. E. Park (2003). "Highly water-enhanced H-ZSM-5 catalysts for dehydration of methanol to dimethyl ether." Bulletin of the Korean Chemical Society **24**(1): 106-108.

www.manaraa.com

Jungsuttiwong, S., J. Limtrakul and T. N. Truong (2005). "Theoretical Study of Modes of Adsorption of Water Dimer on H-ZSM-5 and H-Faujasite Zeolites." The Journal of Physical Chemistry B **109**(27): 13342-13351.

Kamarudin, R., N. Nordin, N. Buang and S. Ahmad (1998). "A Kinetic Study on the Esterification of Palmitic Acid in Methanol." Pertanika Journal of Science & Technology **6**(1): 71-79.

Kasai, P. and P. M. Jones (1984). "MAS-NMR Spectroscopic Study of Water in Zeolites." Journal of Molecular Catalysis A: Chemistry **27**: 81-93.

Kirumakki, S. R., N. Nagaraju and K. V. R. Chary (2006). "Esterification of alcohols with acetic acid over zeolites Hβ, HY and HZSM5." Applied Catalysis A: General **299**(1-2): 185-192.

Kirumakki, S. R., N. Nagaraju and S. Narayanan (2004). "A comparative esterification of benzyl alcohol with acetic acid over zeolites Hβ, HY and HZSM5." Applied Catalysis A: General **273**(1-2): 1-9.

Larsen, S. C. (2007). "Nanocrystalline zeolites and zeolite structures: Synthesis, characterization, and applications." Journal of Physical Chemistry C **111**(50): 18464-18474.

Lee, J.-S. and S. Saka (2010). "Biodiesel production by heterogeneous catalysts and supercritical technologies." Bioresource Technology **101**(19): 7191-7200.

Lestari, S., P. Mäki-Arvela, J. Beltramini, G. M. Lu and D. Y. Murzin (2009). "Transforming triglycerides and fatty acids into biofuels." ChemSusChem **2**(12): 1109-1119.

Liu, Y., E. Lotero and J. G. Goodwin (2006a). "A comparison of the esterification of acetic acid with methanol using heterogeneous versus homogeneous acid catalysis." Journal of Catalysis **242**(2): 9p.

Liu, Y., E. Lotero and J. G. Goodwin (2006b). "Effect of water on sulfuric acid catalyzed esterification." Journal of Molecular Catalysis A: Chemistry **245**(1/2): 9p.

Lucena, I. L., G. F. Silva and F. A. N. Fernandes (2008). "Biodiesel production by esterification of oleic acid with methanol using a water adsorption apparatus." Industrial & Engineering Chemistry Research **47**(18): 6885-6889.

Müller, J. A. (2001). "Prospects and problems of sludge pre-treatment processes." Water science and technology : a journal of the International Association on Water Pollution Research **44**(10): 121-128.

www.manaraa.com

Navalon, S., M. Alvaro and H. Garcia (2009). "Highly dealuminated Y zeolite as efficient adsorbent for the hydrophobic fraction from wastewater treatment plants effluents." Journal of Hazardous Materials **166**(1): 553-560.

Park, J.-Y., Z.-M. Wang, D.-K. Kim and J.-S. Lee (2010a). "Effects of water on the esterification of free fatty acids by acid catalysts." Renewable Energy: An International Journal **35**(3): 5p.

Revellame, E., R. Hernandez, W. French, W. Holmes, E. Alley and R. Callahan Ii (2011). "Production of biodiesel from wet activated sludge." Journal of Chemical Technology & Biotechnology **86**(1): 61-68.

Shirazi, L., E. Jamshidi and M. R. Ghasemi (2008). "The effect of Si/Al ratio of ZSM-5 zeolite on its morphology, acidity and crystal size." Crystal Research and Technology **43**(12): 1300-1306.

United States Environmental Protection Agency: Office of Wastewater Management. (June 2011). "Introduction to the National Pretreatment Program." Retrieved January 31, 2013, from http://www.epa.gov/npdes/pubs/pretreatment_program_intro_2011.pdf.

Xin, J., H. Imahara and S. Saka (2008). "Oxidation stability of biodiesel fuel as prepared by supercritical methanol." Fuel **87**(10–11): 1807-1813.

Zheng, S. (2002). Surface modification of HZSM-5 zeolites. Doctoral.

www.manaraa.com

CHAPTER V

BIODIESEL PRODUCTION FROM *RHODOTORULA GLUTINIS* AND ACTIVATED SEWAGE SLUDGE

5.1 Introduction

Biodiesel, as discussed in Chapter 1, has been shown to be a promising fuel but still has challenges with production volumes due to the high cost and limited availability of feedstocks.

Typically catalysts (homogeneous and heterogeneous) are used for the production of biodiesel. However the biggest disadvantage with using catalysts in working with microbial feedstocks, including sludge is the presence of large amounts of water, which if not removed from the system, could deactivate the catalysts and thus reduce FAME yield. Chapters 3 and 4 investigated the use of heterogeneous catalysts for biodiesel production from triglycerides and palmitic acid (as a surrogate of free fatty acids) with high water content. While the results of Chapter 3 showed that the porous metal oxide catalysts were not suitable for use with oil feedstock containing relatively high moisture, the optimum zeolite catalyst studied in Chapter 4 had better FAME yields as a result of adding an optimum amount of water of 50% (by volume). Other problems with catalyst use include high cost and difficulty with separating catalysts from the products (Demirbas 2007a). Thus, the benefit of investigating non-catalytic transesterification.

www.manaraa.com

An alternative way to avoid the high cost of dewatering sludge (as high as 50% of biodiesel production cost (Mondala et al. 2009)) prior to reaction is to develop a process where wet sludge can be introduced with little or no drying to produce biodiesel. The objective of this part of the project is to examine the feasibility of using sludge with high water content as a feedstock to produce biodiesel by investigating the optimum yield that could be obtained using a 1-step method of direct transesterification at supercritical methanol conditions and a 2-step method of hydrolysis followed by esterification in supercritical methanol. High yields of FAMEs from either method could result in a process to avoid the dewatering costs.

Reactions in supercritical methanol have the potential of producing high FAME yields faster and with relatively high tolerance to water content. Supercritical methanol allows the use of the original microbial media instead of extracted and purified oil as the source of triglycerides for transesterification. It can work with any lipid-containing feedstock and allows for cost savings on the solvent (typically hexane) extraction process**.** By reducing the multiple process steps to extract oil before producing alkyl esters, the use of additional reagents, solvents and unit operations is reduced, potentially reducing the cost of the final product. Therefore, this study will contribute to the improvement of the in-situ transesterification supercritical methanol process for microbial feedstocks using a high-temperature, high-pressure batch reactor system. The supercritical methanol process is described in Section 5.1.1.

The overall aim of this study was to evaluate an alternative, cost-efficient method for producing biodiesel from wet sludge by avoiding processing costs involved in: drying the sludge, adding catalysts, and separating catalysts from products. This was done using

www.manaraa.com

2 methods: 1) the 1-step direct transesterification method, and 2) the 2-step method of hydrolysis of the lipids followed by esterification.

The goals of the 1-step direct transesterification method were to: 1) optimize the reaction conditions for highest FAME yields by varying temperatures, methanol:solid ratios, and reaction times, 2) study the effect of water on biodiesel yield, 3) study the kinetics of the reaction to determine rate constants that can be used in the feasibility study for scale-up, and 4) compare yields and efficiency to the 2-step method of hydrolysis and esterification.

The aim of the 2-step method, investigated by hydrolysis of *Rhodotorula glutinis* followed by esterification with supercritical methanol, is to assess the feasibility of reducing methanol consumed and energy consumption due to severe reaction conditions, while increasing biodiesel yield. This study also determines the rates of reaction, reaction mechanism and the effect of water in the system.

Rhodotorula glutinis, an oleaginous yeast, is used as a surrogate for activated sludge since it has a more uniform composition and less variation between batches compared to raw activated sludge from the wastewater treatment plant which could have large inconsistencies depending on the days it was withdrawn from the treatment plant.

Activated sewage sludge is a great alternative for both the 1-step and 2-step methods because the challenges and costs associated with dewatering can be turned to a benefit when the water content is used for hydrolysis whether concurrently (in the 1-step method) or consecutively (in the 2-step method).

www.manaraa.com

5.1.1 Supercritical methanol properties and advantages

A pure substance can exist in 3 phases: solid, liquid and gas. Of these, there is a critical point that exists between the gas and the liquid phases. Beyond this critical point, the fluid exists as a high density fluid that cannot be condensed any further, even if pressure and temperature are increased (e.g. in the case of methanol), this is referred to as a 'supercritical fluid' (Lee and Saka 2010). Supercritical methanol is a non-condensable, dense fluid with density approaching that of a liquid, while the viscosity and transport properties behave like that of a gas (de Boer and Bahri, 2011). The phase diagram for methanol is shown in Figure 5.1. The critical temperature and pressure for methanol is 239 °C and 8.09 MPa.

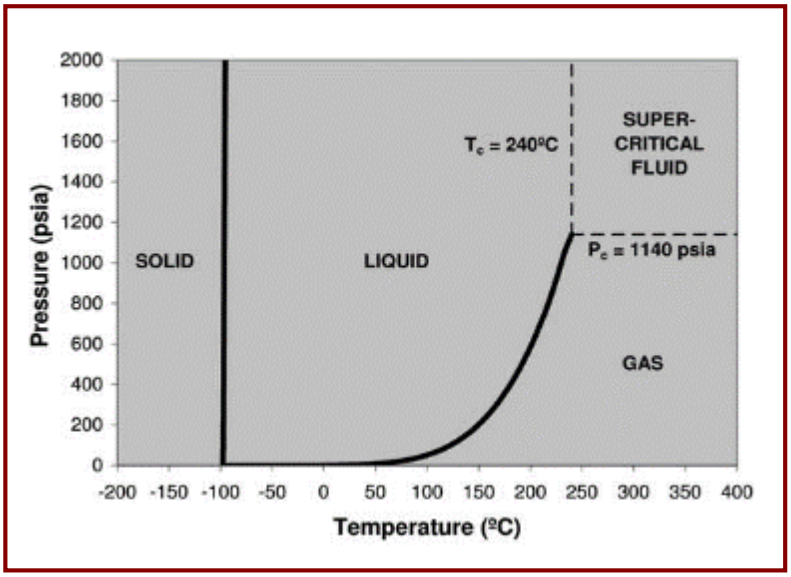

Figure 5.1 The pressure-temperature phase diagram of methanol Source (Ebert 2008)

www.manaraa.com

Supercritical methanol as a reactant has several outstanding properties and advantages for the transesterification and esterification reactions sludge oil compared to the conventional transesterification methods as described in Chapters 1 and 3. Some of the advantages include: 1) high product yields in short reaction times, 2) no catalyst needed, 3) production efficiency, 4) high water tolerance, and 5) feedstock flexibility.

5.1.1.1 High product yields in short reaction times

Supercritical methanol has different avenues by which it allows high conversion of reactants in relatively short reaction times. The supercritical method has a shorter reaction time in the order of minutes compared to a number of hours in conventional processes.

5.1.1.1.1 Increased miscibility of lipids with methanol

Under supercritical methanol conditions, the miscibility of lipids with methanol increases (He et al. 2007) and the 2-phase mixture of oil and methanol behaves as one phase due to the decrease in the dielectric constant of methanol (Kusdiana and Saka 2001) and thus, produces an increase in reaction rates. Solubility of triglycerides in methanol is reported to increase at a rate of 2-3% (w/w) per 10 °C as the reaction temperature increased (Saka and Kusdiana 2001), which makes the reaction faster. Demirbas et al. (2005) showed that methyl ester yield averaged about 55% under subcritical conditions and 95% yield under supercritical conditions after 5 min reaction time (Demirbas 2005); while de Boer and Bahri report as high as 1000% increase in reaction rate between 270 °C and 300°C (de Boer and Bahri 2011). Alenezi et al. describes the occurrence as resulting from ions produced from the alcohol causing the

www.manaraa.com

mixture of oil and alcohol to combine as a single phase which accelerates the reaction (Alenezi et al. 2010).

Also, improved mixing with nonpolar oil occurs due to the hydrophobic behavior of supercritical methanol. Lee and Saka state that the homogeneous reaction under supercritical conditions can be explained by two reasons: one is that an increase in temperature and pressure increases the solubility of triglycerides and the other is that the polarity of methanol decreased because the degree of hydrogen bonding decreases with increasing temperature (Lee and Saka 2010). This means that SCM has a hydrophobic nature with the lower dielectric constant that causes good mixing with oil which is nonpolar (Kusdiana and Saka 2001).

5.1.1.1.2 Methanol also acts as a catalyst

The increase in reaction rate with supercritical methanol is due to the fundamental structural change caused by the polarity, as it facilitates a much stronger direct nucleophilic attack by the methanol on the carbonyl carbon (Kusdiana and Saka 2004a). Thus, the hydrogen bonding of methanol causes the use of a catalyst to be unnecessary (de Boer and Bahri, 2011).

5.1.1.1.2.1 Production Efficiency

The supercritical methanol process can allow higher production efficiency (smaller number of processing steps) because it allows the elimination of the pre-treatment (removal of fatty acids and moisture) capital and operating cost (van Kasteren and Nisworo 2007). Easier product separation (de Boer and Bahri 2011) also allows the

www.manaraa.com

reduction in the post-treatment (e.g. neutralization, washing and drying) steps and costs (Ngamprasertsith and Sawangkeaw 2011).

This also makes this process less harmful to the environment because it does not need any catalysts or chemicals, and the waste from pretreatment and post-treatment steps are reduced since these steps are not necessary.

5.1.1.1.2.2 Tolerance of Water

Kusdiana and Saka report that the supercritical methanol process is highly tolerant of water up to 50% volume (Kusdiana and Saka 2004a), so feedstock drying may not be required and thus, promising for use with sludge. Levine et al. demonstrated that supercritical in-situ transesterification of wet algal biomass (after hydrolysis) in ethanol gave 100% alkyl ester yield (Levine et al. 2010). Similarly, transesterification with supercritical methanol was substantially unaffected by water, compared to alkaline and acid catalysts that are adversely affected. With a water content of 35%, transesterification of rapeseed oil with supercritical methanol demonstrated complete conversion to methyl esters after 4 minutes at 350 °C with a methanol:oil ratio of 42:1(de Boer and Bahri 2011). However, the high probability of the reverse reaction occurring with high water content at equilibrium needs also to be considered.

5.1.1.1.2.3 Feedstock flexibility

It can handle the presence of fatty acids in feedstock (de Boer and Bahri 2011), unlike other conventional methods which produce saponified products when free fatty acids are present. This is an important advantage because it makes the supercritical process for biodiesel production feedstock neutral.

www.manaraa.com

Table 5.1below summarizes the main differences between conventional transesterification method (using sodium hydroxide as catalyst) and supercritical methanol.

Table 5.1 Comparison between supercritical methanol and other common methods

	Conventional Method	**Supercritical Methanol Method**
Reaction time	1-8h	2 – 30 minutes
Reaction Conditions	0.1 MPa, 30 – 65 °C	>8.09 MPa, >239 °C
Catalyst	Acid, base or enzyme	None
Free fatty acids	Saponified products	Methyl esters
Water tolerance	Very low	High
Yield	Normal	Higher
Removal for Purification	Methanol, catalyst, saponified products	Methanol
Process	Complex	Simple

Modified from Table 2 in (Saka and Kusdiana 2001)

The drawbacks of supercritical methanol are the high reaction temperature and pressure which make it energy intensive. Also, the distillation process to recover excess alcohol requires significant energy. To keep the process at an environmentally friendly advantage, it is recommended to use low energy separation methods such as a medium pressure flash drum for alcohol recovery (Diaz et al. 2009).

www.manaraa.com

5.1.2 One-step method: Direct transesterification

In the 1-step method, the transesterification reaction with supercritical methanol proceeds as shown in Figure 5.2, except a catalyst is not needed.

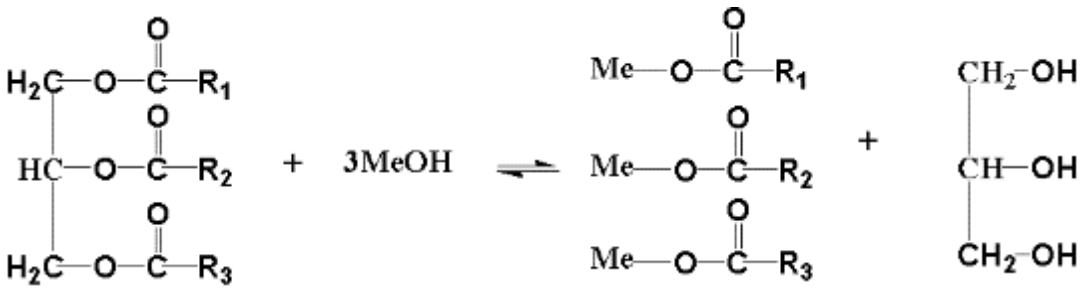

Figure 5.2 Transesterification reaction.

Methanol is most commonly used because of its low critical point and higher activity (Warabi et al. 2004), however ethanol can also be used at supercritical conditions (Pinnarat and Savage 2010). Many authors in the literature have had promising results using supercritical methanol with various feedstocks.

Saka and Kusdiana started work in this area using rapeseed oil and achieved as high as 95% conversion after 240 s at reaction conditions of 342 °C, 45 MPa, and 42:1 methanol:oil molar ratio. Valle et al. studied the transesterification of fodder radish oil and found optimum operating conditions to be 592K, 39:1 methanol: oil molar ratio, and 22 min reaction time to obtain an ester yield of 96% by weight fraction (Valle et al. 2010).

Patil et al. studied the transesterification of wet algae and found the optimal conditions from their response surface methodology analysis were: wet algae-to-methanol (wt/vol) of 1:9, temperature of 255 °C and time of 25 min, while they obtained

www.manaraa.com

a maximum fame yield of 86% at conditions of 260 °C, wet algae to methanol ratio of 12 (wt/vol) and 30 minutes reaction time (Patil et al. 2011).

5.1.2.1.1 Reaction Variables

Temperature and pressure are very important factors that affect the yields of the transeterification reaction. When Saka and Kusdiana investigated the reaction rate from 200 °C/7 MPa to 487 °C/105 MPa, they reported that the rate constant increased 35 times from 200 °C/7 MPa to 300 °C/14 MPa, and 400 times from 200 °C/7 MPa to 487 °C /105 MPa (Kusdiana and Saka 2001). Although high temperature is beneficial to the transesterification yield, it causes thermal decomposition of unsaturated fatty acids above 300 °C (Imahara et al. 2008).

de Boer and Bahri point out that the pressure of supercritical methanol reactions under batch conditions depends on 3 factors: the temperature of the experiment, the methanol to oil ratio and the quantity of reactants (de Boer and Bahri 2011). They report, along with Kusdiana and Saka, that pressure increases at least 5 fold above 320 °C (Kusdiana and Saka 2001).

While transesterification with supercritical methanol has been reported to produces high yields, severe conditions like a high temperature of about 350 °C are often required to achieve complete conversion. This can be very expensive and could cause loss in FAME yield by degradation of some FAMEs at high temperature. To reduce the severity of the combination of high temperature, high pressure, and high methanol:oil ratio conditions, three methods can be used: 1) adding a catalyst, 2) co-solvent use, and 3) two-stage processing (de Boer and Bahri 2011).

www.manaraa.com

5.1.2.1.1.1 Adding a catalyst

Use of catalysts in supercritical methanol conditions has similar problems as acid or base-transesterification catalysis in the presence of water and FFA, and is not seen as beneficial to the process. The problems of separating the catalysts and catalyst poisoning would be issues dealt with. Moreover, the aim of this work was to avoid the additional cost of using catalysts, so this method was not used.

5.1.2.1.1.2 Use of Co-solvents

de Boer et al. defines a co-solvent as a material that is added to the reactive mixture to adjust the critical point and lessen severe reaction conditions (de Boer and Bahri 2011). Cao et al. also report that the addition of propane as a co-solvent increases the solubility between methanol and vegetable oil, allowing the formation of a single phase at a much lower temperature. This required a much lower molar ratio of methanol-to-oil, causing the reaction pressure to reduce significantly (Cao et al. 2005). In their study, they were able to lower the optimal reaction temperature from 350 °C to 280 °C by incorporating a propane/molar ratio of 0.05. With this ratio at 280 °C and methanol/oil ratio of 24, they obtained a soybean oil conversion of 98% in 10 minutes at a pressure of only 12. 8 MPa (Cao et al. 2005). This is a much less severe reaction condition compared with Saka and Kusdiana's process conditions of 350 °C and 45 MPa on rapeseed oil mentioned above. Hegel et al. studied supercritical transesterification with co-solvents and found that the addition of 24% by weight of propane decreased the transition temperature of soybean oil-methanol (from a vapor-liquid to a one-phase supercritical system), from 315 °C to 243 °C when a methanol to oil molar ratio of 65:1 was used (Hegel et al. 2007). While it can serve as a positive alternative, it was not in the scope of

www.manaraa.com

this study since the aim is to reduce additional raw material costs and use already-available material.

5.1.2.1.1.3 2-stage processing

Saka's group was the first to evaluate this study when they developed a two stage supercritical methanol process called the "Saka-Dadan" method (Kusdiana and Saka 2004b). In this study, we will be evaluating a similar 2-step process of hydrolysis followed by esterification to take advantage of the presence of water in the system. This process is described in the following section.

5.1.3 Two-step method of hydrolysis followed by esterification

Studies have been conducted to evaluate the production of biodiesel using a combination of hydrolysis and supercritical fluid technologies. This study is beneficial because: 1) increasing the water tolerance potentially reduces the cost of biodiesel production by reducing drying, 2) there is no additional costs incurred for catalysts, 3) supercritical esterification can be performed at lower temperatures, with less methanol and in less time, and can achieve higher conversions compared to SC transesterification (Levine et al. 2010). The 2-step process proposes that the oils (triglycerides) are first hydrolyzed to form fatty acids and then esterification reaction follows the hydrolysis to convert the fatty acids to FAMEs.

Hydrolysis of oils and fats is a reaction in which water molecules split a triglyceride to form glycerol and fatty acids. It is a 3-step mechanism where one molecule of triglyceride (TG) is hydrolyzed to 1 molecule of diglyceride (DG) and fatty acid (FA), onwards until one molecule of monoglyceride (MG) is hydrolyzed to 1 molecule of

www.manaraa.com

glycerol and FA giving a total of 3 molecules of FAs. Typically, hydrolysis is carried out at 100–260 °C and 100–7000 kPa using 0.4–1.5 (w/w) initial water to oil ratio with or without catalysts (Moquin and Temelli 2008). This hydrolysis and its reverse reaction occurs without catalyst in subcritical water (Minami and Saka 2006). The supercritical esterification reaction is the same reaction as that at subcritical temperatures discussed in Chapter 4, except a catalyst is not used. The hydrolysis and esterification reactions are shown in Figure 5.3 and Figure 5.4, respectively.

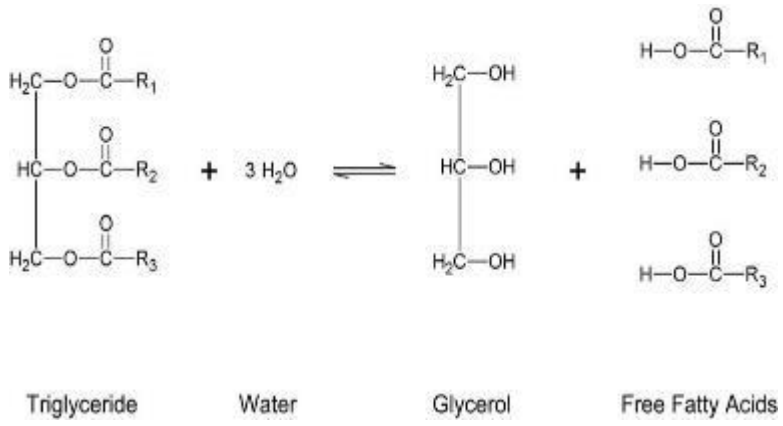

Figure 5.3 Hydrolysis of reaction for converting triglycerides to glycerol and free fatty acids.

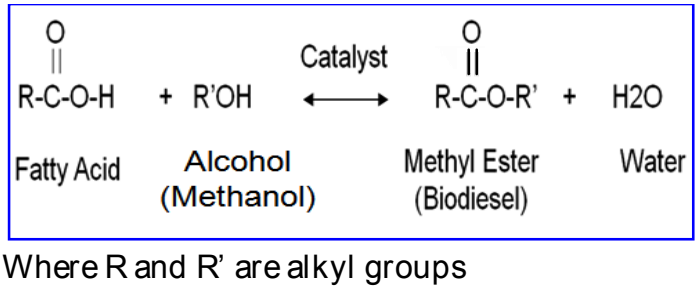

Figure 5.4 Esterification reaction for converting free fatty acids to esters and water.

www.manaraa.com

Researchers have demonstrated that following this 2-step process can allow moderate reaction conditions (270°C/7-20MPa) as opposed to a one-step process (350°C/20-50MPa) (Minami and Saka 2006). They showed that temperature could be increased from 250 °C to 270 °C to improve fatty acid yield for hydrolysis since they obtained a complete conversion of triglycerides to fatty acids when the reaction pressure was above 7 MPa (Minami and Saka 2006). Minami and Saka point out that with hydrolysis at lower temperatures e.g. 250°C and 270°C, the yield of FA increases very slowly in the early stage of the reaction (Minami and Saka 2006). They also found that the hydrolysis reaction always reached equilibrium at around 90 wt.% yield of fatty acids at higher temperatures (even though there was a higher rate of fatty acid formation), when the volumetric ratio of water to rapeseed oil was 1/1, which might be due to the backward reaction of hydrolysis. Under the conditions of 270 °C and 20 MPa, the yield of FA reached 90 wt.% after 60 min (Minami and Saka 2006). The treatment time for hydrolysis is critical to the prevent reverse reaction from occurring (de Boer and Bahri 2011).

5.1.3.1 Benefits of the 2-step Hydrolysis followed by Esterification Method

There are numerous benefits that can be gained using the 2-step method which include: 1) reduction in methanol use since supercritical esterification requires much less methanol than transesterification (Kusdiana and Saka 2004b, Minami and Saka 2006) and thus, less energy for the process, 2) reduction in severity of reaction conditions compared to the 1-step method. Esterification can be performed at a lower reaction temperature and at a faster rate than transesterification (Kusdiana and Saka 2004b, Warabi et al. 2004), 3)

www.manaraa.com

the reaction is faster because esterification has only one reaction step unlike transesterification which has 3 reaction steps (de Boer and Bahri 2011). In a comparison study, Kusdiana and Saka showed that transesterification reached a plateau of 76% conversion after 40 min, while esterification reached a conversion of more than 95% after 20 min, 4) the excess water that comes with the sludge feedstock serves as a benefit and can be used for hydrolysis without supplying additional water, and 5) reduces loss of FAMEs due to thermal degradation at high temperatures.

In the Saka-Dadan process, Kusdiana and Saka studied hydrolysis of rapeseed oil in subcritical water followed by methyl esterification of the fatty acids in supercritical methanol and reported optimum condition as 270 °C for 20 min for hydrolysis and methyl esterification. This was conducted using a 5ml Inconel reactor heated in molten tin (Kusdiana and Saka 2004b). They reacted 1ml oil and 4ml water for hydrolysis (1:217 molar ratio of oil to water). It took 12 seconds to reach their reaction temperature. Afterwards, the product settled for 30 min and separated into the upper (hydrolyzed product) from lower (water and glycerol) portions. They found that at 350 °C, they were able to achieve complete hydrolysis conversion after 3 minutes. However, at 270 °C and 300 °C, it took about 12 and 20 minutes respectively to reach the same yield of fatty acids. They also discussed the effect of reaction pressure on the yield of fatty acids from rapeseed oil treated at 270°C for 20 min, reporting that a complete conversion of triglycerides to fatty acids was achieved when the reaction pressure was above 7 MPa (Kusdiana and Saka 2004). Since the hydrolysis reaction is a reversible reaction, it has higher fatty acid yields when a large excess of water is used or if one of the products is removed from the reaction mixture. Conversely, the presence of water in fatty acids

www.manaraa.com

would have a negative effect on the methyl esterification reaction (Kusdiana and Saka 2004b).

The same procedure and equipment was used for conducting subsequent esterification at 270 °C and 17 MPa. They charged the reaction vessel using authentic fatty acids as well as fatty acids prepared from hydrolysis with a methanol-to-fatty acid molar ratio of 42, obtained almost complete conversion in 20 min. From their comparison of the 1- and 2-step method FAME yields, they reported that a significantly higher FAME yield could be produced via the 2-step method than the 1-step method. For example, at the same reaction time of 40 min, the 2-step method produced almost 30% more in FAME yield than the 1-step method (Kusdiana and Saka 2004b). It is important to note that the reaction time for the 2-step method refers to the sum of those of hydrolysis and methyl esterification steps.

Interestingly, Minami and Saka found that in supercritical esterification, having a higher concentration of fatty acid was more important than having an excess concentration of methanol to prevent the backward reaction because the fatty acid acted as a catalyst so the higher FA concentration as a result of a small amount of methanol used in the reaction can enhance the FAME yield.

5.1.3.1.1 Effect of Initial Water Content

In conventional catalyzed biodiesel production, the presence of water initially in biodiesel feedstock could cause negative effects such as consuming the catalyst and reducing the catalyst efficiency (Kusdiana and Saka 2004a). It could also allow the reverse of the esterification reaction to occur where the formed methyl esters are converted back to fatty acids.

www.manaraa.com

To avoid water's negative effects with conventional acid and base method, Kusdiana and Saka evaluated the effect of the presence of water (up to 50%) in the supercritical methanol method at 350 °C, 43MPa and 42:1 methanol:oil molar ratio and found that it did not have a significant effect on FAME yield, as almost complete conversions were always achieved irrespective of the water content (Kusdiana and Saka 2004). Holliday et al. state that water can dissolve both non-polar and polar solutes since its dielectric constant can be modified from a value of 80 at room temperature to a value of 5 at its critical point (Holliday et al. 1997). Therefore, they point out that water can solubilize most non-polar organic compounds like hydrocarbons at temperatures above 250 °C. Also, they report that water at temperature between 280°C and 350 °C is rich with ionic products and when mixed with polar methanol, the mixture will have both strong hydrophilic and hydrophobic properties and this could be one of the reasons why the reaction rate is higher in the water-added supercritical methanol treatment (Holliday et al., 1997).

5.1.4 Rhodotorula glutinis

Microbial oils produced by oleaginous microorganisms that include bacteria, yeasts, molds and algae are currently seen as promising potential feedstock for biodiesel production due to the similarity in their fatty acids composition to that of vegetable oils (Saenge et al. 2011). However, not all lipids obtained from microbial biomass are suitable for making biodiesel. Only free fatty acids and saponifiable lipids (lipids with fatty acid ester linkages) can be converted to alkyl esters (Saenge et al. 2011). Oleaginous species are microbes that are able to accumulate at least 20% of their biomass as oils in the form of triacylglycerols, and include yeasts, fungi and algae (Ratledge and Wynn 2002,

www.manaraa.com

Ratledge and Cohen 2008). The oil accumulation occurs as a trait of an unbalanced metabolism. When all necessary nutrients are present in the growth medium for the microbes, new cells are synthesized with minimal levels of lipids. However, when the cells run out of a key nutrient they start to accumulate oils. Thus for lipid accumulation to occur, the growth medium has to have an excess of carbon and to have the deprivation of a key nutrient. In the case where microorganisms or sludge produce a small amount of lipid, this strategy can also be used to enhance/increase the lipid content produced by the microbes (Mondala et al. 2012).

Oleaginous yeasts are single-celled fungi that have at least 20% of their dry weight made up of lipids (Khot et al. 2012). They also contain membrane lipids in addition to triacylglycerols. *Rhodotorula glutinis* (RG) is an oleaginous, red yeast that was used in this study as a model for sludge to optimize the production of biodiesel using supercritical methanol and avoid the variation in sludge constituent compounds. For oleaginous yeasts like RG, it has been well established that the lipid yield is high when they are grown in a medium with high carbon to nitrogen ratio (C:N) (Saenge et al. 2011). Therefore, only in low nitrogen medium will they channel carbon towards the accumulation of triacylglycerols (or triglycerides) as storage lipids. The amount of oil that the cells can store depends on the species. For example, Ratledge and Cohen report *Rhodotorula glutinis* to have a maximum lipid content of 72% (w/w) and a fatty acid acid profile of 37% of C16:0, 3 % of C18:0, 47% of C18:1, and 8% of C18:2 (Ratledge and Cohen 2008).

www.manaraa.com

5.2 Experimental Materials and Methods

5.2.1 Chemicals and Gases

37-component FAMEs and FAMEs mix C8-C24 of with saturated, mono-unsaturated and poly-unsaturated fatty acid methyl esters (Supelco, Bellefonte, PA), monoolein, diolein and triolein standards, N-Methyl-N-trimethylsilyltrifluoroacetamide (MSTFA) were obtained from Sigma Aldrich. Heptane, chloroform, pyridine, methanol and sodium sulphate were obtained from Fisher Scientific (Pittsburgh, PA, USA). All the gases used (He, H_2, and air) for gas chromatography were of high purity grade and distributed by NexAir (Columbus, MS, U.S.A.). All chemicals, standard, and gases were used as received without further purification.

5.2.2 Equipment

5.2.2.1 Four hundred and fifty milliliter (450-ml) batch Parr® reactor

The Parr® reactor set-up (Figure 5.5) was initially used because it allowed larger amounts to be reacted and could allow stirring and internal pressure reading. However, set-up for the batch reactor does not allow accurate study of the kinetics of the reaction due to heat loss at the top of the reactor, causing heating times to vary from 2 – 3 hr on different runs. Therefore, a new setup consisting of a fluidized sand bath and Swagelok® 46ml reactor was later chosen to allow accurate analysis of kinetics.

www.manaraa.com

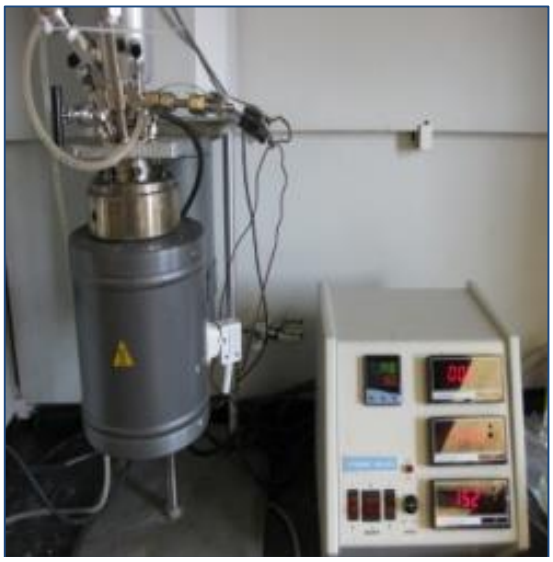

Figure 5.5 Four hundred and fifty milliliter (450-ml) Parr® reactor for the supercritical methanol transesterification of activated sewage sludge.

5.2.2.2 Fluidized sand bath and Swagelok® 46ml reactor

Having reviewed the literature, the types of equipment used for similar reactions at high temperatures were: autoclave in an electric furnace (Demirbas 2005), Reactor equipped with condenser, preheater, and separator (He et al. 2007), Swagelok® unions heated in a molten tin bath (Warabi et al. 2004), Swagelok® unions heated in a sand bath (Levine et al. 2010) and flow-type reactor with resistance heater and pump (Krammer and Vogel 2000). For our purposes which include kinetic analyses from samples at different time points, a compact set-up would offer easier sampling with minimal heating and cooling (e.g. 3-5 minutes) and at least allow reaction of triplicates at once. These were narrowed down to 2 types based on cost, and quick and relatively easy set-up: Swagelok® unions heated in a molten tin bath or Swagelok® unions heated in a sand bath. While heating small reactors in a molten tin bath has the advantage of quick heat

www.manaraa.com

transfer, it has the disadvantages of releasing tin fumes, which was considered unsafe, and having a crude set-up. Thus, it was determined that a reactor with smaller volume in combination with the fluidized sand bath (Figure 5.6) was the best medium for our purposes. The features are listed below:

5.2.2.2.1 Forty-six ml 1-in diameter tube reactors

These were made by swaging (2) 1-inch Swagelok® caps onto the ends of a 5-inch length of 1-inch diameter tubing and 1" Swagelok® tubing and caps (to make 46 ml reactors). The pressure rating was 3100 psi with wall thickness of 0.083 in and volume of 46 ml. The use of a 1-inch diameter reactor would allow the addition of a fitting to accommodate an internal temperature probe to ensure temperature accuracy.

5.2.2.2.2 Fluidized sand bath

These baths use aluminum oxide (Al_2O_3) fluidized by low-pressure air as a dry bath medium with excellent heat transfer properties to heat vessels placed in it. It gave fast heating, a wide temp range from 50 °C to 600 °C, and was safe to use because aluminum oxide is nonflammable and does not produce toxic fumes. The 51 lb capacity fluidized sand bath was obtained from Omega Engineering. Two heaters at the base heated the sand being fluidized. Multiple calibration tests were run to determine time for sand bath and internal temperature probe to reach set point. Aluminum oxide sand was 96% purity.

The disadvantage is that there was loss of some sand as it spilled out occasionally during fluidizing. A modification (Figure 5.7) was made to curtail the spills by adding a piece of air duct on top of the flange to keep the sand in.

www.manaraa.com

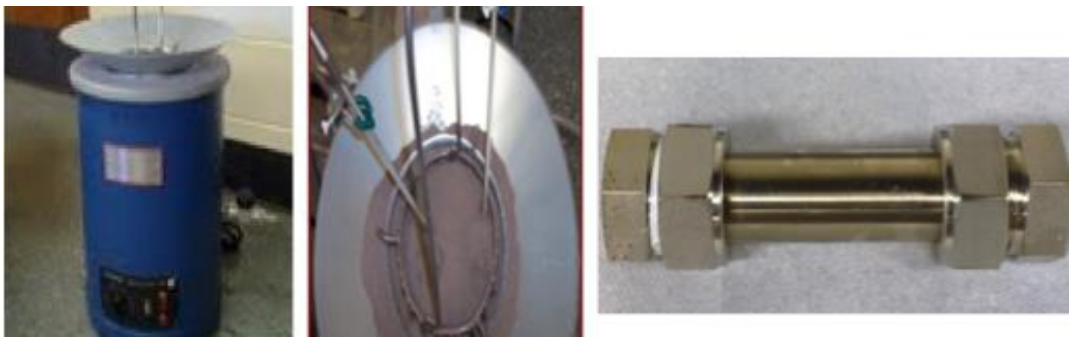

Figure 5.6 Fluidized sand bath and 46-ml reactor from Swagelok® tubing for the supercritical methanol transesterification of activated sewage sludge and *Rhodotorula glutinis*.

Figure 5.7 Modification to sand bath to limit spills

Note-worthy concerns are that the stirring was not controlled, and the pressure inside the Swagelok® reactor could not be measured. These were addressed by: 1) assuming that at supercritical conditions, increased diffusivity allowed good mixing and mass transfer was not an issue, 2) purchasing a pressure transducer that could be added to measure the internal pressure on the reactor.

www.manaraa.com

5.2.2.2.2.1 Additional Precautions

Applied Teflon tape to reactor cap's thread for tighter seal, tightened with vice and dropped into sand bath at desired temperature. Monitored and recorded time till internal temperature stabilized at set point. The volume of methanol/product after reaction was measured to check for volume balance.

5.2.2.3 Internal probe

For accurate kinetics of the reaction, a reactor was modified to include the addition of a temperature probe for measuring the internal temperature of the reactor contents during reaction. For each reaction, this reactor fitted with the probe was always charged with the same amount of reactants as the other reactors, and was used to determine the internal temperature of the other reactors. The parts were obtained from Omega Engineering and included a combination of a thermocouple, a thermowell, a Swagelok® connector and ferrule fittings to attach the probe to the reactor as seen in Figure 5.8 and Figure 5.9 below. This combination rated for up to 5400 psi. The temperature probe with a wire made of fiberglass material had a temperature limit of 480 °C which was satisfactory for our needs.

a)  b)  c) 

Figure 5.8 a) Internal temperature probe, b) thermowell for probe, c) female connector used on reactor end

www.manaraa.com

Figure 5.9 Temperature probe fitted to the reactor

5.2.2.4 Pressure Transducer

A DXD Digital pressure transducer was purchased from Heise® to monitor reaction pressure. The pressure transducer was connected to one end of the reactor via a piece of 1/8-inch tubing to prevent the pressure transducer from being inserted into the hot sand bath in the range of 250 °C - 300 °C. The 1/8-inch tubing allowed the transducer to be directed away from excessive heat due to radiation from the sand bath, although the tubing would need to be changed often between runs to not contaminate samples since it is tougher to clean. A ¼-inch female NPT hole was drilled into the reactor cap to allow the connection to the transducer. The connection is shown in the Figure 5.10 below.

a)  b)  c) 

Figure 5.10 a) Heise ® DXD Digital pressure transducer, b) Initial transducer connection, c) 1/8-in tubing wrapped with heating tape

www.manaraa.com

It was used to test the pressure of 9 ml of methanol in the reactor at its boiling point (65 °C). Initial results of that test indicated a pressure that slowly rose to 3 psi but did not hold which suggested that the length of the 1/8 inch tubing was too long and there was probably a leak. The tubing length was reduced and the pressure indicated increased to ~ 8psi. Since the 1/8-inch tubing was not submerged in the sand bath but was exposed to ambient temperatures which would cool the reactor contents and reduce the pressure, the 1/8-inch tubing was wrapped with heating tape that was heated with a rheostat to 65 °C. This ensured that it was maintained at the set point and the reactor contents would not condense. With that modification, the pressure obtained was 13.8 psi, which is 6% lower than the expected atmospheric pressure of 14.7 psi, but a marked improvement.

The pressure transducer was then used to try to determine the pressure of plain methanol at the supercritical condition of 275 °C but gave an error which turned out to be caused by the transducer being damaged from overheating. Thus, the transducer was not able to be used to investigate reaction pressures at the supercritical methanol reaction conditions.

5.2.3 Procedures

5.2.3.1 Sludge prep and Initial Lipid content determination

Activated sludge samples were obtained from the Hillard Fletcher wastewater treatment plant in Tuscaloosa, AL in 4-gallon plastic buckets and were transported in ice chests to the Renewable Fuels and Chemicals Laboratory at the Dave C. Swalm School of Chemical Engineering at Mississippi State University. Sludge was concentrated by vacuum filtration overnight. The supernatant was discarded and the filtered solids were

www.manaraa.com

centrifuged using an IEC Centra GP6 centrifuge (Thermo Electron Corp., Milford, MA, U.S.A.) operated at 3000 rpm for 20 min. The concentrated sludge was spread into 150 x 15 mm standard polystyrene petri dishes (Fisher Scientific, Pittsburgh, PA, USA), frozen at -18 C using a ColdTech freezer (Jimex Corp., Hayward, CA, USA) and freeze-dried using Freezone 2.5 freeze dry system (LABCONCO, Kansas City, MO, USA) for 5 days. The freeze-dried sludge contained about 95% (weight) solid, determined by Ohaus MB45 infrared heater (Ohaus, Pine Brook, NJ, USA). The freeze-dried sludge was crushed using mortar and pestle, homogenized and stored in the freezer until use. For the reactions in 46 ml reactors, sludge was completely dried using freeze-drier and rehydrated to 90% water (based on solids) before use.

5.2.3.2 Feedstock (*Rhodotorula glutinis*) Production and Initial Lipid content determination

Rhodotorula glutinis (RG) was grown in the laboratory from a mixture of yeast, nutrient solution and Y-M broth in 2000 ml baffled flasks with a foam seal to improve flow of oxygen and lipid yield. The flasks were placed in a shaker (New Brunswick Scientific Co., Edison, NJ, USA) at 30°C over 7 days. The nitrogen-rich medium was developed from a mixture of various nutrients which include (per liter): yeast extract [Fisher Scientific], 0.5g; $Na_2HPO_4 \cdot 12H_2O$, 1.0 g; KH_2PO_4, 1.0 g; $MgSO_4 \cdot 7H_2O$, 0.4 g; $(NH_4)_2SO_4$, 4.0 g; $FeSO_4$ solution (4.0 g/L $FeSO_4 \cdot 7H_2O$, Fisher Scientific), 6.0 ml; and trace mineral solution, 10 ml. The trace mineral solution consisted of (per liter): $CaCl_2 \cdot 2H_2O$, 3.6 g; $ZnSO_4 \cdot 7H_2O$, 0.75 g; $CuSO_4 \cdot 5H_2O$, 0.13 g; $MnSO_4 \cdot H_2O$, 0.50 g; $CoCl_2 \cdot 6H_2O$, 0.13 g; $Na_2MoO_4 \cdot 2H_2O$, 0.17 g (Fisher Scientific). The carbon and energy source was 60g (or 80g) of glucose.

www.manaraa.com

The media containing the cells was transferred to 50-ml plastic centrifuge tubes and centrifuged at 3200 rpm for 15 minutes. The supernatant was decanted and the cells rinsed with 40 ml of water, centrifuged, and decanted to remove nutrient media and stop growth of the cells. The centrifuged, wet RG in tubes were stored in a -80°C freezer before freeze-drying to 95% solids. Freeze-dried cells were stored in the -20°C freezer until use. Before use, 90% moisture content is determined from (1.8g of water)/(0.2g of cells + 1.8g of water). Figure 5.11 illustrates the steps for RG production

Figure 5.11 Steps for the growth of *Rhodotorula glutinis* cells

5.2.3.3 Supercritical Methanol Transesterification

5.2.3.3.1 Reactions in 450ml Parr® Reactor

Activated sludge obtained from a wastewater treatment plant in Tuscaloosa, AL was filtered to a wet paste of 93% water and reacted with methanol in a 450-ml batch reactor at 300°C, 300 rpm for 6 hours. The pressure obtained in the reactor was approximately 2300 psi.

www.manaraa.com

5.2.3.3.1.1 Parr® Reactor Work-Up Procedure

The reaction product was collected and filtered first by vacuum filtration before extraction. The volume of the filtrate was recorded, and 20 ml of the filtrate was transferred to a 60-ml borosilicate vial on which a modified Bligh & Dyer extraction was done twice. First by adding chloroform and water to get the chloroform - methanol - water volume ratio of 1:2:0.8 for a monophasic extraction, followed by a biphasic extraction twice at the chloroform - methanol - water volume ratio of 2:2:1.8 (Bligh and Dyer 1959). After the addition, the mixture was stirred using a vortex mixer for 2 minutes and centrifuged at 2000 rpm for 5 minutes. The extracted chloroform layer was evaporated to dryness at 45°C under a 15 psi stream of nitrogen using TurboVap LV (Caliper Life Sciences). The dry product was weighed, re-dissolved in chloroform and analyzed by gas chromatography (GC) and gas chromatography-mass spectrometry (GCMS). The identification of FAMEs was confirmed by using the Supelco FAMEs standard for 37 FAMEs. The solids on the filter paper were also dissolved in chloroform and analyzed for any residual compounds.

5.2.3.3.2 Reactions in 46 ml batch reactors

The configuration in the sand bath for all reactions, except where noted, was 1 temperature probe reactor with (3) 46-ml reactors for each sample. All four reactors would have the same content for any given reaction so the internal temperature probe could more accurately predict the internal temperature in the other reactors, assuming uniform heating in the sand bath. The temperature controller was set to a temperature 15 - 20 degrees higher than the desired set point initially and changed to the desired set point after reactors were dropped into the sand bath to reduce delay in heating. Internal

www.manaraa.com

temperature equilibrating times were 10 minutes or less after reactors were first dropped into the sand bath. Reactors were dropped in a bucket of cold water to cool after reaction.

5.2.3.4 Work-Up Procedure for 46ml batch reactor

The reaction product was collected, reactor walls rinsed and pooled, volume recorded, and lipids were extracted using a similar modified Bligh & Dyer procedure as described in section 5.2.3.3.1 (Bligh and Dyer 1959). The extraction was done by adding chloroform and water to get the chloroform - methanol - water volume proportion of 1:2:0.8 for a monophasic extraction. This was followed by adding more chloroform and water for a biphasic extraction at the chloroform - methanol - water volume proportion of 2:2:1.8. After the chloroform and water addition, the mixture was stirred using a platform shaker (New Brunswick Scientific Co., Edison, NJ, USA) for 10 minutes and centrifuged at 1800 rpm for 15 minutes before removing the bottom chloroform layer containing the lipids. The biphasic extraction was done twice and the pooled chloroform layer extract was evaporated to dryness at 45°C under a 15-psi stream of nitrogen using TurboVap LV (Caliper Life Sciences). The dry product was weighed, re-dissolved in chloroform and analyzed by GC and GCMS for FAME yields.

Figure 5.12 illustrates the difference in compounds obtained from the sludge product chromatogram and the RG product chromatogram. The RG chromatogram is much cleaner with 3 predominant FAMEs - methyl palmitate, oleate, and stearate, unlike the more diverse sludge profile containing FAMEs and unknowns. Hence, the reason why RG was used to simplify the optimization of reaction conditions instead of sludge.

www.manaraa.com

a)

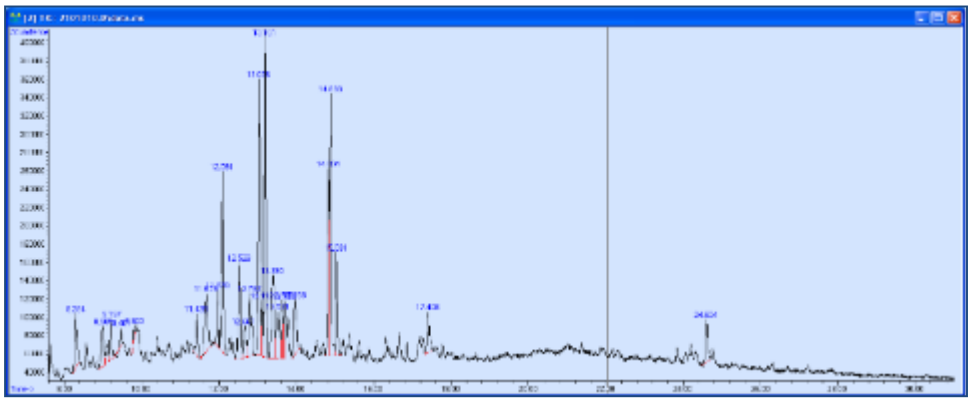

b)

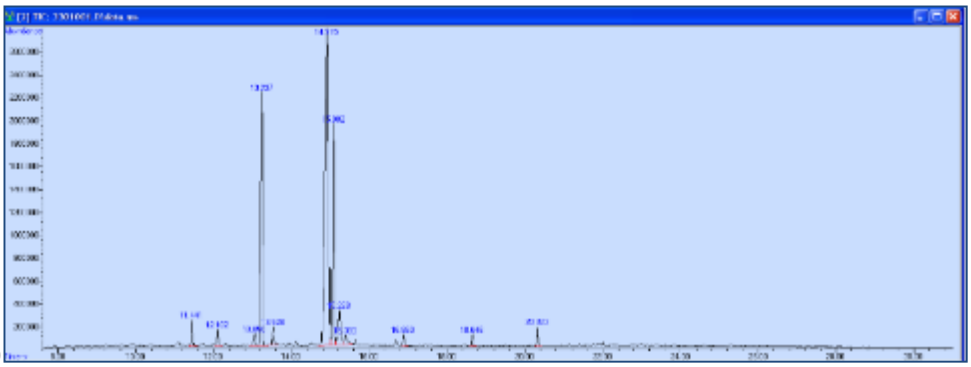

Figure 5.12 Sample chromatogram of products from supercritical transesterification a) sludge, b) Rhodotorula glutinis

5.2.4 Experimental Design

5.2.4.1 Preliminary in situ direct transesterification at 300 °C in Parr reactor

Preliminary reactions for this study were first done in the 450ml Parr® reactor using wet activated sludge from the WWTP in Tuscaloosa, AL until problems with significant heat loss that caused a 2 -3hr heat-up time, instigated the search for a new equipment set-up.

The reactions were conducted in the 450 ml Parr® batch reactor with 20 g or 40 g of sludge (6.75% solids) reacted with 100 ml of methanol (i.e. and 74 ml/1 g and 37 ml/1

www.manaraa.com

g methanol-to-solid ratios) at 300 °C for 6 hours. The pressure obtained in the reactor was approximately 2300 psi.

5.2.4.2 Bligh & Dyer Method of Extracting lipids

Four batches of *Rhodotorula glutinis* (RG) were grown and used over the duration of this study. The batches were made in February 2011, September 2011, January 2012 and June 2012 and were prepared as described in Section 5.2.3.2. The February 2011 batch was only slightly different because 80g/L of glucose was used instead of the 60g/L used in the remaining batches. To determine the initial lipid yield in the cells, a modified Bligh and Dyer extraction method similar to that in Section 5.2.3.3.2 was used for extraction on the unreacted, freeze-dried RG cells. This was done by adding methanol, chloroform and water to get the chloroform - methanol - water volume proportion of 1:2:0.8 for a monophasic extraction, followed by a biphasic extraction twice at the chloroform - methanol - water volume proportion of 2:2:1.8. Once the chloroform layer extract was evaporated to dryness at 45°C under a 15-psi stream of nitrogen using TurboVap LV (Caliper Life Sciences), the dry product was weighed to determine the gravimetric yield of lipids. It is important to note that this lipid yield is only an estimate of the lipids in the cells that were extracted by chloroform. Also, not all the lipids in this extract can be converted to biodiesel. The extract could include some non-saponifiable lipids that do not have ester linkages or phospholipids which cannot be fully converted to FAMEs. Their lipid yield results are shown in Section 5.3.2.

www.manaraa.com

5.2.4.3 In situ direct transesterification and optimization between 275 °C - 325 °C preliminary reactions in 46ml reactors using RG

This initial optimization of FAME yields study was done using the February 2011 RG batch. To simulate wet sludge conditions, water was added to the dry cells to attain a moisture content of 90% for all reactions. The wet cells were reacted with methanol by varying 3 optimization variables using a down-selection method as shown in Table 5.2:

1. Methanol:solid ratios (v/w) of 15 ml:1g, 30 ml:1g, 45 ml:1g
2. Temperatures of 275°C, 300°C, and 325°C
3. Time at 0.5, 1, and 3 hours

Table 5.2 Order of experimental reactions for initial optimization

Reaction order	Methanol:solid ratios (ml/g)	Temperature (°C)	Time (hr)	Substrate
1	15	300	1	RG
	30	300	1	RG
	45	300	1	RG
2	30	275	1	RG
	30	300	1	RG
	30	325	1	RG
3	30	300	0.5	RG
	30	300	1	RG
	30	300	3	RG
4	30	300	3	Sludge

Activated sludge that was obtained from a wastewater treatment plant in Tuscaloosa, AL was filtered, freeze-dried and also reacted at 90% moisture to compare FAME yields with those obtained from *R. glutinis* at the same reaction conditions.

The reactions were run in triplicates, dropping in 3 reactors with the same reactants into the sand bath already at the temperature set point. The timing was started immediately after dropping the reactors into the sand bath and it initially was assumed

www.manaraa.com

that they would heat up uniformly and quickly to the sand bath temperature. The FAME yield obtained was the basis for optimization. Additional experiments were also run using a different batch to compare FAME yields.

5.2.4.4 Timed samples at 250 °C, 90% water content from 10 – 60 minutes

Since the FAME yields obtained from the preliminary optimization reactions were not significantly different between the temperatures and times tested, timed samples at a lower temperature (250°C) were studied for shorter durations to examine the conversion of the initial triglycerides present in the *R. glutinis* cells to FAMEs and monitor other compounds such as diglycerides, and monoglycerides. Three reactors and the internal temperature probe reactor were charged with the same contents and the reactors dropped into the sand bath at the desired temperature. The samples were taken out at 10-minute intervals up to a maximum of 60 minutes starting when the reactors were dropped in without waiting for internal temperature to reach set point before starting timing. This was done so we could capture the FAME yield of the first few minutes of reaction.

5.2.4.5 In situ transesterification yield at 60 °C

To estimate biodiesel yield and fatty acid profile using a different reaction method, Bligh-Dyer extraction was conducted on 0.2 g of freeze-dried RG cells and the extracts were treated with a more conventional method of acid transesterification of the lipid extracts at 60°C to produce FAMEs (Mondala et al. 2012).

For the transesterification, two milliliters of a 2% (v/v) sulfuric acid in methanol was added to the lipid extract samples, vortex-mixed, and heated at 60°C in a water bath for 2 hours. The samples were cooled to room temperature and quenched with 5 ml of an

www.manaraa.com

aqueous solution containing 3% (w/v) $NaCHO_3$ and 5% (w/v) NaCl. FAMEs were extracted from the reaction mixture with two washings of 2 ml toluene containing 200 ug/ml of 1,3-dichlorobenzene as the internal standard and 100 µg/ml of BHT as an antioxidant. The toluene extracts were dried over anhydrous sodium sulfate, diluted, analyzed and quantified using the Agilent 6890 Gas Chromatograph.

5.2.4.6 Two-step in situ Hydrolysis and Supercritical Esterification

Based on literature findings described in section 1.1.3, a two-step method of cell hydrolysis followed by esterification in supercritical methanol was designed. Minami and Saka had tested hydrolysis at 270 °C, (subcritical state of water, <374 °C), with 1:1 volumetric ratio of triglyceride and water at pressure 7MPa, and found that it took 60 min to reach 90 wt% FFA yield (Minami and Saka 2006), those conditions were tested for hydrolysis. At this point, an internal temperature probe was added to a reactor in sand bath and was used in conjunction with a datalogger to monitor set-point equilibrating times.

Water (1.8 ml) was added to 0.2 g of freeze-dried *Rhodotorula glutinis* for 90% moisture content (based on solids). The mixture was hydrolyzed at 270 °C in a 46-ml tubular reactor placed in the heated fluidized sand bath for 30 minutes and 1 hr to assess the effect of reaction time on the fatty acid yield of hydrolysis.

After hydrolysis, the reactor was cooled and 6 ml of methanol was added to the reactor, and subjected to the esterification step in supercritical methanol at 250 °C for 20 minutes. The hydrolysis and hydrolysis-esterification products were analyzed on the GC for fatty acid and FAME yields.

www.manaraa.com

The proposed two-step method used in this study is slightly different from that done by Kusdiana and Saka in 3 ways: 1) the oil phase was not separated from the water phase in the filtrate from the hydrolysis product before reacting with supercritical methanol for esterification because the small amount made it more complex and we also wanted to avoid losing some of the fatty acids with the solids if filtered and discarded; 2) solids are used – cells with membranes, instead of plain oils; and 3) the solids are initially at high water content (90%) as the aim of this study was to evaluate esterification in the presence of high water content.

Additional experiments were conducted to study the effect of temperature on the hydrolysis reactions. Hydrolysis was conducted using 0.2g RG and 1.8ml water at 150 °C and 200 °C for 30 minutes in triplicates.

5.2.4.7 Further optimization

To address the previous optimization study that did not give a result that was significantly different from other conditions, a second optimization study was conducted using RG that aimed for savings on energy consumption and methanol use by using a lower temperature range and lower methanol-to-solid ratios. Three levels of temperature (250°C, 265°C and 280 °C) and 3 levels of methanol-to-solid ratio (7.5ml/g, 15ml/g and 30ml/g) were considered in triplicates, giving a total of 27 runs. A shorter reaction time of 20 minutes plus 10-minute heat-up time was used for all reactions. Table 5.3 shows the experimental design.

www.manaraa.com

Table 5.3 Experimental runs for second optimization study

Methanol:solid ratios (ml/g)	Temperature (°C)
7.5	250
	250
	250
15	265
	265
	265
30	280
	280
	280

Temperature control was ± 3 °C. Reaction conducted in triplicates, reaction time was 20 minutes plus 10-minute heat-up time

5.2.4.8 1-step direct transesterification kinetics at 280 °C on RG with 30ml/g methanol:solid ratio and 0% water

The aim of this experiment was to determine the FAME yields in the absence of water and the rate constant of the reaction. This information is different from other rate constant data found in the literature because cells are involved instead of plain oil. The reactors were charged with 0.2g RG and 6ml methanol. For this reaction, the sand bath configuration was modified to allow 5 reactors to fit in with the temperature probe reactor by using a piece of air duct to keep sand from spilling out Figure 5.13. Once the sand bath had reached the temperature set point, the 6 reactors were inserted, and the internal temperature monitored until it stabilized at the desired set point, time was recorded and 1 reactor was taken out as the 0min sample. The remaining samples were taken out at 5, 10, 15, and 20 minutes. Two reaction replicates were obtained.

www.manaraa.com

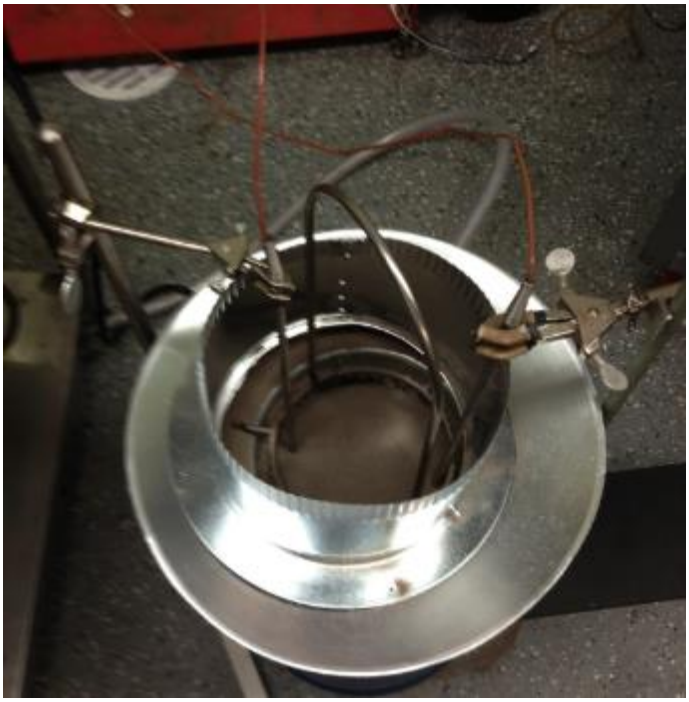

Figure 5.13 Modified fluidized sand bath with air duct restraining sand loss

5.2.4.9 1-step direct transesterification kinetics at 280 °C on RG at 30ml/g methanol:solid ratio and 90% water

The aim of this experiment was to compare the yields at 90% water composition and the rate constant achieved on RG cells to those obtained in the absence of water. This reaction could also represent the 2-step in situ method happening at the same time. Using a similar configuration as in the above section, the reactors were charged with 0.2g RG, 1.8ml water and 6ml methanol and reacted at 280 °C. Timed samples were taken out at 0, 5, 10, 15, and 20 minutes. Two reaction replicates were obtained.

5.2.4.10 Hydrolysis reaction kinetics on RG at 280 °C with 90% water

The aim of this experiment was to determine the yield of fatty acids and the rate constant of the hydrolysis reaction. This illustrates how the hydrolysis could occur in the

www.manaraa.com

90% wet transesterification reaction if eliminating the concurrent transesterification, hydrolysis and esterification reactions taking place due to the presence of water. It allows the comparison of the hydrolysis reaction rate to the transesterification reaction rates at 0% and 90% water composition at the same reaction temperature. The reactors were charged with 0.2g RG and 1.8ml methanol and reacted at 280 °C. Timed samples were taken out at 0, 5, 10, 15, and 20 minutes. Two reaction replicates were obtained.

5.2.5 Analytical Method

5.2.5.1 Standard preparation and sample dilution/preparation for GC

Standard and sample preparations for FAME and glyceride analysis were done using the same method discussed in section 3.2.7 in Chapter 3. Samples dissolved in a toluene diluents were analyzed using gas chromatography-mass spectrometry for compound identification.

5.2.5.2 Gas Chromatography

5.2.5.2.1 Gas Chromatograph for FAME analysis

The concentrations and amounts of FAMEs in the Bligh-Dyer extract were analyzed and quantitated using the Agilent GC 6890N gas chromatograph equipped with a flame ionization detector (GC-FID) (Agilent, Santa Clara, CA, USA. Approximately 4 mg of crude extract sample was dissolved in 1ml standard solution (toluene diluent containing 100 µg/ml butylated hydroxytoluene (BHT) and 200 µg/ml of 1,3-dichlorobenzene (DCB), which was the internal standard for GC analysis) and filtered using a 0.45 µm filter attached to a syringe. One µL of this solution was injected in splitless mode on an Agilent 6890 Gas Chromatograph (Agilent Technologies, Santa

www.manaraa.com

Clara, CA) at a constant injector temperature of 260 °C. The GC (Figure 5.14) was equipped with a 30 m × 0.25 mm ID Restek 11023 Stabilwax DA Capillary Column (Restek, Bellefonte, PA) having a 0.25-µm film thickness. The GC oven was programmed at an initial temperature of 50 °C, held for 2 min, ramped up to 250 °C at 10 °C min^{-1}, and held for 18 min, giving a total of 40 min analysis time. A flame ionization detector (FID) operating at 260°C and using helium carrier gas (14 psi, 53.5 mL/min flow rate) was used to detect the FAMES. The instrument was calibrated using a standard FAME mixture containing 14 FAMEs from C8 – C24 (Sigma-Aldrich, St. Louis, MO). The total FAME concentration obtained was used to estimate the total biodiesel yield from each reactor set.

Figure 5.14 Agilent 6890 series GC system with DA Stabilwax column for quantifying FAMEs and FFA Initial and final temperatures of 50 °C and 250 °C

5.2.5.2.2 High Temperature Varian Gas Chromatograph for glyceride analysis

The high temp GC was used to analyze the glyceride content in the reaction products for quantification. The equipment used was the Varian 3600 GC (Figure 5.15) equipped with a flame ionization detector (FID). The column used was the ZB-5HT

www.manaraa.com

Inferno™ (Phenomenex, Torrance, CA, USA) having dimensions of 15m, internal diameter of 0.32mm and film thickness of 0.10µm, and 400 °C maximum temperature. The initial and final injector temperatures will be 50°C and 380°C respectively and the FID temperature of 380°C in accordance with the ASTM Method D 6584 (ASTM). (ASTM)(ASTM)(ASTM)(ASTM)(ASTM)(ASTM)The GC oven was programmed at an initial temperature of 50°C for 1 minute, then ramped to 180°C at 15°C/minute, to 230°C at 7°C/minute, and then to 370°C/minute at 10°C/minute was held constant at 380°C for 5 minutes.

Figure 5.15 High temperature GC

5.2.5.3 GCMS

Gas Chromatography-Mass Spectrometry (GCMS) was used to identify the FAME compounds. An Agilent 5975 GCMS equipment (Figure 5.16) was used with a Restek Rxi-5SiL MS column. Initial and final temperatures of the oven were 50 °C and 320 °C. An Electron Ionization (EI) scan was run from 50 – 450 m/z.

www.manaraa.com

Figure 5.16 Agilent 5975 GCMS with Mass Selective Detector (MSD)

5.2.5.4 Calculations

FAME yields were calculated as:

$$FAME\ yield\ (\%) = \frac{\text{mass of FAMEs in product}}{mass\ of\ initial\ cells} * 100\% \qquad (5.1)$$

5.3 Results and Discussion

5.3.1 Preliminary in situ direct transesterification at 300 °C in Parr reactor

The yields on these reactions were relatively high after 6 hours of reaction using sludge of 6.75% solids. However, since the reactions were not very reproducible when duplicate reactions were conducted; these results only give a rough estimate of the distribution of FAMEs in the liquid and solid product. The results show an average FAME (biodiesel) yield of 7.8 % (based on initial solids) was obtained after analyzing the liquid product. The FAME yield on the leftover solid product was deemed negligible as only ~0.05 - 0.1% so there is no significant FAME loss by discarding the solids. Analysis of the product by Gas Chromatography-Mass Spectrometry (GCMS) showed

www.manaraa.com

the FAME profile obtained from the sludge transesterification product in Table 5.4. As expected, the predominant FAMEs in sludge were C16:0, C16:1, C18:0, and C18:1.

Table 5.4 FAME profile on sludge transesterification product

Methanol: Solids Ratio	74 ml:1 g	37 ml:1 g
% Yield of Methyl Palmitoleate (C16:1)	2.06	2.13
% Yield of Methyl Palmitate (C16:0)	2.32	2.51
% Yield of Methyl Oleate (C18:1)	2.23	1.84
% Yield of Methyl Stearate (C18:0)	1.05	1.42
Overall Yield from Sludge solids (% wt of solids)	7.66 ± 1.31	7.90 ± 3.94

Comparing that FAME yield with other conventional methods as seen in Table 5.5 below, we see that the supercritical methanol method produces a higher yield without the addition of catalyst but at a much higher temperature and pressure.

www.manaraa.com

Table 5.5 Comparison of supercritical methanol reaction with other methods

	Dried Sludge (Revellame et al. 2010)	Wet Sludge (Revellame et al. 2011)	Supercritical Methanol (This study)
% Water (g/g solid)	~ 5	~ 84.5	~ 93
Methanol Loading (ml/g solid)	25/1	30/1	37/1, 74/1
Catalyst Loading (% vol)	4	10	-
Reaction Temperature (°C)	55	75	300
Reaction Pressure (atm)	1	1	157
% FAME Yield (g/g solid)	4.79 ± 0.02	3.93 ± 0.15	7.78 ± 4.15

Although the 74ml/g reaction appeared to have a high yield, that reaction needs to be confirmed as reproducible in a different set-up that has more consistent and minimum heat-up times. Also, *Rhodotorula glutinis* (RG) was used as a more consistent substrate that also reduced the variance in the sludge substrate composition.

5.3.2 Bligh & Dyer Method of Extracting lipids in *Rhodotorula glutinis* (RG)

The gravimetric lipid yields from the modified Bligh-Dyer extract for the 4 RG batches used in this study are listed in Table 5.6 below. All batches had similar yields with an average of 37 %.

www.manaraa.com

Table 5.6 Table showing variation in lipid yield between batches

	February 2011	September 2011	January 2012	June 2012
Lipid Yield (% wt of initial cell weight)	35	36	35	41

Derivatization (Section 5.2.5.1) and analysis of the Bligh-Dyer extract of RG indicated only about 20% of the Bligh-Dyer extract was triglycerides, leaving 80% of the extract as other compounds such as phospholipids.

5.3.3 In situ direct transesterification and optimization between 275 °C - 325 °C

The results of the optimization reactions conducted in 46ml reactors using RG are shown in Figure 5.17 - Figure 5.19. The study to determine the best reaction conditions for producing the highest FAME yields efficiently did not yield an optimum set of conditions at this point. For all the varying conditions (methanol:solid ratio, temperature, and time), the FAME yields increased as each variable increased but were not significantly different within the ranges tested. The fact that the reaction timing was started upon dropping the reactors into the sand bath did not affect the results because all reactions in this set were treated the same way and the absence of an optimum indicated that would not have made a significant difference.

www.manaraa.com

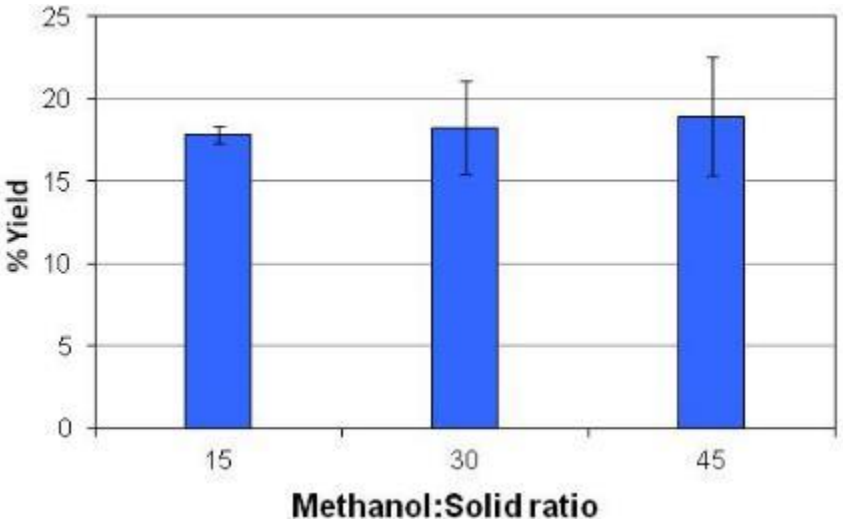

Figure 5.17 Effect of Methanol:Solids ratio on the FAMEs yield for supercritical transesterification of *Rhodotorula glutinis*

300 °C, 1 hour, 90% water

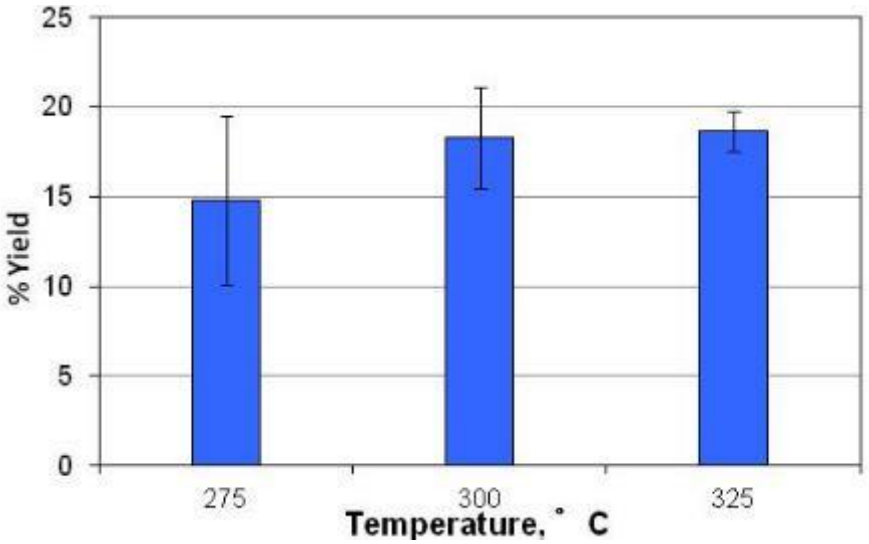

Figure 5.18 Effect of reaction temperature on the FAMEs yield for supercritical transesterification of *Rhodotorula glutinis*

Methanol:Solids ratio = 30 ml/g, 1 hour, 90% water

www.manaraa.com

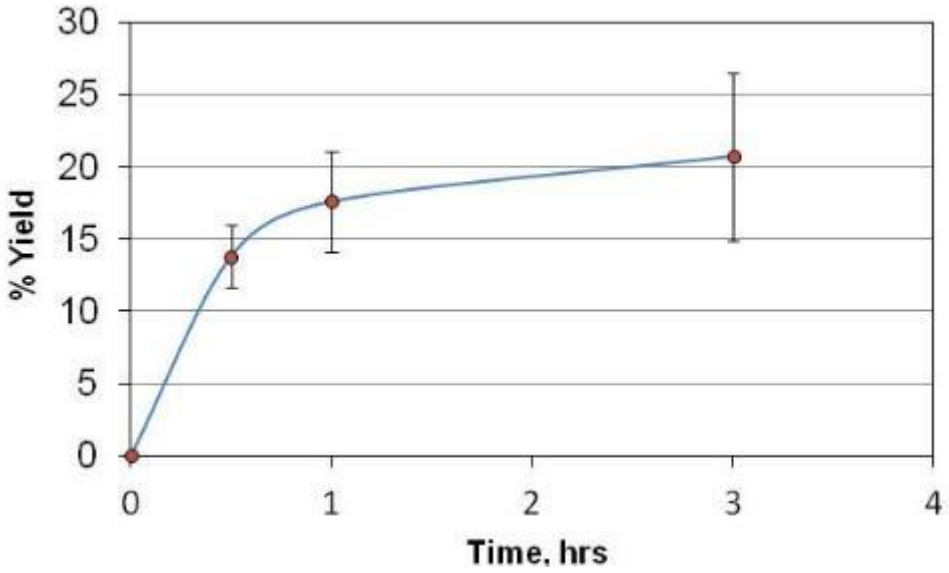

Figure 5.19 Effect of reaction time on the FAMEs yield for supercritical transesterification of *Rhodotorula glutinis*

Methanol:Solids ratio = 30 ml/g, 300 °C, 90% water

It was also observed that the highest yield (21%) after 3 hours of reaction time was still not at the estimated maximum original lipid yield obtained from Bligh-Dyer extraction on unreacted *R. glutinis* cells which was approximately 35% cell dry weight (gravimetric). However, there are non-saponifiable lipids (lipids that cannot be converted to biodiesel) in the 35% estimate, which prevent the complete conversion of the lipid extract from occurring. The 3 predominant FAMEs that were observed - methyl palmitate, oleate, and stearate were also reported by Zhang et al. (Zhang et al. 2011).

When sludge and *R. glutinis* were compared at the same reaction conditions of 300 °C, 30 ml methanol:1 g cells, 3 hours and 90% water, the sludge produced a lower analytical FAME yield of 2.24 ± 0.4% than the *R. glutinis* at 20.71 ± 5.8% (Table 5.7). Although relatively low, the sludge FAME yield can still be improved by growing the cells under high carbon-to-nitrogen ratios to enhance the initial lipids present in the cells

www.manaraa.com

(Mondala et al. 2012). In the study by Mondala et al., they increased the lipid content of sludge from 11 % (raw activated sludge) to 18% (enhanced activated sludge) by cultivating at high C:N ratios. Their FAME yields also increased from 3 % to 10 % after sludge was enhanced. Furthermore, the transesterification condition used were only at 60 °C and not supercritical conditions, which indicates the possibility for higher yields.

Table 5.7 Comparison of FAME yields for transesterification of *Rhodotorula glutinis* and activated sewage sludge with supercritical methanol

Reaction Conditions 300 °C, 30 ml:1 g, 3 hours, 90% water	**Sludge**	***Rhodotorula glutinis***
FAME Yield (%)	2.24 ± 0.4	20.71 ± 5.8

5.3.3.1 Experiments to compare FAME yields between the batches:

Since the February 2011 batch was used for these results, a similar study for comparison at 2 reaction conditions was done on the September 2011 batch at the same reaction conditions of 1 hour at 275 °C and 300 °C to determine if they gave similar yields. The same reactant mix of 0.2g RG, 6ml methanol, and 1.8ml water (i.e. 30ml/g methanol:solid ratio and 90% wet solids) was reacted and results are shown in Table 5.8.

www.manaraa.com

Table 5.8 Experiments to compare FAME yields and effect of reaction times using September 2011 batch

	275 °C	**300 °C**
15 min		5.2 ± 0.9%
1 hr	32 ± 1.7% (15%)*	35.2 ± 5.3% (17%)*
5 hr		28.5 ± 4.4%

*Previous values from February 2011 batch are in parentheses

Overall, the September 2011 RG batch had higher FAME yields than the first February 2011 batch at the same 1 hour supercritical reaction conditions. This may have been due to the slight difference in the RG yeast preparation compared to the remaining 3 batches.

5.3.3.2 Effect of Reaction Time

A 15 min reaction was conducted to evaluate how far the reaction proceeded in a very short period of time. The 15 minutes was timed immediately after the reactors were placed in the sand bath. The 5.2 ± 0.9 % yield obtained indicates how fast the FAMEs are produced during the heating time before the system equilibrates to the temperature set point. Compared with literature data that has ~ 80% conversion in 15 minutes for a smaller system, the difference in these results lies in the fact that cells with cell membranes instead of plain oil are involved here and the cells also have 90% moisture content that could affect the conversion rate.

A 5 hr reaction was also run to see if a longer reaction time would produce a FAME yield significantly different from the 1 hr runs enough to justify the extra energy expense. However, reacting for 5 hours did not increase FAME yield but decreased it

www.manaraa.com

slightly. This yield was lower than expected given the high yields at shorter reaction times. This could be due to FAME degradation at the high temperature (Imahara et al. 2008) and also side reactions like hydrolysis of triglycerides to fatty acids and reverse esterification of those fatty acids occurring due to the presence of water.

Since no optimum was observed in this initial study and the yield based on varying reaction times were not significantly different, it was decided that a shorter reaction time would be economically beneficial to the process by saving energy. The next study was designed to study the production of FAMEs over a shorter time period. Furthermore, triglycerides, diglycerides and monoglycerides were quantitated to get a better picture of the reaction progress.

5.3.4 Timed results at 250 °C, 90% water content from 10 – 60 minutes

Previous experiments varying reaction time from 30min to 1.5hr for 0.2g of RG with 90% water content at 300°C showed that FAME yields (based on initial 0.2g of cells) were not significantly different, as seen in Figure 5.19.

The results of additional experiments to study conversion of glycerides and generation of FAMEs in a lower time range of 1-hour total reaction time at 10-minute intervals are shown in Figure 5.20. Since the internal temperature probe could take 12 minutes to settle at the temperature set point for a given reaction, the reaction time for these tests was started immediately after dropping the reactors into the sand bath to not miss the conversions that take place in the first couple minutes of heating. This helped investigate if there were any significant changes in FAME yield at a lower reaction time period (between 0 and 1 hour as seen in Figure 5.20) and to investigate the concentration changes in glycerides and FAMEs as reaction time progressed. A reaction temperature of

www.manaraa.com

250°C was chosen to investigate the FAME yield at a lower temperature. The results achieved at 250°C (16% after 1 hr) were comparable to the yields between 275 °C and 325°C, which could help reduce costs. However, the highest FAME yield was not achieved after 60 minutes but after 30 minutes (17%).

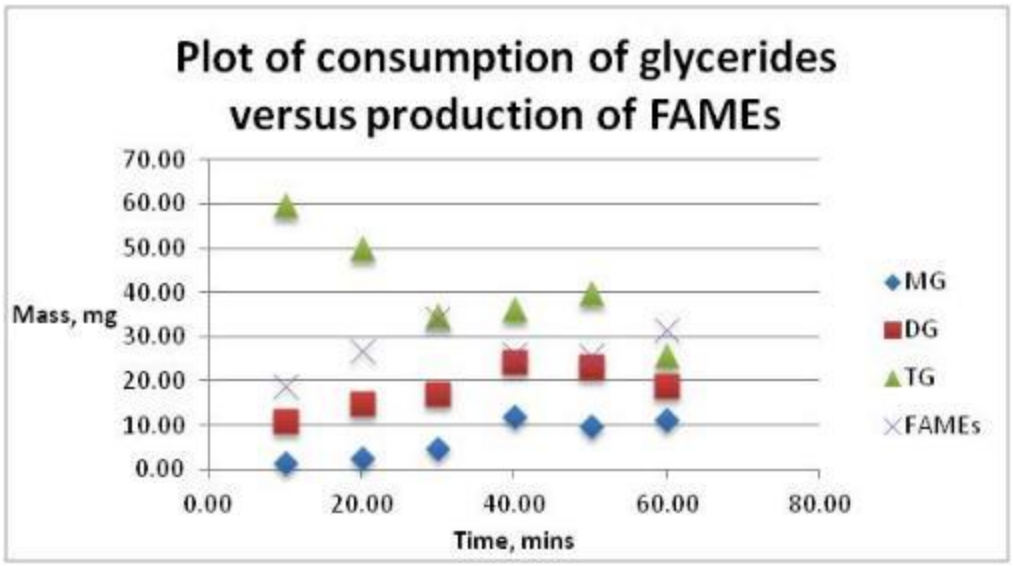

Figure 5.20 Product profiles at different reaction times for supercritical transesterification of *Rhodotorula glutinis*

Methanol:Solids ratio = 30 ml/g, 250 °C, 90% water

In the first 30 minutes, the trends on the 4 components are as expected with triglyceride amounts decreasing as it is being converted to diglycerides and monoglycerides, and FAMEs increasing as it is being produced from the glycerides as seen in the mechanism in Figure 5.21.

www.manaraa.com

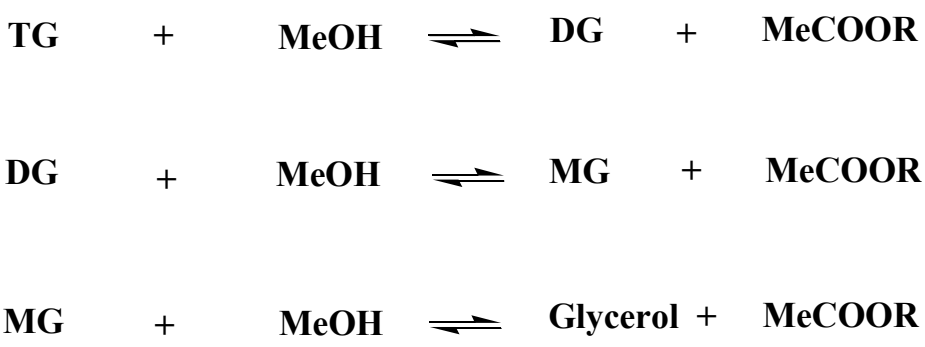

Figure 5.21 The mechanism of transesterification of triglyceride.

After the 30-minute sample, the glyceride amounts seem to stabilize at the 40 and 50 minute times although the triglyceride amount still decreases by the 60 minute sample and the FAME increase by the 60 minute time. These results between the 40 – 60 minute time periods could be due to the conversion of triglycerides to fatty acids and fatty acids converting to FAMEs. The triglyceride would be able to produce a fatty acid molecule if hydrolysis is concurrently taking place especially with the presence of water in these reactions. These were only run in duplicates as a preliminary test before the kinetic reactions in Sections 5.3.8 and 5.3.9.

Based on the glyceride consumption and FAME production, it was determined that the reaction time does not need to be higher than 30 minutes in further reactions since a higher FAME yield was not obtained after 30 minutes. Thus, for studying kinetics, it was decided to have sample points in the first 30 minutes. The time taken for the internal temperature probe to reach the set point (heat-up time) was ~ 13 minutes.

www.manaraa.com

5.3.5 In situ transesterification yield at 60 °C

The yield of FAMEs from this transesterification of RG lipid extracts was 19% based on the initial 0.2g of freeze-dried RG cells used and 59% based on initial lipid extract mass. In 2 hours, transesterification of lipid extracts with added catalyst and 0% water content generated 19% FAME yield, while in 10 minutes, transesterification of 90% wet RG with supercritical methanol produced 10% FAME yield (cell basis) as seen in Figure 5.20 and reached 17 % FAME yield in 30 minutes. At this point, the supercritical methanol process still has the promising advantages of: saving cost in catalyst usage and separation, reducing reaction time, high water tolerance and avoids the very expensive processing steps of removing water and extracting lipids before sludge oil can be reacted with catalyst to produce biodiesel.

5.3.6 Two-step in situ Hydrolysis and Supercritical Esterification

In Figure 5.22, the sample 'Before hydrolysis' represents the lipid extract of the unreacted RG cells and it indicates that there is a high amount of triglycerides initially that is drastically reduced in the other samples that were hydrolyzed proving that the triglycerides were converted to fatty acids as expected. We found that the yield in fatty acid if hydrolyzing at 270 °C for 30 minutes or 1 hour was very close. The fatty acid yields (based on initial cell weight) of hydrolysis after the 30 min and 60 min reaction times were 27.1 and 26.5% respectively which indicated that it was not necessary to hydrolyze for 60 minutes to get a higher fatty acid yield. It was also observed that only 18% of the fatty acids formed were converted to FAMEs with a yield of 15% when hydrolysis was followed by esterification in supercritical methanol at 250 °C for 20 minutes, indicating that the FAME yield from the 2-step reaction could be increased

www.manaraa.com

significantly. Based on these results, however, the 2-step process is comparable to the 1-step process in FAME yields.

Kusdiana and Saka's 2-step study showed that the 2-step method provided much higher yields than the 1-step for the same reaction time (Kusdiana and Saka 2004b). Reaction times for the 2-step method were obtained by summing the times for hydrolysis and esterification. For example, after 40 min reaction time at 270 °C, their 1-step method had a FAME yield of ~70% while their 2- step method had a yield of at least 95%.

The numbers obtained in this study cannot be compared to those in Kusdiana and Saka's study as they have different bases e.g. reaction time and water removal. Their studies suggest the reason the yield increase was not seen with the 2-step method is because: 1) our 1-step method already contained water that would have simultaneously hydrolyzed the triglycerides to fatty acids, thus performing reversible, supercritical methanol transesterification and esterification concurrently and producing high yields that were similar to the 2-step method. This would not happen in the absence of water; 2) water and glycerol were not separated out after hydrolysis in this study, which would have increased the yield. However, the scope of this study was to evaluate the effect of high water content on FAME yields in both methods. For future work, separating oil and aqueous phases before esterification could give the advantage of higher FAME yields and reduced glycerol production since glycerol is removed with the aqueous phase prior to methyl esterification (Minami & Saka, 2006).

www.manaraa.com

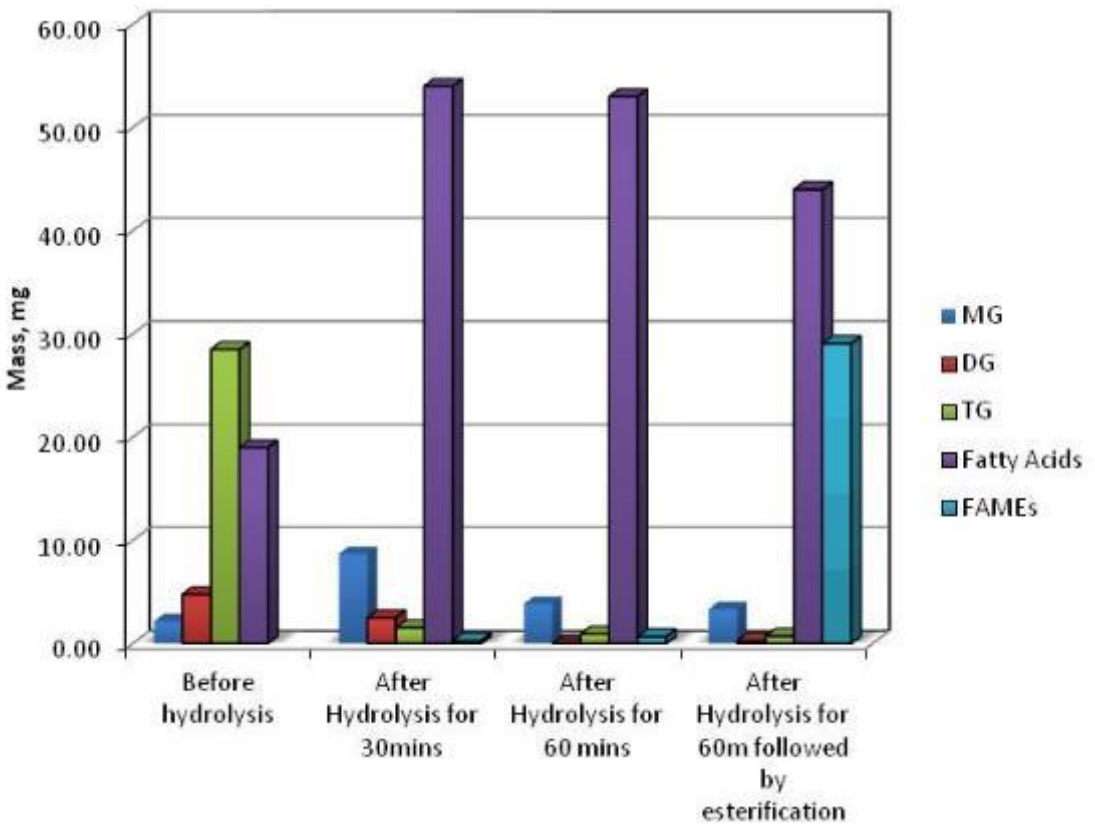

Figure 5.22 Product profiles for the hydrolysis and esterification

250 °C, 90% water

The predominant fatty acids obtained from hydrolysis were palmitic, oleic, stearic and linoleic acids and were identified by matches with model FAMEs analyzed by the GC. Figure 5.23 shows pictures of the RG cells before and after hydrolysis.

www.manaraa.com

a)  b) 

Figure 5.23 a) Freeze-dried *Rhodotorula glutinis* (RG) cells, b) residue of hydrolyzed RG

5.3.6.2 Effect of change in hydrolysis temperature

The fatty acid yields from hydrolysis of 90% wet RG cells for 30 min at 150 °C and 200 °C were 31.9 % and 26 % respectively. These were very similar to the fatty acid yield from hydrolysis at 270 °C (27%), which indicates that hydrolysis can be done at a lower temperature and save on energy costs for the 2 - step process. Interestingly, this was an unexpected trend especially since Kusdiana and Saka had the fatty acid yield increase by ~ 35% as temperature was increased from 255 C to 270 °C with a hydrolysis reaction time of 20 min (Kusdiana and Saka 2004b). This result can be attributed to system differences such as: water ratio, reaction pressure and the presence of cell membranes.

Although the 2-step process produces high yields, the large scale process could be a little more complicated than a single-step process. The process will require high-pressure reactors that could connect with a high-pressure water-glycerol-fatty acid phase separator (if increasing yield by removing aqueous phase); and the glycerol-water stream

www.manaraa.com

which is still contaminated by fatty acids will require more separation units that will only consume more energy if distillation columns are used for example (Ngamprasertsith and Sawangkeaw 2011).

5.3.7 Further optimization of the 1-step process at 90% water composition

5.3.7.1 Statistical Analysis and Regression

The statistical analyses were on the yields obtained from the optimization study were done using SAS® software*, a statistical analysis software package. The software's ADX interface was used for generating response surface plots, numerical optimization, and for data analyses and presentation. Regression analyses were done at a significance level of 0.05.

In combination with partial linear regression, the SAS ADX interface was used to determine the main and interactive effects of the factors on the response. A fourth order response surface model was used to relate the experimental response, Y, to the factors. The model is represented by:

$$Y = \beta_0 + \beta_1 X_1 + \beta_2 X_2 + \beta_{11} X_1^{\,2} + \beta_{22} X_2^{\,2} + \beta_{12} X_1 X_2 + \beta_{112} X_1^{\,2} X_2 + \beta_{122} X_1 X_2^{\,2} + \beta_{1122} X_1^{\,2} X_2^{\,2} + \varepsilon \quad (5.2)$$

Equation 5.2 represents the full response surface model (master model) including both the significant and insignificant effects. The R^2 fit at the 95% confidence level obtained was 0.88 which indicates good agreement between the model and experimental data. A fitted surface response model (predictive model) based only on significant factor effects was also obtained with an R^2 fit of 0.84:

$$Y = \beta_0 + \beta_1 X_1 + \beta_2 X_2 + \beta_{12} X_1 X_2 + \beta_{122} X_1 X_2^{\,2} + \beta_{1122} X_1^{\,2} X_2^{\,2} + \varepsilon \quad (5.3)$$

www.manaraa.com

The response surface and contour plots obtained from the SAS ® analysis are in Figure 5.24.

---

*SAS and all other SAS Institute Inc. product or service names are registered trademarks or trademarks of SAS Institute Inc. in the U.S.A. and other countries. ® indicates U.S.A. registration.

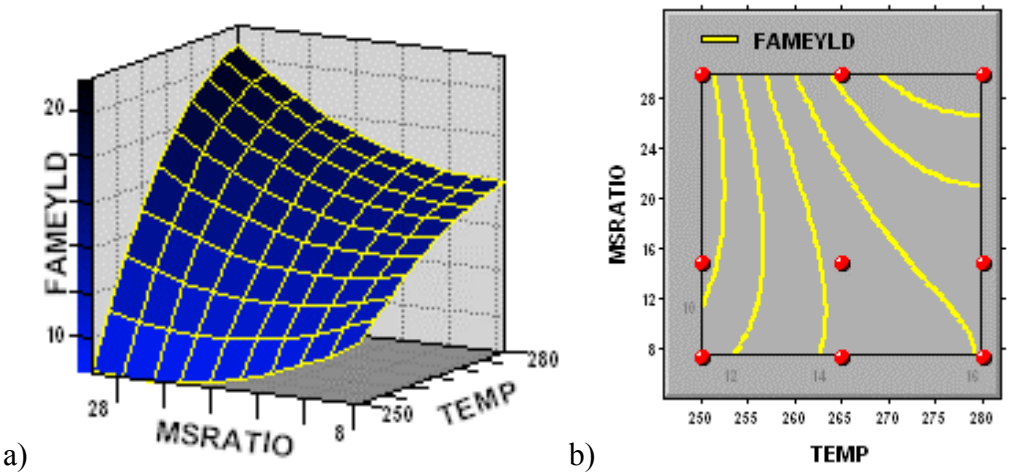

a) b)

Figure 5.24 a) RSM plot, and b) Contour plot from SAS® optimization

An ANOVA table (Figure 5.25) obtained using the SAS® software was used to identify significant effects.

www.manaraa.com

Effect	DF	Sum of Squares	Mean SS	F Ratio	P Value
TEMP	1	253.18	253.18	68.49	<.0001
MSRATIO	1	84.938	84.938	22.977	0.0001
TEMP*MSRATIO	1	67.005	67.005	18.126	0.0004
TEMP*TEMP	1	17.297	17.297	4.6793	0.0435
MSRATIO*MSRATIO	1	11.53	11.53	3.1192	0.0934
TEMP*TEMP*MSRATIO	1	54.436	54.436	14.726	0.0011
TEMP*MSRATIO*MSRATIO	1	59.094	59.094	15.986	0.0008

Figure 5.25 ANOVA table

All the factors except the quadratic factors of temperature and methanol were found to be statistically significant at a significance level of 0.05, and the uncoded predictive model was found to be with R^2 of 0.8 and statistically insignificant lack of fit ($p = 0.1$) which indicates that the predictive model is adequate. The optimum condition for FAME production from RG was obtained at the combination of 280 °C and 30ml/g methanol-to-solid ratio, producing a FAME yield of 21.5%. This condition is suitable for our needs as Xin et al. suggests that the favorable reaction temperature used in supercritical methanol processes should be less than 300 °C to avoid degradation of the methyl esters (Xin et al. 2008).

The coded model was expressed as:

$$\begin{aligned} FAMEYLD = {} & 14.8 + 7.5\times TEMP + 3.7\times MSRATIO + 2.4\times TEMP\times MSRATIO - \\ & 3.4\times TEMP\times TEMP\times MSRATIO - 4.4\times TEMP\times MSRATIO\times MSRATIO \end{aligned} \quad (5.4)$$

The SAS ® generated estimates for the coded model are shown in Figure 5.26. Figure 5.27 shows the numerical optimization values generated using the model and Table 5.9 shows the experimental runs and yields for comparison.

www.manaraa.com

Effects for FAMEYLD

	Master Model				Predictive Model			
Term	Estimate	Std Err	t	Pr > |t|	Estimate	Std Err	t	Pr > |t|
TEMP	7.530104	0.909884	8.275898	<.0001	7.530104	1.027853	7.326052	<.0001
MSRATIO	3.717425	0.775522	4.793451	0.0001	3.688362	0.865605	4.261021	0.0003
TEMP*MSRATIO	2.363	0.555024	4.257475	0.0004	2.363	0.626984	3.768834	0.0011
TEMP*TEMP	-1.71301	0.791899	-2.16316	0.0435				
MSRATIO*MSRATIO	1.588167	0.899241	1.766118	0.0934				
TEMP*TEMP*MSRATIO	-3.62255	0.944007	-3.83742	0.0011	-3.35208	1.057004	-3.1713	0.0046
TEMP*MSRATIO*MSRATIO	-4.40344	1.101341	-3.99825	0.0008	-4.40344	1.244134	-3.53936	0.0019

Figure 5.26 SAS ® generated estimates for coded model

Numerical Optimization Results:

	TEMP	MSRATIO	FAMEYLD
1	280	30	21.489866719
2	272.5	30	20.837166138
3	280	24.375	19.075936439
4	265	30	18.505342677
5	272.5	24.375	18.463352391
6	280	18.75	17.365309778
7	272.5	18.75	16.774003773
8	265	24.375	16.486481002
9	280	13.125	16.357986737
10	280	7.5	16.053967315
11	272.5	13.125	15.769120285
12	272.5	7.5	15.448701926
13	265	18.75	15.133245968
14	257.5	30	14.494396336
15	265	13.125	14.445637573
16	265	7.5	14.423655818
17	257.5	24.375	13.145322274
18	257.5	7.5	12.978828989
19	257.5	18.75	12.443036363
20	257.5	13.125	12.387538601
21	250	7.5	11.114221441
22	250	13.125	9.5948233693
23	250	30	8.8043271159
24	250	18.75	8.7033749579
25	250	24.375	8.4398762068

Figure 5.27 SAS ® generated numerical optimization result

www.manaraa.com

Table 5.9 Experimental runs and yields

RUN	TEMP	MSRATIO	FAMEYLD
1	250	7.5	14.675
2	250	7.5	13.509
3	250	7.5	13.09
4	250	15	7.19
5	250	15	6.751
6	250	15	7.143
7	250	30	10.611
8	250	30	7.795
9	250	30	9.324
10	265	7.5	14.197
11	265	7.5	12.425
12	265	7.5	11.603
13	265	15	15.159
14	265	15	12.267
15	265	15	13.351
16	265	30	17.4
18	265	30	20
28	265	30	23
19	280	7.5	14.905
20	280	7.5	14.181
21	280	7.5	16.77
22	280	15	20.714
23	280	15	17.423
24	280	15	20.466
25	280	30	16.266
26	280	30	24.127
27	280	30	20.275

5.3.8 1-step direct transesterification at 280 °C on RG with sample times 0, 5, 10, 15, and 20 minutes without water

Many authors in the literature show that the kinetics of supercritical transesterification typically follows the first-order rate law with respect to triglyceride concentration (Kusdiana and Saka 2001, He et al. 2007) due to the high methanol:oil ratio in the reaction. We hypothesize that our reaction would follow a similar model due to the

www.manaraa.com

high 654:1 molar ratio of methanol to oil present. The kinetic data obtained was fitted to a first order model based on unesterified compounds at any given time (uME) similar to a method used by supercritical methanol researchers (Kusdiana and Saka 2001, He et al. 2007). The unesterified compounds refer to the triglycerides (TG), diglycerides (DG), monoglycerides (MG), and unreacted fatty acids (FA) present at any given time. We determined this would be more accurate for our system since there could potentially be a significant amount of fatty acids produced from concurrent hydrolysis of the triglycerides. The rate constant was determined based on decreased amount of the unesterified compounds starting with the expression:

$$Rate = -d\frac{[uME]}{dt} \tag{5.5}$$

which can be written as

$$-d\frac{[uME]}{dt} = k[uME] \tag{5.6}$$

where *[uME]* is the concentration of the species excluding the methyl esters and glycerol product. Integrating,

$$ln[uME,0] - ln[uME,t] = kt \tag{5.7}$$

Rearranging,

$$-\ln(\frac{[uME,t]}{[uME,0]}) = kt \tag{5.8}$$

where *uME,0* is the initial species concentration at time zero, and *uME,t* is the concentration of the species at time *t*. The apparent rate constant, *k*, was obtained by the linear fit of Equation 5.8.

www.manaraa.com

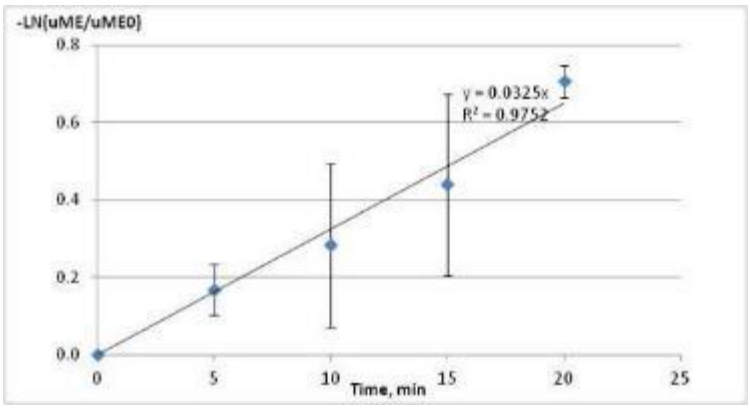

Figure 5.28 First order calculation for 0% transesterification

Since there was a 8 – 10 minute internal temperature equilibrating time when the reactors were first dropped in, which made it difficult to capture the initial changes in the reaction, the analysis was made using differences between the remaining time points. The rate constant obtained from the calculation in Figure 5.28 was 5.4×10^{-4} s^{-1}, which corresponds well with literature data. Irreversible first order reaction was used by these authors and they had similar rate constants of ~7.0×10^{-4} s^{-1}. Kusdiana and Saka used rapeseed oil at 270 °C and 12 MPa while He et al. used soybean oil at 270 °C and 28MPa. Literature shows that a rate constant of 3×10^{-4} s^{-1} was obtained at 230 °C for the noncatalytic transesterification of soybean oil (Dasari et al. 2003). The difference between the RG rate constant obtained of 5.4×10^{-4} s^{-1} and these literature values could be indicative of the effect of cell walls present, which may result in a mass transfer resistance prior to reaction.

www.manaraa.com

5.3.9 1-step direct transesterification at 280 °C on RG at 30ml/g methanol:solid ratio and 90% water with sample times 0, 5, 10, 15, and 20 minutes

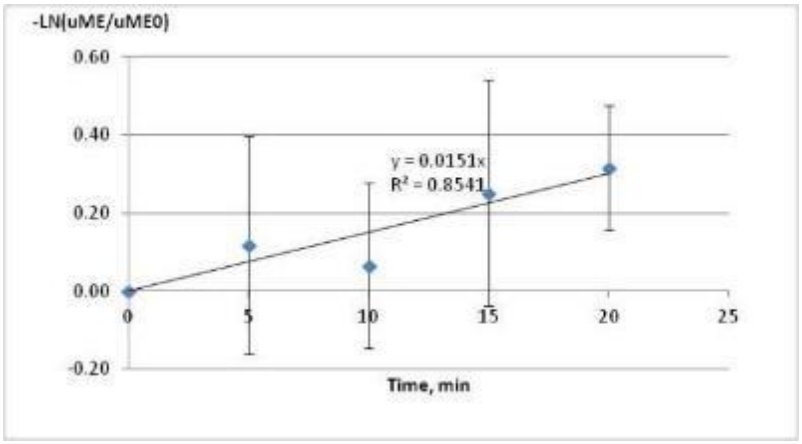

Figure 5.29 First order calculation for 90% transesterification

Using a similar approach as above, the rate constant obtained was 2.5×10^{-4} s^{-1} as obtained from the slope in Figure 5.29. The rate decreased by ~ 50%.

There are 4 major reactions that could be occuring in this system:

1. Forward reaction on transesterification of lipids
2. Hydrolysis of lipids producing FFAs
3. Esterification of FFAs
4. Reverse esterification reaction consuming FAMES and producing FFAs

The 50% decrease in rate constant indicates that these are the predominant reactions expected, based on the high methanol and water content.

5.3.10 Hydrolysis kinetics on RG at best temperature 280 °C at 0, 5, 10, 15, and 20 minutes

The rate constant of 2.15×10^{-3} s^{-1} obtained from Figure 5.30 is very fast compared to the transesterification reaction and indicates strong dominance of the

www.manaraa.com

hydrolysis reaction (instead of transesterification) occuring with in situ water during the 90% wet transesterification reaction. It also illustrates that the 2-step method can work in absence of water and can produce higher yields of FAMEs since the production of fatty acids will be significantly faster.

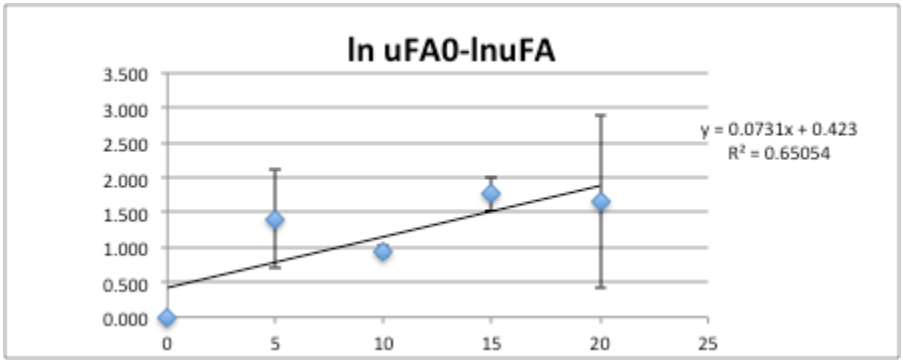

Figure 5.30 First order calculation for 90% water hydrolysis reaction

5.4 Conclusions

Two different reaction set-ups were used for the 1-step direct transesterification method: the stirred 450-ml Parr reactor gave an average FAME yield of 7% on sludge, while the smaller 46-ml batch reactors gave a 2.2% FAME yield. When compared at same conditions of 300 °C, 30 ml: 1 g, 3 hours and 90% water, sludge produced a lower yield of 2.24 ± 0.4% than *Rhodotorula glutinis* at 20.71 ± 5.8%. The FAME yield on the *R. glutinis* at supercritical conditions was very promising considering that as high as 60% of the original lipid content (35% cell dry weight) was converted to biodiesel at 90% water and no catalyst. Although, the FAME yield on the sludge reaction compared to the *R. glutinis* was significantly lower, it could be optimized by growing sludge under high

www.manaraa.com

carbon:nitrogen ratios. Regardless of the sludge source, as long as there is secondary sludge, the microbes can be fed present to increase the oil content.

Optimum condition for 1-step direct transesterification on the yeast at 90% water content is 280 °C with 30ml/g methanol:solid ratio and FAME yield of 21.5%. There is an opportunity for lower energy and methanol use to make this more economical without compromising significantly on yield.

The 2 hour in situ transesterification at 60°C of the Bligh & Dyer extract from the same 0.2g mass of RG cells used produced 19 % in FAME yield while the FAME yield obtained from 30 minutes of 250°C reaction with supercritical methanol was 17% (based on initial 0.2g of dry RG cells). At this point, the supercritical methanol process still has the promising advantages of: saving cost in catalyst usage and separation, reducing reaction time, avoiding the costly extraction process of drying down water and extracting lipids before sludge oil can be reacted to produce biodiesel.

From the comparison made of the 1-step and 2-step method at similar reaction conditions, both methods were comparable at 17% FAME yield for the 1-step reaction and 15% FAME yield for the 2-step method and are promising for use with wet sludge as feedstock. The two-step method did not produce a significantly higher amount of FAMEs at the reaction conditions tested, but still had a significant amount of fatty acids that were not converted. The kinetics from these systems showed that hydrolysis was faster and thus was occurring in the 90% wet 1-step reaction. Both have the potential for similar high yield and it could be more profitable to use the 1-step method if the same high temperature will be used in both cases, as the 2-step method could require more energy. Thus, depending on the process size, it could still be profitable to use the 1-step method

www.manaraa.com

rather than expend the energy to reach supercritical methanol twice. If taking the 2-step route, separating oil and aqueous phases before esterification could give the advantage of higher FAME yields and reduced glycerol production since glycerol is removed with the aqueous phase prior to methyl esterification. The result of the economic analysis demonstrates which method is better for a particular application, but both methods show that activated sludge could be potential feedstock for biodiesel production.

www.manaraa.com

5.5 References

Alenezi, R., G. A. Leeke, J. M. Winterbottom, R. C. D. Santos and A. R. Khan (2010). "Esterification kinetics of free fatty acids with supercritical methanol for biodiesel production." Energy Conversion and Management **51**(5): 1055-1059.

ASTM "ASTM D6584 - 00 Test Method for Determination of Free and Total Glycerin in B-100 Biodiesel Methyl Esters By Gas Chromatography." ASTM International.

Bligh, E. and W. Dyer (1959). "A Rapid method of total lipid extraction and purificatin " Canadian Journal of Biochemistry and Physiology **37**(8): 911-917.

Cao, W. L., H. W. Han and J. C. Zhang (2005). "Preparation of biodiesel from soybean oil using supercritical methanol and co-solvent." Fuel **84**(4): 347-351.

Dasari, M. A., M. J. Goff and G. J. Suppes (2003). "Noncatalytic alcoholysis kinetics of soybean oil." JAOCS, Journal of the American Oil Chemists' Society **80**(2): 189-192.

de Boer, K. and P. A. Bahri (2011). "Supercritical methanol for fatty acid methyl ester production: A review." Biomass and Bioenergy **35**(3): 983-991.

Demirbas, A. (2005). "Biodiesel production from vegetable oils by supercritical methanol." Journal of Scientific and Industrial Research **64**(11): 858-865.

Demirbas, A. (2007a). "Biodiesel from sunflower oil in supercritical methanol with calcium oxide." Energy Conversion and Management **48**(3): 937-941.

Diaz, M. S., S. Espinosa and E. A. Brignole (2009). "Model-Based Cost Minimization in Noncatalytic Biodiesel Production Plants." Energy & Fuels **23**(11): 5587-5595.

Ebert, J. (2008). "Supercritical Methanol for Biodiesel Production." Retrieved 02/14/13, from http://www.biodieselmagazine.com/articles/2212/supercritical-methanol-for-biodiesel-production.

He, H., S. Sun, T. Wang and S. Zhu (2007). "Transesterification Kinetics of Soybean Oil for Production of Biodiesel in Supercritical Methanol." Journal of the American Oil Chemists' Society **84**(4): 399-404.

Hegel, P., G. Mabe, S. Pereda and E. A. Brignole (2007). "Phase Transitions in a Biodiesel Reactor Using Supercritical Methanol." Industrial & Engineering Chemistry Research **46**(19): 6360-6365.

Holliday, R. L., J. W. King and G. R. List (1997). "Hydrolysis of Vegetable Oils in Sub- and Supercritical Water." Industrial & Engineering Chemistry Research **36**(3): 932-935.

Imahara, H., E. Minami, S. Hari and S. Saka (2008). "Thermal stability of biodiesel in supercritical methanol." Fuel **87**(1): 1-6.

www.manaraa.com

Khot, M., S. Kamat, S. Zinjarde, A. Pant, B. Chopade and A. RaviKumar (2012). "Single cell oil of oleaginous fungi from the tropical mangrove wetlands as a potential feedstock for biodiesel." Microbial Cell Factories **11**(1): 71.

Krammer, P. and H. Vogel (2000). "Hydrolysis of esters in subcritical and supercritical water." The Journal of Supercritical Fluids **16**(3): 189-206.

Kusdiana, D. and S. Saka (2001). "Kinetics of transesterification in rapeseed oil to biodiesel fuel as treated in supercritical methanol." Fuel **80**(5): 693-698.

Kusdiana, D. and S. Saka (2004a). "Effects of water on biodiesel fuel production by supercritical methanol treatment." Bioresource Technology **91**(3): 289-295.

Kusdiana, D. and S. Saka (2004b). "Two-step preparation for catalyst-free biodiesel fuel production." Applied Biochemistry and Biotechnology **115**(1): 781-791.

Lee, J.-S. and S. Saka (2010). "Biodiesel production by heterogeneous catalysts and supercritical technologies." Bioresource Technology **101**(19): 7191-7200.

Levine, R. B., T. Pinnarat and P. E. Savage (2010). "Biodiesel Production from Wet Algal Biomass through in Situ Lipid Hydrolysis and Supercritical Transesterification." Energy & Fuels **24**(9): 5235-5243.

Minami, E. and S. Saka (2006). "Kinetics of hydrolysis and methyl esterification for biodiesel production in two-step supercritical methanol process." Fuel **85**(17-18): 2479-2483.

Mondala, A., K. W. Liang, H. Toghiani, R. Hernandez and T. French (2009). "Biodiesel production by *in situ* transesterification of municipal primary and secondary sludges." Bioresource Technology **100**(3): 1203-1210.

Mondala, A. H., R. Hernandez, T. French, L. McFarland, J. W. Santo Domingo, M. Meckes, H. Ryu and B. Iker (2012). "Enhanced lipid and biodiesel production from glucose-fed activated sludge: Kinetics and microbial community analysis." AIChE Journal **58**(4): 1279-1290.

Moquin, P. H. L. and F. Temelli (2008). "Kinetic modeling of hydrolysis of canola oil in supercritical media." The Journal of Supercritical Fluids **45**(1): 94-101.

Ngamprasertsith, S. and R. Sawangkeaw (2011). Transesterification in Supercritical Conditions. Biodiesel - Feedstocks and Processing Technologies.

Patil, P. D., V. G. Gude, A. Mannarswamy, S. Deng, P. Cooke, S. Munson-McGee, I. Rhodes, P. Lammers and N. Nirmalakhandan (2011). "Optimization of direct conversion of wet algae to biodiesel under supercritical methanol conditions." Bioresour Technol **102**(1): 118-122.

www.manaraa.com

Pinnarat, T. and P. E. Savage (2010). "Noncatalytic esterification of oleic acid in ethanol." The Journal of Supercritical Fluids **53**(1–3): 53-59.

Ratledge, C. and Z. Cohen (2008). "Microbial and algal oils: Do they have a future for biodiesel or as commodity oils?" Lipid Technology **20**(7): 155-160.

Ratledge, C. and J. P. Wynn (2002). The biochemistry and molecular biology of lipid accumulation in oleaginous microorganisms. Advances in Applied Microbiology, Academic Press. **Volume 51:** 1-51.

Revellame, E., R. Hernandez, W. French, W. Holmes and E. Alley (2010). "Biodiesel from activated sludge through *in situ* transesterification." Journal of Chemical Technology and Biotechnology **85**(5): 614-620.

Revellame, E., R. Hernandez, W. French, W. Holmes, E. Alley and R. Callahan Ii (2011). "Production of biodiesel from wet activated sludge." Journal of Chemical Technology & Biotechnology **86**(1): 61-68.

Saenge, C., B. Cheirsilp, T. T. Suksaroge and T. Bourtoom (2011). "Potential use of oleaginous red yeast Rhodotorula glutinis for the bioconversion of crude glycerol from biodiesel plant to lipids and carotenoids." Process Biochemistry **46**(1): 210-218.

Saka, S. and D. Kusdiana (2001). "Biodiesel fuel from rapeseed oil as prepared in supercritical methanol." Fuel **80**(2): 225-231.

Valle, P., A. Velez, P. Hegel, G. Mabe and E. A. Brignole (2010). "Biodiesel production using supercritical alcohols with a non-edible vegetable oil in a batch reactor." The Journal of Supercritical Fluids **54**(1): 61-70.

van Kasteren, J. M. N. and A. P. Nisworo (2007). "A process model to estimate the cost of industrial scale biodiesel production from waste cooking oil by supercritical transesterification." Resources, Conservation and Recycling **50**(4): 442-458.

Warabi, Y., D. Kusdiana and S. Saka (2004). "Reactivity of triglycerides and fatty acids of rapeseed oil in supercritical alcohols." Bioresource Technology **91**(3): 283-287.

Xin, J., H. Imahara and S. Saka (2008). "Oxidation stability of biodiesel fuel as prepared by supercritical methanol." Fuel **87**(10–11): 1807-1813.

Zhang, G., W. T. French, R. Hernandez, E. Alley and M. Paraschivescu (2011). "Effects of furfural and acetic acid on growth and lipid production from glucose and xylose by Rhodotorula glutinis." Biomass Bioenergy **35**(1): 7-7.

www.manaraa.com

CHAPTER VI

ENGINEERING SIGNIFICANCE

6.1 Introduction

This study has demonstrated that activated sludge is a high-potential feedstock for biodiesel production especially since the lipid content of the microorganisms that comprise it can be enhanced. The supercritical methanol process showed potential of reducing overall production costs by reducing drying costs. Mondala et al. demonstrated that 307, 000 gallons of biodiesel could be produced annually at a cost of $3.23/gallon using activated sludge as a feedstock, based on processing of approximately 30 million gallons of wastewater/day. However, 53% of that cost was attributed to drying costs (Mondala et al. 2009).

Chapter 5 demonstrated that 2 methods: the 1-Step and 2-Step processes, can be used efficiently for biodiesel production while tolerating water content, and the economic analysis is discussed in Section 6.2 below.

6.2 Economic Analysis of 1-Step and 2-Step processes

This work was done for a plant that could process 30 million gallons of wastewater per day, based on the annual treatment capacity of the wastewater treatment plant in Tuscaloosa, AL (Mondala et al. 2009) and produce 140, 000 kg of influent sludge solids per day. The biodiesel production rate based on the influent sludge solids rate was

www.manaraa.com

4260 gallons/day for both the 1- and 2-step processes. This was done assuming that 10% of the entering sludge solids produced in the wastewater was saponifiable lipids that were fully converted to FAMEs (biodiesel). Operating time was assumed to be 8000 hr in a year (~333 days). The process simulation software, SuperPro Designer v6.0 (Intelligen 1991) was used for all costing except for those of the PFR reactors which were calculated using the costing model for a pressurized vessel (Peters et al. 2003). Additional costing references are included in the Appendices.

Table 6.1 illustrates the determination of the incoming sludge solids flow rate. This assumed a total solids concentration of 10,000 mg/L, a total BOD_5 removal of 95% from the wastewater treatment steps was estimated. The total sludge produced was calculated using a ratio of 0.65 kg of sludge produced/kg BOD_5 removed (Rittmann and McCarty 2001). It was assumed that 20% of the sludge is wasted and this waste stream is used as the wet sludge feedstock to the processes.

www.manaraa.com

Table 6.1 Calculation of sludge produced from 3 $\times 10^7$ million gallons/day WWTP at Tuscaloosa, AL

	Daily
Influent flow rate, daily WW capapcity in Tuscaloosa plant, gallons/day	3.00×10^7
Assumed concentration of solids in influent wastewater, mg/L	10000
Mass of Solids in influent WW, kg/day	1.14×10^6
BOD5 removal (95%), kg/day	1.08×10^6
Sludge produced (0.65kg sludge produced/kg BOD5 removed), kg/day	7.01×10^5
Amount of sludge wasted (20% of sludge produced), kg/day	1.40×10^5
Incoming Mass flowrate of sludge solids into process (Wasted), kg/day	**1.40×10^5**
Incoming Mass flowrate of wet sludge, kg/day	1.40×10^6
Actual % of solids in sludge wastewater	10
Methanol:solids ratio, ml/g	30
Incoming methanol flowrate needed for above kg of solids/day, in gal/day:	1.11×10^6
Incoming methanol flowrate needed for above kg of solids/day, in kg/day:	**3.32×10^6**

6.2.1 The 1-step process

A schematic for the 1-step process is shown in Figure 6.1. It was assumed that the wastewater sludge was obtained free from a wastewater treatment plant near the biodiesel production plant, neglecting transportation costs. The wet sludge and methanol streams were combined via a mixer after preheating them to 95 °C and 60°C respectively. These were reacted in a stoichiometric plug flow reactor (PFR) at the optimal reaction condition obtained from the experimental study in Chapter 5: temperature of 280 °C and methanol:solid ratio of 30ml/g for the base case. A residence time of 60 minutes was utilized and pressure of 14 MPa was assumed from data in He et al. (He et al. 2007). The stoichiometry used in the kinetic PFR was:

www.manaraa.com

78 Sludge + 3 Methanol → 3 FAME + 1 Glycerol + 2.27sludge remnant (6.1)

Sludge was represented by the empirical formula $C_5H_7O_2N$ (Revellame et al. 2012). The stoichiometry was calculated assuming that 78 moles of sludge (113 g/mol molecular weight) were equivalent to 1 mole of saponifiable triglyceride which was assumed to be triolein (885g/mol molecular weight). FAME was represented by methyl oleate (296.5 g/mol molecular weight). The sludge remnant ($C_{138}H_{167}O_{70}N_{39}$) was added to balance the stoichiometric reaction and was assumed to have a molecular weight of ~ 3489 g/mol.

The PFR product was run through a phase separation device, where it was assumed that 90% of the methanol and water in the product stream exit as the top component (since they exist as vapor at 280 °C). This top component is further separated using a distillation column (C-103). The remaining product stream from the reactor exits through the bottom stream and is filtered using 3 microfiltration systems, and separated in a second distillation column (C-101) where methanol is removed for additional recycling. The bottom stream of C-101 was routed to a distillation column to purify the FAME (diesel) product. Actual FAME produced was 4260 gallons per day, assuming full conversion of 10% of sludge solids, and neglecting process losses (Table 6.2).

www.manaraa.com

Table 6.2 Calculation of biodiesel yield from 1-step process

Incoming hourly rate of sludge solids, kg/h	5843
10% of sludge is triglyceride (TG) that is converted to fame, kg/h	584
1 mole of triglyceride (TG), g/mol	885
Molar flowrate of TG(in sludge), mol/h	660
Molar rate of FAME produced (Since 1 mol TG = 3 mol FAME), mol/hr	1981
Mass rate of FAME produced (Since 1 mol TG = 3 mol FAME), kg/hr	587
Yearly mass production rate of biodiesel, kg/yr	4.70×10^6
Yearly volume production rate of biodiesel, gal/yr	1.42×10^6
Daily volume production rate of biodiesel, gal/day	**4261**

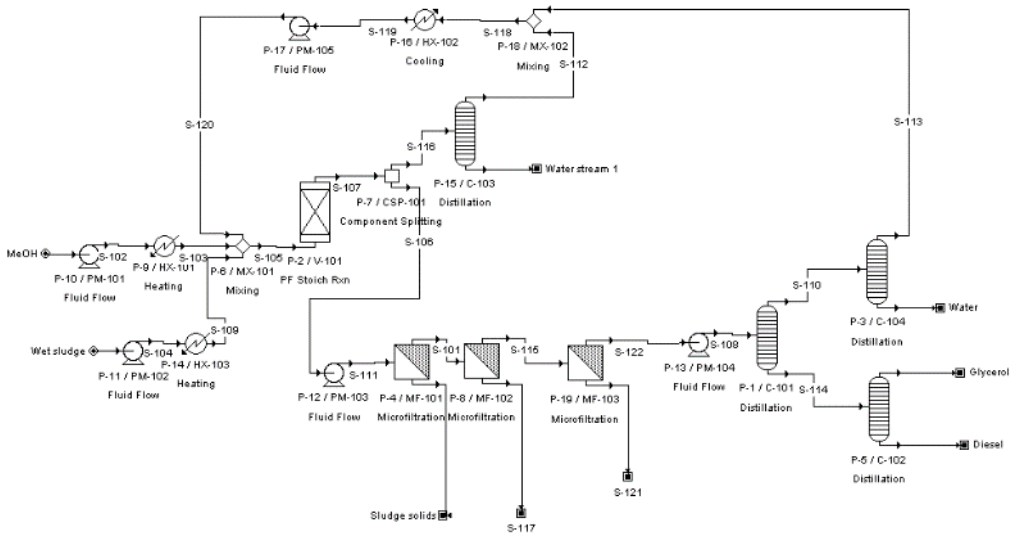

Figure 6.1 1-step process schematic

The breakdown of the estimated costs associated with the 1-Step process is shown in Table 6.3. To determine the influence of methanol:solids ratio, the calculations were made using reduced methanol-to-solid ratio at 7.5ml/g, but assuming the same yield. The basis for these calculations was also 4260 gallons of biodiesel produced daily.

www.manaraa.com

Table 6.3 Calculation of biodiesel breakeven price from the 1-step process

		Costs ($) for 30ml/g	Costs ($) for 7.5ml/g
Total capital investment cost, TCC (FCC + WCC)		4.93×10^7	4.48×10^7
1. Equipment cost, EC		7.05×10^6	6.34×10^6
Fixed capital cost, FCC		4.29×10^7	3.90×10^7
Working capital, WCC (15% of FCC)		6.43×10^6	5.85×10^6
B. Total annual production cost, TAPC (DOC+IOC+DEPC+GE)		6.82×10^7	4.45×10^7
1. Direct operating costs, DOC		4.75×10^7	2.79×10^7
Labor	7.06×10^6		
2. Indirect operating costs, IOC		5.10×10^6	5.02×10^6
a. Overhead, packing, storage (60% of labor)		4.24×10^6	4.24×10^6
b. Local taxes (1.5% of FCC)		6.43×10^5	5.85×10^5
c. Insurance (0.5% of FCC)		2.14×10^5	1.95×10^5
3. Depreciation, DEPC (10% of FCC)		4.29×10^6	3.90×10^6
4. General expenses, GE		1.13×10^7	7.74×10^6
a. Administrative expenses (25% of overhead)		1.06×10^6	1.06×10^6
b. Distribution and selling (≈10% of TAPC)		6.82×10^6	4.45×10^6
c. Research and development (≈5% of TAPC)		3.41×10^6	2.23×10^6
Price of biodiesel per gallon to break even ($)		48.00	31.37

The results show a biodiesel production break-even price of $48.00 at 30ml/g and $31.37 at 7.5ml/g, which is quite expensive if comparing to a petroleum diesel price of $3.38/gallon. Marchetti et al (Marchetti and Errazu 2008) who performed an economic analysis on biodiesel production from acid oils at a rate of 36,036 ton/yr obtained a biodiesel unitary cost of $0.98/kg (or $3.24/gallon). However, the biggest differences that exist between these processes occur with the feedstock used and the chemical process. Marchetti et al. treated 36,000 tons/year of acid oils (> 90% triglycerides), while this

www.manaraa.com

study treats 47,000 ton/year of 90% wet sludge (approximately < 20% saponifiable lipids).

6.2.2 The 2-step process

A schematic for the 2-step process is shown in Figure 6.2. The same incoming mass flow rate of sludge solids as in the 1-step process was used. The 90% wet sludge was charged into a stoichiometric PFR at hydrolysis reaction condition of 200 °C. Residence time in the hydrolysis reactor was 30 minutes and it was assumed that 10% of the entering sludge solids produced in the wastewater were triglycerides that were fully converted to free fatty acids. The hydrolysis reactor had a pressure of 7 MPa, which was assumed from data in the paper by Moquin et al. (Moquin and Temelli 2008). The stoichiometry used in the hydrolysis PFR was:

$$78\ \text{Sludge} + 3\ \text{Methanol} \rightarrow 3\ \text{Fatty acid (FFA)} + 1\ \text{Glycerol} + 2.25\ \text{sludge remnant} \quad (6.2)$$

This was calculated assuming that 78 moles of sludge (113 g/mol) were equivalent to 1 mole of saponifiable triglyceride (triolein), which was hydrolyzed to oleic acid. The sludge remnant ($C_{138}H_{167}O_{72}N_{39}$) was added to balance the stoichiometric reaction and was assumed to have a molecular weight of ~ 3521g/mol.

www.manaraa.com

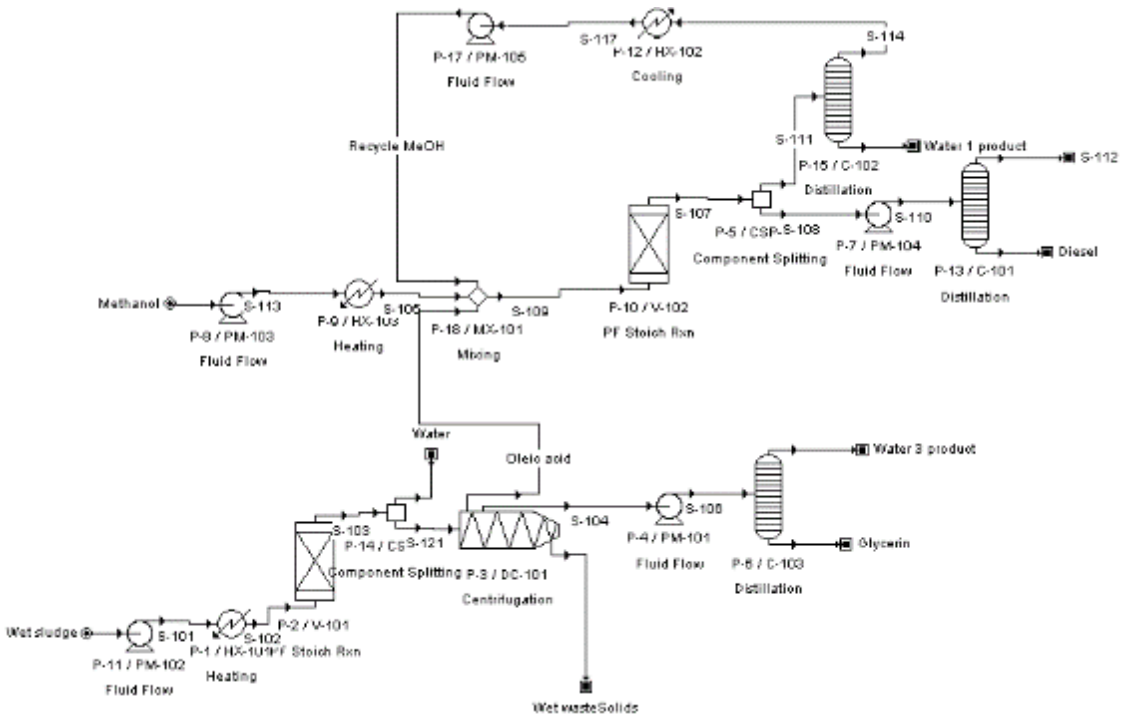

Figure 6.2 2-step process schematic

After hydrolysis, the product was run through a phase separation device, where it was assumed that 90% of the water in the product stream exit as the top. The bottom component was further separated using a centrifuge for solid/oil/fat removal (DC-101). Oleic acid was removed from the top section of the centrifuge and combined with methanol coming in at a 7:1 methanol:fatty acid ratio for the supercritical esterification reaction in the stoichiometric PFR (V-102). The 7:1 ratio was obtained from the supercritical esterification study done by Alenezi et al (Alenezi et al. 2010). Complete conversion of the FFAs during esterification at 280 °C and a residence time of 30 minutes was assumed, also neglecting process losses.

A splitter was also used to remove 90% of the methanol and water content in the esterification product stream which was followed by a series of distillation separations to

www.manaraa.com

generate the methanol recycle and purify the diesel product stream. Actual FAME produced was also ~ 4260 gallons per day. Table 6.4 illustrates the calculation of the biodiesel yield.

Table 6.4 Calculation of biodiesel yield from the 2-step process

Test yield of fatty acid from hydrolysis	**Hourly**
incoming hourly rate of sludge solids, kg/h	5843
10% of sludge is triglyceride (TG) that is converted to fame, kg/h	584
1 mole of TG, g/mol	885
molar flowrate of TG(in sludge), mol/h	660
Molar rate of FFA produced (Since 1 mol TG = 3 mol FFA), mol/hr	1981
Mass rate of FFA produced (Since 1 mol TG = 3 mol FFA), kg/hr	560
Methanol:ffa molar ratio	7
Incoming methanol flowrate needed for above kg of solids/day, in mol/hr	13865
Incoming methanol flowrate needed for above kg of solids/day, in kg/hr	444
Test yield of FAME from esterification	**Hourly**
incoming hourly molar flow rate of ffa	1981
Molar rate of FAME produced (Since 1 mol FFA =1 mol FAME), mol/hr	1981
Mass rate of FAME produced(Since 1 mol FFA =1 mol FAME), kg/hr	587
Yearly mass production rate of biodiesel, kg/yr	4.70×10^6
Yearly volume production rate of biodiesel, gal/yr	1.42×10^6
Daily volume production rate of biodiesel, gal/day	**4261**

The breakdown of the estimated costs associated with the 2-Step process is shown in Table 6.5. Using the same biodiesel production basis as the 1-step process, the breakeven price for the 2-step process at the conditions described was $11.77, which was at least 62% lower than either of the 1-step processes analyzed in Table 6.3. This can attributed to the smaller reactor and downstream processing equipment needed for esterification after most of the water content has been removed upon exiting the

www.manaraa.com

hydrolysis stage. The fast hydrolysis conversion to fatty acids that initially takes place at a lower temperature (200 °C), in addition to the lower methanol volume needed for esterification, also reduced the energy requirements and thus, the cost.

Table 6.5 Cost breakdown for 2-step process

Total capital investment cost, TCC (FCC + WCC)a		**1.47×10^7**
1. Equipment cost, EC		2.09×10^6
Fixed capital estimate, FCC		1.28×10^7
Working capital, WCC (15% of FCC)		1.92×10^6
B. Total annual production cost, TAPC (DOC+IOC+DEPC+GE)b		**1.67×10^7**
1. Direct operating costs, DOC		8.83×10^6
Labor	5.11×10^6	
2. Indirect operating costs, IOC		3.32×10^6
a. Overhead, packing, storage (60% of labor)		3.07×10^6
b. Local taxes (1.5% of FCC)		1.92×10^5
c. Insurance (0.5% of FCC)		6.39×10^4
3. Depreciation, DEPC (10% of FCC)		1.28×10^6
4. General expenses, GE		3.27×10^6
a. Administrative expenses (25% of overhead)		7.67×10^5
b. Distribution and selling (≈10% of TPC)		1.67×10^6
c. Research and development (≈5% of TPC)		8.35×10^5
Price of biodiesel per gallon to break even		**11.77**

6.2.2.1 Comparison of both processes

The purpose of the economic analysis was to compare the two methods, not to give absolute cost values for each process. Although, the 2-step method has a lower breakeven price, it is still not competitive with petroleum diesel price at ~ $3.38 per gallon. There are a number of possibilities to improve the economic viability of the 2-step process which include: 1) reducing the temperature of the hydrolysis and esterification reactors to lower energy requirements, 2) reducing the methanol-to-solid ratio, 3)

www.manaraa.com

including heat integration to maximize efficiency, and 4) adding tipping fees from the WWTP and from sale of the spent solids.

For example, the spent solids (~126,000 kg/day) obtained from the process can be used as a source of additional revenue if sold (e.g. for composting). It could generate ~ \$106/day if assuming \$11/yd^3 as the selling price (SolidWasteDistrict.com 2013). The use of one or more of these options could potentially make the biodiesel break-even price competitive with petroleum fuels. This can generate a plethora of opportunities globally by utilizing a waste material for local, sustainable fuel production that will ultimately improve the economic security of any country.

www.manaraa.com

6.3 References

Alenezi, R., G. A. Leeke, J. M. Winterbottom, R. C. D. Santos and A. R. Khan (2010). "Esterification kinetics of free fatty acids with supercritical methanol for biodiesel production." Energy Conversion and Management **51**(5): 1055-1059.

He, H., S. Sun, T. Wang and S. Zhu (2007). "Transesterification Kinetics of Soybean Oil for Production of Biodiesel in Supercritical Methanol." Journal of the American Oil Chemists' Society **84**(4): 399-404.

Intelligen (1991). SuperPro Designer.

Marchetti, J. M. and A. F. Errazu (2008). "Technoeconomic study of supercritical biodiesel production plant." Energy Conversion and Management **49**(8): 2160-2164.

Mondala, A., K. W. Liang, H. Toghiani, R. Hernandez and T. French (2009). "Biodiesel production by *in situ* transesterification of municipal primary and secondary sludges." Bioresource Technology **100**(3): 1203-1210.

Moquin, P. H. L. and F. Temelli (2008). "Kinetic modeling of hydrolysis of canola oil in supercritical media." The Journal of Supercritical Fluids **45**(1): 94-101.

Peters, M. S., K. D. Timmerhaus and R. E. West (2003). Plant design and economics for chemical engineers, McGraw Hill.

Revellame, E. D., R. Hernandez, W. French, W. E. Holmes, T. J. Benson, P. J. Pham, A. Forks and R. Callahan Ii (2012). "Lipid storage compounds in raw activated sludge microorganisms for biofuels and oleochemicals production." RSC Advances **2**(5): 2015-2031.

Rittmann, B. E. and P. L. McCarty (2001). Environmental Biotechnology: Principles and Applications. New York, NY, McGraw-Hill.

SolidWasteDistrict.com (2013) "Compost Rates and Tipping Fees."

www.manaraa.com

CHAPTER VII

CONCLUSION

The economic feasibility of using activated sludge from municipal wastewater with little or no drying as a feedstock for cost-efficient biodiesel production was investigated. This work sought after catalytic and non-catalytic processes that could lower the produce biodiesel production cost from activated sludge.

The research began with the study of the effect of water on tranesterification of soybean oil using porous metal oxides. The results demonstrated that there is strong water deactivation on these catalysts. Therefore, these catalysts were not recommended for use with wet sludge to generate an economic yield of biodiesel.

In the study of the effect of water on esterification of palmitic acid using zeolites, the most active zeolite was the H-ZSM-5 catalyst with silica:alumina ratio of 80. An optimum water content of 50 % was identified using this catalyst and a mechanism of Langmuir-Hinshelwood form was proposed for moisture contents tested in the range of 0 - 70%:

$$r = k\frac{(C_a C_b - \frac{C_c C_d}{K_e})}{(1+K_a C_a + K_d C_d)^2} \quad (7.1)$$

The mechanism demonstrated that the adsorption of palmitic acid and water molecules on two different catalytic sites during the reactions was significant. This

www.manaraa.com

demonstrated that at this optimum, fatty acids produced from hydrolyzed sludge do not have to be dried completely before reaction, but can be dried partially to 50% and used to produce biodiesel.

For the non-catalytic process, two methods (1-step and 2-step processes) were studied and compared in terms of FAME yields and kinetic rate constants. A model system of oleaginous yeast - *Rhodotorula glutinis* (RG) was used to evaluate the biodiesel production in a system similar to sludge. The optimization of reaction conditions for the 1-step method of direct transesterification of RG gave the optimum as 280 °C, 30ml/g, producing a FAME yield of 21.5% while at 90% moisture content.

An economic analysis was used to compare the biodiesel break-even price for the 2-step method (hydrolysis followed by esterification) with the 1-step method (direct transesterification) at this optimum reaction condition. The 2-step method had a break-even price for biodiesel production at $11.77 compared to $48 for the 1-step process. This was attributed to the smaller methanol volume needed for the 2-step process which causes smaller reactors and downstream processing equipment to be needed. Although the 2-step break-even price is still relatively expensive, some cost savings can be made to reduce production costs by making some changes such as: 1) reducing the temperature of the hydrolysis and esterification reactors to lower energy requirements, 2) reducing the methanol-to-solid ratio, 3) including heat integration to maximize efficiency, and 4) adding tipping fees from the WWTP and from sale of the spent solids.

The results show that the use of the non-catalytic process of supercritical methanol with wet sludge for biodiesel production is feasible. Although not yet economical, it is promising in terms its high water tolerance, no use of catalysts, no soap

www.manaraa.com

products, short reaction times, and relatively easier separation. Further sensitivity analyses could enable commercial production of biodiesel at a relatively low cost from this readily available, non-food feedstock. And in the case of the 2-step method, the water already present in sludge is an advantage for use in hydrolysis.

7.1 Research Needs

Further study at the 50% water composition optimum on the esterification with zeolite should be done and an economic analysis to compare with the non-catalytic process. In addition, additional research on improving the 2-step method by determining cost savings in the above-mentioned areas (heat integration, tipping fee revenue, reduced methanol volume, and reduced reaction temperatures) will help improve the economics.

www.manaraa.com

APPENDIX A

X-RAY DIFFRACTOGRAMS OF METAL-SUBSTITUTED HYDROTALCITES

www.manaraa.com

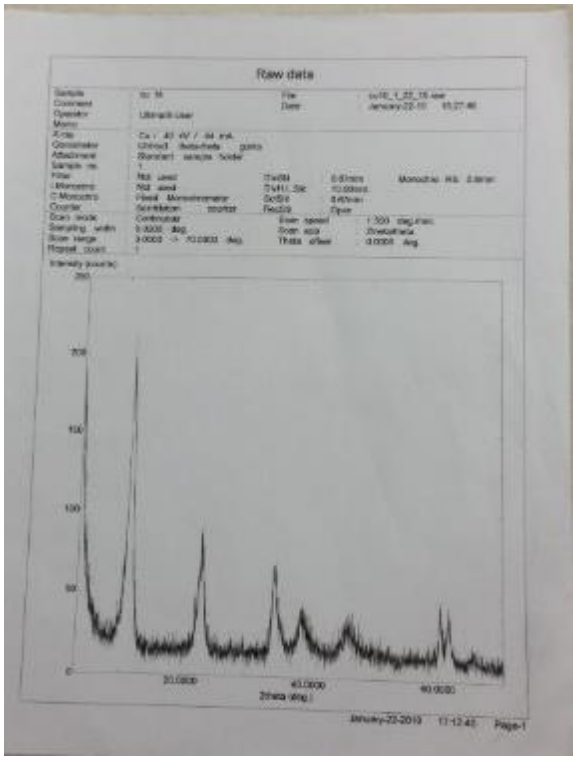

www.manaraa.com

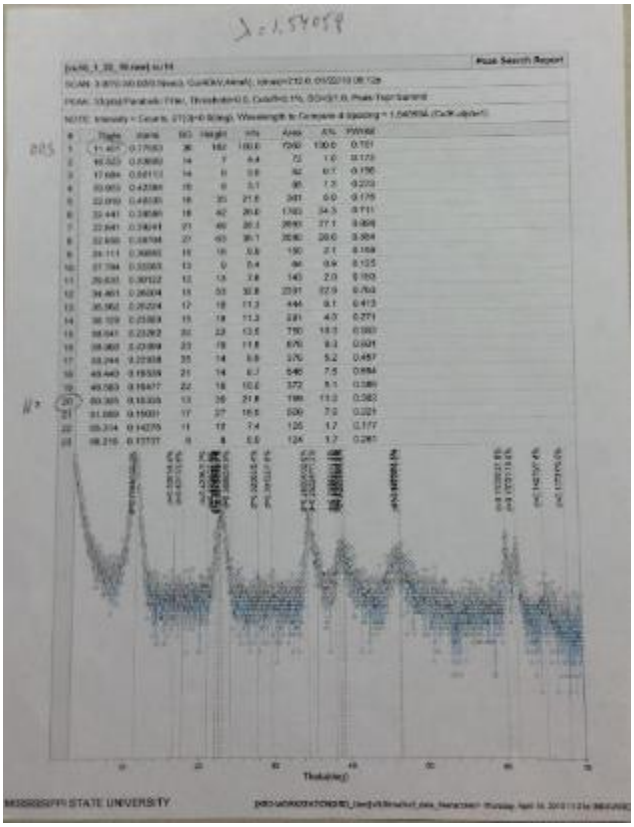

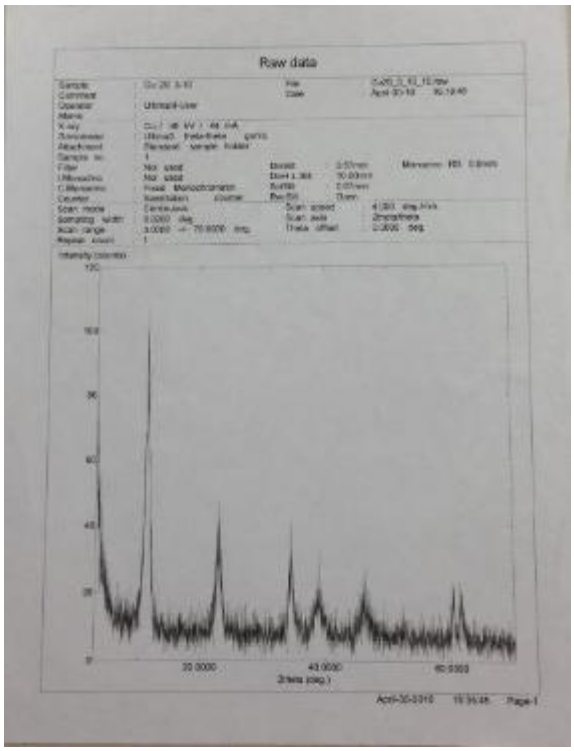

www.manaraa.com

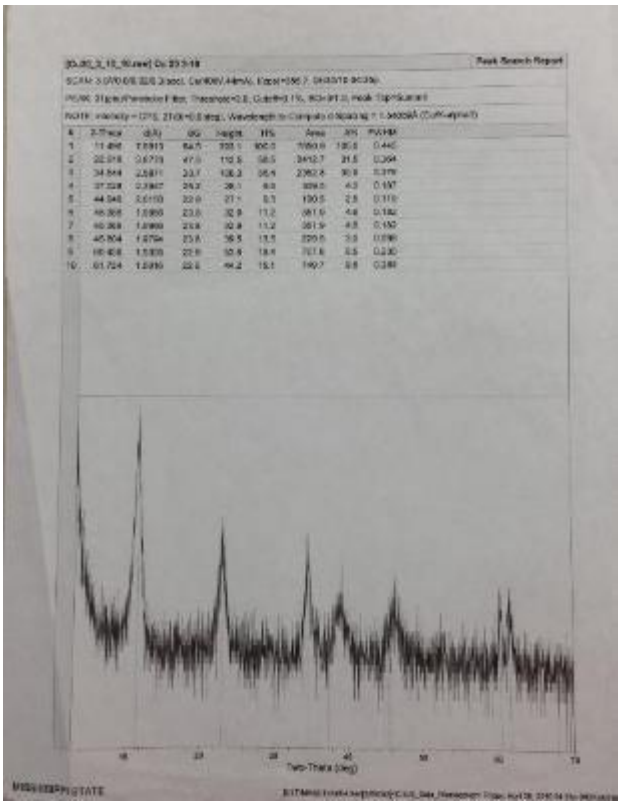

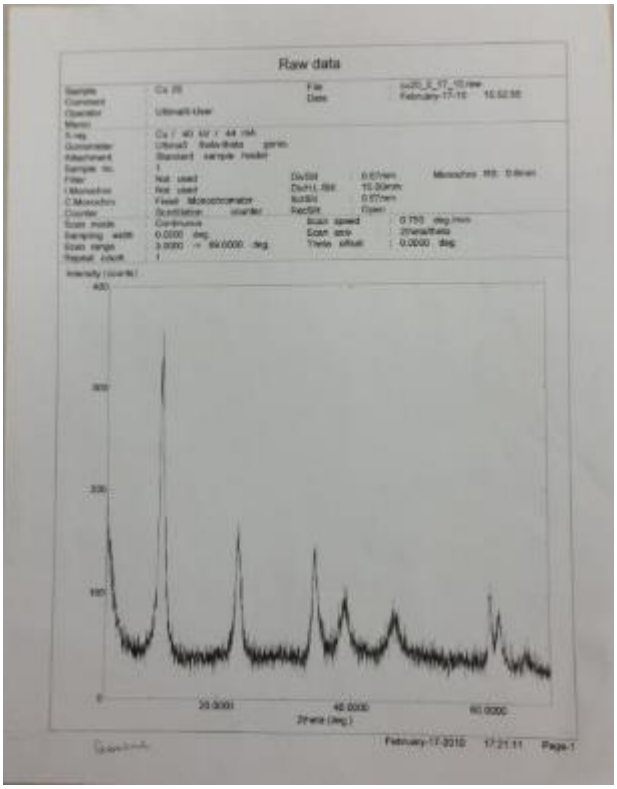

www.manaraa.com

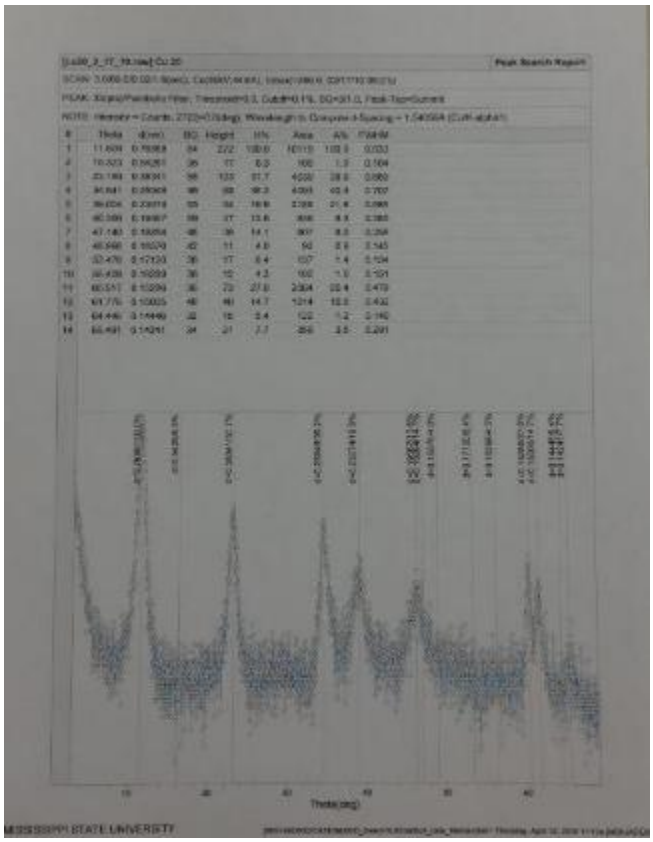

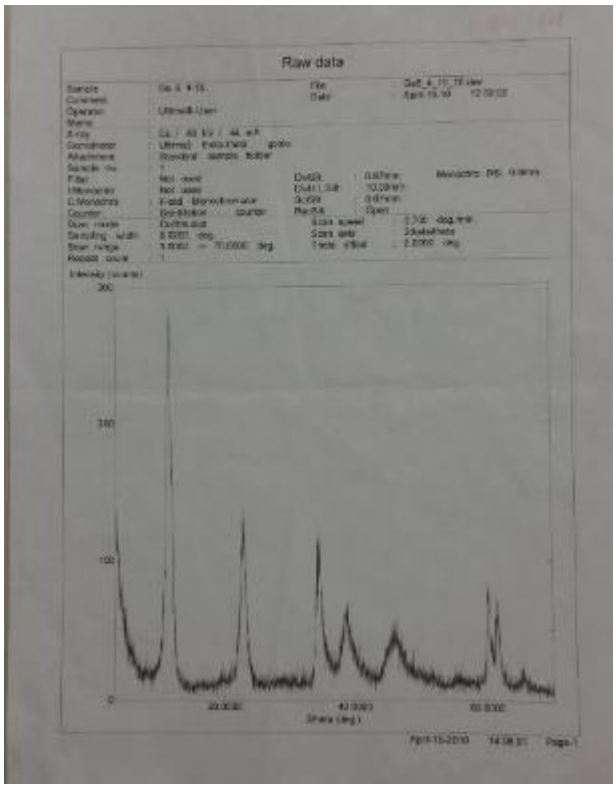

www.manaraa.com

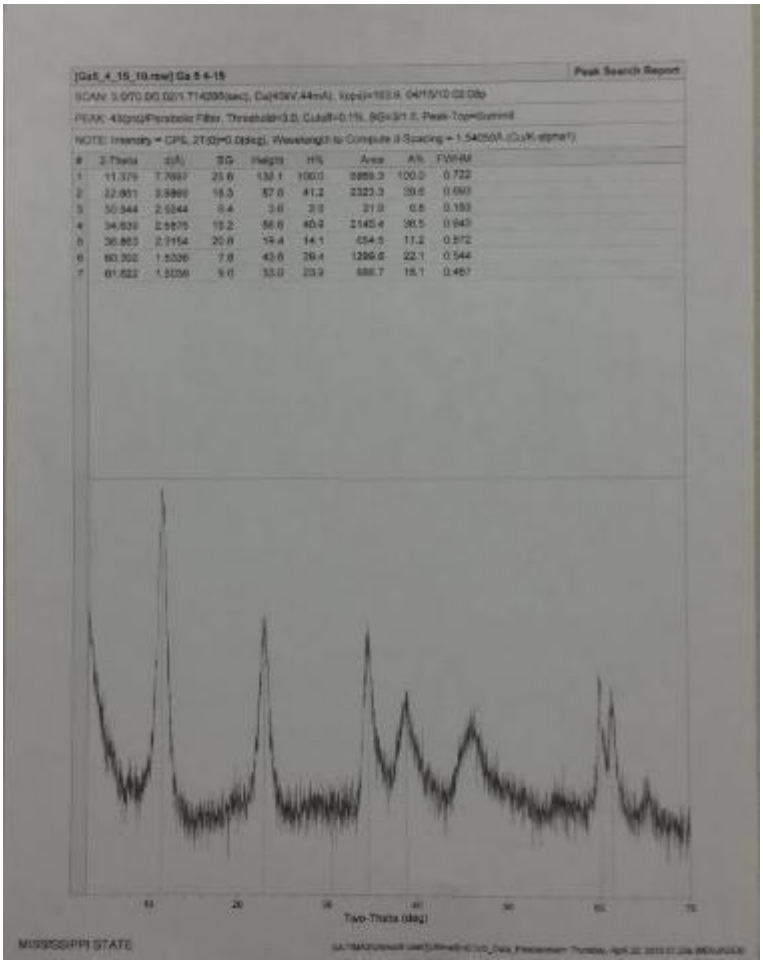

www.manaraa.com

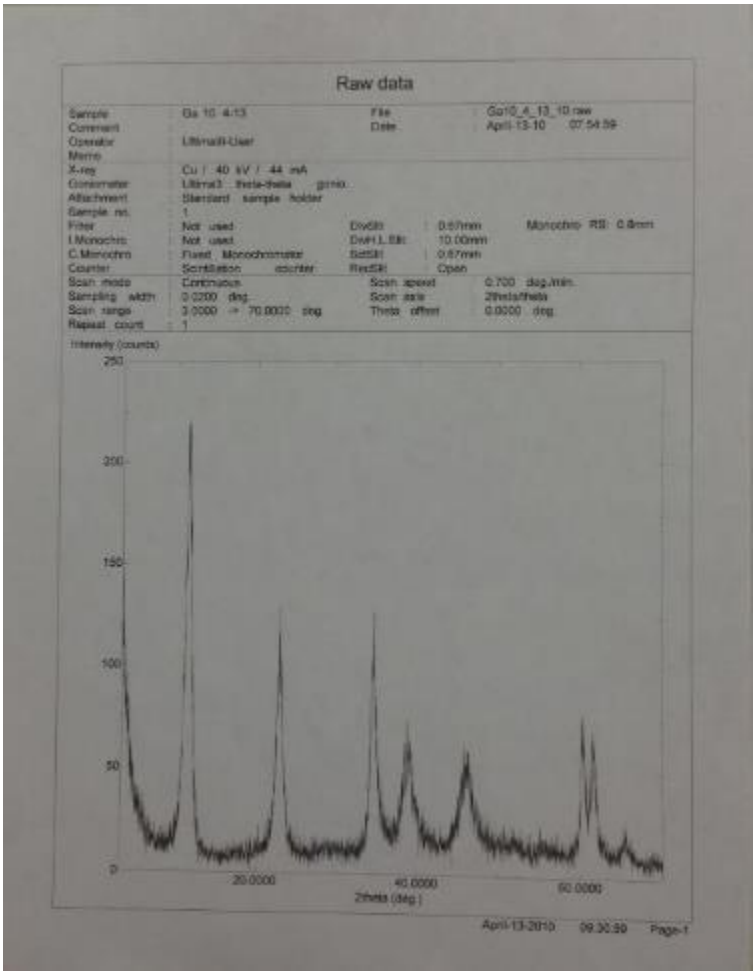

www.manaraa.com

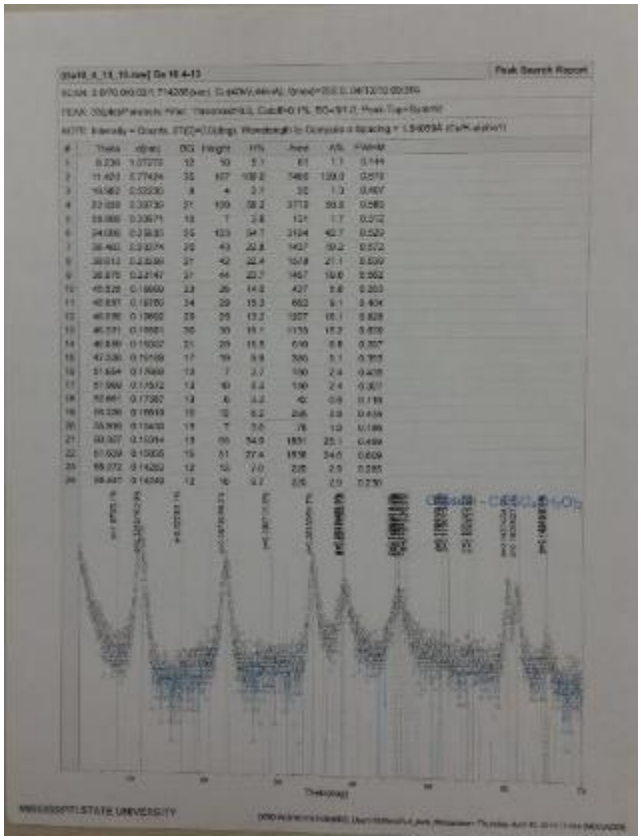

www.manaraa.com

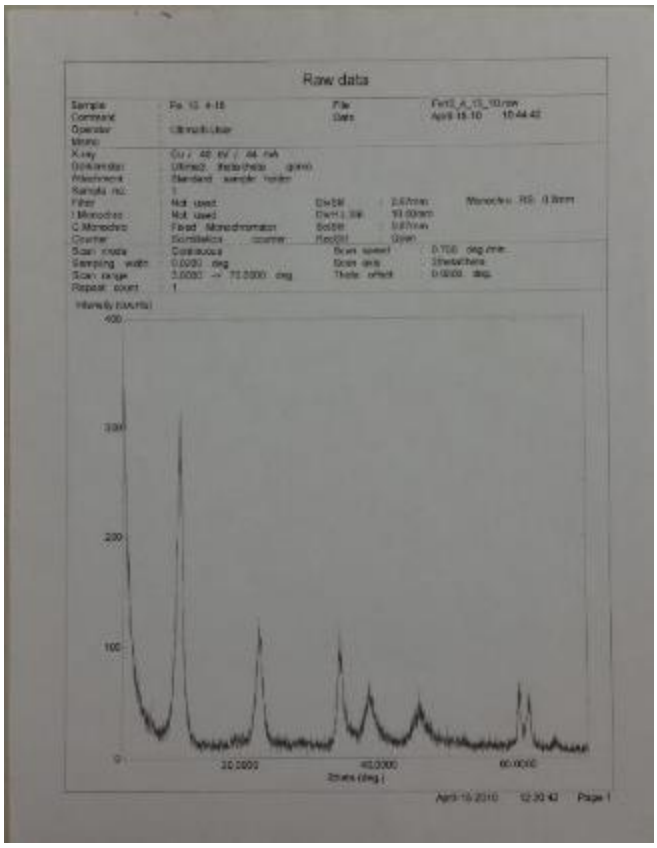

www.manaraa.com

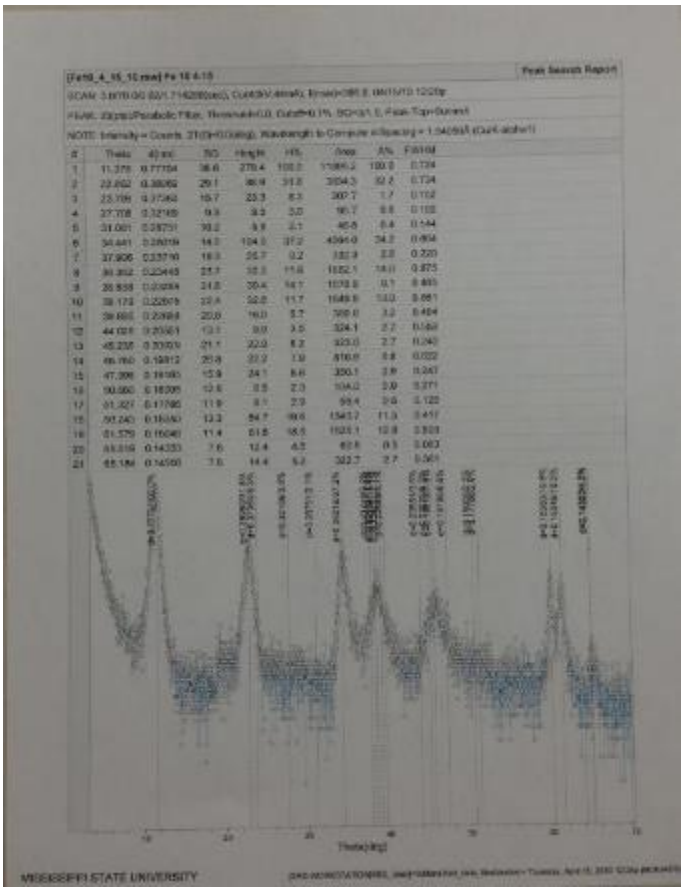

www.manaraa.com

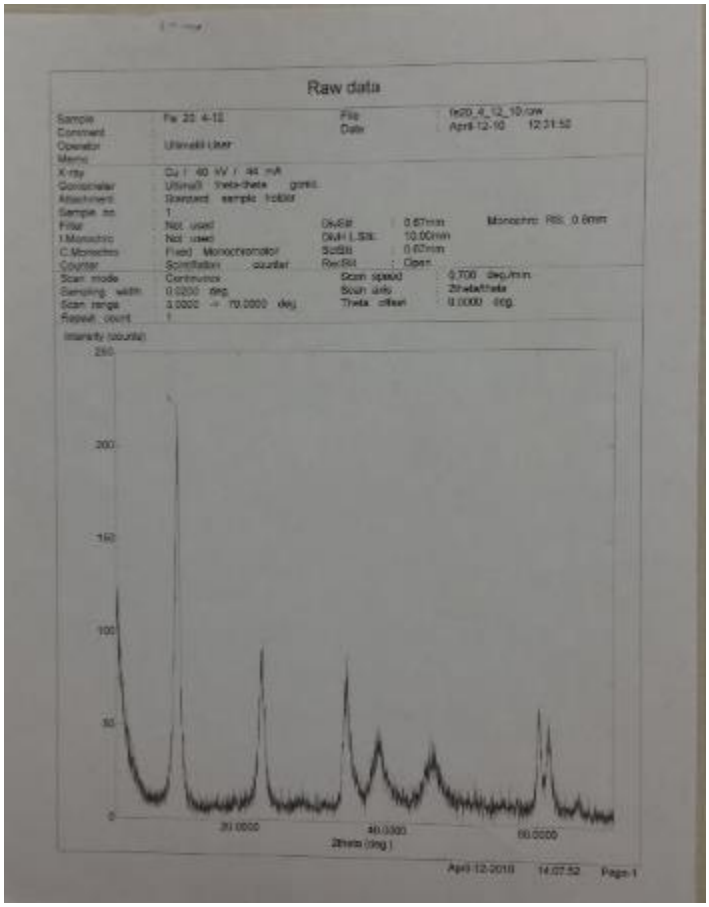

www.manaraa.com

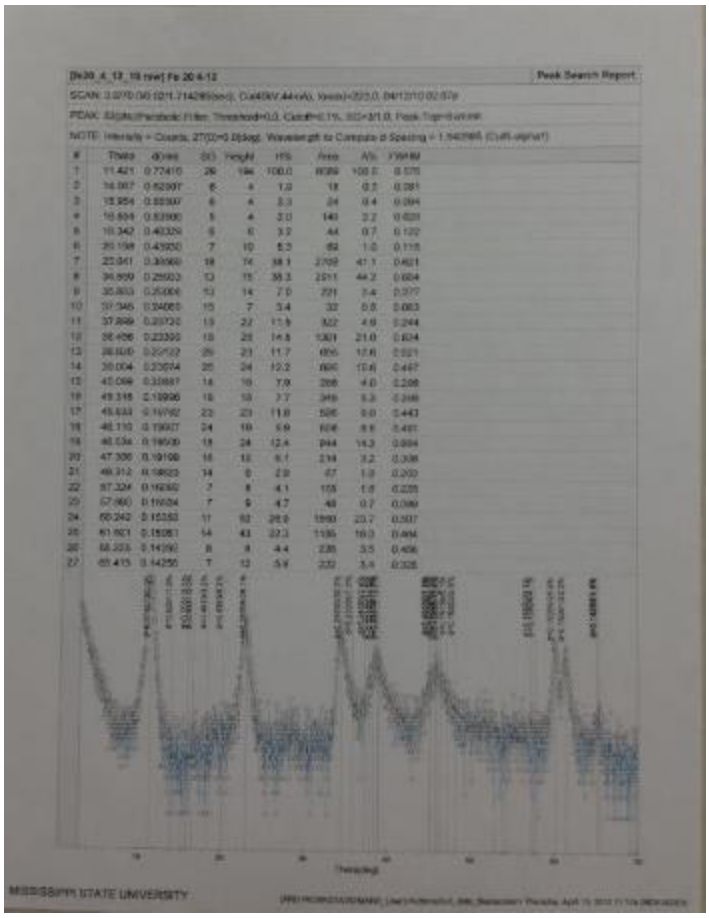

www.manaraa.com

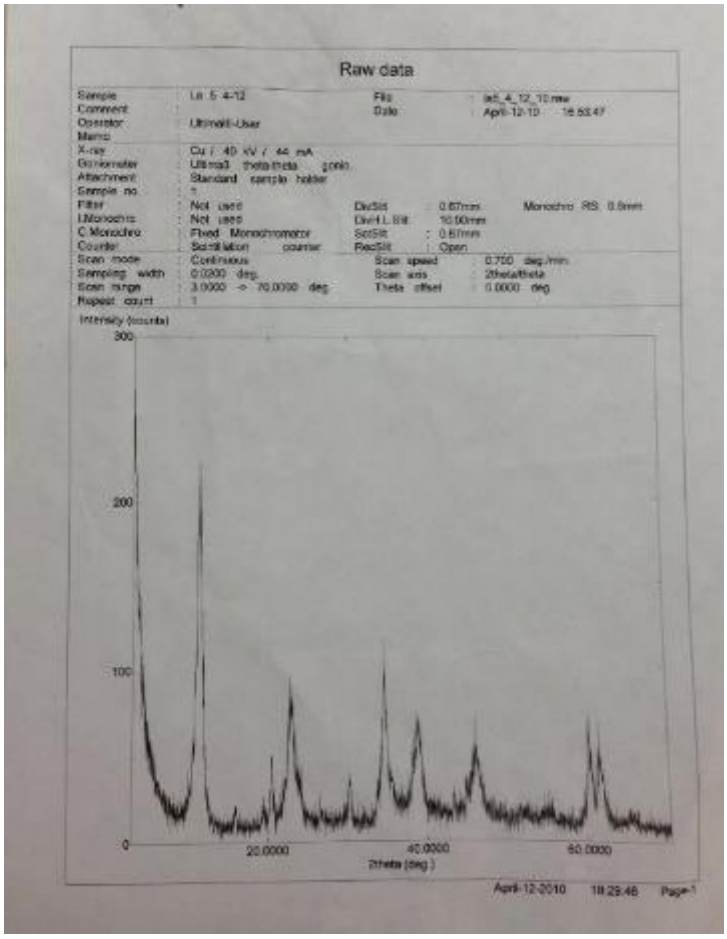

www.manaraa.com

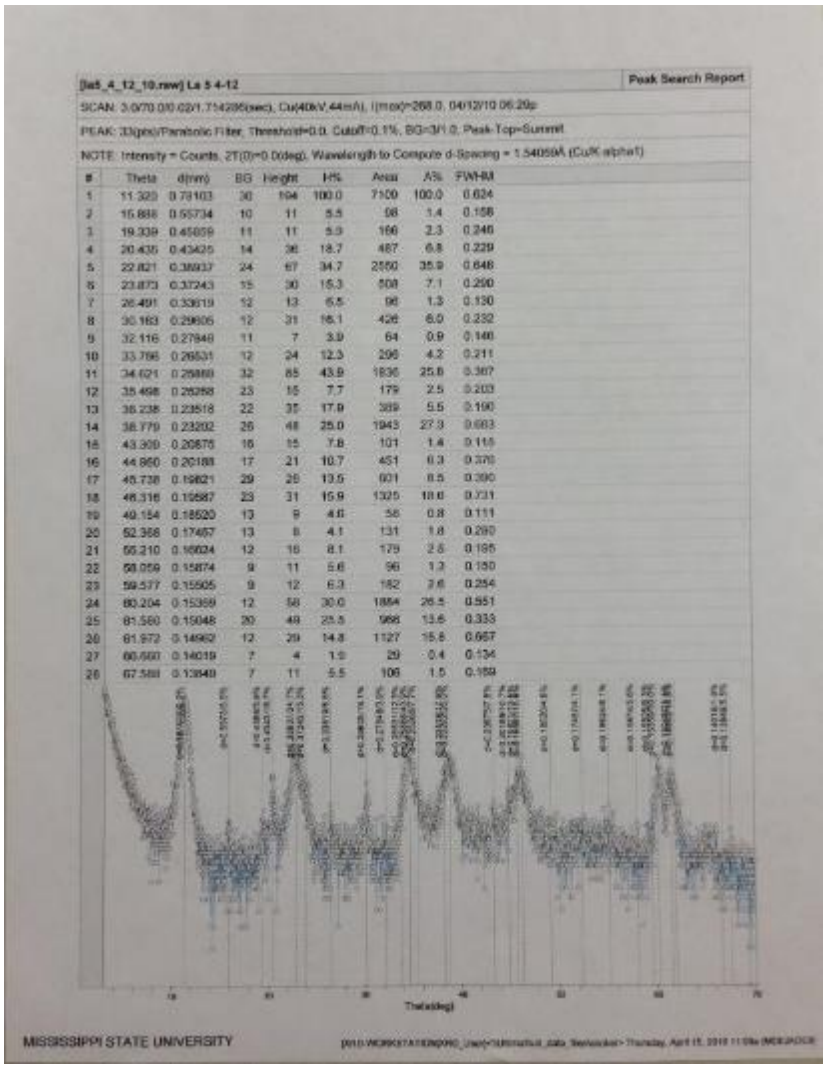
[la5_4_12_10.raw] La 5-4-12 Peak Search Report

SCAN: 3.0/70.0/0.02/1.714286(sec), Cu(40kV,44mA), ((max)=268.0, 04/12/10 06:29p

PEAK: 3(pix)/Parabolic Filter, Threshold=0.0, Cutoff=0.1%, BG=3/1.0, Peak-Top=Summit

NOTE: Intensity = Counts, 2T(0)=0.0(deg), Wavelength to Compute d-Spacing = 1.54056Å (CuK alpha1)

#	Theta	d(nm)	BG	Height	H%	Area	A%	FWHM
1	11.323	0.78103	30	194	100.0	7100	100.0	0.624
2	15.888	0.55734	10	11	5.5	98	1.4	0.158
3	19.339	0.45859	11	11	5.3	166	2.3	0.246
4	20.435	0.43425	14	36	18.7	487	6.8	0.229
5	22.821	0.38937	24	67	34.7	2550	35.9	0.646
6	23.873	0.37243	15	30	15.3	508	7.1	0.290
7	26.491	0.33619	12	13	6.5	96	1.3	0.130
8	30.163	0.29606	12	31	16.1	426	6.0	0.232
9	32.116	0.27848	11	7	3.9	64	0.9	0.146
10	33.766	0.26531	12	24	12.3	296	4.2	0.211
11	34.621	0.25889	32	85	43.9	1836	25.8	0.367
12	35.498	0.25268	23	16	7.7	179	2.5	0.203
13	36.238	0.23518	22	35	17.9	389	5.5	0.190
14	38.779	0.23202	26	48	25.0	1943	27.3	0.683
15	43.309	0.20875	16	15	7.8	101	1.4	0.115
16	44.860	0.20188	17	21	10.7	451	6.3	0.370
17	45.738	0.19821	29	29	13.5	601	8.5	0.390
18	46.316	0.19587	23	31	15.9	1325	18.6	0.731
19	49.154	0.18520	13	9	4.6	56	0.8	0.111
20	52.368	0.17457	13	8	4.1	131	1.8	0.280
21	55.210	0.16624	12	16	8.1	179	2.5	0.195
22	58.059	0.15874	9	11	5.6	96	1.3	0.150
23	59.577	0.15505	9	12	6.3	182	2.6	0.254
24	60.204	0.15359	12	58	30.0	1864	26.5	0.551
25	61.560	0.15048	20	49	25.5	966	13.6	0.333
26	61.972	0.14962	12	29	14.8	1127	15.8	0.667
27	66.560	0.14019	7	4	1.9	29	0.4	0.134
28	67.588	0.13849	7	11	5.5	106	1.5	0.169

MISSISSIPPI STATE UNIVERSITY

www.manaraa.com

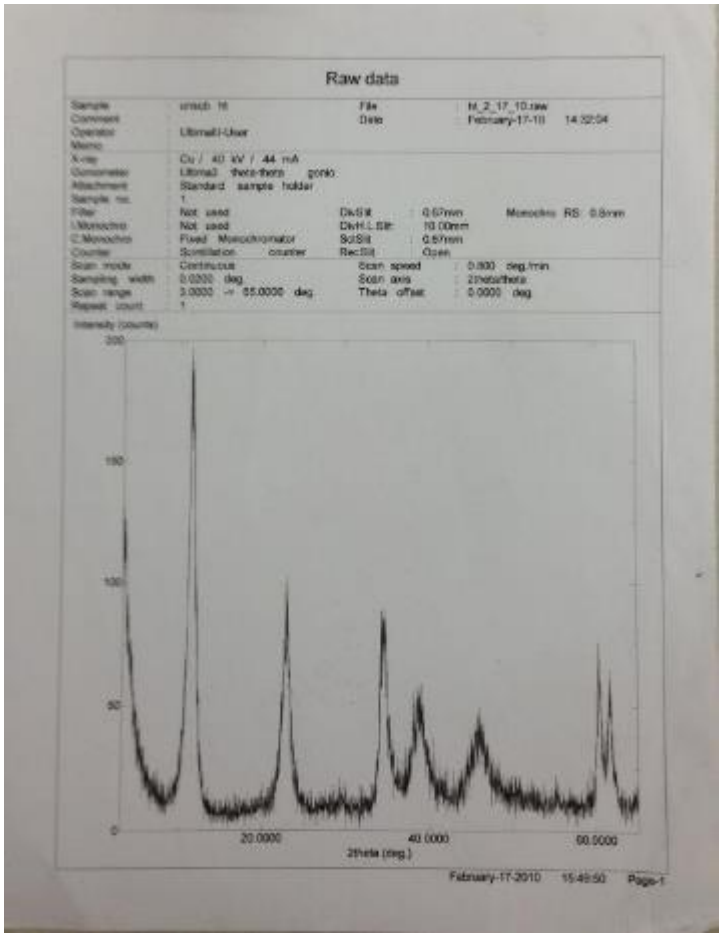

www.manaraa.com

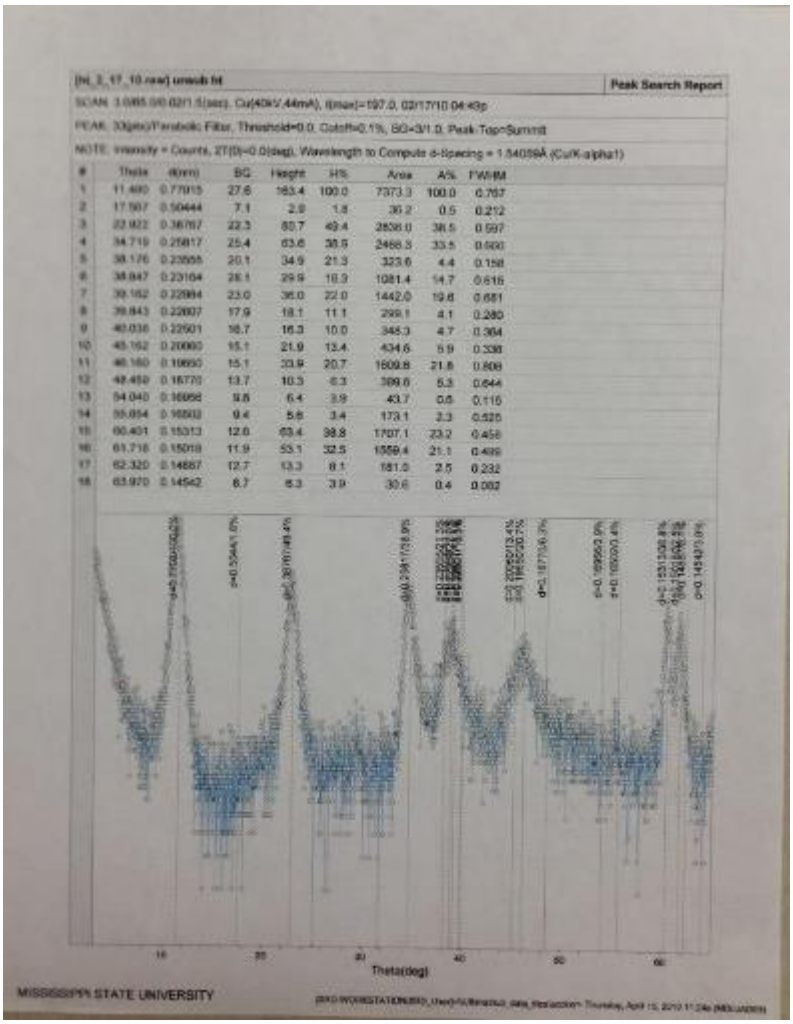

www.manaraa.com

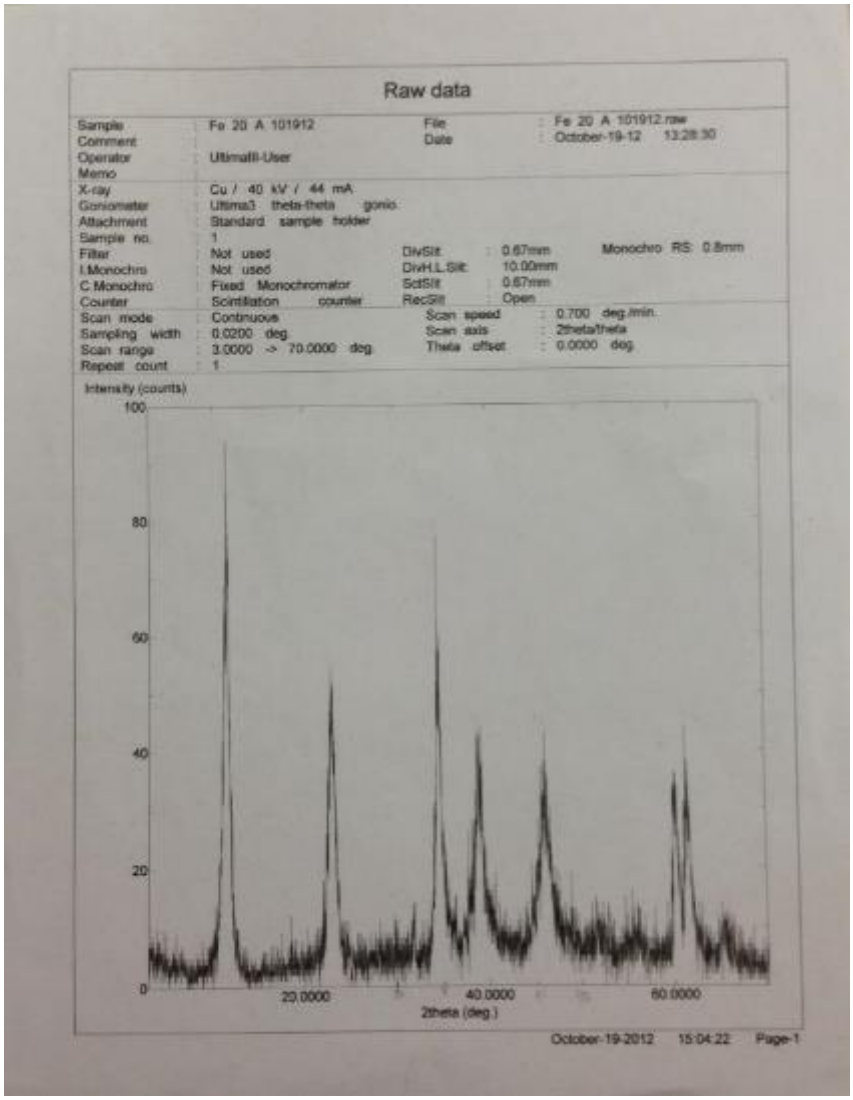

www.manaraa.com

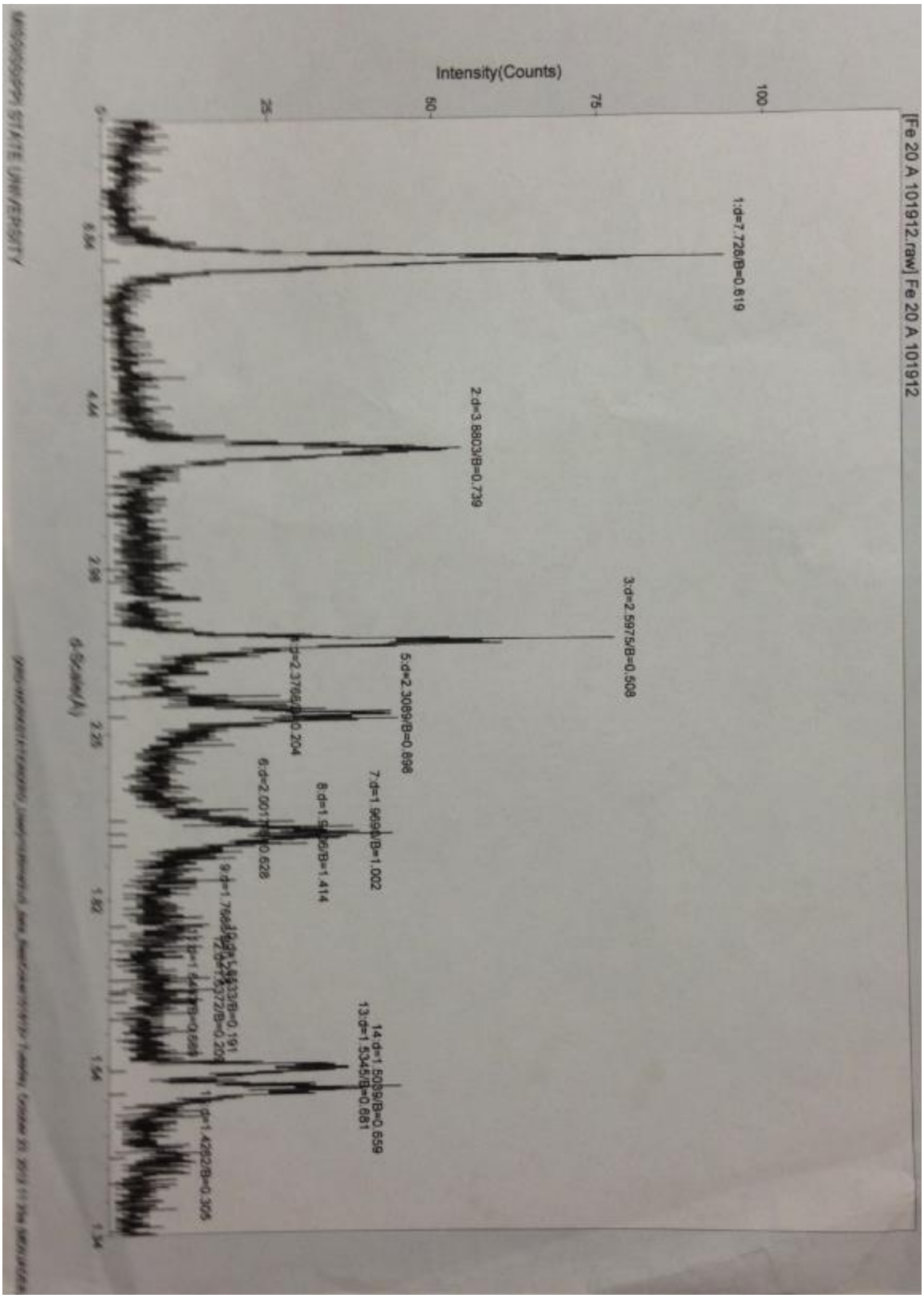

www.manaraa.com

PDF#00-041-1428(RDB): QM=Doubtful(O); d=Diffractometer; I=Diffractometer | PDF Card

Hydrotalcite (Magnesium Aluminum Carbonate Hydroxide Hydrate) (SJO)

$Mg_6Al_2(CO_3)(OH)_{16}\cdot 4H_2O$

Radiation=CuKa1 Lambda=1.5406 Filter=

Calibration= 2T=5.479-82.181 I/Ic(RIR)=O

Ref: Jiang, S., Zhang, G., Liang, H., Huang, W.
Acta Mineral. Sinica, v1984 p296 (1984) CAS#12304-65-3

Rhombohedral - Powder Diffraction, R3m (166) Z=3 mp=

CELL: 6.151 x 6.151 x 46.5 <90.0 x 90.0 x 120.0> P.S=hR56.00

Density(c)=1.975 Density(m)=2.04 Mwt=603.98 Vol=1523.61 F(20)=0.8(0.172,153/4)

Ref: Allmann, R., Jepsen, H.
Neues Jahrb. Mineral., Monatsh. p544 (1969)

Additional Patterns: To replace 00-014-0191 and 00-022-0700. See PDF 01-070-2151. Analysis: Chemical analysis (wt.%): "Al2 O3" 17.18, "Cr2 O3" 0.66, MgO 39.57, "C O2" 7.22, "H2 O"+ 35.14, NiO 0.12: "(Mg5.98 , Ni0.01)5.99 (Al2.04 , Cr0.05)2.09 (O H)16 C O3 ·3.87 H2 O". Color: Light red. Reason O Quality Was Assigned: O assigned because four reflections are unindexed. Sample Source or Locality: Specimen from Jianshibao asbestos mine, Sichuan, China. Unit Cell Data Source: Powder Diffraction.

Color: Light red

Strong Lines: 7.84/X 3.91/8 16 12/6 2.61/3 1.86/2 2.02/1 1.58/1 4.34/1

24 Lines, Wavelength to Compute Theta = 1.54059Å(Cu), I%-Type = (Unknown)

#	d(Å)	I(f)	(hkl)	2-Theta	Theta	1/(2d)	#	d(Å)	I(f)	(hkl)	2-Theta	Theta	1/(2d)
1	16.1160	55.0	(003)	5.479	2.740	0.0310	13	2.1910	9.0	(1,1,15)	41.167	20.584	0.2282
2	7.8440	100.0	(006)	11.271	5.636	0.0637	14	2.0230	12.0	(211)	44.763	22.381	0.2472
3	4.3410	10.0		20.442	10.221	0.1152	15	1.9730	9.0	(1,1,18)	45.961	22.981	0.2534
4	3.9140	80.0	(018)	22.700	11.350	0.1277	16	1.9570	10.0	(0,2,16)	46.359	23.179	0.2555
5	2.8350	5.0	(0,1,14)	31.532	15.766	0.1764	17	1.8620	15.0	(2,1,10)	48.874	24.437	0.2685
6	2.7710	5.0		32.280	16.140	0.1804	18	1.8640	4.0	(0,2,22)	55.151	27.576	0.3005
7	2.6080	30.0	(024)	34.358	17.179	0.1917	19	1.5760	12.0	(1,0,28)	58.519	29.260	0.3173
8	2.5160	10.0		35.656	17.828	0.1987	20	1.5400	6.0	(3,0,15)	60.025	30.013	0.3247
9	2.4020	3.0	(1,1,12)	37.409	18.705	0.2082	21	1.5060	7.0	(226)	61.525	30.763	0.3320
10	2.3700	9.0		37.933	18.967	0.2110	22	1.3040	10.0	(407)	72.416	36.208	0.3834
11	2.3110	9.0	(0,2,10)	38.940	19.470	0.2164	23	1.2540	5.0	(1,2,29)	75.796	37.899	0.3987
12	2.1990	10.0	(0,0,21)	41.011	20.505	0.2274	24	1.1720	3.0	(2,3,11)	82.181	41.090	0.4266

Simulation Parameters: Fixed-Slit Intensities, Two-Theta Range =3.48/84.18/0.02, FWHM = 0.1

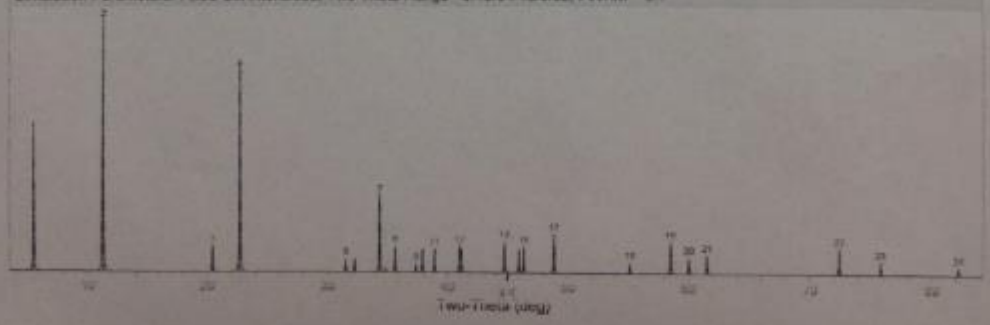

Two-Theta (deg)

MISSISSIPPI STATE UNIVERSITY

www.manaraa.com

APPENDIX B

DERIVATION OF BEST MECHANISM MODEL FOR WET AND DRY FREE FATTY ACID ESTERIFICATION

www.manaraa.com

The mechanism for the best model identified is shown below:

$$r = k\frac{(C_aC_b - \frac{C_cC_d}{K_e})}{(1+K_aC_a+K_dC_d)^2} \quad \text{(B.1)}$$

In this model and subsequent derivation steps, the subscripts: *a*, *b*, *c*, and *d* represent the compounds: palmitic acid (PA), methanol (M), methyl palmitate (MP), and water (W) respectively.

Based on the mechanism discussed in Chapter 4, with the adsorption, surface reaction and desorption steps in consecutive order below (Equations B.1 -B. 3)

$$PA + S_1 \underset{k_{-A}}{\overset{k_A}{\rightleftharpoons}} PA \cdot S_1 \quad \text{(B.2)}$$

$$PA\ S_1 + MeOH + S_2 \underset{k_{-S}}{\overset{k_S}{\rightleftharpoons}} MP + S_1 + W\text{-}S_2 \quad \text{(B.3)}$$

$$W \cdot S_2 \underset{k_{-D}}{\overset{k_D}{\rightleftharpoons}} W + S_2 \quad \text{(B.4)}$$

Derivation:

It was assumed that the surface reaction step is rate-limiting.

The concentration of palmitic acid (PA) adsorbed onto the catalytic site, $C_{PA}\cdot S_1$, in the adsorption reaction is given by:

$$C_{PA} \cdot S_1 = K_aC_{PA}C_v \quad \text{(B.5)}$$

The concentration of water (W) adsorbed onto the catalytic site, $C_W\cdot S_2$, in the adsorption reaction is given by:

$$C_W \cdot S_2 = \frac{C_WC_v}{K_{dw}} = K_dC_WC_v \quad \text{(B.6)}$$

The rate of the surface reaction, r_s, can be expressed as:

www.manaraa.com

$$r_s = k_s C_{PA} \cdot S_1 C_M C_v - \frac{C_{MP} C_W \cdot S_2 C_v}{K_s} \quad \text{(B.7)}$$

Where C_v represents the concentration of vacant sites; K_a, K_s, and K_{dw} represent the equilibrium constants for the adsorption, surface reaction, and desorption steps.

To simplify Equation 5 to a non-fraction, a new term K_d was defined, which is the inverse of the K_{dw} term that is the equilibrium constant for the desorption of water. Thus, K_d represents the equilibrium constant for the adsorption of water in Equation 3.

Plugging Equations 4 and 5 into Equation 6,

$$r_s = k_s (K_a C_{PA} C_M {C_v}^2 - \frac{K_d C_{MP} C_W {C_v}^2}{K_s}) \quad \text{(B.8)}$$

The total concentration of sites, C_t, is:

$$C_t = C_v + C_{PA} \cdot S_1 + C_W \cdot S_2 \quad \text{(B.9)}$$

$$C_t = C_v (1 + K_a C_{PA} + K_d C_W) \quad \text{(B.10)}$$

Therefore,

$${C_v}^2 = \frac{{C_t}^2}{(1 + K_a C_{PA} + K_d C_W)^2} \quad \text{(B.11)}$$

Plugging Equation 10 into Equation 7:

$$r_s = \frac{k_s {C_t}^2 (K_a C_{PA} C_M - \frac{K_d C_{MP} C_W}{K_s})}{(1 + K_a C_{PA} + K_d C_W)^2} \quad \text{(B.12)}$$

An overall equilibrium constant, K_e, is defined as:

$$K_e = K_a * K_s * K_{dw} = \frac{K_a * K_s}{K_d} \quad \text{(B.13)}$$

Therefore, substituting Equation 12 into Equation 11 produces:

www.manaraa.com

$$r_s = \frac{k_s K_a C_t{}^2 (C_{PA} C_M - \frac{C_{MP} C_W}{K_e})}{(1 + K_a C_{PA} + K_d C_W)^2} \quad \text{(B.14)}$$

Simplifying, and defining an apparent rate constant, *k*, as:

$$k = k_s K_a C_t{}^2 \quad \text{(B.15)}$$

The final model for the reaction rate becomes:

$$r = k \frac{(C_a C_b - \frac{C_c C_d}{K_e})}{(1 + K_a C_a + K_d C_d)^2} \quad \text{(B.16)}$$

www.manaraa.com

APPENDIX C

ADDITIONAL EQUIPMENT USED FOR SUPERCRITICAL METHANOL EXPERIMENTS

www.manaraa.com

Turbovap

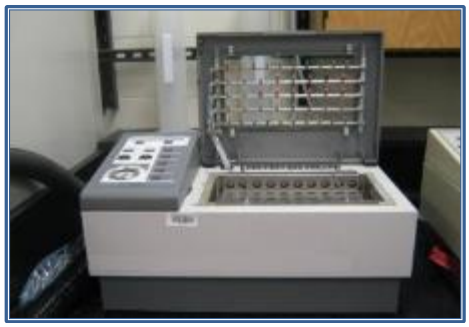

Figure C.1 TurboVap LV

(Caliper Life Sciences, Hopkinton, MA, U.S.A.)

Rotavap

Figure C.2 Büchi R-205 rotary evaporato

(Brinkmann Instruments, Inc., Westbury, NY, U.S.A)

www.manaraa.com

Temperature controller

Figure C.3 Benchtop temperature controller for sand bath

(Omega Engineering, Stamford, Connecticut, U.S.A.)

Datalogger

Figure C.4 Datalogger used to record internal probe and sand bath temperature changes

(Omega Engineering, Stamford, Connecticut, U.S.A.)

www.manaraa.com

Dessicator

Figure C.5 Dessicator used for holding catalysts till use

(Fisher Scientific, Pittsburgh, PA, USA)

Air filters

Figure C.6 Air filters upstream of sand bath

Changed airfilter crystals when pink, regenerated in oven for 1.5hr at 120°C

www.manaraa.com

Platform shaker

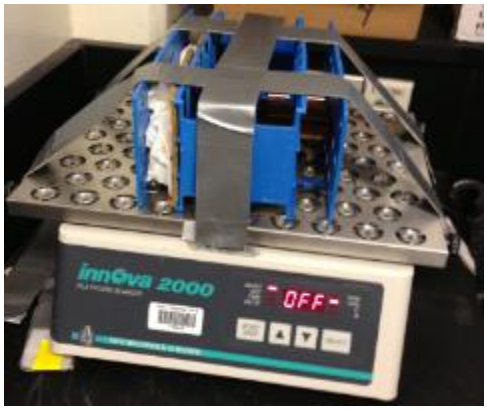

Figure C.7 Platform shaker used during Bligh-Dyer extraction

(New Brunswick Scientific Co., Edison, NJ, USA)

www.manaraa.com

APPENDIX D

ADDITIONAL DATA ON ECONOMIC ANALYSIS

www.manaraa.com

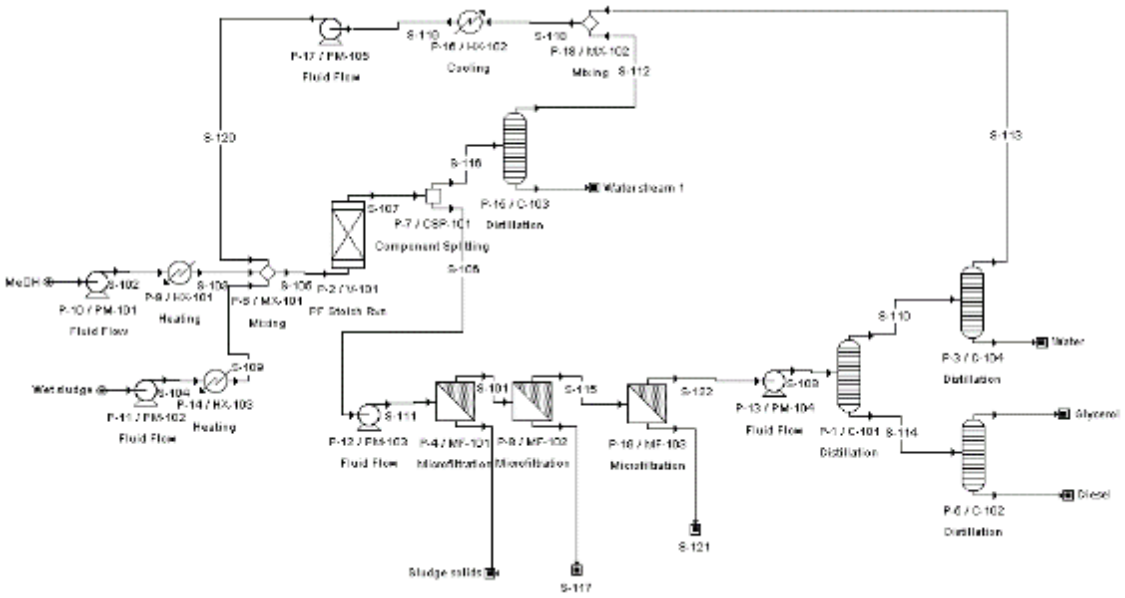

Figure D.1 One-step plant schematic

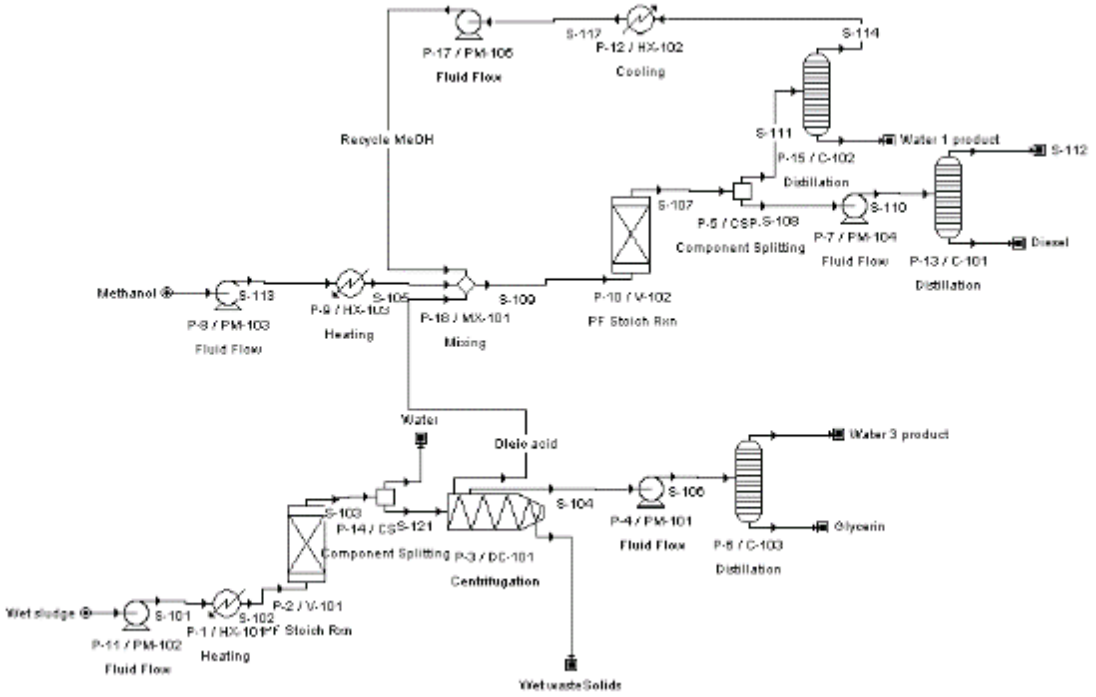

Figure D.2 Two-step plant schematic

www.manaraa.com

المنارة للاستشارات

Book used: Plant design and economics for chemical engineers, Peters and Timmerhaus, 5th ed.

	Hydrolysis Reactor	Esterification Reactor	1-step Transesterification reactor
Temperature, °C	200	280	280
Pressure, kPa	7000	10000	14000
Pressure with 10% allowance, kPa	7700	11000	15400
Shape	Cylindrical	Cylindrical	Cylindrical
Length (L), m	15.88	3.6	20
Diameter (d), m	1.59	0.36	2
Inside radius (ri), m	0.79	0.18	1
Material assumption	SS 316, spot examined, double-welded butt joints	SS 316, spot examined, double-welded butt joints	SS 316, spot examined, double-welded butt joints
Corrosion allowance, Cc	0.0032	0.0032	0.0032
Stress, S (Table 12-10, page 555)	79300	79300	79300
Joint Efficiency (Ej)	0.85	0.85	0.85
0.385 × S × Ej	25950.9	25950.9	25950.9
Thickness, t depends on if P > or < 0.385 × S × Ej			
P greater or less than 0.385 × S × Ej?	<	<	<
Thickness (t), m	0.091	0.033	0.240
Density of steel (ρ), kg/m^3	8000	8000	8000
Weight of shell, π × d × L × t × ρ	57772.87	1076.31	241842.13
Head diameter factor (Table 12-11)	1.6	1.6	1.6
Weight of 2 heads (Page 634)	9245.41	173.65	38694.74
Total weight of vessel including 20% increase for nozzles, etc	80421.93	1499.95	336644.25
Cost factor based on pressure (Table 12-12)	5.4	5.4	8.8
F.o.b. cost for reactor based on eqn 12.50 = (cost per kg) × Total weight × Wv^-0.34	681182.96	49195.76	2855870.58
cost index in 2011	585.7	585.7	585.7
cost index in 2002	395.6	395.6	395.6
Cost of vessel in 2011	1008515.82	72836.09	4228218.90

Figure D.3 Cost calculation for hydrolysis, esterification and transesterification reactors used in Superpro Designer® simulation for economic analysis

www.manaraa.com

Table D.1 Superpro Designer ® software output for 1-step plant simulation at 30ml/g methanol-to-solid ratio

2. MAJOR EQUIPMENT SPECIFICATION AND FOB COST (2012 prices)

Quantity/ Standby/ Staggered	Name	Description	Unit Cost ($)	Cost ($)
1/0	MF-101	Microfilter Membrane Area = 36.53 m2	82,000	82,000
1/0	PM-101	Centrifugal Pump Power = 0.20 kW	9,000	9,000
1/0	PM-102	Centrifugal Pump Power = 6.96 kW	41,000	41,000
1/0	PM-103	Centrifugal Pump Power = 0.09 kW	9,000	9,000
1/0	PM-104	Centrifugal Pump Power = 0.09 kW	9,000	9,000
1/0	C-102	Distillation Column Column Volume = 75.29 gal	76,000	76,000
1/0	CSP-101	Component Splitter Size/Capacity = 195680.63 kg/h	0	0
1/0	HX-101	Heat Exchanger Heat Exchange Area = 0.20 m2	1,000	1,000
1/0	HX-103	Heat Exchanger Heat Exchange Area = 33.35 m2	12,000	12,000
6/0	C-103	Distillation Column Column Volume = 6510.86 gal	79,000	474,000
2/0	C-101	Distillation Column Column Volume = 8690.05 gal	146,000	292,000
1/0	C-104	Distillation Column Column Volume = 12224.17 gal	164,000	164,000
1/0	MF-102	Microfilter Membrane Area = 36.53 m2	82,000	82,000
1/0	HX-102	Heat Exchanger Heat Exchange Area = 28.89 m2	11,000	11,000
1/0	PM-105	Centrifugal Pump Power = 21.39 kW	68,000	68,000
1/0	MX-101	Mixer Size/Capacity = 195704.37 kg/h	0	0
1/0	MX-102	Mixer Size/Capacity = 135933.37 kg/h	0	0
1/0	V-101	Plug Flow Reactor Vessel Volume = 16633.91 gal	4,228,000	4,228,000
1/0	MF-103	Microfilter Membrane Area = 36.52 m2	82,000	82,000
		Unlisted Equipment		1,409,000
			TOTAL	7,045,000

Table D.1 (continued)

3. FIXED CAPITAL ESTIMATE SUMMARY (2012 prices in $)

3A. Total Plant Direct Cost (TPDC) (physical cost)

1. Equipment Purchase Cost	7,045,000

www.manaraa.com

2. Installation	3,021,000
3. Process Piping	2,466,000
4. Instrumentation	2,818,000
5. Insulation	211,000
6. Electrical	705,000
7. Buildings	3,170,000
8. Yard Improvement	1,057,000
9. Auxiliary Facilities	2,818,000
TPDC	23,312,000

3B. Total Plant Indirect Cost (TPIC)

10. Engineering	5,828,000
11. Construction	8,159,000
TPIC	13,987,000

3C. Total Plant Cost (TPC = TPDC+TPIC)

TPC	37,299,000

3D. Contractor's Fee & Contingency (CFC)

12. Contractor's Fee	1,865,000
13. Contingency	3,730,000
CFC = 12+13	5,595,000

3E. Direct Fixed Capital Cost (DFC = TPC+CFC)

DFC	42,894,000

4. LABOR COST - PROCESS SUMMARY

Labor Type	Unit Cost ($/h)	Annual Amount (h)	Annual Cost ($)	%
Operator	69.00	102,394	7,065,000	100.00
TOTAL		102,394	7,065,000	100.00

5. RAW MATERIALS COST - PROCESS SUMMARY

Bulk Raw Material	Unit Cost ($/kg)	Annual Amount (kg)	Annual Cost ($)	%
Wet sludge	0.000	462,773,520	0	0.00
Methanol	0.482	10,612,800	5,115,000	100.00
TOTAL		473,386,320	5,115,000	100.00

www.manaraa.com

Table D.1 (continued)

6. VARIOUS CONSUMABLES COST (2012 prices) - PROCESS SUMMARY

Consumable	Units Cost ($)	Annual Amount		Annual Cost ($)	%
Dft Membrane	400.000	868	m2	347,000	100.00
TOTAL				347,000	100.00

7. WASTE TREATMENT/DISPOSAL COST (2012 prices) - PROCESS SUMMARY

THE TOTAL WASTE TREATMENT/DISPOSAL COST IS ZERO.

8. UTILITIES COST (2012 prices) - PROCESS SUMMARY

Utility	Annual Amount	Reference Units	Annual Cost ($)	%
Electricity	501,279	kWh	50,128	0.19
Steam	1,649,286,431	kg	6,927,003	26.81
Cooling Water	114,433,280,695	kg	11,443,328	44.28
Chilled Water	3,923,441,831	kg	1,569,377	6.07
B's VHPsteam	585,116,553	kg	5,851,166	22.64
TOTAL			25,841,001	100.00

9. ANNUAL OPERATING COST (2012 prices) - PROCESS SUMMARY

Cost Item	$	%
Raw Materials	5,115,000	10.77
Labor-Dependent	7,065,000	14.87
Facility-Dependent	8,070,000	16.99
Laboratory/QC/QA	1,060,000	2.23
Consumables	347,000	0.73
Waste Treatment/Disposal	0	0.00
Utilities	25,841,000	54.40
Transportation	0	0.00
Miscellaneous	0	0.00
Advertising/Selling	0	0.00
Running Royalties	0	0.00
Failed Product Disposal	0	0.00
TOTAL	47,499,000	100.00

Table D.2 Superpro Designer ® software output for 1-step plant simulation at 7.5ml/g methanol-to-solid ratio

2. MAJOR EQUIPMENT SPECIFICATION AND FOB COST (2012 prices)

Quantity/

www.manaraa.com

Standby/ Staggered	Name	Description	Unit Cost ($)	Cost ($)
1/0	MF-101	Microfilter	82,000	82,000
		Membrane Area = 36.53 m2		
1/0	PM-101	Centrifugal Pump	9,000	9,000
		Power = 0.05 kW		
1/0	PM-102	Centrifugal Pump	41,000	41,000
		Power = 6.96 kW		
1/0	PM-103	Centrifugal Pump	9,000	9,000
		Power = 0.09 kW		
1/0	PM-104	Centrifugal Pump	9,000	9,000
		Power = 0.09 kW		
1/0	C-102	Distillation Column	76,000	76,000
		Column Volume = 74.50 gal		
1/0	CSP-101	Component Splitter	0	0
		Size/Capacity = 89879.80 kg/h		
1/0	HX-101	Heat Exchanger	1,000	1,000
		Heat Exchange Area = 0.05 m2		
1/0	HX-103	Heat Exchanger	12,000	12,000
		Heat Exchange Area = 33.35 m2		
2/0	C-103	Distillation Column	73,000	146,000
		Column Volume = 6295.12 gal		
1/0	C-101	Distillation Column	151,000	151,000
		Column Volume = 9423.98 gal		
1/0	C-104	Distillation Column	102,000	102,000
		Column Volume = 4351.78 gal		
1/0	MF-102	Microfilter	82,000	82,000
		Membrane Area = 36.52 m2		
1/0	HX-102	Heat Exchanger	4,000	4,000
		Heat Exchange Area = 6.66 m2		
1/0	PM-105	Centrifugal Pump	36,000	36,000
		Power = 4.88 kW		
1/0	MX-101	Mixer	0	0
		Size/Capacity = 89876.56 kg/h		
1/0	MX-102	Mixer	0	0
		Size/Capacity = 31110.56 kg/h		
1/0	V-101	Plug Flow Reactor	4,228,000	4,228,000
		Vessel Volume = 16703.27 gal		
1/0	MF-103	Microfilter	82,000	82,000
		Membrane Area = 36.51 m2		
		Unlisted Equipment		1,267,000
			TOTAL	6,337,000

Table D.2 (continued)

3. FIXED CAPITAL ESTIMATE SUMMARY (2012 prices in $)

3A. Total Plant Direct Cost (TPDC) (physical cost)

www.manaraa.com

1. Equipment Purchase Cost	6,337,000
2. Installation	2,931,000
3. Process Piping	2,218,000
4. Instrumentation	2,535,000
5. Insulation	190,000
6. Electrical	634,000
7. Buildings	2,852,000
8. Yard Improvement	951,000
9. Auxiliary Facilities	2,535,000
TPDC	21,182,000

3B. Total Plant Indirect Cost (TPIC)

10. Engineering	5,296,000
11. Construction	7,414,000
TPIC	12,709,000

3C. Total Plant Cost (TPC = TPDC+TPIC)

TPC	33,892,000

3D. Contractor's Fee & Contingency (CFC)

12. Contractor's Fee	1,695,000
13. Contingency	3,389,000
CFC = 12+13	5,084,000

3E. Direct Fixed Capital Cost (DFC = TPC+CFC)

DFC	38,975,000

4. LABOR COST - PROCESS SUMMARY

Labor Type	Unit Cost ($/h)	Annual Amount (h)	Annual Cost ($)	%
Operator	69.00	102,394	7,065,000	100.00
TOTAL		102,394	7,065,000	100.00

www.manaraa.com

Table D.2 (continued)

5. RAW MATERIALS COST - PROCESS SUMMARY

Bulk Raw Material	Unit Cost ($/kg)	Annual Amount (kg)	Annual Cost ($)	%
Wet sludge	0.000	462,773,520	0	0.00
Methanol	0.482	2,653,200	1,279,000	100.00
TOTAL		465,426,720	1,279,000	100.00

6. VARIOUS CONSUMABLES COST (2012 prices) - PROCESS SUMMARY

Consumable	Units Cost ($)	Annual Amount		Annual Cost ($)	%
Dft Membrane	400.000	868	m2	347,000	100.00
TOTAL				347,000	100.00

7. WASTE TREATMENT/DISPOSAL COST (2012 prices) - PROCESS SUMMARY

THE TOTAL WASTE TREATMENT/DISPOSAL COST IS ZERO.

8. UTILITIES COST (2012 prices) - PROCESS SUMMARY

Utility	Annual Amount	Reference Units	Annual Cost ($)	%
Electricity	336,357	kWh	33,636	0.31
Steam	707,950,140	kg	2,973,391	27.50
Cooling Water	45,171,099,808	kg	4,517,110	41.77
Chilled Water	904,732,945	kg	361,893	3.35
B's VHPsteam	292,757,881	kg	2,927,579	27.07
TOTAL			10,813,608	100.00

www.manaraa.com

Table D.2 (continued)

9. ANNUAL OPERATING COST (2012 prices) - PROCESS SUMMARY

Cost Item	$	%
Raw Materials	1,279,000	4.58
Labor-Dependent	7,065,000	25.33
Facility-Dependent	7,328,000	26.27
Laboratory/QC/QA	1,060,000	3.80
Consumables	347,000	1.24
Waste Treatment/Disposal	0	0.00
Utilities	10,814,000	38.77
Transportation	0	0.00
Miscellaneous	0	0.00
Advertising/Selling	0	0.00
Running Royalties	0	0.00
Failed Product Disposal	0	0.00
TOTAL	27,892,000	100.00

Table D.3 Superpro Designer ® software output for 2-step plant simulation

2. MAJOR EQUIPMENT SPECIFICATION AND FOB COST (2012 prices)

Quantity/ Standby/ Staggered	Name	Description	Unit Cost ($)	Cost ($)
1/0	PM-102	Centrifugal Pump Power = 6.96 kW	41,000	41,000
1/0	HX-101	Heat Exchanger Heat Exchange Area = 29.85 m2	11,000	11,000
1/0	DC-101	Decanter Centrifuge Throughput = 206.44 gal/h	270,000	270,000
1/0	PM-101	Centrifugal Pump Power = 0.01 kW	9,000	9,000
1/0	PM-103	Centrifugal Pump Power = 0.01 kW	9,000	9,000
1/0	HX-103	Heat Exchanger Heat Exchange Area = 0.01 m2	1,000	1,000
1/0	PM-104	Centrifugal Pump Power = 0.08 kW	9,000	9,000
1/0	C-101	Distillation Column Column Volume = 10.23 gal	52,000	52,000
1/0	C-103	Distillation Column Column Volume = 5663.68 gal	123,000	123,000
1/0	CSP-102	Component Splitter Size/Capacity = 58426.81 kg/h	0	0
1/0	CSP-101	Component Splitter Size/Capacity = 1008.34 kg/h	0	0

Table D.3 (continued)

www.manaraa.com

1/0	C-102	Distillation Column	56,000	56,000
		Column Volume = 244.91 gal		
1/0	V-102	Plug Flow Reactor	73,000	73,000
		Vessel Volume = 97.13 gal		
1/0	HX-102	Heat Exchanger	1,000	1,000
		Heat Exchange Area = 0.06 m2		
1/0	PM-105	Centrifugal Pump	9,000	9,000
		Power = 0.04 kW		
1/0	MX-101	Mixer	0	0
		Size/Capacity = 1008.33 kg/h		
1/0	V-101	Plug Flow Reactor	1,009,000	1,009,000
		Vessel Volume = 8303.72 gal		
		Unlisted Equipment		418,000
			TOTAL	2,091,000

3. FIXED CAPITAL ESTIMATE SUMMARY (2012 prices in $)

3A. Total Plant Direct Cost (TPDC) (physical cost)

1. Equipment Purchase Cost	2,091,000
2. Installation	930,000
3. Process Piping	732,000
4. Instrumentation	836,000
5. Insulation	63,000
6. Electrical	209,000
7. Buildings	941,000
8. Yard Improvement	314,000
9. Auxiliary Facilities	836,000
TPDC	6,951,000

3B. Total Plant Indirect Cost (TPIC)

10. Engineering	1,738,000
11. Construction	2,433,000
TPIC	4,170,000

3C. Total Plant Cost (TPC = TPDC+TPIC)

TPC	11,121,000

3D. Contractor's Fee & Contingency (CFC)

12. Contractor's Fee	556,000
13. Contingency	1,112,000
CFC = 12+13	1,668,000

3E. Direct Fixed Capital Cost (DFC = TPC+CFC)

DFC	12,789,000

Table D.3 (continued)

www.manaraa.com

4. LABOR COST - PROCESS SUMMARY

Labor Type	Unit Cost ($/h)	Annual Amount (h)	Annual Cost ($)	%
Operator	69.00	74,109	5,113,000	100.00
TOTAL		74,109	5,113,000	100.00

5. RAW MATERIALS COST - PROCESS SUMMARY

Bulk Raw Material	Unit Cost ($/kg)	Annual Amount (kg)	Annual Cost ($)	%
Wet sludge	0.000	462,773,520	0	0.00
Methanol	0.482	752,400	363,000	100.00
TOTAL		463,525,920	363,000	100.00

6. VARIOUS CONSUMABLES COST (2012 prices) - PROCESS SUMMARY

THE CONSUMABLES COST IS ZERO.

7. WASTE TREATMENT/DISPOSAL COST (2012 prices) - PROCESS SUMMARY

THE TOTAL WASTE TREATMENT/DISPOSAL COST IS ZERO.

8. UTILITIES COST (2012 prices) - PROCESS SUMMARY

Utility	Annual Amount	Reference Units	Annual Cost ($)	%
Electricity	76,959	kWh	7,696	0.30
Steam	169,996,326	kg	713,985	27.57
Cooling Water	6,489,590,724	kg	648,959	25.06
Chilled Water	8,095,712	kg	3,238	0.13
B's VHPsteam	121,583,764	kg	1,215,838	46.95
TOTAL			2,589,715	100.00

www.manaraa.com

Table D.3 (continued)

9. ANNUAL OPERATING COST (2012 prices) - PROCESS SUMMARY

Cost Item	$	%
Raw Materials	363,000	3.23
Labor-Dependent	5,113,000	45.50
Facility-Dependent	2,405,000	21.40
Laboratory/QC/QA	767,000	6.83
Consumables	0	0.00
Waste Treatment/Disposal	0	0.00
Utilities	2,590,000	23.04
Transportation	0	0.00
Miscellaneous	0	0.00
Advertising/Selling	0	0.00
Running Royalties	0	0.00
Failed Product Disposal	0	0.00
TOTAL	11,238,000	100.00

www.manaraa.com